CIVIL ENGINEERING STUDIES

Structural Research Series No. 328

FATIGUE BEHAVIOR OF WELDED THIN WEB GIRDERS AS INFLUENCED BY WEB DISTORTION AND BOUNDARY RIGIDITY

by

D. W. GOODPASTURE

and

J. E. STALLMEYER

A Technical Report
of a Research Program
Sponsored by
BUREAU OF PUBLIC ROADS
DEPARTMENT OF COMMERCE
Contract No. CPR-11-4204

UNIVERSITY OF ILLINOIS
URBANA, ILLINOIS
AUGUST 1967

FATIGUE BEHAVIOR OF WELDED THIN WEB GIRDERS AS INFLUENCED BY WEB DISTORTION AND BOUNDARY RIGIDITY

by
D. W. Goodpasture
and
J. E. Stallmeyer

A Report of an Investigation Conducted
by
The Civil Engineering Department
University of Illinois
In Cooperation with
Department of Commerce-Bureau of Public Roads
Contract No. CPR-11-4204

University of Illinois
Urbana, Illinois
August 1967

ACKNOWLEDGMENT

The study reported herein is part of an investigation of the Flexural Fatigue Strength of All-Welded Beams and Girders which is being conducted at the University of Illinois under the sponsorship of the Department of Commerce, Bureau of Public Roads. This investigation is part of the structural research program of the Department of Civil Engineering.

The author wishes to express his appreciation to Professor J. E. Stallmeyer for his aid, advice and encouragement during the investigation. The writer wishes to thank Mr. G. E. Rymer for his helpful advice and suggestions during the welding experimentation and his care in the preparation of the specimens. The efforts of Mr. O. H. Ray and other members of the laboratory shop in preparing specimens and maintaining test equipment are greatly appreciated.

The author also wishes to express his deep appreciation to his wife, Marion, for her assistance, encouragement, and understanding during the past four years.

TABLE OF CONTENTS

TABLE OF CONTENTS (Continued)

LIST OF TABLES

LIST OF FIGURES

LIST OF FIGURES (Continued)

LIST OF FIGURES (Continued)

LIST OF FIGURES (Continued)

LIST OF FIGURES (Continued)

LIST OF FIGURES (Continued)

1. INTRODUCTION

1.1 Background

Plate girders are structural members which are designed to resist both shearing forces and bending moments. Shearing forces are resisted by the web and bending moments are resisted primarily by the flanges if the forces are resisted by pure beam action. Plate girders are primarily moment resisting members in most civil engineering applications. In order to accomplish an economical design, it has been general practice to place as much material as possible in the flanges of the girder and to locate the flanges as far apart as possible. Therefore, a deep thin web results. This optimization of material is limited by the fact that when the web thickness becomes small relative to the web depth, the web plate becomes unstable.

For years civil engineers have assumed in design that the strength of a plate girder was limited by the theoretical buckling strength of the individual girder panels. Extensive theoretical and experimental research has been focused on the problem of stiffened plates under combined bending and shearing stresses. Most of this research was conducted to determine the magnitude of various combinations of boundary stresses at which perfectly plane plates become unstable and cease to be perfectly plane.

Most design specifications limit the web slenderness ratio d/t, in order to insure that a plane web will not buckle at design loads. It is assumed that the girder carries shear and moment by pure beam action.

The limiting stresses are based on the theoretically computed buckling stresses of an ideal panel.

Aeronautical engineers require structural members with minimum weight and have taken advantage of the full strength of a girder. Tests have shown that the ultimate strength of a girder is not limited by the buckling of individual panels. After a panel buckles, the girder changes from beam action to a more efficient manner of carrying the additional load instead of resisting increases in load by pure beam action alone. The girder begins to act as a Pratt truss with the web panels performing the function of tension diagonals and the transverse stiffeners behaving as vertical compression members. Wagner (1)* proposed the pure diagonal tension theory for plate girders in which it was assumed that the web acted as a membrane and resisted no compression. Kuhn (2) assumed the shear was resisted partly by beam action and partly by diagonal tension field action. Thus, the design of girders in the aeronautical field evolved to the proportioning of the girder on the basis of its ultimate load and a suitable factor of safety.

Civil Engineers have been convinced that more efficient use could be made of the material in plate girders if advantage was taken of the post-buckling strength of the girders. A comprehensive investigation involving the application of the diagonal tension field theory to civil engineering structures was conducted at Lehigh University from 1957 to 1961. The purpose of the investigation was to develop simple but general formulae to predict the ultimate capacity of girders subjected

* Numbers in parentheses refer to entries in the list of references.

to pure shear, pure bending, and combined shear and bending. One of the results of this experimental and analytical investigation was the conclusion that the stresses in plate girder web panels could exceed the theoretical buckling stresses of the panels without ill effects. As a result of such investigations, the new AISC building specification allows the proportioning of the web in a plate girder with a much higher web slenderness ratio, d/t.

Recently, an investigation of the effect of longitudinal stiffeners on the strength of plate girders was initiated at Lehigh University. Incomplete results indicate that the main beneficial effect was the reduction of lateral web deflections. No increase in ultimate capacity was experienced in the few tests conducted thus far.

Very few reports of fatigue tests on thin web girders are available. One such investigation was conducted at the University of Illinois by L. R. Hall and J. E. Stallmeyer (3) in which several parameters were varied in order to study their effect on the fatigue behavior of scale model girders. Flange rigidity, transverse stiffener rigidity, and type of loading were the principal parameters considered. From the investigation, it was concluded that the rigidity of boundary members had a significant effect on the fatigue behavior of thin web girders. Failures were caused by two effects, namely the fluctuating membrane stresses and the web flexing action at the panel boundaries.

1.2 General Discussion

For the purpose of this report, a thin web girder is defined as any plate girder in which the web depth-to-thickness ratio is sufficiently large so that buckling of any of the individual web panels of the girder occurs before the allowable working load of the girder is attained.

Buckling of individual panels is generally not experienced because an initially plane panel is seldom obtained. Instead, initial web deflections occur as a result of fabrication and when the girder is subjected to load these initial web distortions increase gradually. Thin web girders are being considered for inclusion in the AASHO specification and a knowledge is needed of the influence of initial web deflections, and also of the deflections due to loading, on the fatigue behavior of the plate girder. As the web deflects laterally, membrane stresses are increased and bending stresses increase in relation to the curvature of the web along the boundary. For an understanding of the fatigue behavior of thin web girders the interrelationship of the membrane stresses, web bending stresses, and residual stresses along the boundary of a panel is required.

1.3 Object and Scope

The objectives of the research program described herein were to determine the influence of initial web distortion on the fatigue behavior of thin web girders and to determine the distribution of stresses along the panel boundaries. Longitudinally stiffened plate girders were also studied in order to determine their fatigue behavior in relation to girders without longitudinal stiffeners.

Many factors affect the fatigue strength of plate girders. It would be impossible to study the effect of all of these parameters in a program of limited scope. Therefore, the investigation reported herein is limited to the consideration of flange rigidity, and type of loading in addition to the initial web deflections and the inclusion of longitudinal stiffeners.

Full size girder tests are very costly and time consuming, therefore, it was decided to use scale model girders in order to obtain the desired information. A scaling method developed earlier was used to proportion the scale model girders.

Ten fatigue tests were performed on three different types of girders. Four of these tests were conducted on girders with longitudinal stiffeners. Two of the girders without longitudinal stiffeners were subjected to a high shearing force and a very small bending moment, while the remainder of the girders were subjected to combined shearing forces and bending moments. Nine static tests were performed on the scale model girders in order to study the distribution of stress around the boundary of the web. The static tests were performed on the girders used in the fatigue tests. The results of these tests have been analyzed and the fatigue behavior of the girders were compared to twenty additional tests in which the variables were identical to those considered in the investigation reported herein, except for the magnitude of the initial web deflections and the presence of longitudinal stiffeners.

1.4 Notation

A_{ls}	Area of longitudinal stiffener.
a	Transverse stiffener spacing.
b	Clear depth of web between flanges.
D	Flexural rigidity of unit width of plate, $Et^3/12(1-\mu^2)$.
d	Clear depth of web between flanges.
E	Young's modulus of elasticity.
I	Moment of inertia of flange about its own horizontal centroidal axis.

I_s	Moment of inertia of stiffener about an axis in the plane of the web.
k	Factor used to obtain the design rigidity of a longitudinal stiffener.
t	Thickness of plate.
W	Load applied to girder.
W_{cr}	Theoretical critical buckling load of an ideal web panel with simply supported rigid boundaries.
W_{mf}	Maximum fatigue loading.
w	Lateral web deflection.
w_c	Deflection at center of panel.
$w_{l.s.\ max.}$	Maximum lateral deflection of longitudinal stiffeners.
$w_{max.}$	Maximum lateral web deflection.
EI_s/Da	Transverse stiffener rigidity parameter.
α	d/a, the aspect ratio of a panel.
β	d/t, web depth to web thickness ratio.
γ	EI_s/Dd, longitudinal stiffener rigidity.
γ^*	Optimum rigidity of longitudinal stiffener.
δ	Area of longitudinal stiffener, As, divided by the depth, d, and the thickness, t, of the web plate.
μ	Poisson's ratio.
σ	Normal stress.
τ	Shearing stress.

2. REVIEW OF LITERATURE

2.1 Strength of Plate Girders

As outlined in the preceding chapter, the criteria of limiting the strength of a girder to the buckling of an individual web panel was found to be inadequate in predicting the ultimate capacity of plate girders used in civil engineering applications. The capacity of girders which are subjected to bending depends on the strength of the compression flange acting with a portion of the web as a column (4). The flange column may fail either by buckling or yielding. In thin web girders subjected to shear the web lateral deflections increase gradually as the load is increased. Tension field action results from the stress redistribution in the web, and the ultimate capacity is obtained when the beam action shear stresses and the tension field normal stress fulfill the yield condition (5). The effect of interaction between bending and shear is not pronounced. The influence of bending moments on the ultimate capacity should be very small for the girders reported herein according to Reference 6.

Most of the analytical and experimental research on plate girders has centered on determining the buckling strength of individual panels, whether the girders are transversely stiffened or both transversely and longitudinally stiffened. Perhaps the most comprehensive investigation of this type is represented by the work of Kloppel and Scheer (7). A computer was utilized in the determination of buckling coefficients for various types of stiffened rectangular plates. The results are presented in

graphical form for plates with stiffeners in one direction, stiffeners in two directions, and multiple stiffeners. Extensive experimental investigations have been conducted by Ch. Massonnet and K. C. Rockey involving the use of longitudinal stiffeners to improve the static behavior of thin web girders. Massonnet (8) concluded from his tests that his theoretical optimum longitudinal stiffener rigidity was inadequate for the design of stiffeners which would isolate the webs of girders into subpanels. For design purposes Massonnet (10) recommended a stiffener rigidity seven times that of the optimum rigidity for a longitudinal stiffener placed at the fifth point nearest the compression flange. A lower multiplication factor is suggested for stiffeners placed nearer the neutral axis of the girder. K. C. Rockey (11) has conducted an experimental investigation involving bolted aluminum girders and has suggested design rules for the spacing and proportioning of longitudinal stiffeners identical to the design recommendations of Massonnet.

Bending tests on longitudinally stiffened plate girders conducted at Lehigh University (12) indicate that the bending strength of plate girders may be increased by the use of a properly proportioned stiffener located at the upper fifth point of the web. In several tests longitudinal stiffeners were provided which exceeded the minimum requirements of several specifications including the British, German, and AASHO specifications and no increase in bending strength was experienced in any of the girders. The investigators concluded that the use of larger stiffeners would result in an increase in static strength. The stiffener rigidities provided in the Lehigh tests were not as large as those proposed by Massonnet for design. Although the bending strength was not increased by the use of longitudinal stiffeners, the stress redistribution was

effectively controlled in the web. After the web buckles in thin web girders, the web cannot resist its share of the compressive stress and a redistribution of compressive stress occurs. The force no longer resisted by the web is transferred to the compression flange. If a longitudinal stiffener is located in the compressive zone of the web, it limits the lateral deflection of the web and inhibits the redistribution of compressive stress.

The shear strength of girders may be increased by the use of longitudinal stiffeners. Two subpanels are created in which separate diagonal tension fields are formed. The Lehigh tests (12) indicate that the increase in strength is dependent on the aspect ratio of the panel, web slenderness ratio and stiffener position.

2.2 Deflections of Thin Web Girders

Initial lateral web deflections are expected to have an influence on the fatigue behavior of thin web girders. Both the magnitude and the distribution of the initial web deflections will influence the fatigue behavior. The distribution of web deflections due to the distortion of the web will be referred to hereafter as the web deflection pattern, distribution, or configuration. Fabrication procedures, the size of individual component parts of the girder, and the geometrical arrangement of the parts will all influence the initial deflections. Residual stresses which result from the welding process cause the distortion of the web. Different shapes and magnitudes of the deflection pattern are due to different welding procedures.

Initial deflections equal to the web thickness are prevalent in test girders and the use of the linear theory of plates is inapplicable in

the analysis of the web. Table 1 lists the order of magnitude of the initial web deflection of selected panels of girders tested at Lehigh University (13) with a girder depth of fifty inches, which corresponds to a full sized small plate girder. Comparison of the values in this table shows the influence of the aspect ratio and web slenderness ratio on initial deflections. Generally the initial deflections are smaller with girders having smaller web slenderness ratios and lower aspect ratios.

Many theoretical investigations have been reported pertaining to the behavior of plates with small initial deflections in the order of 0.1 to 0.25 times the thickness of the web. The analysis has been limited to either simply supported or clamped boundaries and to simple loading conditions such as uniform compression on two opposite edges or a uniform shear on all edges. In welded plate girders the edges of the web are neither simply supported nor fully clamped, but are between these two extremes. Bergman (14) made an analytical study of square plates subjected to shear along the boundaries and included maximum initial deflections of 0.05t, 0.5t, 1.0t, 2.0t, and 3.0t where t is the thickness of the plate. The initial deflections of the plate were represented by the function

$$w(x,y) = f_o \sin \frac{\pi x}{a} \sin \frac{\pi y}{a} \qquad (2.2.1)$$

with the origin of the coordinate system taken at one corner of the plate. The additional deflection due to load was taken as a Fourier series in three terms,

$$w(x,y) = f_1 \sin \frac{\pi x}{a} \sin \frac{\pi y}{a} + f_2 \sin \frac{2\pi x}{a} \sin \frac{2\pi y}{b} + f_3 \sin \frac{3\pi x}{a} \sin \frac{3\pi y}{a} \qquad (2.2.2)$$

where f_1, f_2, and f_3 are parameters. The symbol a is used to denote the length of a side of a square plate. The increase in deflection due to increase in load is shown in Fig. 1 for a square plate subjected to shear. Theoretically a plate which has very small initial deflections will exhibit a rapid growth of deflections at a load near that of the buckling load for an initially plane plate. At loads much smaller or larger than the buckling value, the plate with smaller initial deflections behaves much like an originally plane plate. However, this is not the case for plates with initial deflections which are two or three times the thickness of the plate.

It is generally known that the plate has considerable post buckling strength in contrast to the behavior of compression members such as columns or truss members. When a plate buckles, there are certain stresses which are created due to the fact that the edges of the plate do not deform freely. Tensile membrane stresses are present which tend to restrict the increase in plate deflection. The tensile membrane stresses are anchored in the flanges and in the adjacent panels of the plate girder. The ability of the flanges to resist the membrane stresses depends on the rigidity of the flanges. The flange rigidity parameter, I/a^3t, was used by Hall and Stallmeyer (3) in an investigation of its effect on web deflections, and ultimately on the fatigue behavior of a plate girder. Rockey (11) has proposed a minimum value of the flange rigidity parameter which should be used in the design of thin web girders. The depth of the buckles is dependent upon both the load and the flange rigidity parameter I/a^3t as shown in Fig. 2. The circle on each curve represents the minimum value of flange rigidity at which the value of w_{max}/t is almost constant.

The circles correspond closely to the values obtained by the use of the recommended empirical formula for the minimum flange rigidity

$$\frac{I}{a^3 t} \geq 0.00035 \left(\frac{W}{Wcr} - 1\right) \qquad (2.2.3)$$

where I = moment of inertia of flange about it horizontal centroidal axis

a = stiffener spacing, center to center

t = thickness of web

W = actual load on web panel

Wcr = theoretical buckling load of web panel

In addition to the membrane stresses, plate bending stresses are created at the edges of the panel because the boundaries of a panel of a welded plate girder are not simply supported. The magnitude of these plate bending stresses depend mainly on two factors, namely the magnitude of the deflection and the rotational restraint of the boundaries. As the plate deflection increases, the membrane and the plate bending stresses increase also. The membrane stresses have a stabilizing effect on the plate. Therefore, a plate with larger initial deflections whould deflect less for a given increment of load than a plate with smaller initial deflections. This conclusion is borne out in Fig. 1 where a comparison of the average slopes of the curves shows a larger increase in deflection per unit load for plates with smaller deflections. At higher loads, all of the curves parallel each other so that this effect is no longer observed. From these observations it is apparent that web panels with smaller initial deflections should have a larger range of deflections than those girders with larger initial deflections.

With regard to the fatigue behavior of thin web girders, both of the two previously mentioned stresses are important. If a girder is

fabricated with panels having large initial deflections, then the plate bending or web flexing stresses due to the cyclic loading are reduced. If, on the other hand, the initial web deflections are small, then the web flexing stresses subsequent to loading should be larger. Thus the most undesirable stress condition occurs when the addition of the two types of stress is at a maximum value. Residual stresses are a third type of stress which, when combined with the membrane stresses and the web flexing stresses, may create the most undesirable stress condition at some point along the boundary of the web panel. No quantitative reports on the distribution of residual stresses in thin web girders are presently available.

Hall and Stallmeyer (3) reported that the shape of the initial deflection pattern may influence the fatigue behavior of thin web girders. Initial web deflections were rather large in several of the test girders, and the deflection configuration due to load did not conform to the theoretical shape. The initial shape was only modified by the addition of load. As a result the distribution and intensity of the membrane stresses and web flexing stresses along the boundary of the panel may also be modified. Therefore because web flexing and membrane stresses are expected to affect the fatigue behavior of thin web girders, the shape of the initial deflection pattern may influence the fatigue behavior of thin web girders.

In the preliminary tests conducted at Lehigh University (12) on girders with longitudinal stiffeners, one of the conclusions of the investigation was that the use of a longitudinal stiffener minimized the lateral deflections of the web when the girder was subjected to load. The maximum web deflection at working load, the maximum web deflection at zero load, and the percent increase of the web deflection between zero and the working load is given in Table 2 for the girders tested at Lehigh. The first

specimen in the table had no longitudinal stiffener. It has been pointed out previously that the deflections of the web influence both the membrane and the web flexing stresses, and that these stresses are related to the fatigue behavior of thin web girders. Therefore, the inclusion of longitudinal stiffeners should influence the fatigue behavior of thin web girders.

2.3 Longitudinal Stiffeners

In girders subjected to bending there is a redistribution of stress when the web panel buckles. Since the initial deflections lead to a gradual increase in the web deflections, this transfer of compressive stress in the web to the compression flange begins with the initiation of loading. No such redistribution occurs near the tension flange because the stresses due to beam action of the girder are tensile and tend to decrease the size of the buckle. Addition of a longitudinal stiffener in the compression zone of the web restricts the development of increased lateral deflections and therefore limits, to some extent, the redistribution of compressive stress.

The longitudinal stiffener forms, ideally, a nodal line in the web. In order to accomplish this the stiffener must have a rigidity large enough to resist buckling with the web. Ch. Massonnet (9) has derived requirements for the optimum rigidity of stiffeners. The optimum rigidity is defined by Massonnet as the smallest stiffener which will theoretically remain straight at any value of the applied load. Any larger stiffener would only contain material which was not required for the stiffening purpose of the component, and a smaller stiffener would allow the web to deflect due to the applied loads. Therefore, the "optimum" rigidity is

the boundary between these two types of behavior. For a longitudinal stiffener at the upper fifth point of the web, the fifth point nearest the compression flange, the optimum rigidity is given in Eq. 2.3.1 for the case of pure bending:

$$\gamma^* = 3.87 + 5.1\,\alpha + (8.82 + 77.6\,\delta)\,\alpha^2 \qquad (2.3.1)$$

valid over the range $0.5 \leq \alpha \leq 1.5$,

where γ^* = optimum rigidity = $\frac{EI_s}{Dd}$

E = Young's modulus of elasticity

I_s = moment of inertia of the longitudinal stiffener about a vertical axis through the central plane of the web

D = flexural rigidity of a unit width of web plate, $Et^3/12\,(1 - \mu^2)$

d = clear depth of web between flanges

t = web thickness

μ = Poisson's ratio

α = aspect ratio, a/d

a = stiffener spacing

δ = area of longitudinal stiffener, A_{ls}, divided by the depth, d, and thickness, t, of the web plate.

For girder panels subjected to pure shear, a condition which is most unlikely in a beam type structure, the most efficient location of the longitudinal stiffener is at the mid-depth of the web. The optimum rigidity for the longitudinal stiffener is given in Eq. 2.3.2 for a panel subjected to pure shear.

$$\gamma^* = 5.4\,\alpha^2\,(2\alpha + 2.5\,\alpha^2 - \alpha^3 - 1) \qquad (2.3.2)$$

Equation 2.3.2 is valid over the range $0.5 \leq \alpha \leq 2.0$ and γ^* and α are as defined earlier.

For panels subjected to combined shear and bending no specific value is given for the stiffener rigidity. Massonnet recommends that the calculation of the stiffener size be made for both pure shear and pure bending, and the larger of the two stiffeners is the recommended choice. All of the values for the optimum stiffener rigidity are based on the assumption that the web is initially plane. For practical design purposes Massonnet (10) recommends the use of a factor, k, to determine the design rigidity of the longitudinal stiffeners. The values of k were based on tests to collapse of girders and represent a mean value for each location of the stiffener. The influence on the value of k of other parameters such as the aspect ratio, α; web slenderness, β; and stress ratio τ/σ were found to be minimal. The values of k are as follows:

Distance Between Horizontal Stiffener and Compressed Flange	Value of k
b/2	3
b/3	4
b/4	6
b/5	7

In contrast to the recommendations of Massonnet, the German specification (15) specifies the optimum stiffener rigidity for the design of longitudinal stiffeners. Charts were developed by Massonnet (16) for the determination of the factor of safety with regard to buckling of the web when the German specifications are utilized. In the United States, the AASHO specifications (17) allow the design of a girder with a

longitudinal stiffener 0.2d from the compression flange having the following minimum moment of inertia

$$I_s \geq t^3 d \left[2.4 \left(\frac{b}{d}\right)^2 - 0.13 \right] \qquad (2.3.3)$$

where I_s = moment of inertia of longitudinal stiffener about a vertical axis through the central plane of the web

d = clear depth of web between flanges

t = thickness of web

b = clear distance between transverse stiffeners

The moment of inertia of a one sided stiffener is computed with respect to an axis through the stiffener web interface. It may be shown that the area required for a single sided stiffener is 63% of that required for double sided stiffeners if the only consideration is the moment of inertia furnished. Reference to Fig. 3 will show that for stiffeners of the same thickness, t, the moment of inertia of a single sided stiffener is $I_1 = b^3 t/3$ and that of double sided stiffeners is $I_2 = 2(b')^3 t/3$ if the thickness of the web is neglected. For the provision of equal moments of inertia, b must equal 1.26 b'. The resulting areas of the stiffeners are bt = 1.26 b't and 2b't, indicating that indeed the area of the single sided stiffener is 63% of the area of the double sided stiffener. Therefore, from the previous calculation it would seem to be more economical to employ single sided stiffeners. However, if the function of the stiffener is reconsidered, it is desired that the stiffener provide a straight rigid boundary for the web panel. The use of a single sided stiffener creates an eccentricity between the force carried by the stiffener and the centroid of the stiffener area. Rockey (11) has shown that double sided stiffeners have a much smaller lateral deflection than single sided stiffeners.

The relationship between the maximum lateral deflection of the longitudinal stiffener and the stiffener rigidity is shown in Fig. 4. The maximum lateral deflections of the stiffeners were obtained at a load equivalent to 1.12 times the critical buckling load for the web panels. If double sided longitudinal stiffeners are to be used and the maximum proposed design load is not greater than 1.5 times the buckling load, Rockey suggests that stiffeners having an inertia double the theoretical optimum values will operate quite effectively.

When the German, British and AASHO specifications are compared, as in Fig. 5, it is apparent that the AASHO specification is the least conservative. In view of the reported test results by Rockey and Massonnet, the stiffeners proportioned by the use of the ASSHO specification are not capable of performing their stiffening function. The points in Fig. 5 labeled 1, 2, and 5 represent three of the tests performed at Lehigh University (12). No increase in ultimate capacity was obtained from the use of longitudinal stiffeners. Only the control of stress redistribution in the web and the minimizing of the lateral web deflections was achieved. The triangular points labeled HSB and HVSB represent the stiffener rigidities used in the investigation reported herein.

Since longitudinal stiffeners influence both the magnitude of the lateral deflection of the web and the distribution of stresses along the web panel boundary, it is expected that the addition of longitudinal stiffeners will have an influence on the fatigue of thin web girders.

2.4 Fatigue Behavior of Thin Web Girders

2.4.1 General Discussion

In previous sections it has been pointed out that many factors influence the fatigue behavior of thin web girders. The magnitude and distribution of the initial web deflections, flange rigidity, web slenderness, transverse stiffener rigidity, longitudinal stiffener rigidity, type of loading and the range of loading have all been mentioned. Several of these parameters will be discussed in more detail in the following sections with particular reference to the series of plate girder tests carried out at the University of Illinois by Hall and Stallmeyer (3).

2.4.2 Influence of Flange Rigidity

The effect of flange rigidity has already been discussed with reference to initial web deflections. If the flange rigidity is maintained above a certain minimum value, lateral deflections of the web can be controlled. Lateral deflections of the web cause both web flexing stresses and membrane stresses. These stresses are expected to be related to the fatigue strength of thin web girders. Therefore as the flange rigidity affects the lateral web deflections, it affects the fatigue behavior of thin web girders.

The analyses of Wagner (1) and Kuhn (2) considered flange rigidity and expressions were developed for the calculation of the secondary bending moments in the flange. As the tension field develops, it creates tensile membrane stresses which are anchored at the boundaries of the panel, in particular the flanges on two edges of the panel. The transverse stiffeners act as supports and the flange was assumed to act like a continuous beam subjected to a distributed load. The foregoing results

were obtained by investigators working in the aircraft industry. Secondary flange bending moment were not expected to be significant in civil engineering structures according to Kuhn (2) and Legett and Hopkins (18). Rockey (19) and Hall and Stallmeyer (3) found that large secondary flange bending moments did indeed exist in civil engineering girders. The most significant research on the flange rigidity of girders for civil engineering applications were performed by Rockey (11, 19). Figure 2 indicates that the maximum web deflection depends on two factors, the load ratio and the flange rigidity. On the basis of the tests represented in Fig. 2, Rockey recommended the minimum flange rigidity given in Eq. 2.2.3.

Hall and Stallmeyer (3) investigated the influence of flange rigidity on the fatigue behavior of thin web girders and concluded that the rigidity of boundary members (flanges and stiffeners) of the individual web panels had a significant effect on the fatigue behavior. Rockey's minimum flange rigidity (Eq. 2.2.3) was recommended for the design of plate girders which are to be subjected to fatigue type loadings.

2.4.3 Influence of Transverse Stiffener Rigidity

The statement was made in the previous section that the fatigue behavior of a thin web girder was affected by the rigidity of the boundary members of the individual web panels. Two of the boundary members are the transverse stiffeners. The static behavior of girders depends on the size and spacing of the transverse stiffeners. Most theoretical investigations reported in the literature have dealt with the calculation of buckling coefficients for ideal plate-stiffener combinations. Two types of plate-stiffener combinations have been reported with regularity. One type consisted of weak stiffeners closely spaced and the problem reduced to the

study of the buckling of an orthogonal plate. The other type of plate-stiffener combination is more closely related to the webs of civil engineering girders. In such girders, the stiffeners are usually relatively rigid and normally not closely spaced. Based on tests performed on aluminum alloy girders an empirical design formula was determined by Moore (20) and was used as the basis for the proposed transverse stiffener rigidity requirements in the British specification, B.S. 153(21). Rockey (22) carried out extensive tests on girders employing both single sided and double sided stiffeners. Very definite stability limits were obtained and design formulae were presented for single sided stiffeners and double sided stiffeners. For aspect ratios between 0.55 and 1.4, the formula proposed by Moore represents a value of transverse stiffener rigidity between the two values given by Rockey. Rockey's formulae and Moore's empirical equation are shown in graphical form in Fig. 6. The main purpose of the investigations was to determine the properties of a transverse stiffener which would effectively isolate each individual web panel. In actual practice a perfectly plane web or initially straight stiffener is rarely encountered. With the application of load and particularly after the web panel has distorted extensively, it is highly unlikely that the transverse stiffener will remain straight even though the stiffener may function as desired by carrying the vertical component of the tension field force.

With regard to fatigue behavior of thin web girders two types of stresses have been mentioned, namely, the web flexing stress and the membrane stress. The web flexing stress is influenced by the relative deflection and rotation of the stiffener at the web. If the diagonal tension membrane stresses are not anchored to the transverse stiffener, they are transferred to the adjacent web panels. The only fatigue tests on thin web girders

in which the effect of transverse stiffeners was investigated were reported by Hall and Stallmeyer (3). Five girders were tested representing a large range in transverse stiffener rigidity. Very short fatigue lives were encountered with girders having intermediate sized stiffeners, approximately the size recommended by present U.S. specifications.(17, 23). The use of transverse stiffeners with a larger rigidity increased the fatigue lives of the thin web girders.

It is expected that the rigidity of the transverse stiffeners will have an effect on both membrane stresses and web flexing stresses, and therefore, ultimately affect the fatigue behavior of thin web girders.

2.5 Scaling Parameters

A welded plate girder is composed of three basic components, namely, the flanges, web and stiffeners. The web is designed primarily to resist the shear, and the flanges are designed primarily to resist the applied moment. The stiffeners serve to divide the web into panels bounded on two sides by the flanges and on the other two sides by the stiffeners. In order to test model girders it was desired to relate the behavior of the model to the prototype by means of non-dimensional parameters. The behavior of the panels depends on the relative rigidities of the components, and these rigidities are expresses in terms of the geometrical properties of the individual components. Hall and Stallmeyer (3) have shown that there are four dimensionless parameters which may be used to describe the relative rigidities of the girder components. The parameter,

$$\frac{I}{a^3 t} \qquad (2.5.1)$$

where I = moment of inertia of flange about its horizontal centroidal axis, ins.^{4}

a = stiffener spacing, in.

t = thickness of web, in.

was used by several investigators to describe the magnitude of flange rigidity. The effect of stiffeners on the behavior of girders can be related to the ratio of the rigidity of the transverse stiffeners to the flexural rigidity of the web panel. This ratio is described by the parameter

$$\frac{EI_s}{Da} \qquad (2.5.2)$$

where E = Young's modulus of elasticity

I_s = Moment of inertia of the transverse stiffener or stiffeners about a horizontal axis through the central plane of the web

D = Flexural rigidity of a unit width of web plate, $Et^3/12\ (1 - \mu^2)$

a = Stiffener spacing

The remaining two parameters which describe the web are the aspect ratio, α, and the web slenderness ratio, β, where

$\alpha = a/d$

$\beta = d/t$, the ratio of web depth to web thickness

In addition to the four parameters used by Hall and Stallmeyer, another parameter is required to describe the relative rigidity of longitudinal stiffeners. Actually the parameter is identical to that used for transverse stiffeners, except that the web distance perpendicular to the stiffener is now the depth, d, which replaces the stiffener spacing a in Eq. 2.5.2. The resulting parameter is as shown below

$$\frac{EI_s}{Dd} \qquad (2.5.3)$$

where E, D, d are defined above and

I_s = Moment of inertia of the longitudinal stiffener about a vertical axis through the central plane of the web.

3. TEST SPECIMENS

3.1 General Discussion

Fatigue tests on thin web girders performed at the University of Illinois were reported by L. R. Hall & J. E. Stallmeyer (3). Variables in that study included the flange rigidity, type of loading, and transverse stiffener rigidity. In those early tests the initial web distortions resulting from fabrication of the specimens were large. Subsequent to those tests, the development of an improved welding technique enabled specimens to be fabricated with smaller initial web deflections. One of the objectives of this investigation was to determine the influence of these initial web deflections on the fatigue behavior of the girders. Test specimens and configurations were chosen to duplicate specific tests in the previous investigation.

Of related interest was the investigation of the effectiveness of longitudinal stiffeners in reducing the initial web deflections and the web deflections under load. The subsequent fatigue behavior of a thin web girder with such web deflection reductions was to be examined. For this purpose additional specimens were designed to be equivalent to specimens previously used in the investigation of initial web deflections, except that a longitudinal stiffener was included. The specimens of the present investigation are discussed in detail in the following sections.

3.2 Girders with Various Flange Rigidities Subjected to Shear

The fatigue performance of a thin web girder panel subjected to a high shear was studied in the earlier tests. Eight specimens with

varying flange rigidities were tested. An increase in fatigue life was observed when the flange rigidity was increased. All other variables, except initial web distortion and flange rigidity, were identical for all eight tests. Duplicate specimens of the earlier girders which had the smallest flange rigidity and the largest flange rigidity were fabricated. The objective in duplicating the extreme cases of the earlier investigation was to determine if the flange rigidity would be a significant parameter in determining the fatigue life of the girder when coupled with decreased initial deflections. Each specimen had a central test panel with a web slenderness ratio, d/t, of 267 and an aspect ratio of 0.75. Web material with a thickness of 0.075 in. was used and the depth and width of the test panel were 20 in. and 15 in., respectively. An aspect ratio of 0.3 was used for the panels on either side of the central test panel in order to make them stronger than the test panel. Figure 7 depicts the test panel and its position within the test specimen and the girder as a whole. Double sided stiffeners were used and were cut from 2 in. by 1/8 in. bar stock. A 5 in. flange width was used for both specimens. The two flange thicknesses were 1/4 in. and 1 in. resulting in flange rigidity parameter values $1/a^3$ t, of 0.0000258 and 0.00159.

3.3 Girders with Various Flange Rigidities Subjected to Shear and Bending

Exact duplicates of the earlier test panels with various flange rigidities subjected to shear and bending could not be fabricated because of a difference in the thickness of available web material. It was desired to keep the web slenderness ratio, d/t; aspect ratio; bending stresses; shearing stresses; and the flange rigidity parameter, I/a^3t, equal to the values used in the prior tests. As in the earlier tests, a

web slenderness ratio of 267 and an aspect ratio of 0.75 were used. The nominal flexural stress in both specimens was equal to that used in the earlier tests. No fatigue life was reported for the girder with the smallest flange rigidity in the earlier tests; therefore, the girder with flanges which were next higher in stiffness was chosen for duplication. Again, in order to determine the effect of flange rigidity on the fatigue life of a thin web girder, the test girder with the largest flange rigidity was chosen to be duplicated. This selection permitted the further investigation of the hypothesis that increased flange rigidity leads to improve fatigue behavior.

For both specimens the web thickness was 0.0747 in. and the depth and width of each of the two test panels were 20 in. and 15 in., respectively. Double sided stiffeners were chosen to comply with the AISC building specification requirements for thin web girders. The flexural stress was identical for both specimens and the shear stress was constant in the test panels. Location of the test panels and the loading arrangement is shown in Fig. 8. Sizes of the flanges for the two specimens were 4 in. by 3/8 in. and 1 1/2 in. by 1 in. providing flange rigidity parameter values of 0.0000753 and 0.000494, respectively.

3.4 Girders with Various Transverse Stiffener Sizes Subjected to Shear Bending

In the earlier tests it was discovered that the girder with the smallest transverse stiffeners sustained a very long fatigue life compared to three other girders with larger transverse stiffeners. Only the specimen with the stiffest stiffeners achieved a longer fatigue life. The very flexible stiffeners did not restrain the web, but deflected and rotated

with the web. Due to this phenomenon only a small amount of curvature of the web was present at the junction of the web and the transverse stiffener. As a result, only small secondary bending stresses were present at these panel boundaries. All of the stiffeners in the remainder of the tests offered some measure of fixity at the boundary of the web panels. Since the very flexible stiffener does not perform its intended function and would not be considered a practical design, it was decided to duplicate two of the tests in which the stiffeners provided a semblance of restraint to the web. The girder with the largest transverse stiffeners was duplicated and one specimen was provided with stiffeners with a rigidity between the smallest and second smallest used in the earlier phase of the program.

In the original tests a web material having a thickness of 0.0625 in. was used. An aspect ratio of 0.5 and a web slenderness ratio, d/t, of 320 were maintained in the earlier tests. Web material with a thickness of 0.0598 in. was used in the two duplicate specimens. A web slenderness ratio, d/t, of 312 and an aspect ratio of 0.50 were utilized. Three test panels were included in the specimen which was subjected to a constant shear force and an increasing bending moment from one edge of the test panels to the other (See Fig. 9). Dimensions of each of the three panels were a depth of 18.6 in. and a width of 9.3 in.

In the previous tests the flanges were tapered linearly in order to maintain a constant flexural stress to shear stress ratio of 1.52. For the specimens in this investigation flange width was maintained at a constant value and, as a result, the flexural stress to shear stress ratio varied from 0.86 to 1.52 over the length of the test panel. From static tests on shear panels K. C. Rockey (11) proposed a minimum value of the

flange rigidity parameter, I/a^3t. The flanges in the present program were proportioned so that Rockey's minimum value of the flange rigidity parameter was exceeded in both the previous tests and those reported herein. The resulting flange width and thickness were 4 1/2 in. and 1/2 in., respectively.

One-eighth inch by one-half inch double sided stiffeners were provided for one test specimen to render a minimum value of 57 for the stiffener rigidity. A stiffener rigidity of 3640 was obtained by the use of 1/8 in. by 2 in. double sided stiffeners on the second specimen. All transverse stiffeners were cut from bar stock. Sizes of the stiffeners used on the earlier tests are given in Table 6.

3.5 Longitudinally Stiffened Girders with Various Flange Rigidities Subjected to Shear and Bending

It was desired to determine the effects of the presence of a longitudinal stiffener on the fatigue behavior of thin web girders. To this end, it was decided to test girders similar to the girders described in the two previous sections. Satisfactory fatigue lives obtained in the tests on girders with various flange rigidities subjected to shear reduced the need for seeking improved fatigue lives. Variables being held constant in relation to the specimens described in Section 3.3 were the web slenderness ratio, d/t of 267; the aspect ratio of 0.75; and the web thickness, 0.0747 in. In addition, shear stresses were identical to the specimens described in Section 3.3. Each of the two test panels were 20 in. deep and 15 in. wide (See Fig. 10).

An analytical investigation by Ch. Massonnet (9, 10) led to the determination of an optimum longitudinal stiffener rigidity and also to design recommendations for longitudinal stiffeners. Present AASHO (17)

specification requirements allow a stiffener which is smaller than the optimum stiffener defined by Massonnet. The optimum stiffener rigidity referred to above was used as the basis for the design of the longitudinal stiffeners.

As a result, the longitudinal stiffeners were conservative with respect to the AASHO specification requirements. For both specimens the width and thickness of the longitudinal stiffener were 1 5/8 in. and 1/8 in., respectively. The longitudinal stiffener was extended three inches beyond each end of the test section and terminated at transverse stiffeners included for this purpose. The longitudinal stiffener was located at the upper fifth point of the girder cross section.

For the specimen with the smallest flange rigidity, the flanges were identical to the earlier test of this investigation. The flange size was 3/8 in. by 4 in. and the flexural stresses were identical to the nominal values for the earlier test. An unrealistic transverse stiffener size resulted when a one sided stiffener was proportioned to fit in the 3/4 in. half width of the flange of the girder with the largest flange rigidity. As a compromise, a flange width and thickness of 2 1/2 in. and 3/4 in., respectively, was used. The resulting maximum flexural stress in the test section was 11.6 ksi as opposed to the nominal value of 14 ksi in the other specimens. Both girders utilized transverse stiffeners which were 1/4 in. thick and 1 1/4 in. wide which satisfied the requirements of the AISC building specification.

3.6 Longitudinally Stiffened Girders with Various Transverse Stiffener Rigidities Subjected to Shear and Bending

As outlined in the preceding section a specimen fabricated with a longitudinal stiffener was desired in order to study its fatigue behavior. Variables held constant for the girders with various transverse stiffener sizes subjected to shear and bending were the web slenderness ratio, 312; aspect ratio, 0.5; flange rigidity; shear stress and flexural stress. Three panels were included in the test section and the dimensions of each panel were 18.6 in. deep, 9.3 in. wide, and 0.0598 in. thick. The flanges were 4 1/2 in. wide and 1/2 in. thick. Single sided transverse stiffeners were chosen to be 2.4 times the area of one of the double sided stiffeners discussed in Section 3.4. A minimum transverse stiffener rigidity of 445 was obtained by the use of 1/8 in. by 1 1/4 in. stiffeners. 7,130 was the maximum transverse stiffener rigidity and was obtained by using 1/4 in. by 2 1/2 in. stiffeners. Again, the longitudinal stiffener was proportioned to satisfy Massonnet's criteria for an optimum stiffener. The longitudinal stiffener was 1/16 in. thick and 9/16 in. wide. The longitudinal stiffener was located at the upper fifth point of the cross section of the girder and was extended three inches beyond the outer transverse stiffeners. Two additional transverse stiffeners were provided for connection to the ends of the longitudinal stiffener (See Fig. 11).

The shear force was constant through the test section and the bending moment increased linearly from one edge of the test zone to the other edge. The flexural stress to shear stress ratio varied from 0.86 to 1.52 through the test section.

4. MATERIALS AND FABRICATION OF SPECIMENS

4.1 Materials

Four different types of materials were used in the fabrication of the test girders. All of the webs for the girders with various flange rigidities were sheared from 6 by 10 ft. plates of 0.0747 inch thick A415-58T rolled carbon sheet steel. The webs for the girders with various transverse stiffener rigidities were sheared from 5 by 10 ft plates of 0.0598 inch thick A441-64T rolled steel sheets. All flanges were flame cut. Flanges for the girders subjected to shear were taken from 6 by 12 ft plates of A441-64T steel plates. The flanges were cut from 6 by 12 ft plates of A7 steel for the girders with various flange rigidities subjected to shear and bending. Flanges of the girders with various stiffener rigidities were obtained from 6 by 12 ft plates of A441-64T steel.

The longitudinally stiffened girders with various flange rigidities were fabricated with webs of A415-58T rolled carbon sheet steel. The webs were sheared from 6 by 10 ft plates of A415-58T having a thickness 0.0747 inches. Flanges for the girder with a longitudinal stiffener and having the smallest flange rigidity were cut from a 6 by 12 ft plate of A441-64T steel. A373 steel was used for the flanges for the girder with the stiffest flanges. The webs of the girders with longitudinal stiffeners and various transverse stiffener sizes were sheared from a 5 by 10 ft plate of 0.0598 inch thick A441-64T rolled steel sheet. The flanges for these girders were obtained from 6 by 12 ft plates of A441-64T steel plates. The physical properties and chemical composition of the web materials are given in Table 3.

4.2 Fabrication of Test Specimens

The test specimens were formed by bolting sturdy girder sections to each end of a short thin web test specimen (See Fig. 12). The test loads were applied to the end sections and were transmitted to the test section through the bolted connections. This method of fabrication eliminated the possibility of failures due to concentrated stresses at the load and reaction points and also eliminated the need for a complicated lateral support system.

In order to weld the specimen together the flanges and web were clamped in their proper relative positions in positioning stands. The positioning stands consisted of two one inch thick cold rolled plates five inches wide clamped between two rotating stands. The one inch plates served to form a solid base to which the specimens were clamped during welding and to help keep the web plane during welding. The stands allow the specimen to be rotated freely in order that all welding can be done in the downhand position. The girder components were then tack welded to hold them in place during the welding of the specimen.

Semi-automatic metallic-inert gas welding equipment and a 0.030 inch diameter electrode wire was used for all welding. The welding sequence for the specimens is shown in Fig. 13. Various sequences were used in order to obtain the least web distortion and the sequence shown is the result of these observations. Twelve inch passes were used in attaching the web to the flanges. The numbers in Fig. 13(a) refer to the order in which the flange to web fillet weld passes were made. Beginning at the center of the specimen, a twelve inch pass was made toward the end of the specimen. The specimen was then rotated and another fillet weld was made

on the other side of the web. The welding progressed from side to side of the web and from the top flange to the bottom flange as indicated by the numbers and arrows in Fig. 13(a). After the web had been welded to the flanges, the transverse stiffeners were tack welded to the web at the ends and at the quarter points of the stiffeners. The four center passes on all transverse stiffeners were made on both sides of the web in an attempt to minimize and distribute the heat input evenly in the web. Back stepping passes were used on the stiffeners as indicated in Fig. 13(b). After the center section of all the transverse stiffeners had been welded to the web, the remaining four passes were made on each transverse stiffener, taking each stiffener in the same order as before.

The girders with longitudinal stiffeners were provided with one sided transverse stiffeners and the transverse stiffeners were attached in the same manner as described above. After the transverse stiffeners had been attached, the longitudinal stiffener was tack welded into position. Six inch passes were used in attaching the longitudinal stiffener to the web (See Fig. 13(c)). Again short, distributed passes were used to minimize the web distortion resulting from welding. Holes were drilled in the ends of all of the specimens to receive the splice bolts.

5. TEST PROCEDURES

5.1 Measurement of Initial Web Deflections

It is inevitable that during the fabrication of a welded plate girder some distortion will occur. Initial buckles of the web are the most apparent features of this distortion due to welding. One of the main features of this investigation was to determine the effects of initial web deflections upon the behavior of thin web girders.

After the specimens had been bolted to the stronger end pieces and placed in the 250,000 lb. Wilson lever type fatigue machine, Fig. 14, the initial web deflection readings were taken. A jig was used in making the web measurements and it consisted of two vertical bars attached firmly to the flanges of the specimen. Attached to the two vertical bars was a horizontal bar with a key-way milled along the length of the bar. An Ames dial was mounted on the horizontal bar by means of a sliding collar and a key to limit the rotation of the collar around the bar. Measurements of the distance from the plane of the jig to the web were made by sliding the Ames dial horizontally along the web at two inch vertical intervals. Measurements were also taken near the stiffeners and the compression flange with the resulting distance between these measurements and the typical grid being less than two inches. The four corner measurements of the web panel were taken as reference values and an undistorted reference surface was generated by connecting the four corners with straight lines in proximity to the boundary of the panel. The remaining measurements were compared to the reference surface and initial web deflections were obtained. A simple computer program was used to do the computations described above.

5.2 Measurement of Web Deflections Due to Load

A cyclic loading was applied to the specimens after which the web deflection measurements were again taken at various values of loading. Normally measurements were made with no load and were then made at each load interval as the load was increased in four increments to the maximum fatigue loading. In several of the static tests web deflections were measured at loads larger than the maximum fatigue load. The measurements were made exactly as described in the previous section and the computer was utilized in the reduction of data as before.

5.3 Static Tests

5.3.1 Selection of Specimens

To determine the distribution of stresses around the boundary, static tests were performed on all of the specimens subjected to fatigue tests. Upon completion of the fatigue tests, to be described in a following section, no increase in deflection was experienced at the maximum fatigue test load. Similar tests at Lehigh (24) indicate that there is no loss in strength of the girder although extensive fatigue cracks have formed. In one test of the current investigation a girder was repaired by means of placing a new weld over the fatigue crack. The girder was then subjected to fatigue loading. The repair was still sound after an additional 500,000 cycles of loading were applied. Due to these factors it was decided that static tests could be satisfactorily performed on the same test specimens used in the fatigue tests.

Repairing the girders consisted of placing a new weld on both sides of the web at the location of the fatigue crack. The weld was extended approximately one-half to one inch beyond both ends of the crack.

5.3.2 Location and Type of Strain Gages

Preparation of the web for the application of strain gages was performed by removing all mill scale by the use of emery cloth and an abrasive cylinder in a hand drill. Lines were scribed on the web to serve as a guide in the installation of the gages. AR-1-S-6 rosettes and A-1 single element SR-4 strain gages were used in all cases. A typical gage layout is shown in Fig. 15. In most of the test panels rosettes were located at the positions indicated by the gages shown as solid lines. Dashed lines indicate the locations of gages which were included in approximately one-half of the test panels. Gages shown as dotted lines were used on only one or two test panels. A-1 single element SR-4 strain gages were also placed on the transverse and longitudinal stiffeners. Gages were placed on both sides of the transverse stiffeners at mid-height, the upper quarter point and near the top of the girder in most of the tests. Gages were located on both sides of the longitudinal stiffener at its intersection with each panel boundary and at the centers of the panels.

5.3.3 Loading

Nominal values of the stresses used in the earlier tests performed at the University of Illinois dictated the loads applied to the girders of the current investigation. All values of loads or stresses are given in terms of the maximum fatigue loading. Four equal load increments of one-fourth of the maximum fatigue loading were used in the static tests. Higher loads were obtained by the application of increments of 10% to 15% of the maximum fatigue load. A stress ratio of one-quarter was used for all fatigue tests.

A maximum nominal shear stress of 10.8 ksi was used for the test panel of the shear girders. This value of stress was chosen originally to equal the AISC building specification allowable shear stress. For the girders with various flange rigidities subjected to shear and bending, a nominal maximum shear stress of 10.9 ksi and a nominal bending stress which varied from 0 to 14 ksi through the test section were used. Anticipation of AASHO specification requirements and a factor of safety of 1.33 for fatigue were considered in determining the stresses in the earlier tests on girders with varying flange rigidities. The allowable stresses dictated by the AISC building specification were used as the basis for the selection of the nominal stresses used in the original tests on girders with various transverse stiffener rigidities. A nominal shear stress of 10.7 ksi and a maximum nominal bending stress of 16.3 ksi were furnished for the girders with various transverse stiffener rigidities. Because of the change in the size of the flanges of the longitudinally stiffened girder with the most rigid flanges, the maximum nominal bending stress was only 11.6 ksi. The maximum bending stress in the other specimen with a smaller flange rigidity was 14 ksi and the nominal shear stress was 10.9 ksi for both test specimens. The longitudinally stiffened girders with varying transverse stiffener sizes were subjected to identical nominal stresses as were their counterparts without longitudinal stiffeners, namely, a shear stress of 10.7 ksi and a maximum flexural stress of 16.3 ksi.

Figures 7, 8, 9, 10, and 11 depict the location of the loads, reactions and test panels in addition to the shear and bending moment diagrams for each series of tests.

5.3.4 Other measurements

At selected load levels during the static tests, measurements of the lateral deflection of the web were taken using the jig which was described in Section 5.1. Ames dials were also included in order to measure the vertical deflection of the girder subjected to load. The vertical deflection measurements were made at the location where the deflection would be the largest within the test panels.

5.4 Fatigue Tests

The assembled girders were positioned in a 250,000 lb. Wilson lever type fatigue machine and the initial web deflections were measured as described in an earlier section. A stress ratio of one-quarter was used as in the earlier tests. Section 5.3.3 gives the details pertaining to the magnitude of the maximum fatigue loading. Figure 14 shows the fatigue machine as adapted for the girder tests. Failure of the test specimen was declared when a crack length of three inches was observed. No noticeable loss of load was experienced in any of the tests at the failure just defined. Crack growth was relatively slow during the first two or three inches of propagation. If repairs were not made to the girder then actual failure would occur when the cracks eliminated the ability of the web to sustain the tension field forces. Repairs have been successful in prolonging the life of thin web girders and a crack of three inches in a girder eighteen to twenty inches deep was thought to be of sufficient size to necessitate repairs. Observation of the crack location and growth was achieved with the aid of magnifying glasses.

6. TEST RESULTS

6.1 Lateral Web Deflections

6.1.1 Initial Web Deflections

6.1.1.1 Girders Subjected Primarily to Shear

Fabrication techniques were developed in order to minimize the initial web deflections, and the resulting initial web deflection patterns for girders FT-1A and FT-10A are illustrated in Fig. 16. The maximum initial web deflections of the girders in the earlier investigation at the University of Illinois are recorded in Table 4 for comparison with the values obtained in the present investigation. The girders which were fabricated as duplicates of girders in the earlier tests are designated by the suffix "A". The shape of the initial distortion is a single buckle, just as in six of the eight previous tests. Figure 17 illustrates the initial web deflections for girders FT-1 and FT-10.

6.1.1.2 Girders with Various Flange Sizes Subjected to Shear and Bending

The initial configuration of the web of girder FTSB-6A is shown in Figure 18. Due to an oversight on the investigator's part, the web deflections of girder FTSB-2A were not measured until after 600 cycles of loading had been applied. While the web deflections due to load change very little with repeated applications, the initial web deflections are changed markedly upon first application of the maximum fatigue loading. Therefore the initial deflections were not obtained, but were of the same general magnitude and shape as those recorded for FTSB-6A.

For comparison, the initial web deflections of the girders of the earlier tests are shown in Fig. 19. It is apparent that the magnitudes of

the deflections in the original tests are much larger than those of the present investigation. Table 5 contains information pertaining to the maximum initial web deflections for both panels of each of the girders included for consideration.

6.1.1.3 Girders with Various Transverse Stiffener Rigidities Subject to Shear and Bending

The initial deflection patterns for girders VST 8-4A and VST 8-16A are shown in Figs. 20 and 21, respectively. The effect of the closer spacing of the stiffeners can be seen in the generally lower magnitude of the initial web deflections listed in Table 6 for the earlier test girders as well as those in the present investigation. The deflections in all three test panels are given for girders VST 8-4A and VST 8-16A, whereas only the web deflections of the center panel were reported in the previous investigation. The trend of decreasing initial web deflections with increasing stiffener rigidity is not supported by the two girders tested as a part of this investigation.

6.1.1.4 Longitudinally Stiffened Girders with Various Flange Rigidities

Figures 22 and 23 illustrate the initial web deflection patterns for the two longitudinally stiffened girders with different flange rigidities subjected to shear and bending. The initial deflections were approximately of the same magnitude as the other girders with varying flange rigidities recorded in Table 5. The presence of longitudinal stiffeners did not serve to decrease the initial web distortions in the case of these two girders, HSB-1 and HSB-2. The effect of the longitudinal stiffener was to shift the buckle to a lower position, leaving the portion of the web

between the longitudinal stiffener and the compression flange relatively undistorted.

6.1.1.5 Longitudinally Stiffened Girders with Varying Transverse Stiffener Rigidities

The initial web deflections of girders HVSB-1 and HVSB-2 are depicted in Figs. 24 and 25, respectively. The patterns for these two longitudinally stiffened girders differed markedly from the VST series girders which were fabricated without longitudinal stiffeners. Several buckles in each panel appeared in the VST series girders. Only one buckle was present in two of the three panels of girder HVSB-1 and, only one very small buckle was detected in one of the three panels of girder HVSB-2. The maximum initial web deflection in each of the three panels is included in Table 6 for girders HVSB-1 and HVSB-2.

6.1.2 Web Deflections Due to Load

6.1.2.1 Girders Subjected to Shear

The development of the buckle due to applied load for girder FT-1A is shown in Figs. 26 and 27. Contour lines of equal lateral deflection are used to illustrate the process. A contour interval of one-third of the web thickness was used. Web deflection measurements were made at four load increments after the girder had been subjected to 118,000 cycles of loading. The applied load is given in the figure as a ratio of the load to the maximum fatigue loading, W/Wmf. After the girder had been subjected to 1,000,000 cycles, the web deflection measurements were again made at the smallest and the largest values of load used in each cycle of loading. It was desired to learn of any changes in the deflection pattern due to the repeated loads. Failure of the girder was declared at 2,250,000 cycles of

loading and web deflection measurements were made at W/Wmf equal to 0, 1/4, 1/2, 3/4, and 1. The results of these measurements are shown in Figs. 28, 29, and 30.

Girder FT-10A was subjected to 1,000 cycles of loading before web deflection measurements were made at the four equally incremented loads from 1/4 Wmf to Wmf, inclusive. These values of web deflection are shown in Figs. 31 and 32. Web deflections were measured again after 2,075,000 cycles of loading and the measurements were taken with the girder subjected to the minimum and the maximum loads of the fatigue cycle. Figure 33 depicts the results of the measurements. After completion of the fatigue test, the girder was subjected to a static test and web deflections were measured at loads larger than the maximum fatigue loading. At a load of 1.5 Wmf the web deflections were as shown in Fig. 34.

6.1.2.2 Girders with Various Flange Rigidities Subjected to Shear and Bending

Girder FTSB-2A was constructed with the least rigid flanges of girders subjected to shear and bending in the present investigation and web deflection measurements were taken at loads equal to the minimum and maximum fatigue cycle loads. Due to the large deflections, the contour interval was chosen to be equal to the thickness of the web. Figure 35 illustrates the deflection pattern for the minimum fatigue loading after 600 load cycles. The pattern corresponding to the maximum fatigue loading is shown in Fig. 36. The deflection pattern after 371,000 cycles of loading is shown in Fig. 37 for W/Wmf = 1.

FTSB-6A was the designation of the girder with the largest flange rigidity in the present investigation, and Fig. 38 shows the web deflections

due to the maximum fatigue loading. After the girder had failed, web deflection measurements were obtained with the girder subjected to no load. These deflections are presented in Fig. 39 and may be compared to the initial web deflections in Fig. 18. The change in the web deflections is quite apparent from such a comparison.

6.1.2.3 Girders with Various Transverse Stiffener Rigidities Subjected to Shear and Bending

The web deflections of the girder with the smallest transverse stiffeners were mapped at loads corresponding to the minimum and maximum fatigue loading, and the results are represented in Figs. 40 and 41, respectively. During the static test, measurements were made at a load equivalent to 1.5 Wmf. The resulting deflection pattern is shown in Fig. 42.

The largest stiffeners were used on girder VST 8-16A and the web deflections are given in Figs. 43 and 44 for the two extremes of the cyclic loading. The foregoing measurements were made upon completion of the fatigue test.

6.1.2.4 Longitudinally Stiffened Girders with Varying Flange Rigidities Subjected to Shear and Bending

The use of a longitudinal stiffener had a considerable effect on the lateral web deflections which occur due to load. Figures 45 and 46 show that one buckle dominates each panel of girder HSB-1. The two figures depict the panel deflections at the minimum and maximum fatigue cycle loads, respectively. A comparison of Figs. 36 and 37 illustrates the differences between the two types of patterns. Two buckles dominated each panel of the girder without longitudinal stiffeners. The development of the deflection

pattern with successively larger loads is portrayed in Figs. 47, 48, 49, and 50 for the longitudinally stiffened girder with the largest value of flange rigidity, HSB-2. Again it may be noted that a single buckle dominates each panel. This buckle became more narrow and the maximum deflection increased, as shown in Fig. 52, when the load was increased to 1.3 W_{mf} during the static test. Two small buckles developed on either side of the primary buckle and were 180 degrees out of phase with the large buckle.

6.1.2.5 Longitudinally Stiffened Girders with Various Transverse Stiffener Rigidities Subjected to Shear and Bending

Initial web deflections influenced the pattern of deflections due to load. The addition of load to the girder with the least rigid transverse stiffeners caused the initial buckles to change in magnitude and to distort a small amount. Negligible distortion was encountered in the subpanel bounded by the longitudinal stiffener and the compression flange. The web deflections corresponding to the minimum and maximum fatigue loading are shown in Figs. 52 and 53, respectively. Due to the small deflections, the contour interval is taken as one-third of the web thickness. After 478,000 cycles of loading, the web deflections were measured with no load on the girder. The results are illustrated in Fig. 54.

Very small initial web deflections were obtained in the girder with the largest transverse stiffeners. Subsequent loading produced little increase in the web deflections. Figure 55 depicts the girder panel deflections while subjected to one-fourth of the maximum fatigue load after 3,000 cycles of loading. The maximum lateral web deflection is approximately two-thirds of the web thickness. At the maximum fatigue loading the maximum

deflection has only increased to about eight-five percent of the web thickness. The web deflections corresponding to the maximum fatigue loading are presented in Fig. 56. Figures 57 and 58 illustrate the change in the deflection pattern after 3,000,000 applications of the load.

6.2 Static Tests

6.2.1 Results Pertaining to Membrane Stresses

6.2.1.1 Shear Girders with Varying Flange Rigidities

In an effort to determine the magnitudes of the web membrane stresses AR-1-S-6 rosettes were mounted on both sides of the web at various locations. Gages were placed on girder FT-1A at points A, B, C, D, E, F, G, H, J, K, and M shown in Fig. 15. Girder FT-10A, with the most rigid flanges, was instrumented with the rosettes at points A, C, E, H, and M. The distance from the edge of the web to the gage lines was 3/4 in. for both specimens instead of 1 in. as specified in Fig. 15. In addition, the rosettes on specimens FT-1A and FT-10A were oriented in such a manner that the 45° gage was turned 90° from the position shown in Fig. 15. The magnitude and the direction of the principal stresses were computed from the measured strains. The strains in each of the three directions were averaged based on the assumption that a linear distribution of strain existed through the thickness of the web. These three computed strains were used to obtain the values of the membrane stresses. Figure 60 illustrates the development of the maximum principal membrane stress at three panel locations for girders FT-1A and FT-10A with increased loading. Also included in the figure are the values of the maximum principal stress computed from the stresses calculated by the use of the ordinary flexural theory for beams. The location of the rosette is indicated in each figure by the dot

on the inset drawing of the test panel. In addition the location is specified by a letter included in the insert which refers to the gage locations shown in Fig. 15. The minimum principal membrane stresses for the same three locations are given in Fig. 61. The principal stresses at various panel locations for girder FT-1A are shown plotted to scale in Fig. 62. Values calculated by assuming that the ordinary flexural theory was valid are shown in black on the figure. Partial diagonal tension field stresses, shown in green, were obtained by assuming that the shear was carried by beam action up to the theoretical buckling stress for a simply supported plate subjected to shear on all four edges and the excess load above that value was carried by the diagonal tension field as outlined by Basler (5). Principal stresses were calculated from the strains measured in the rosettes and are shown in red. Figure 62 relates the magnitude and the direction of the principal stresses for girder FT-1A obtained by the three procedures just mentioned. Similar information for girder FT-10A is shown in Fig. 63.

6.2.1.2 Girders with Varying Flange Rigidities Subjected to Shear and Bending

Web membrane stresses were obtained from strains measured during the static tests of girders FTSB-2A and FTSB-6A. AR-1-S-6 rosettes were mounted on opposite sides of the web at various panel locations. The gages were placed at points A, B, C, D, and E shown in Figure 15. Both panels of the two specimens were instrumented at these points. In addition gages were mounted on girder FTSB-2A at location F (Fig. 15) on panels 1 and 2 and at point G (Fig. 15) in panel 1. The dimensions shown in Fig. 15 are typical for the two FTSB girders. The measured strains were used in order to

calculate the magnitude and the direction of the principal membrane stresses. Again it was assumed that a linear distribution of strain existed through the thickness of the web. Figs. 64, 65, 66, 67, 68, and 69 show the comparison of membrane stresses for girders FTSB-2A and FTSB-6A. Values of the maximum principal stresses are plotted as ordinates with the corresponding load values as the abscissa. Theoretical values of the maximum principal stress, calculated by the use of the ordinary flexural theory for beams are included in each figure. Because of the difference in the size of the flanges of the two girders, the theoretical values differ somewhat for each girder. This difference is very small as may be seen in the left portion of Fig. 64. The difference in the two theoretical values decreases as the ratio of bending stress to shear stress decreases. For the remaining figures only the theoretical value for girder FTSB-2A is shown. The location of each gage is given in the insert of each figure as a dot and the letter in the insert refers to the location as defined in Fig. 15. Maximum principal stresses in panel 1 are shown in Figs. 64 and 65. Panel 2 maximum principal stresses are given in Figs. 66 and 67. Minimum principal stresses for panels 1 and 2 are shown in Figs. 68 and 69, respectively. A comparison of measured values and theoretical values is shown for girders FTSB-2A and FTSB-6A in Figs. 70 and 71, respectively. Black vectors denote flexural theory principal stresses, green vectors represent the partial diagonal tension field stresses and red denotes the experimentally obtained values. Tension is depicted by vectors which point away from the gage point, while compression is illustrated by vectors pointing toward the gage location. Longitudinal strains were measured at six locations on the cross section of the FTSB girders. Gages on the web were

located at points C, D, E, R, and S as shown in Fig. 15. The distribution of longitudinal stresses is shown in Figure 72 for the cross-section indicated on the sketch in the figure. Theoretical values obtained from the ordinary flexural theory are included for reference. A wide variation from the theoretical values was experienced in both girders.

6.2.1.3 Girders with Varying Transverse Stiffener Rigidities

AR-1S-6 rosettes were mounted at fifteen locations on both surfaces of the web of the girders with varying transverse stiffener rigidities. Panels 1 and 2, having the highest and second highest bending stress-to-shear stress ratio, respectively, were instrumented with gages at points B, C, D, and E, as identified in Fig. 15. Panel 3 with the smallest bending stress-to-shear stress ratio was provided with rosettes at locations A, B, C, D, E, F, and L as illustrated in Fig. 15. Both specimens, VST 8-4A and VST 8-16A, were instrumented identically in all three panels. The gages located at points D and E were rotated 90° from the positions shown in Fig. 15. Figures 73, 74, and 75, and 76 illustrate the variation of mid-plane maximum principal web stresses with increase in load. Each of the three graphs in Figs. 73, 74, and 75 shows the stress variation at each of three locations within a particular panel. The maximum principal stress at a particular location in three different panels is depicted in Fig. 76. In each of the figures, the theoretical values, as computed by means of the ordinary flexural theory, are shown as solid straight lines. Minimum principal stresses for the same locations indicated in Fig. 73, 74, 75, and 76 are given in Figs. 77, 78, 79, and 80. It may be noted that the deviation from the theoretical values is, in general, greater for the maximum principal stresses than for the minimum principal stresses.

Predicted and measured principal stresses for girder VST 8-4A are shown in Fig. 81. Beam theory values are shown as black vectors, partial diagonal tension field stresses are green vectors and the measured values are shown in red. Again, vectors pointing away from the gage location are tensile stresses and those pointing toward the gage denote compression. The aforementioned quantities are shown in Fig. 82 for girder VST 8-16A also.

The distribution of longitudinal stresses is shown in Fig. 83 for girders VST 8-4A and VST 8-16A. The cross section in panel 3 having the smallest bending stress-to-shear stress ratio was chosen for representation. Agreement with the theoretical flexural theory values is reasonably good. Figure 84 shows the stress distribution in the compression zone above the neutral axis for girders VST 8-4A and VST 8-16A. One cross-section in each of the three panels is represented; namely those containing the rosette strain gages near the vertical stiffeners. The sketch indicates the location of the cross section with the largest moment present in the top row.

6.2.1.4 Longitudinally Stiffened Girders with Varying Flange Rigidities

Figures 85, 86, and 87 illustrate the variation of maximum principal stress versus the applied load for various panel locations of girders HSB-1 and HSB-2. Rosettes were located in both panels of the specimens at points B, C, D, and E as shown in Fig. 15. In addition, panel 1 was provided with a rosette at the neutral axis near the edge having the largest bending stress-to-shear stress ratio (F in Fig. 15). The location of the gages is indicated in the figure by the use of a sketch of the specimen containing both a dot at the gage location and a letter below the sketch

referring to the positions outlined in Fig. 15. Minimum principal stresses were plotted versus applied load for gage locations C, D, and E (See Fig. 15) in panels 1 and 2 of the girder test section and are shown in Figs. 88 and 89, respectively.

Changes in the girder cross section to maintain reasonable stiffener proportions created a significant difference between the theoretical values calculated for the two girders at certain points. Theoretical values for both girders are included in parts of Figs. 86, 87 and 89 for purposes of comparison. From these figures it may be seen that the normal deviation of the measured values from the theoretical values exceeds the deviation of one theoretical value from the other. The theoretical values for girder HSB-1 are identified in the figures by "1" and those for girder HSB-2 are designated "2".

The comparison of the theoretical principal stresses and the experimental values is shown in Fig. 90 for girder HSB-1. Black, green, and red vectors denote beam theory, partial diagonal tension field theory, and measured values, respectively. Figure 91 represents the same comparison for HSB-2 as that in Fig. 90. The distribution of longitudinal stresses on a vertical cross section for both girders are included with the FTSB girders in Fig. 72. The longitudinal gages used were located at points C, D, E, R, and S as indicated on Fig. 15.

6.2.1.5 Longitudinally Stiffened Girders with Various Transverse Stiffener Rigidities

Only one static test was performed on a longitudinally stiffened girder with various transverse stiffener rigidities, and the girder tested, HVSB-1, contained transverse stiffeners with the minimum rigidity. The

principal stresses in the web of HVSB-1 were plotted in Figs. 73, 74, 75, 76, 77, 78, 79, and 80 in order to facilitate the comparison between girders similar in every way except for the presence of a longitudinal stiffener. The variation of maximum principal stress versus load is shown in Figs. 73, 74, 75, and 76 whereas the variation of minimum principal stresses with load is illustrated in Figs. 77, 78, 79, and 80. Values calculated according to the formulas for ordinary flexure are shown in all figures as straight solid lines.

Figure 92 shows a comparison of principal stresses obtained from beam theory, partial diagonal tension field theory, and experimental results for nine locations on the web of girder HVSB-1. Vectors are shown in black, green, and red in order to distinguish between the beam theory values, partial diagonal tension field values, and the measured values, respectively. The distribution of longitudinal stresses along the vertical cross section having the smallest moment-to-shear ratio is shown in Fig. 83 for girder HVSB-1. A comparison of the stress distribution in the compression zone above the mid-depth of the beam for each panel is shown in Fig. 84.

6.2.2 Flexing Action of the Web

The amount of web flexing action varied from specimen to specimen. Figures 26 to 27 illustrate the changes in the web deflection pattern in the girder having the smallest flange rigidity parameter, I/a^3t, subjected to shear. The slight changes noted for this specimen were typical for all of the girders. In general the original deflection pattern, due to fabrication, was altered by the application of the load. As the load was increased, the pattern shifted so as to align the axis of the buckle with the direction of the tension field stresses. Higher load led to a more

pronounced deflection pattern, in which the buckle was deeper and more narrow. As the load was increased and decreased during the loading cycle, the pattern changed from a deep, narrow buckle to a shallow, rounded buckle even after many cycles of loading. A comparison of Figs. 26 and 27 with Fig. 28 indicates that the changes due to the repeated loading were indeed small. Even at the time of failure of girder FT-1A the web deflection patterns were essentially unchanged from the earlier patterns (See Figs. 29 and 31). The girders subjected to shear developed a single buckle whereas those girders subjected to combined shear and bending contained two or more buckles in each panel.

In the girders with varying flange rigidities subjected to shear and bending, the same type of pattern changes were experienced as for the FT girders. However, with the repetition of the loading these patterns were changed to a greater extent as is evidenced in Figs. 37 and 38 for girder FTSB-2A. In panel 1 the smaller buckle has increased in magnitude and in size with repetition of the load. The companion girders with longitudinal stiffeners, HSB, did not form two buckles in each panel, but one buckle was present and was aligned along the diagonal of the subpanel formed by the transverse and longitudinal stiffeners. Figures 46, 47, 48 and 50 show the web deflection patterns for the minimum and maximum fatigue loads for girders HSB-1 and HSB-2. No significant deflections were measured in the subpanel above the longitudinal stiffener and no flexing of this portion of the web was observed. The flexing action of the lower portion of the web was very evident and could be observed in a casual glance from several feet away. In some instances the flexing action was accompanied by sound.

Web deflections were generally smaller in the girders with various transverse stiffener rigidities and they were particularly small in the companion longitudinally stiffened girders, HVSB. Web flexing was also less pronounced in these specimens. Contrary to the reasoning in Chapter 2, girder panels with smaller initial deflections had a smaller range of deflection also. The columns listed as range of deflections in Tables 4, 5, and 6 give a good indication of the amount of flexing present in the webs of the girders tested by Hall and Stallmeyer (3). A comparison of the initial web deflections and the corresponding range of deflections during a cycle of loading for each girder panel is shown in Fig. 93. The value of the initial deflection in a particular panel may occur at a point other than the point experiencing the largest range of deflections. From the figure it may be noted that a large initial deflection is no assurance of a small web flexing action.

6.2.3 Behavior of Stiffeners

6.2.3.1 Transverse Stiffeners

The size of the transverse stiffeners used in the girders with varying flange rigidities subjected to shear and bending was dictated by the requirements of the AISC Manual of Steel Construction (23). Girders having no longitudinal stiffeners were designed with double stiffeners, i.e., two identical stiffeners, one on each side of the web. The inclusion of the longitudinal stiffener made a single-sided stiffeners the most convenient way to design the transverse stiffening element. Single element wire resistance strain gages were applied to both sides of the stiffener at three levels. The first level was located at the midpoint of the stiffener, the second level at the third level was taken as close to the compression flange

as possible. The top gages were located about one inch from the bottom of the compression flange (top flange). Typical gage locations are shown in Fig. 94. The strains recorded in the stiffeners were very small compared to the theoretical values obtained by assuming that the transverse stiffener carries the vertical component of the partial diagonal tension field force. There are several reasons for this discrepancy. The tension field is anchored to the flange along the web-compression flange interface. This anchoring force causes secondary bending moments in the flange and the transverse stiffeners act with the web in supporting the flange. Strains measured in the web at locations adjacent to the transverse stiffener were comparable and in some instances higher than the average strains in the stiffener. Normally four strain gages were used at each level in the case of double-sided stiffeners, and the average strain of these gages was used in order to eliminate the effects of bending in the stiffeners. The tension field force is theoretically anchored at the boundary of the panel, and the web of the adjoining panel is neglected in the computation of the stiffener force. The web and stiffener are integrally connected and any strain in the stiffener must be accompanied by strain in the web. It was evident from the strains in the stiffeners that the stiffener wasn't performing its assumed role in the partial diagonal tension field theory. Table 7 lists representative strains at the maximum fatigue loading for the girders tested.

The results for girders with varying transverse stiffener sizes subjected to shear and bending are similar to the test results just described. The strains in the stiffeners were small compared to the theoretical values in all cases. Strains less than ten percent of the theoretical values were common in the two girders without a longitudinal stiffener

and the girder with the longitudinal stiffener. The strains for the girders with only transverse stiffeners were of the same order of magnitude throughout the tests. Therefore the force in the larger stiffeners was proportionately larger than the force in the smaller stiffeners. Similar results were reported by Hall and Stallmeyer (3). The strains in the transverse stiffeners of the girder with a longitudinal stiffener, HVSB-1, were very small, being on the order of three to five percent of the theoretical value.

Bending of the smaller stiffeners was apparent from examination of the four separate strain gages at each level of the stiffener. All of the girders except VST 8-16A experienced a significant amount of bending. Compressive strains were present on one side of the web, while tensile strains were registered on the other side in many cases. This indicates that the smaller stiffeners used were not adequate to furnish a rigid boundary for the panels.

6.2.3.2 Longitudinal Stiffeners

Static tests were performed on three of the four girders designed with longitudinal stiffeners. Strain gages were placed on both sides of the stiffener at the points where the transverse stiffeners crossed the longitudinal stiffener and at the center of each test panel. Therefore ten gages were used on the HSB specimens having two test panels, and fourteen gages were used on the HVSB girder containing three test panels. Reference to Figs. 46 through 59 shows that the longitudinal stiffeners were effective in controlling lateral web deflections even at very high loads as evidenced in Fig. 52. In every case no significant buckles formed in the small subpanel formed by the compression flange, longitudinal stiffener, and the transverse stiffeners. The buckling pattern of the girders with an aspect ratio of 0.5 was drastically changed (See Figs. 42 and 54).

Figure 95 depicts the development of the strain in the longitudinal stiffener and an indication of the bending of the stiffener for girder HSB-1. The sketch at the top of the figure shows the location of the strain gages with respect to the entire specimen. Below, the strains are plotted for each location showing the individual strain value on each side of the stiffener. The compressive strain at the left and center longitudinal-transverse stiffener intersection and the tensile strains at the center of each panel indicate that bending was present in the longitudinal stiffener even at low loads. Therefore, while the longitudinal stiffeners were effective in controlling lateral web deflections, a rigid boundary for the panel was not achieved. Girder HSB-2 acted in a similar manner as shown in Fig. 96. The lateral web deflection patterns for the corresponding longitudinally unstiffened and stiffened girders are shown in Fig. 39 and 51, respectively.

Figure 97 illustrates the strain values present in the longitudinal stiffener of the girder with a small transverse stiffener rigidity. It may be seen from this figure that the transverse stiffener did not have much restraining effect on the buckling of the web and longitudinal stiffener. It appears that the longitudinal stiffener over the three panel specimen has a general deflection shape in the form of a half-sine curve. Superimposed on this large deflected shape were sine curve deflections within each panel. The two sine curves were additive in the end panels and of opposite sign in the center panel.

6.2.4 Overall Girder Deflections

Vertical deflections were measured in each static test. An Ames dial was placed at the location of the maximum deflection for each specimen.

For the girders subjected to shear alone, two dials were used on each edge of the single test panel. Deflections were read to the nearest 0.001 in. Figure 98 represents the deflection behavior for the shear girders. Yielding of the test specimen is very apparent for girder FT-1A. The deformation of the shear panel was such that the right side of the panel moved upward with respect to the deflection experienced earlier at a load twenty-five percent greater than the maximum fatigue load (W/Wmf = 1.25). A more gradual yielding was experienced in girder FT-10A. The larger flanges of the second girder were not affected by the tension field stresses of the web to the extent of the influence shown in the girder with smaller flanges.

The load deflection curves for the girders with varying flange rigidities subjected to shear and bending are shown in Fig. 99. Extensive yielding in the specimen was experienced at loads slightly higher than the maximum load used in the fatigue tests. In fact, the FTSB-2A girder having the smallest flanges showed extensive yielding characteristics in the first load increment above the maximum fatigue load value. The companion girders, HSB-1 and HSB-2, acted in much the same manner as the non-longitudinally stiffened FTSB girders as shown in Fig. 100. No increase in yield strength of the longitudinally stiffened girders was experienced. With the application of more load and resulting large deflections, specimen HSB-1 displayed a higher strength than either of the other three similar girders.

The girders with varying transverse stiffener rigidities exhibited a much higher strength in relation to the maximum fatigue loading than the other girders tested in this investigation. The girder with a longitudinal stiffener, HVSB-1, and its counterpart with transverse stiffeners only, VST 8-4A, acted very similarly. The similarity can be seen from the shapes

of the load deflection curves in Fig. 101. Girder VST 8-16A, having larger transverse stiffeners, displayed a smaller deflection at the higher loads.

6.3 Fatigue Tests

6.3.1 Girders with Various Flange Rigidities Subjected to Shear

The results pertaining to the development of the web deflection patterns with increasing load have already been mentioned in section 6.1. Figures 26, 27, 28, 29, 30, and 31 illustrate the development of the deflection pattern at various periods in the life of girder FT-1A. Figures 32, 33, and 34 depict similar results observed with specimen FT-10A. Web deflection measurements were made as the repeated loadings progressed in order to determine changes in the buckling pattern, if any. No significant changes were observed. Most alterations consisted of a slight change in the magnitude of the deflections. Results pertinent to the fatigue behavior of shear panels with varying flange rigidities are given in Table 4 and are combined with the results obtained by Hall and Stallmeyer (3). The suffix "A" denotes the girders of the present investigation. The decrease in maximum web deflections initially and those due to load is readily observed for the latter tests. No crack had initiated in girder FT-10A after 3,500,000 cycles of loading and is designated as no failure in the table.

The location of the crack in girder FT-1A is shown in Fig. 102. Figures 102 and 103 show the location of failures in all girders tested. The influence of the flange rigidity parameter, I/a^3t, on the fatigue life of the girders is shown in Fig. 104. The results of two tests performed at Lehigh University were included and bear the labels LF-1 and LF-2. The improved fatigue behavior of the girders in the present investigation is apparent. The influence of the initial web deflections is considered in

Fig. 105. In Fig. 106 the range of web deflection during each loading cycle is plotted versus the fatigue life of the shear panel. In both of these figures, improved fatigue lives are experienced with a reduction of initial and range of deflection.

6.3.2 Girders with Various Flange Sizes Subjected to Shear and Moment

Web deflection patterns are shown in Figs. 36, 37, 38, and 39 for the minimum and maximum values of the cyclic load at various intervals in the loading history of the two girders with different flange rigidities subjected to shear and bending. Only slight alterations of the pattern are noticeable in the figures.

Table 5 contains the results of the tests reported in this investigation in addition to the results obtained by Hall and Stallmeyer (3). The suffix "A" is used to denote the girders tested in the present investigation. The maximum initial deflection and the maximum deflection due to the maximum fatigue load are given for both panels of each specimen. The maximum range of deflection during one load cycle at a particular point is also indicated. One exception was the determination of the maximum range of deflection for girder FTSB-6A for a load variation from zero to the maximum fatigue load. The value entered in the table was taken as three quarters of the zero to maximum load deflection value. The locations of the failures in girders FTSB-2A and FTSB-6A are shown in Fig. 102.

The effect of the flange rigidity parameter, I/a^3t, on the fatigue life of the FTSB girders is shown in Fig. 107. An increase in fatigue life was encountered with increasing flange rigidity in the earlier investigation which was not verified by the test results of this investigation. The effect of initial deflection and range of deflections on fatigue life are

illustrated in Figs. 108 and 109. In general, longer fatigue lives were experienced with the girders displaying smaller initial and smaller range of deflections.

6.3.3 Girders with Various Transverse Stiffener Rigidities Subjected to Shear and Bending

Web deflection pattern changes due to load are shown in Fig. 41, 42, 44, and 45 for the two girders with different transverse stiffener rigidities. With increasing load the patterns vary a small amount in magnitude and orientation. Table 6 contains information related to the fatigue behavior of the VST girders. The suffix "A" on the specimen code identifies the girders tested in the present program. All web deflections are given as a ratio of the deflection to the thickness of the web. Initial deflections, maximum deflections and the range of deflections in each load cycle are given for each panel. Only partial results were available for the girders tested previously. Figure 102 illustrates the location of the failures in girders VST 8-4A and VST 8-16A.

The relationship between transverse stiffener rigidity and fatigue life is shown in Fig. 110. No trend in the data is readily discernible. Figures 111 and 112 depict the correlation of fatigue life with initial deflections of the web and the range of web deflections, respectively. Again, smaller initial deflections and range of deflections are found in the specimen with longer fatigue lives.

6.3.4 Longitudinally Stiffened Girders with Varying Flange Rigidities

Figures 46, 47, 48, 49, 50, and 51 indicate the development of the web deflection patterns due to applied load for the longitudinally stiffened girders with various flange rigidities. Included in Table 5 are

the results pertaining to the fatigue behavior of girders HSB-1 and HSB-2. The initial and maximum load web deflections are not significantly smaller than the companion girders without longitudinal stiffeners, but the range of deflection due to a cycle of loading is definitely smaller than the corresponding values for the original tests. Figure 107 also includes the HSB girders in the comparison of fatigue life and flange rigidity parameter, I/a^3t. The influence of initial deflection and the range of deflection on fatigue life is shown in Fig. 108 and 109 for the longitudinally stiffened girders. Failure locations for these girders are shown in Fig. 103.

6.3.5 Longitudinally Stiffened Girders with Various Transverse Stiffeners

Web deflection pattern development and changes for girders HVSB-1 and HVSB-2 are shown in Figs. 53, 54, 55, 56, 57, 58, and 59. The change in the web deflection pattern of girder HVSB-2 between the measurements taken at 3,000 cycles and those taken at 3,000,000 cycles of loading was greater than that observed in the other specimens. The web deflection pattern at the minimum load changed very slightly, while the pattern at the maximum loading shifted its position slightly and increased twofold. The presence of the longitudinal stiffener had a definite influence on the development of the buckled web deflections near the compression flange.

Table 6 contains the results pertaining to HVSB girders and relates the values of initial, maximum, and range of deflections to fatigue life and to the other girders with varying transverse stiffener rigidities without longitudinal stiffeners. The location of the failure in HVSB-1 is shown in Fig. 103. Failure of HVSB-2 occurred in the connections and is not shown. The term "no failure" is used to indicate that the test panels did not fail at 3,000,000 cycles of loading.

The transverse stiffener rigidity, EIs/Da, versus fatigue life in Fig. 110 shows the comparison of the two longitudinally stiffened girders with those with transverse stiffeners only. Initial web deflections and range of deflections are plotted against fatigue life in Figs. 111 and 112, respectively. Figure 112 shows a good correlation between decreasing range of deflections and increasing fatigue life.

7. DISCUSSION OF TEST RESULTS

7.1 Web Deflections

7.1.1 Initial Deformation

One of the first objectives of this investigation was to develop a welding procedure which resulted in the fabrication of small thin web girders with small initial lateral web deflections. Short welding passes were used and subsequent passes were made at various locations. The heat input from welding was distributed to different portions of the girder in this way, and no particular portion received the large amounts of concentrated heating which is the main cause of web distortion. The use of a small electrode also minimized the heat input to the girder from welding. The welding sequence shown in Fig. 13 is the result of the welding sequence experimentation.

Large initial web deflections were reported by Hall and Stallmeyer (3) in the girder tests which preceded the present investigation. Initial web deflections are shown in Figs. 16 and 17 for girders fabricated for the two test series. Figure 16 depicts the web deflections of the shear girders with varying flange rigidities constructed for the present investigation and Fig. 17 shows the initial web configurations of the companion girders of the previous investigation. A marked improvement is noted for the girders of the present test series. Further improvement might be obtained in order to restrict the deflection to less than the thickness of the web. The web thickness in the girders shown in Figs. 16 and 17 was 0.0747 inches.

Further proof of the improvement in welding technique may be seen by comparing Figs. 18 and 19. In Fig. 18 the maximum web deflection is only 2.77 times the thickness of the web, whereas web deflection-to-thickness ratios of 3 and 4 are common in Fig. 19. The new welding technique resulted in fewer buckles in each panel also. The addition of a longitudinal stiffener resulted in slightly larger deflections in a single pattern. Figures 22 and 23 illustrate the longitudinally stiffened girders having a web depth to thickness ratio of 267. A larger value of $^{d}/_{t}$, 312, was used with the girders with varying transverse stiffener rigidities. Comparison of Figs. 20 and 21 with Figs. 24 and 25 indicates that the use of a longitudinal stiffener may not decrease the size of the deflections, but it does change the shape of the deflection pattern markedly. The absence of appreciable web deflection is attributed to coincidence rather than a further improvement of welding technique. However, the use of larger transverse stiffeners does have an influence on the web deflections as may be evidenced in Figs. 20 and 21. The only difference in the two girders was the size of the transverse stiffeners with girder VST 8-16A having the larger stiffeners (1/8" x 2" vs. 1/8" x 1/2"). It was found in the previous investigation that the transverse stiffener rigidity did influence the initial deformation of the web.

7.1.2 Web Deflections Due to Load

As mentioned in Chapter 6, the application of load resulted in the rearrangement of the web deflection pattern. No sudden change in web deflections was experienced during the loading cycle. A study of Figs. 26 and 27 illustrates the gradual increase in magnitude and change in shape of the web deflection pattern. As the load was increased, the buckle became deeper and more narrow.

The orientation of the buckle is aligned with the general direction of the maximum principal stresses present in the web. The behavior shown in Figs. 26 and 27 for the girder with the smaller flange rigidity subjected to shear was in general indicative of the behavior of all the test girders. Table 4 lists the values of the maximum fatigue load (Wmf) deflections and the range of deflections during one cycle of loading for the shear girders with varying flange rigidities in the present investigation, in addition to the results obtained in the earlier investigation. In the earlier tests, the web deflection corresponding to the maximum load showed a decreasing trend with increasing flange rigidity. No such results were experienced in the girders tested subsequently.

In the earlier tests two and three buckles were present initially in the girders with varying flange rigidities subjected to shear and bending as shown in Fig. 19. The addition of load merely served to alter the shape of these initial deformations. In the present tests a single buckle dominated the test panels initially and after the load was applied, two distinct buckles appeared, oriented in the direction of the maximum principal stresses. With each repetition of load, the magnitude of the buckles changed slightly. As a result the maximum flexing action of the web was experienced at points other than along the crest of the buckles. The girders having a longitudinal stiffener had only a single buckle in each panel.

Multiple buckles were present in the girders with varying transverse stiffener rigidities subjected to combined shear and bending. The small aspect ratio, $\alpha = 0.5$, is probably responsible for the formation of the numerous buckles. As in the earlier tests, the application of load served to alter the shape of the pattern, increasing the magnitude of most of the buckles. The addition of the longitudinal stiffener increased the

aspect ratio of the lower subpanel and fewer buckles formed in these subpanels formed in these subpanels. After the load had been applied, drastic changes in the deflection patterns occurred as may be seen by a comparison of Fig. 24 with Figs. 53 and 54, and Fig. 25 with Figs. 58 and 59. A drastic change in girder HVSB-2 was expected due to the almost nonexistence of initial deformation. No buckles were encountered in the small subpanels either initially or due to load.

In general the web deflections experienced in the girders of the present investigation are representative of deflections to be expected in full size welded plate girders. The influence of the web deflections on the behavior of the girders under static and fatigue loadings will be discussed in greater detail in subsequent sections of this chapter.

7.2 Static Tests

7.2.1 Discussion of Test Results Pertaining to Membrane Stresses

7.2.1.1 Shear Girders with Varying Flange Rigidities

Figure 60 illustrates the development of the maximum principal stresses with increasing load as determined in the static tests on girders FT-1A and FT-10A. At the flange-web junction, the measured values were larger than the values predicted by ordinary beam theory. The actual maximum principal stresses were expected to exceed the beam theory values due to the partial diagonal tension field. The decrease in stress at loads above the maximum fatigue load in girder FT-10A (location E) was due to the shifting deflection pattern, which may be seen in Figs. 34 and 35. Minimum principal stresses were expected to be less than the beam theory values due to the buckling of the web. The increase in compressive stress at location C indicated on Fig. 61 was in all probability due to secondary

bending of the flange. The junction of the transverse stiffener with the flange restricts the development of tensile stresses due to the compression in the transverse stiffener and the web. Very little deflection of the web was observed near the stiffener-flange junction. The large compressive stresses measured at E for both girders indicates that the web was carrying an appreciable amount of the vertical component of the diagonal tension field force.

From Figs. 62 and 63 it may be seen that the experimental values are intermediate between the beam theory values and the partial diagonal tension field theory values. The stresses shown were obtained for the maximum fatigue loading and not at ultimate load conditions.

7.2.1.2 Girders with Varying Flange Rigidities Subjected to Shear and Bending

Stresses calculated from the measured strains exceeded the beam theory values in the majority of cases in the two panels of the FTSB girders. In particular Figs. 64 and 65 show a large deviation from the theoretical values for panel 1 of the test specimen. Panel 1 had the least amount of moment present. Girder FTSB-2A had the least rigid flanges of two test specimens. Again it may be noted that high values of maximum principal stresses were expected, although stresses of a magnitude greater than 30 ksi at the maximum fatigue loading were not predicted by the partial diagonal tension field theory. Extensive yielding was experienced in both specimens at a load slightly higher than the maximum fatigue load as may be seen in Fig. 99. Initial web deflections were not obtained for girder FTSB-2A due to the fact that one cycle of loading was inadvertantly applied before web deflection measurements were made, and the web was permanently deformed as shown in Fig. 36.

The minimum principal stresses in panel 1 of FTSB-2A were mainly tensile in contrast to the compression stresses present in panel 1 of FTSB-6A and panel 2 of both girders. Figure 68 illustrates the erratic behavior of girder FTSB-2A. None of the remaining eight girders tested exhibited similar behavior. From Fig. 70 it is evident that the experimental maximum principal stresses are very near the magnitude of the partial diagonal tension field theory values in panel 1 and are quite dissimilar in panel 2. The fact that both the maximum and minimum principal stresses are tensile indicates that the large deflection of the web created large tensile membrane stresses. It may also be noted From Figs. 70 and 71 that the experimental values of stress have a magnitude and orientation which are intermediate between the beam theory values and the partial diagonal tension field theory values. Results of tests performed at Lehigh University (24) indicated that the experimental values of stress around the panel boundary did not vary from the ordinary beam theory values to any great extent.

Longitudinal stress distributions across a vertical cross-section for the various girders are shown in Fig. 72. Due to the buckling of the web, the subsequent large lateral deflections due to load and the development of the diagonal tension field, the longitudinal stresses on the cross-section considered differ to a great degree from the theoretical beam values. It is significant to note the difference in the shapes of the stress distribution for the girders with and without a longitudinal stiffener. Both of the FTSB girders exhibit two peaks in the distribution corresponding to the two buckles formed in the panel. Each of the HSB girders displays only a single tensile peak due to the single buckle present in the lower subpanel. The influence of the large secondary bending stresses in the tension flanges

is cited as the reason for the small value of tensile stress in the web near the tension flange.

7.2.1.3 Girders with Varying Transverse Stiffener Rigidities Subjected to Shear and Bending

The experimental values of midplane membrane principal stresses for the VST girders agreed reasonably well with the beam theory predictions. Figures 73, 74, 75, and 76 illustrate the variation of the maximum principal stresses with load. In panel 2 (Fig. 74) the variation in the experimental maximum principal stress is almost linear at the three gage locations. The minimum principal stresses shown in Figs. 77, 78, 79, and 80 also vary only a small amount from the beam theory values. The aspect ratio, α, must have a large influence on the behavior of the tension field action stresses. The VST girders have a $^{d}/_{t}$ ratio of 312 and the theoretical buckling load varies from 0.36 Wmf to 0.45 Wmf for the three test panels as contrasted to the $^{d}/_{t}$ ratio of 267 and theoretical buckling loads of 0.41 Wmf to 0.45 Wmf for the FTSB girders discussed in section 7.2.1.2 The VST girders did have a flange rigidity greater than the FTSB girders. However, the boundary rigidity of the VST 8-4A girder should be approximately equal to that of girder FTSB-6A. There was no great deviation from beam theory values in the tests on the VST girders comparable to that shown in Fig. 64 for the FTSB girders. Figures 81 and 82 further indicate the similarity of the experimental stresses and those calculated by the ordinary beam theory. The experimental values, shown in red, do not exhibit the high values of maximum principal stress predicted by the partial diagonal tension field theory, shown in green. The results just mentioned indicate that the diagonal tension field is not very well developed at the maximum fatigue loading. Figure 83 also

strengthens this conclusion. Some reduction in longitudinal stress is encountered in the compression zone of the VST specimens. No evidence of the secondary flange bending moments is found in the vicinity of the tension flange. The reduction of compressive stress in the compression zone is due to the buckling of the web. It is a well-known fact that the buckles in a girder web subjected to both bending and shear have a larger magnitude in the compression zone of the web than in the tension zone. Figure 84 depicts the compression zone longitudinal stresses for the VST and the HVSB girders. In general the longitudinal stresses are significantly reduced in the girders without the longitudinal stiffener.

7.2.1.4 Longitudinally Stiffened Girders with Varying Flange Rigidities

The use of a longitudinal stiffener is supposed to divide the web panel into two subpanels. For the series of tests reported herein, a longitudinal stiffener was furnished at the upper fifth point of two girders which were similar in other respects to the two FTSB test specimens. Theoretically, the buckling strength of the panel is controlled by each of the subpanels. The critical buckling load for the smallest subpanel is larger than the maximum fatigue load, therefore there should be no partial diagonal tension field in that subpanel. The critical buckling load for the lower subpanel was increased from 0.41 Wmf and 0.45 Wmf to 0.65 Wmf to 0.72 Wmf for panels 2 and 1, respectively, due to the addition of the longitudinal stiffener. The use of the longitudinal stiffener has very little effect on the stresses predicted by the ordinary flexure theory. A small increase in the moment of inertia of the cross-section and a slight shift in the centoidal axis are the only changes in the analysis due to the presence of a longitudinal stiffener.

The variation of the experimental membrane stresses with load is shown in Figs. 85 through 86. The gage locations denoted as B and C (See Fig. 15) are included in the upper small subpanel, while those locations identified as D, E, and F are in the lower subpanel. In all cases the test values of principal stresses exceeded those predicted by the beam theory. Surprisingly, the stresses measured in the small subpanel in which the critical load was not exceeded, exhibited behavior indicative of partial tension field action. Apparently the influence of the longitudinal stiffener was not very large in separating the behavior of the two subpanels. The magnitude and the general variation of the membrane stresses with increase in load were very similar in the corner locations, C and D, of both subpanels as may be seen in Figs. 85, 86, 87, 88, and 89. Figure 90 shows that both theoretical values of stress were exceeded in girder HSB-1 subjected to the maximum fatigue loading. For girder HSB-2 the beam theory values were exceeded at all locations, whereas the partial diagonal tension theory values were not exceeded by the experimental stresses as shown in Fig. 91. Test results reported by Cooper (12) suggested that stress redistribution in the web was reduced when longitudinal stiffeners are used. Figure 72 indicates some redistribution is prevented in the vicinity of the stiffener. Figure 83 also suggests a reduction in the web stress redistribution for the HVSB girder.

7.2.1.5 Longitudinally Stiffened Girders with Varying Transverse Stiffener Rigidities

The principal stresses obtained from girder HVSB-1 for various loads are plotted on Figs. 73 through 80 with the values obtained from the VST specimens. The addition of the longitudinal stiffener served to increase

the theoretical buckling strength of both subpanels. The changes in the theoretical values due to the addition of a longitudinal stiffener were small and were not plotted separately. It has been pointed out in earlier sections that a significant change in the flange thickness did not alter the beam theory values very much (See Fig. 86). The stresses in the VST tests were very close to the beam theory values, and those measured on girder HVSB-1 were even closer to the beam theory values in most cases.

Figure 77 is a good example of the results obtained in the three tests. Figure 92 also gives a good indication of the results obtained in the static test on HVSB-1. It is evident that the partial diagonal tension field has not developed in the web at a load equal to the maximum fatigue loading. The theoretical critical buckling load in the lower subpanels varied from 0.58 Wmf to 0.73 Wmf for the three panels.

7.2.2 Flexing Action of the Web

Prior to these tests, it was thought that a web with small initial deflections would experience a relatively large increase in deflection due to applied loads, while a girder web with a large initial deflection pattern would experience a smaller increase in deflections due to load. While this is probably true at a particular point, it does not hold true if different points are considered for the maximum initial deflection and the increase in deflection due to load. Figure 93 shows that there is no correlation between large initial deflections of a panel and a small range of deflection for the panel. Indeed, it seems that girders having small initial deflections also experience the smallest range of deflection due to load. These results are important in relation to the fatigue behavior of the girders and will be discussed further in section 7.3.

7.2.3 Discussion of the Behavior of the Stiffeners

7.2.3.1 Transverse Stiffeners

It was stated earlier in section 6.2.3.1 that the strains measured in the transverse stiffeners were much less than the theoretical values obtained by assuming that all of the vertical component of the tension field is supported by the stiffener. A decrease in strain is noted with increasing distance from the neutral axis. The maximum strain would theoretically occur in the lower portion of the transverse stiffener. Therefore the strains shown in Table 7 are in general agreement with theory. However, the magnitude of these experimentally obtained strains are not as large as the theoretical values. For example, the largest strain in Table 7 corresponds to a compressive stress of 25,650 psi and a stiffener force of 4.82^{k}. The vertical component of diagonal tension in panel 2 is 8.93^{k}. Therefore the stiffeners account for only 54% of the theoretical force in this case. It should be emphasized that the strain used in the example just cited was very large in comparison to the other strains shown in Table 7. The second largest strain shown for FTSB-6A corresponds to a stiffener force equal to 34% of the theoretical value. The stiffener forces tend to enforce the theory that the theoretical partial diagonal tension field force was only partly developed in the FTSB and the HSB girders.

Even lower values of stiffener strain and force were encountered in the tests on the VST and HVSB girders. This was not unexpected in view of the web membrane stresses discussed earlier. Since the web membrane stresses were almost equal to the beam theory values, very little evidence of partial diagonal tension field action could be expected in the transverse stiffeners.

Examination of the individual strain gage values indicated that a significant amount of bending was present in the stiffeners. Unequal strains were recorded for the four gages at each level of the double-sided stiffeners, and in some cases, both tensile and compressive strains were recorded indicating a large amount of bending. It was evident that the stiffeners in all the FTSB, HSB, VST and HVSB girders with the exception of VST 8-16A and HVSB-2 were inadequate to fulfill the function of providing a rigid boundary for the web panel. HVSB-2 was not tested statically.

7.2.3.2 Longitudinal Stiffeners

As previously mentioned, the longitudinal stiffeners were effective in controlling the lateral web deflections. Reference to Figs. 46 through 59 shows that deflections of the web in the small subpanel were very small, whereas large deflection patterns were encountered in the lower, larger subpanel. The stiffeners used were proportioned to meet the stiffness requirements for Massonnet's (9) optimum rigidity for longitudinal stiffeners. For design purposes, Massonnet (10) recommends the use of an increased stiffness, which would be seven times the optimum stiffness used in the tests reported herein. From Fig. 5 it may be seen that the present AASHO specifications require a stiffness less than Massonnet's optimum rigidity which was used in the German specifications. The longitudinal stiffeners in the HSB and HVSB girders were not adequate to furnish a completely rigid boundary as evidenced in Figs. 95, 96, and 97 where considerable bending of the stiffeners is observed. But, the stiffener did serve to separate the two subpanels and virtually eliminate the web flexing in the small subpanel. Much larger stiffeners were used in tests performed at Lehigh University (12) and no increase in ultimate strength was observed. P. B. Cooper (12)

concludes that an increase in strength is possible with larger stiffeners. Massonnet's factor of seven may be required if an increase in static strength is desired. However, in the present investigation the influence of the longitudinal stiffener on the fatigue behavior of the girder was the important factor. A reduction of the web stress redistribution, the virtual elimination of web deflection due to load in the small subpanel, and the effective separation of the large panel into the two subpanels are important in the fatigue behavior of the girders. From the test results it appears that stiffeners having a rigidity equal to Massonnet's optimum value are adequate to fulfill the above mentioned requirements.

7.2.4 Vertical Deflection of the Test Specimen

In order to determine the overall behavior of the girders, it is desirable to examine the load deflection curves shown in Figs. 98 through 101. The most unexpected behavior of the girders was the large increase in deflection at loads equal to only 1.25 Wmf or less. Girder FT-1A yielded extensively at W = 1.25 Wmf as shown in Fig. 98. A large increase in deflection was recorded for girder FTSB-2A. The nominal shear stress was 10.9 ksi for FTSB-2A at the maximum fatigue loading. The AISC specification allows 10.4 ksi for such a girder not subjected to repeated loads. The maximum bending stress was 14 ksi, which is far below the allowable value. Therefore, extensive yielding was observed at an overload of 10% which was unexpected. Girder FTSB-6A had flanges which were more rigid than FTSB-2A and Fig. 99 indicates that a load equal to 1.20 Wmf was applied before extensive yielding occurred. The longitudinally stiffened companion girders acted in much the same manner. It is thought that such a slight overload (10%) should not result in such large deflections. This behavior certainly doesn't reflect the purported factor of safety of 1.65 against yielding. Further study is recommended to resolve this apparent dilemma.

Higher loads were applied to the VST and HVSB specimens specimens before significant yielding was observed as shown in Fig. 101. Even at a load of 1.50 Wmf, the girders tested had not deflected an unreasonable amount. The high strength web material provided an extra margin of safety. The nominal shear stress applied to the girders was 10.7 ksi at W = Wmf, whereas the allowable shear stress was 17.7 ksi for the web material and geometry used. A depth-to-thickness ratio of 312 for the web is not allowed by the AISC specification which limits the ratio to 216 for the strength steel used. It is interesting to note that the specimens which exceeded the allowable code values had more reserve capacity then the girders judged acceptable by the same specification. For girders subjected to cyclic loadings, the design stresses are reduced, but if the structure is certain to undergo fewer than 2,000,000 cycles of loading this reduction is minimal.

7.3 Fatigue Behavior

7.3.1 Shear Girders with Varying Flange Rigidities

Flange rigidity is a factor which influences the fatigue behavior of thin web girders. Hall and Stallmeyer reported an increase in fatigue life with increasing flange rigidity. Figure 104 shows the fatigue lives plotted against the flange rigidity parameter for the FT girders. A general increase in the cycles to failure with increasing flange rigidity is noted for the earlier tests. There were not enough tests in the present investigation to conclude that the flange rigidity had a definite effect on the fatigue behavior, but the trend observed in the earlier tests is also evident in the latter tests. Two girders tested at Lehigh University (24) are included in the graph (designated as LF-1 and LF-2). It may be noted here that girders, such as those tested at Lehigh, with normal proportions as designed today, do not furnish a high flange rigidity. The only

difference between the specimens tested earlier and those of this investigation was the type of fabrication and the resulting smaller initial deflections. Therefore, the initial web deflections were thought to be important in influencing the fatigue behavior of the girders. An increase in fatigue life with decreasing initial deflections was noted. Figure 105 includes test results for the two larger Lehigh girders memtioned previously. No influence of size is noted in this figure. Three major types of stress influence the fatigue behavior of thin web girders and large initial deflections are indicative of the presence of two of these stresses, namely residual stress and membrane stress. The third type of stress, that due to the flexing of the web during each load cycle, was qualitatively measured by the range of deflection of the web. Figure 106 illustrates the variation in the number of cycles to failure with respect to the range of deflection during each loading cycle. With the exception of girders FT-1 and FT-4, a reasonably linear relationship is achieved on the semi-logarithmic plot. As expected, the fatigue behavior of thin web girders subjected to shear depends on three interacting stress conditions. The initial deflections of a girder web influence the initial membrane stresses and the geometry of the panel influences the development of that midplane stress after the load has been applied. The flexing action of the web due to the cyclic loading creates conditions of high stress at certain points. Added to this were the residual stresses which were not measured in these tests.

7.3.2 Girders with Varying Flange Rigidities Subjected to Shear and Bending

The fatigue cracks were located near the ends of the buckles in the panels as shown in Fig. 102. The fatigue crack initiated along the

web-stiffener junction. The crack formed at the base of the weld in the web and propagated vertically until the bottom of the crack turned and advanced into the web panel in a direction perpendicular to the tension field force. Figure 65 indicates that the tension present in girder FTSB-2A near the crack location was much higher than the beam theory predicted. In fact, the stress was slightly larger than the partial diagonal tension field value shown in Fig. 70.

Flange rigidity did not appear to have any effect on the fatigue behavior, whereas the earlier tests indicated an improvement in fatigue life with increasing flange rigidity; (see Fig. 107). The longitudinally stiffened girders were influenced by flange rigidity to about the same extent as the girders of the prior investigation. No correlation between the initial deflections and the fatigue lives was found in Fig. 108. However, Fig. 109 does indicate an improvement in fatigue life with decreasing flexing of the web. All of the girders of the present investigation enjoyed longer fatigue lives and one probable cause in addition to those evaluated in this study was the reduction of the heat input during welding and the resultant smaller residual stresses.

The longitudinally stiffened girders sustained higher fatigue lives than their unstiffened counterparts. This difference cannot be ascribed to the flange rigidity, initial deflections, or range of web deflections since these values were approximately equal for all the girders involved. There was no significant difference in the membrane stresses for girders FTSB-6A and HSB-2. The membrane stresses were largest in panel 1 of girder FTSB-2A and largest in panel 2 of HSB-1. No explanation can be given for the increase in fatigue life for the longitudinally stiffened girders at this time.

7.3.3 Girders with Varying Transverse Stiffener Rigidities

Hall and Stallmeyer (3) reported an increase in fatigue life for girders with very stiff or very flexible transverse stiffeners as opposed to those with intermediate sized stiffeners. Figure 110 indicates that the fatigue life was increased for girders with intermediate sized stiffeners and also for those with large stiffeners. The addition of the longitudinally stiffened girders to the graph reinforces the theory that intermediate size stiffeners are related to relatively shorter fatigue lives. Figures 111 and 112 suggest that perhaps the initial web deflection and range of deflection may have more of a bearing on the fatigue behavior than the transverse stiffener rigidity. Of course all of these factors are intermingled because the stiffness of the panel boundaries influences the web deflections.

8. SUMMARY AND CONCLUSIONS

8.1 Summary

The objectives of this investigation were to determine the influence of initial web distortion on the fatigue behavior of thin web girders and to determine the distribution of stresses along the panel boundaries. Plate girders with and without longitudinal stiffeners were tested in order to determine the influence of longitudinal stiffeners on fatigue behavior. Several parameters were chosen in order to study their effects on girder behavior. Flange rigidity and transverse stiffener rigidity were parameters used in earlier tests on girders subjected to fatigue loadings. Six model girders were fabricated with small initial web distortions in order to determine any influence of web distortion as compared to similar girders in the previous investigation. Four of the girders had varying flange rigidities, two of which were subjected to a large shearing force in conjunction with a small bending moment and the other two girders were subjected to combined shear and bending. Flange rigidities chosen were approximately equal to the extreme values in the previous tests. Two girders were tested having transverse stiffeners with intermediate and large rigidity values.

Four additional girders were tested having a longitudinal stiffener located at the upper fifth point of the web. Two of these girders had a variation in flange rigidity and two contained transverse stiffeners of rigidities similar to the girders without longitudinal stiffeners. All longitudinally stiffened girders were subjected to combined shear and

bending. Massonnet's optimum rigidity was used as the basis for the design of the longitudinal stiffener sizes.

Fatigue tests were performed with all ten girders. Upon completion of the fatigue tests, the girders were instrumented with electrical wire resistance strain gages and strain measurements were made during static tests to failure of the girder test section. One girder, longitudinally stiffened with the largest transverse stiffener rigidity, developed a fatigue crack in the tension flange in the region of the flange connection and was unsuitable for static testing.

The results obtained from these tests were analyzed and compared with the results obtained from nineteen similar tests performed in a previous investigation.

8.2 Conclusions

Initial web deformations were reduced by the use of a small diameter electrode and the selection of a welding sequence in order to reduce and distribute the heat input during fabrication of the specimens. As a result of this investigation, it was determined that model girders can be fabricated with web distortions comparable to those present in full size girders.

Web deflections changed gradually with the application of load to the girders. No critical buckling load for the panels was observed as was expected in panels having initial deflections. The orientation of the buckles shifted with increasing load and were, in general, parallel to the direction of the partial diagonal tension field. The deflection

patterns did not change appreciably with numerous applications of the load. The number of buckles in each panel was influenced by the geometry of the panel. Panels having a lower aspect ratio, α, contained a greater number of buckles than those panels with an aspect ratio nearer unity. No buckles were recorded in the small subpanels of the longitudinally stiffened girders.

Girders with varying flange rigidities, a $^{d}/t$ ratio of 267, and an aspect ratio, α, of 0.75 exhibited stresses along the web boundary which were intermediate in magnitude between the beam theory stresses and the partial diagonal tension field stresses. Secondary flange bending moments were observed in the girders with varying flange rigidities. The girders with varying transverse stiffener rigidities exhibited membrane stresses along the panel boundaries which were very close to the ordinary flexural theory values. The web depth to thickness ratio, $^{d}/t$, was 312 and the aspect ratio, α, was 0.5 for these girders.

The longitudinal stiffeners served to limit stress redistribution in the compression zone of the web near the location of the stiffener. In the girders with different flange rigidities, large membrane stresses were recorded even in the small subpanel where the theory predicts that the diagonal tension field will not develop. Massonnet's requirements for optimum rigidity for longitudinal stiffeners does not furnish a stiffener large enough to completely separate the panel into two subpanels and does not increase the static strength of the plate girder. The results pertaining to strength agree with results obtained from tests performed

at Lehigh reported by Cooper (12). The boundary rigidity afforded by the longitudinal stiffener influences the flexing action of the web due to cyclic loading. Therefore it is thought that the AASHO minimum requirements for longitudinal stiffeners should be increased to at least equal Massonnet's optimum rigidity value. Increase in size of the stiffener in order to obtain a higher static strength is apparently not economically feasible in view of the Lehigh results from girders with much stiffer longitudinal stiffeners.

An unexpected result was the lack of reserve strength in the girders with varying flange rigidities subjected to shear and bending. Extensive yielding and resulting large deflections were encountered at very small overloads above the maximum fatigue loading. Additional research on the static strength of similar girders is required.

Fatigue behavior of thin web girders is a very complex problem. The interaction of residual stresses, membrane stresses, and flexing stresses near the panel boundaries influences the initiation of a fatigue crack and its subsequent growth. The boundary rigidity of the panels influences the distortion of the web which, in turn, affects the membrane and flexing stresses. Initial distortion had a pronounced effect on the fatigue behavior of the girders tested. Improved fatigue lives were obtained for girders with small initial distortions which also displayed small flexing action due to load. Growth of the fatigue crack was slow and no loss of load nor increase in deflection was encountered with crack

lengths of one-sixth the depth of the girder. Rewelding cracks did not seem to affect the strength of the girders during the static tests. Inspection and repair of girders could be accomplished with comparative ease.

LIST OF REFERENCES

1. Wagner, H., "Flat Sheet Metal Girders with Very Thin Metal Web," Pts. I, II, III, N.A.C.A. T.M. Nos. 604, 605, 606, 1931.

2. Kuhn, P., "Investigation of the Incompletely Developed Diagonal Tension Field," N.A.C.A. Report No. 697, 1940.

3. Hall, L. R., and Stallmeyer, J. E., "Thin Web Girder Fatigue Behavior as Influenced by Boundary Rigidity," Structural Research Series No. 278, University of Illinois, January 1964.

4. Basler, K., and Thurlimann, B., "Strength of Plate Girders in Bending," Journal of the Structural Division, A.S.C.E., Vol. 87, No. ST6, August 1961.

5. Basler, K., "Strength of Plate Girders in Shear," Fritz Engineering Laboratory Report No. 251-20, Lehigh University, December 1960.

6. Basler, K., Yen, B. T., Mueller, J. A., and Thürliman, B., "Web Buckling Tests on Welded Plate Girders, Part 4, Tests on Plate Girders Subjected to Combined Bending and Shear," Fritz Engineering Laboratory Report No. 251-14, Lehigh University, May 1960.

7. Klöppel, K., and Scheer, J. S., Beulwerte Ausgesteifter Rechteckplatten, Verlag von Wilhelm Ernst and Sohn, Berlin, 1960.

8. Massonnet, Ch., "Essai de Voilement sur Poutres a Ame Raidie," Publ. I.A.B.S.E., Vol. 14, 1954.

9. Massonnet, Ch., "Voilement des Plaques Planes Sollicitees dan Leur Plan," C.E.C.M. Notes Techniques, B-13.2, Brussels.

10. Massonnet, Ch., "Stability Considerations in the Design of Steel Girders," Transactions of the American Society of Civil Engineers, Vol. 127, Part II, 1962.

11. Rockey, K. C., "Web Buckling and the Design of Webplates," The Structural Engineer, February and September, 1968.

12. Cooper, P. B., "Bending and Shear Strength of Longitudinally Stiffened Plate Girders," Fritz Engineering Laboratory Report No. 304.6, Lehigh University, September, 1965.

13. Dudley, K. E., Mueller, J. A., and Yen, B. T., "Lateral Web Deflections of Welded Test Girders," Fritz Engineering Laboratory Report No. 303.4, Lehigh University, June 1966.

14. Bergman, S. G. A., Behavior of Buckled Rectangular Plates Under the Action of Shearing Forces Along All Edges, Victor Pettersons Bokindustriaktiebolag, Stockholm, 1948.

15. Deutscher Normanausschuss, DIN 4114, Blatt 1 and 2, Beuth-Vertrieb B.m.b.H., Berlin WI5 and Koln, 1952.

16. Massonnet, Ch., and Greisch, R., "Beulsicherheitsberechnung Entsprechend der DIN 4114 mit Helfe eines Nomogramms," Stahlbau, Vol. 26, 1957.

17. American Association of State Highway Officials, Standard Specifications for Highway Bridges, 1961.

18. Legett, D.M.A., and Hopkins, H. G., "The Effect of Flange Stiffness on the Stresses in a Plate Web Spar Under Shear," R.& M. No. 2434, H.M. Stationery Office.

19. Rockey, K. C., "Plate Girder Design, Flange Stiffness and Web Plate Behavior," Engineering, December 20, 1957.

20. Moore, R. L., "An Investigation on the Effectiveness of Stiffeners on Shear-Resistant Plate-Girder Webs," N.A.C.A. T.N. No. 862, September 1942.

21. Longbottom, E., and Heyman, J., "Experimental Verification of the Strengths of Plate Girders Designed in Accordance with the Revised British Standard 153: Tests on Full-size and on Model Plate Girders," Proceedings of the Institution of Civil Engineers, Vol. 5, Part 3, Structural Paper No. 49, 1956.

22. Rockey, K. C., "The Design of Intermediate Vertical Stiffeners on Web Plates Subjected to Shear," Aeronautical Quarterly, Vol. VII, November 1956.

23. American Institute of Steel Construction, Manual of Steel Construction, 1963.

24. Yen, B. T., "On the Fatigue Strength of Welded Plate Girders," Fritz Engineering Laboratory Report No. 303.1, Lehigh University, November 1963.

25. D'Apice, M. A., and Cooper, P. B., "Static Bending Tests on Longitudinally Stiffened Plate Girders," Fritz Engineering Laboratory Report No. 304.5, Lehigh University, April 1965.

TABLE 1

INITIAL WEB DEFLECTIONS IN GIRDER PANELS

Reported by Dudley, Mueller, and Yen (13)

Aspect Ratio α	Web Slenderness Ratio $\beta = d/t$	Initial Deflections w_o (inches)	$\frac{w_o}{t}$
1.5	264	0.608	3.217
1.5	264	0.493	2.609
1.0	294	0.131	0.771
1.0	294	0.101	0.594
1.0	294	0.171	1.006
1.0	288	0.255	1.465
1.0	288	0.150	0.860
1.0	288	0.135	0.776
1.0	275	0.362	1.989
1.0	275	0.191	1.049
1.0	275	0.280	1.538
1.0	274	0.253	1.390
1.0	274	0.184	1.011
1.0	274	0.279	1.533
1.0	263	0.206	1.084
1.0	263	0.191	1.005
1.0	263	0.053	0.394
1.0	260	0.208	1.083
1.0	260	0.161	0.838
1.0	260	0.142	0.739
1.0	255	0.34	1.8

TABLE 2

WEB DEFLECTION COMPARISON FOR LEHIGH GIRDERS (25)

Specimen	α	γ	w_{max} (in.)	w_o (in.)	Δw %
LB1	1.0	0	0.221	0.092	140
LB2	1.0	38.4	0.215	0.186	16
LB3	1.0	75.1	0.256	0.225	14
LB4	1.5	38.4	0.232	0.166	40
LB5	0.75	38.4	0.076	0.065	17

TABLE 3

PHYSICAL PROPERTIES AND CHEMICAL ANALYSIS OF WEB MATERIALS

ASTM Designation	A 415-58T	A 441-64T
	0.075	0.060
Yield Strength psi	33,300	57,500
Ultimate Strengty psi	43,200	71,800
Elongation in 8 inches	28.7	22.0
Carbon Percent	0.15	0.17
Manganese	0.60	1.20
Phosphorus	0.040	0.014
Sulfer	0.050	0.010
Silicon	--	0.030
Copper	--	0.07
Nickel	--	0.04

TABLE 4

RESULTS OF TESTS ON GIRDERS WITH VARIOUS FLANGE SIZES SUBJECTED TO SHEAR

Girder	Flange Thickness in.	Fabrication Distortion Initial w_o/t	Maximum Load w/t	Range w/t	Cycles to Failure
FT-1	1/4	3.2	6.8	0.60	251,900
FT-1A	1/4	1.2	1.9	0.48	2,250,000
FT-2	3/8	2.8	5.3	0.91	293,900
FT-3	1/2	2.1	2.9	0.66	915,600
FT-9	1/2	2.0	2.2	0.77	508,600
FT-4	5/8	3.3	4.5	0.37	476,900
FT-5	3/4	2.8	3.8	0.91	408,300
FT-6	1	2.1	3.5	0.53	863,400
FT-10	1	3.4	3.2	0.77	621,400
FT-10A	1	1.8	2.2	0.45	3,500,000 (no failure)
LF1		3.22			330,000
LF2		1.13			~ 2,000,000

TABLE 5

RESULTS OF FLANGE RIGIDITY ON GIRDERS SUBJECTED TO SHEAR AND BENDING

Girder	Flange Size	Initial w		Max. Load w/t		Range w/t		Cycles to
		Panel 1	Panel 2	Panel 1	Panel 2	Panel 1	Panel 2	Failure
FTSB-1	4-3/8x1/4	3.64	4.79	3.72	4.70	1.38	1.25	--
FTSB-2	2-7/8x3/8	3.86	3.47	4.21	3.50	1.32	1.06	40,000
FTSB-2A	4 x3/8	4.64	1.46*	4.52	3.32	0.57	0.60	356,400
FTSB-3	2-1/8x1/2	3.34	3.96	--	--	--	--	32,000
FTSB-4	1-5/8x5/8	3.18	3.03	3.89	3.38	1.11	0.88	49,000
FTSB-5	1-3/8x3/4	3.76	1.94	3.78	2.85	1.04	0.72	84,000
FTSB-6A	1-1/2x 1	2.90	2.09	3.43	4.04	1.09	0.84	362,000
FTSB-6	1 x 1	4.20	3.50	4.32	4.52	1.21	1.23	101,000
HSB-1	4 x3/8	3.28	3.62	4.54	3.06	0.60	0.59	500,900
HSB-2	2-1/2x3/4	3.28	3.20	4.30	4.05	0.67	0.59	1,266,000

* Web deflection after full load had been applied.

TABLE 6

TEST RESULTS FOR GIRDERS WITH VARIOUS STIFFENER SIZES

Specimen	Stiffener Size in.	Initial w/t			Maximum w/t			Cycles to Failure	Range s/t		
		Panel 1	Panel 2	Panel 3	Panel 1	Panel 2	Panel 3		1	Panel 2	3
VST 16-8	1/16 x 1/2	--	3.4	--	--	3.5	--	239,000		1.2	
VST 8-4	1/8 x 1/2	--	2.7		--	2.8	--	55,000		0.5	
VST 8-4A	1/8 x 1/2	1.33	1.28	0.90	1.88	1.27	0.90	1,454,000	0.85	0.45	0.55
VST 8-6	1/8 x 3/4	--	2.4	--	--	2.8	--	52,000		0.7	
VST 8-10	1/8 x 1 1/4	--	2.0	--	--	2.2	--	52,000		0.7	
VST 8-16	1/8 x 2	--	1.7	--	--	2.5	--	250,000		0.6	
VST 8-16A	1/8 x 2	0.97	1.02	2.06	1.03	1.17	2.30	1,121,000	0.85	0.42	0.97
HVSB-2	1/8 x 1 1/4	1.68	0.88	2.02	1.97	1.20	1.63	510,000	0.41	0.50	1.15
HVSB-2	1/4 x 2 1/2	0.52	0.32	0.35	0.62	0.55	0.87	3,000,000 (no failure)	0.25	0.32	0.45

TABLE 7

AVERAGE TRANSVERSE STIFFENER STRAINS

Girder	Strain (microinches/inch) Location*								
	Edge Panel 1			Panel 1 - Panel 2			Edge Panel 2		
	X	Y	Z	X	Y	Z	X	Y	Z
FTSB2A	-150	-215	-180	-855	-445	-177	-187	-107	-35
FTSB-6A	- 82	- 87	- 35	-547	-310	-116	- 77	- 70	-32
HSB-1	- 30	+ 70	---	-255	-175	---	- 90	- 70	--
HSB-2	- 10	+ 40	---	- 70	- 46	---	- 90	-135	--

* See Fig. 94 for gage locations.

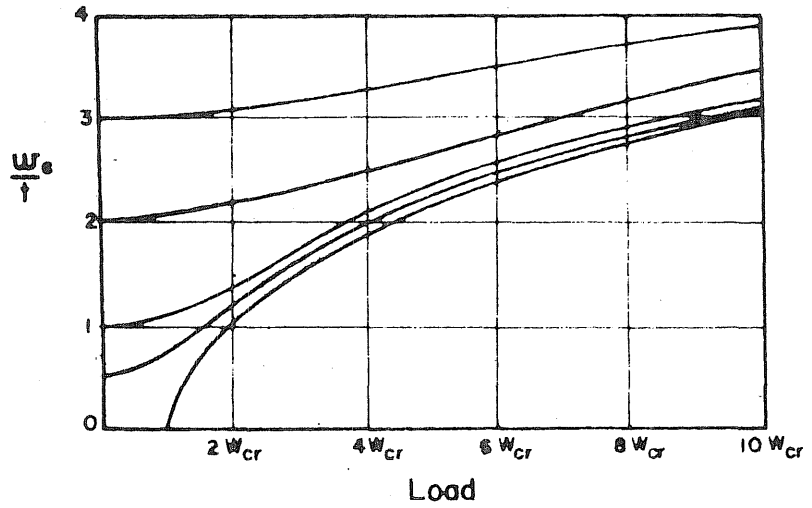

w_c Lateral web deflections at center of web panel.
t Thickness of web plate.
w_{cr} The theoretical buckling load of an ideal web panel with simply supported rigid boundaries.

FIG. 1 MAXIMUM DEFLECTIONS AT THE CENTERS OF SQUARE SHEAR PANELS WITH INITIAL DEFLECTIONS AND RIGID BOUNDARIES.

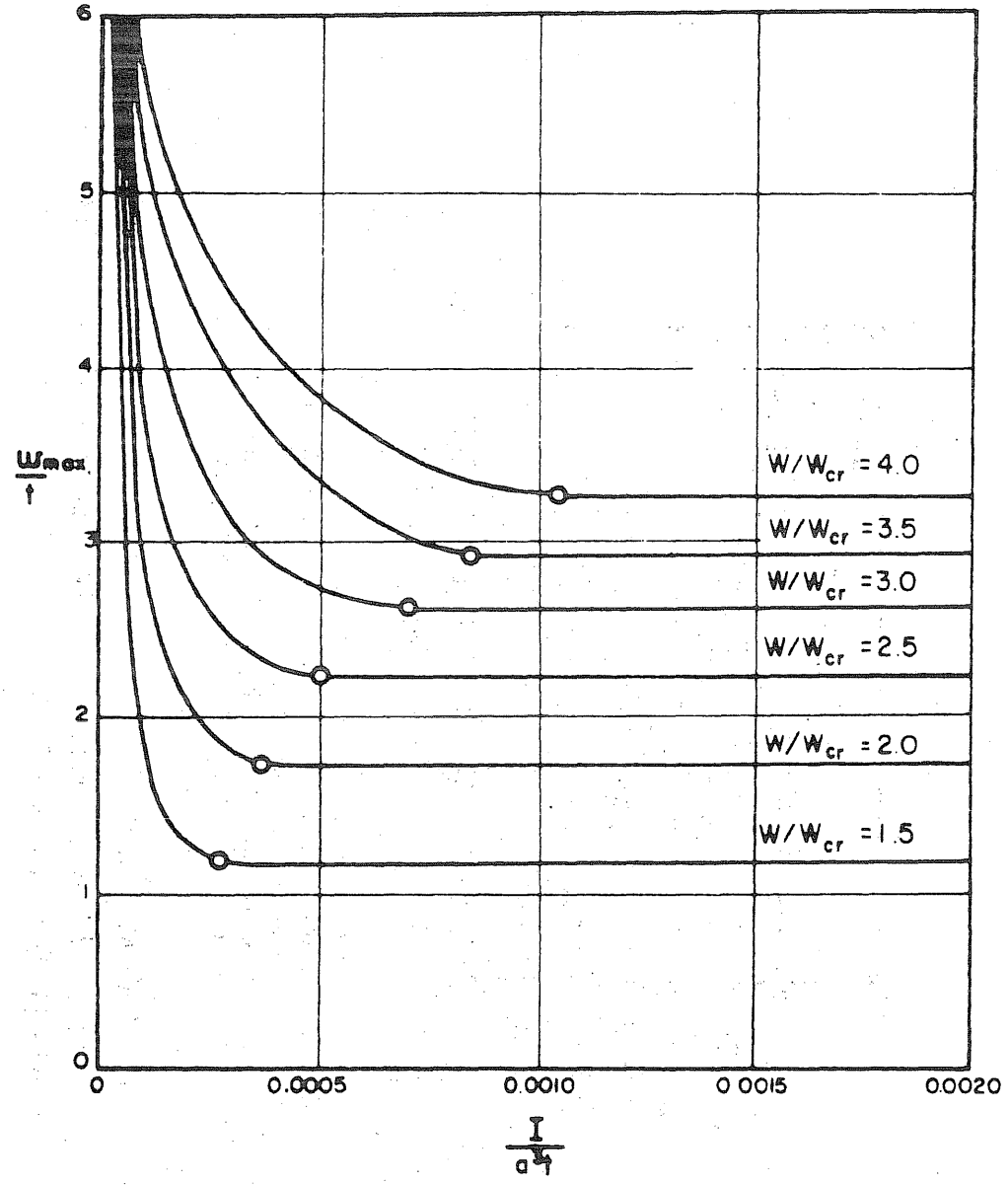

w_{max} Maximum lateral web deflection

FIG. 2 RELATIONSHIP BETWEEN LATERAL WEB DEFLECTION, FLANGE RIGIDITY AND LOAD FOR PLATE GIRDER WEB PANELS.

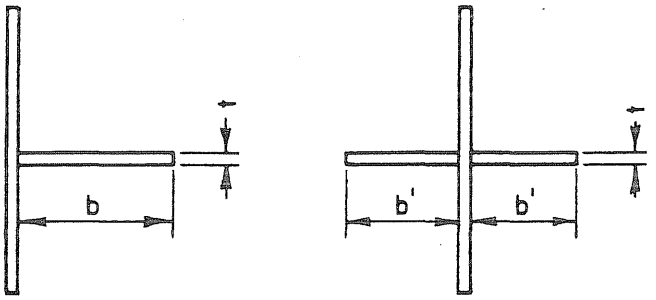

FIG. 3 SINGLE AND DOUBLE SIDED STIFFENERS.

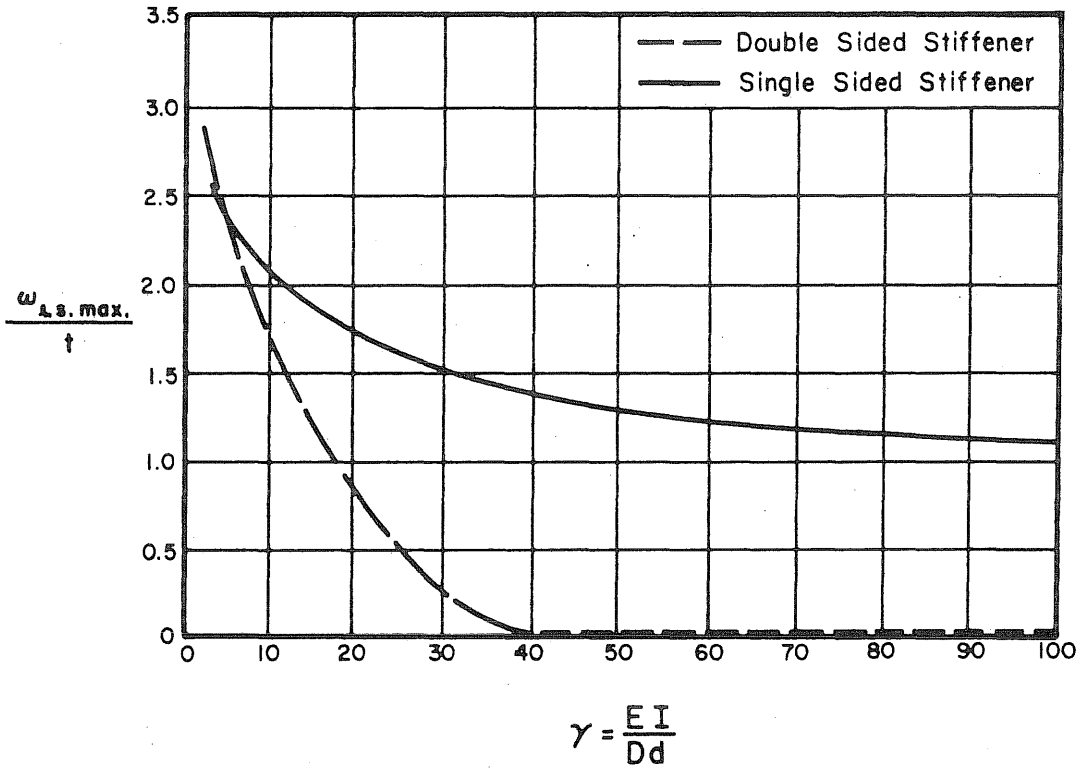

FIG. 4 MAXIMUM LATERAL DEFLECTION OF LONGITUDINAL STIFFENER VS. STIFFENER RIGIDITY.

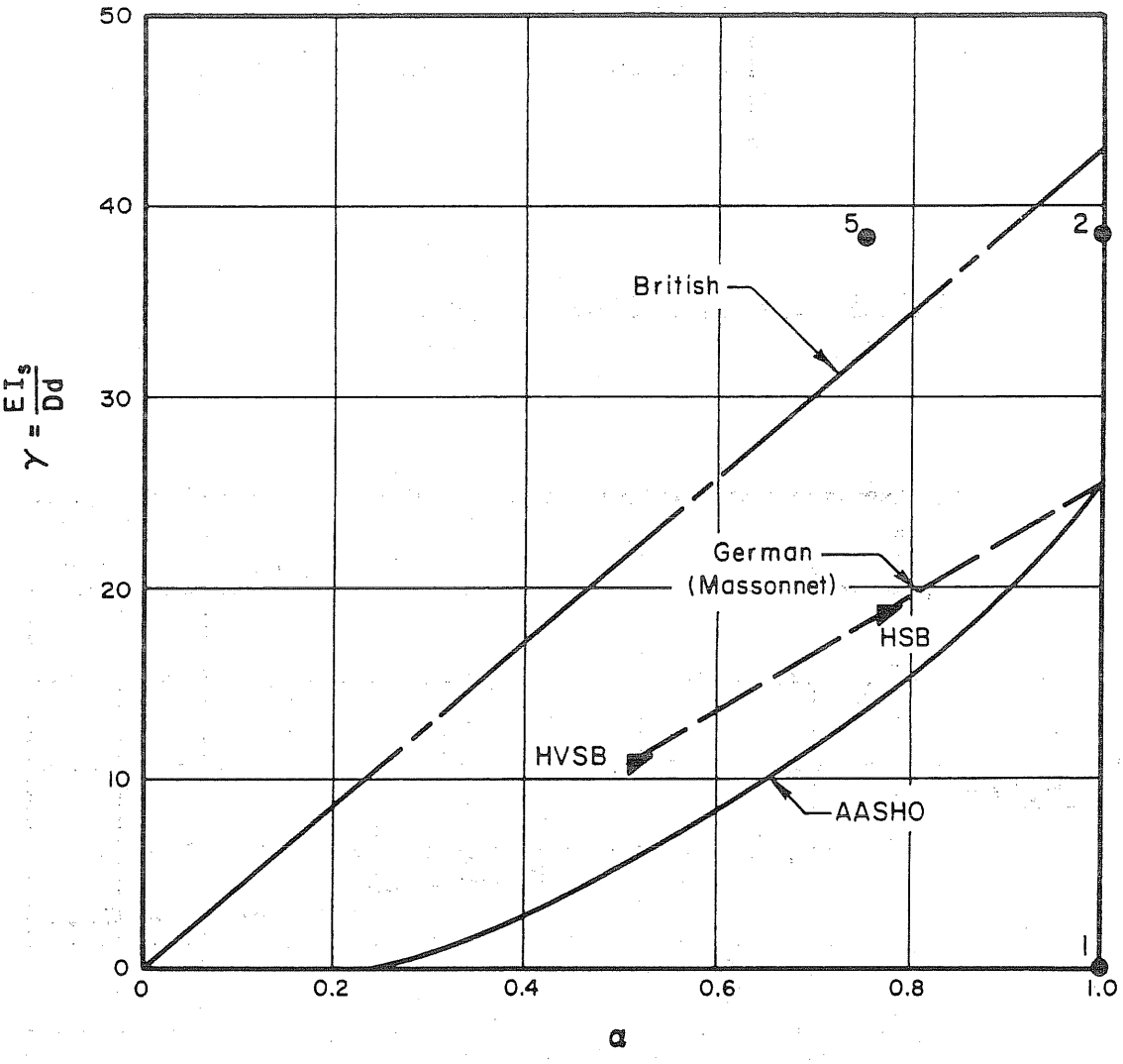

FIG.5 LONGITUDINAL STIFFENER RIGIDITY REQUIREMENTS.

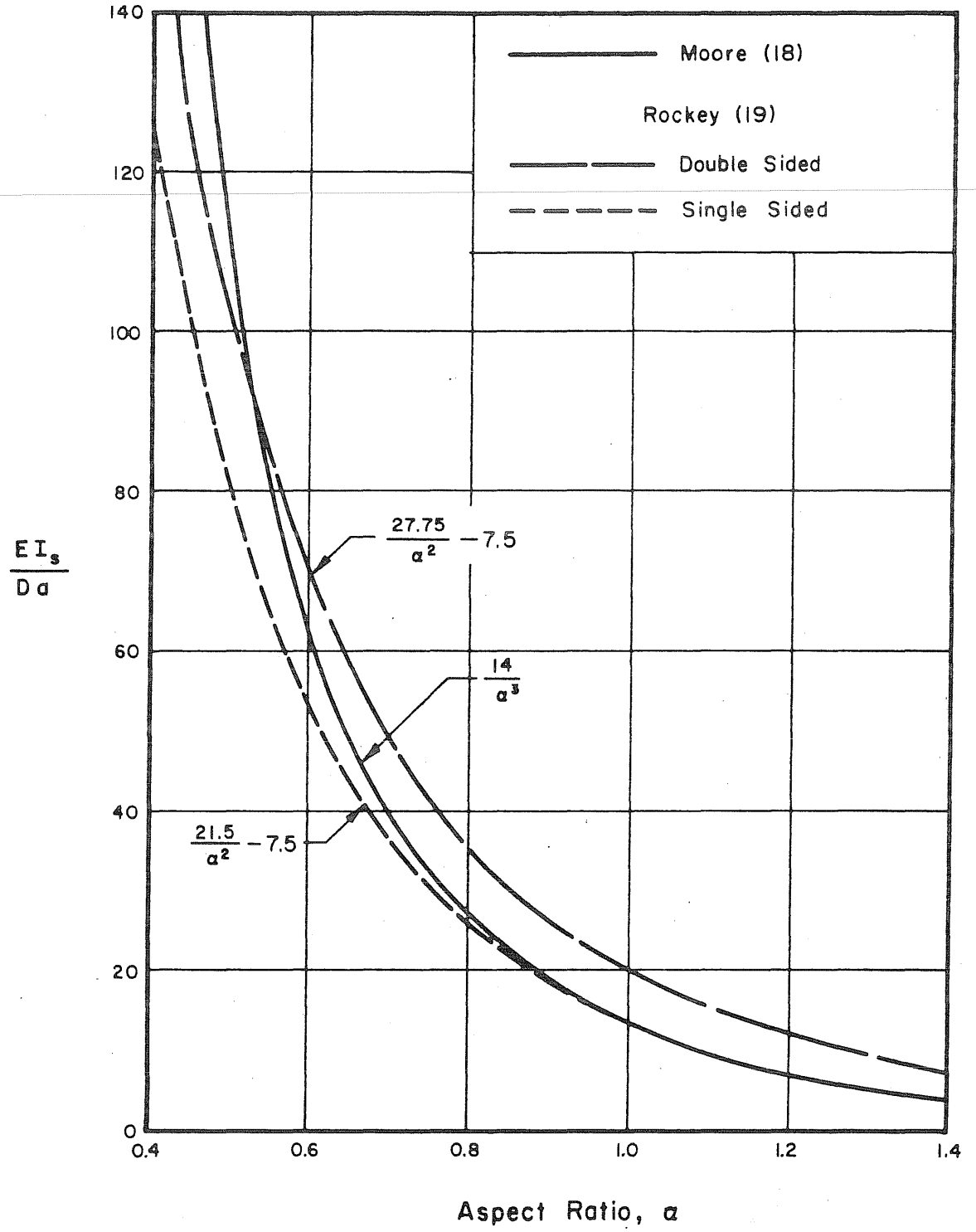

FIG. 6 LIMITING VALUES OF TRANSVERSE STIFFENER RIGIDITY AS A FUNCTION OF THE ASPECT RATIO.

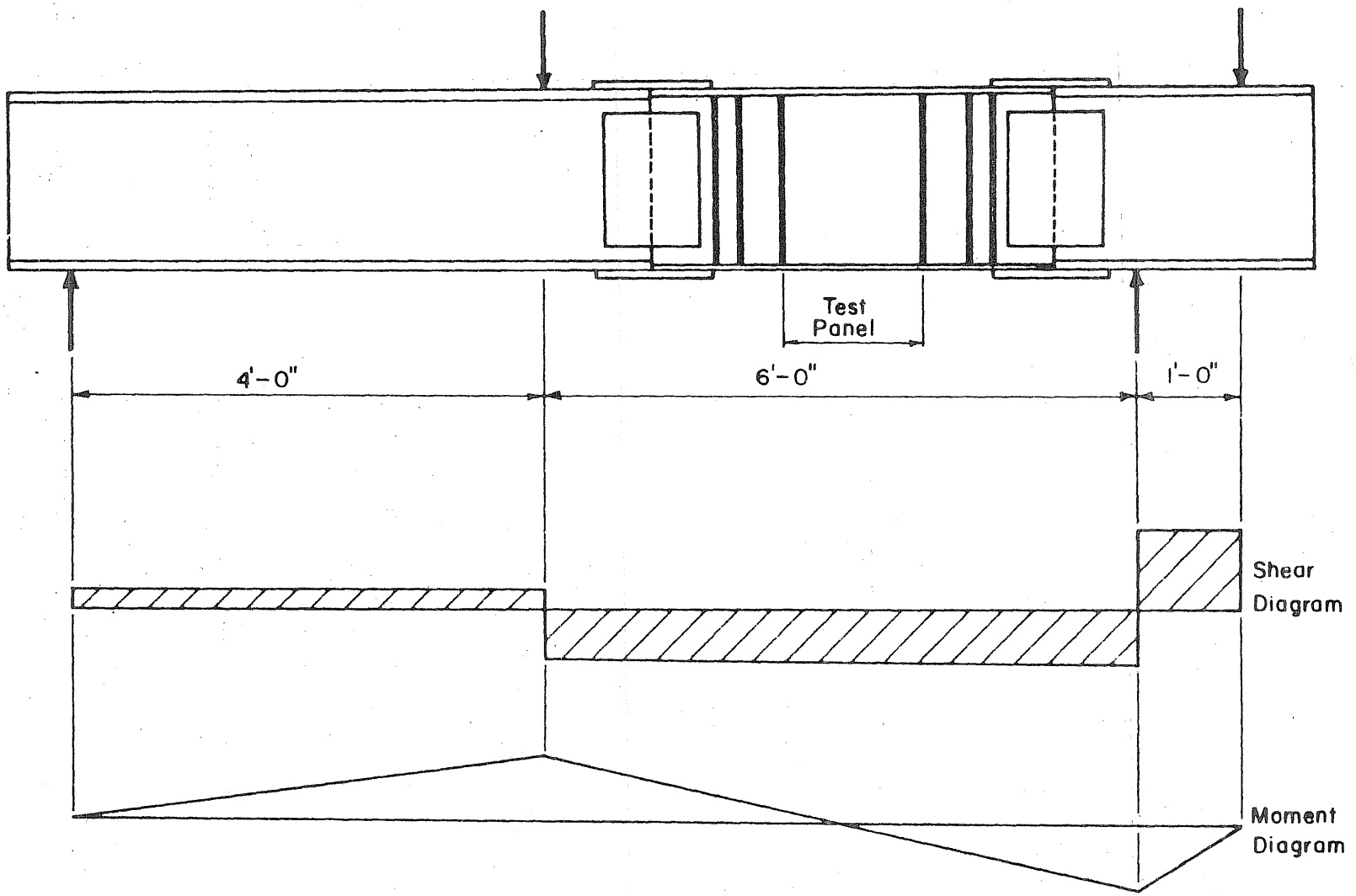

FIG. 7 GIRDERS WITH VARIOUS FLANGE SIZES SUBJECTED TO SHEAR.

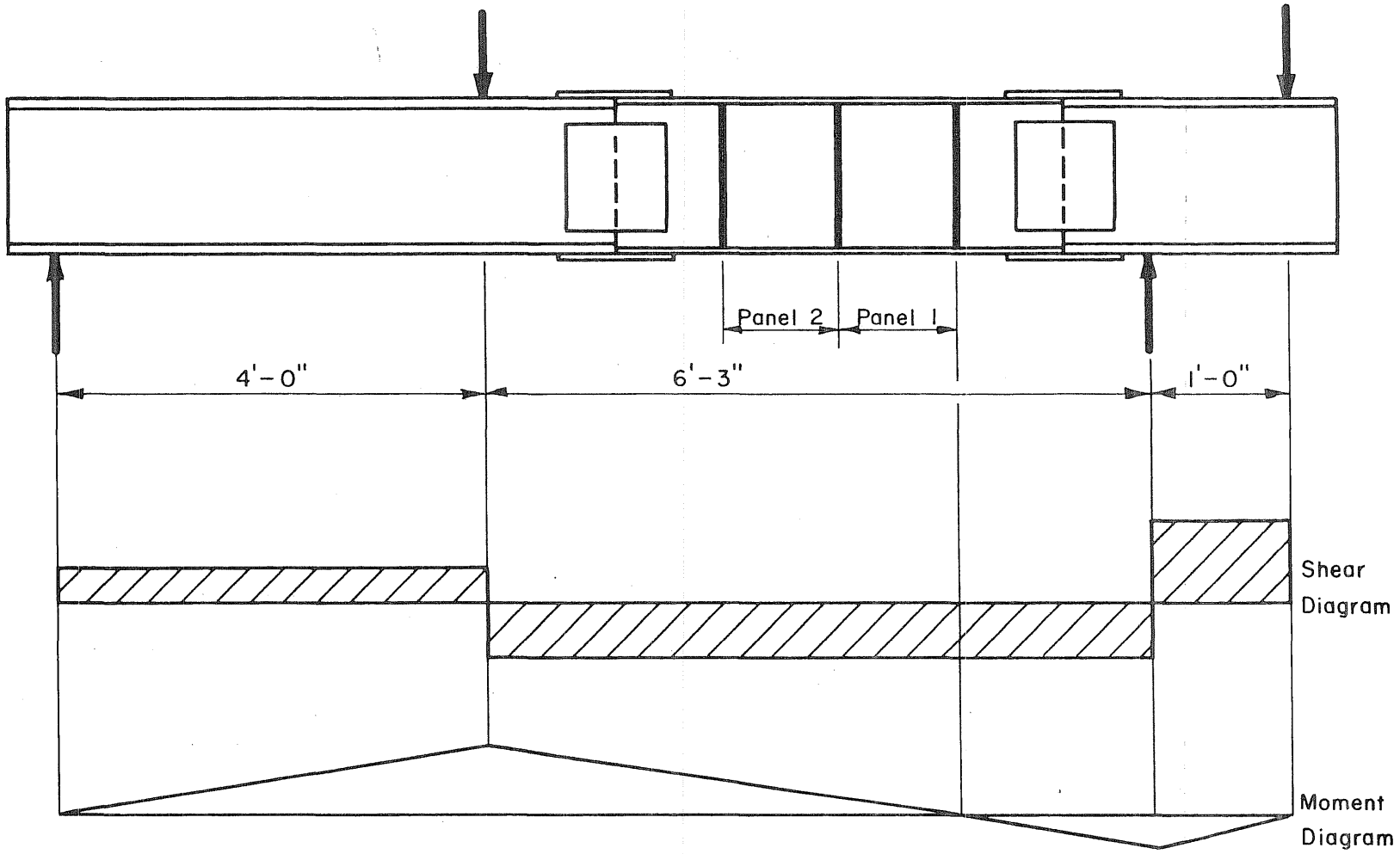

FIG. 8 GIRDERS WITH VARIOUS FLANGE SIZES SUBJECTED TO SHEAR AND MOMENT.

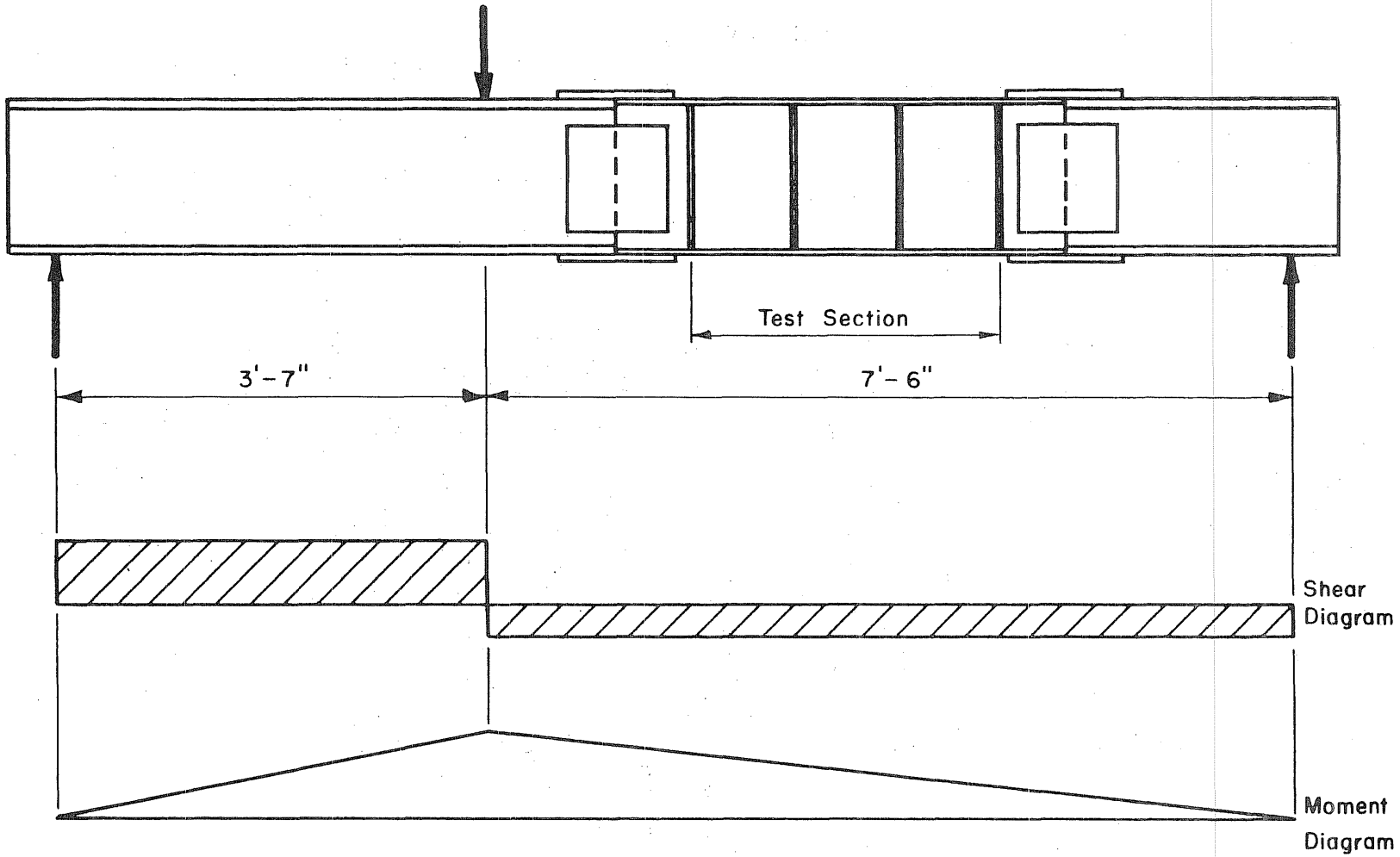

FIG. 9 GIRDERS WITH VARIOUS STIFFENER SIZES.

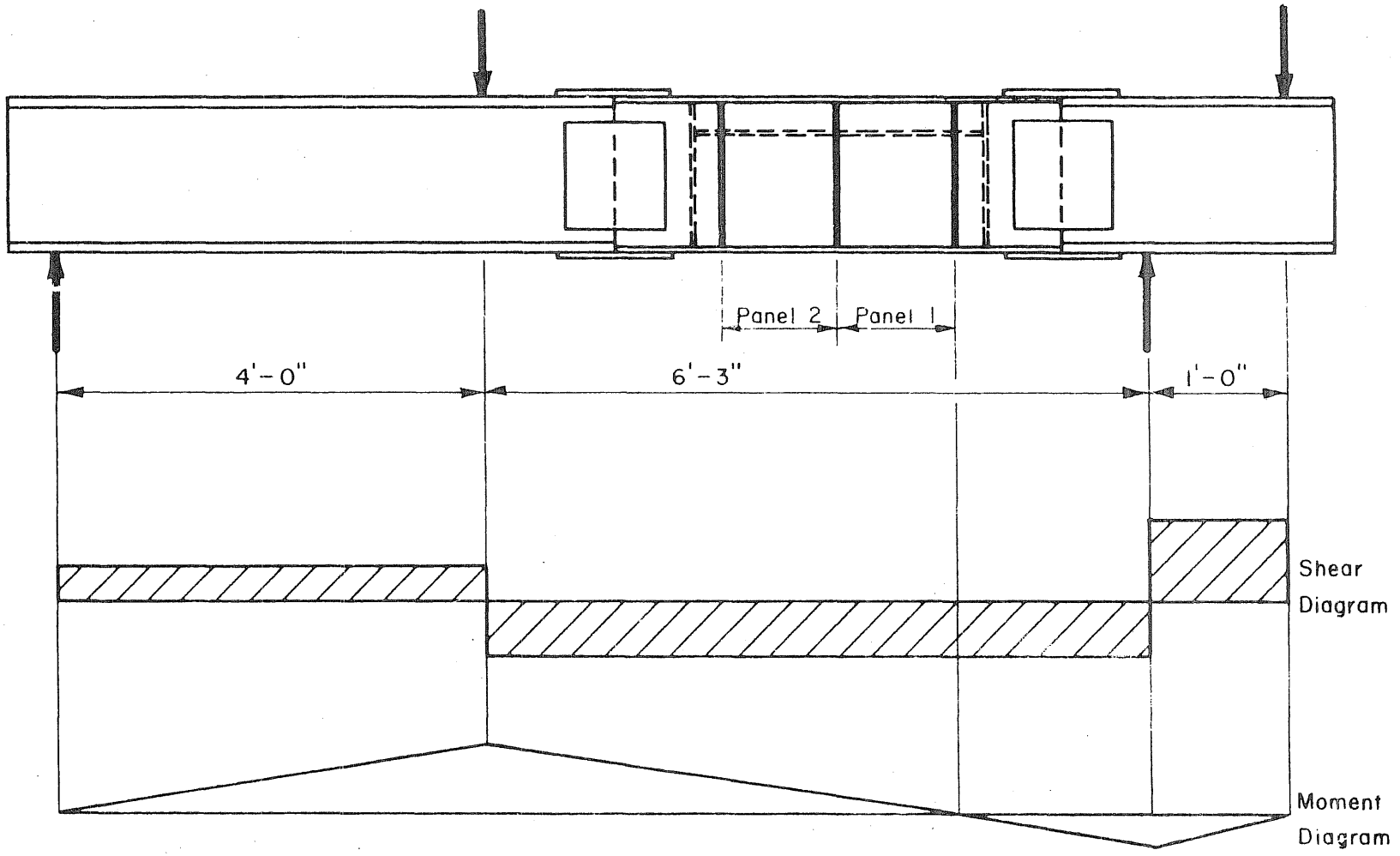

FIG. 10 LONGITUDINALLY STIFFENED GIRDERS WITH VARIOUS FLANGE RIGIDITIES SUBJECTED TO SHEAR AND MOMENT.

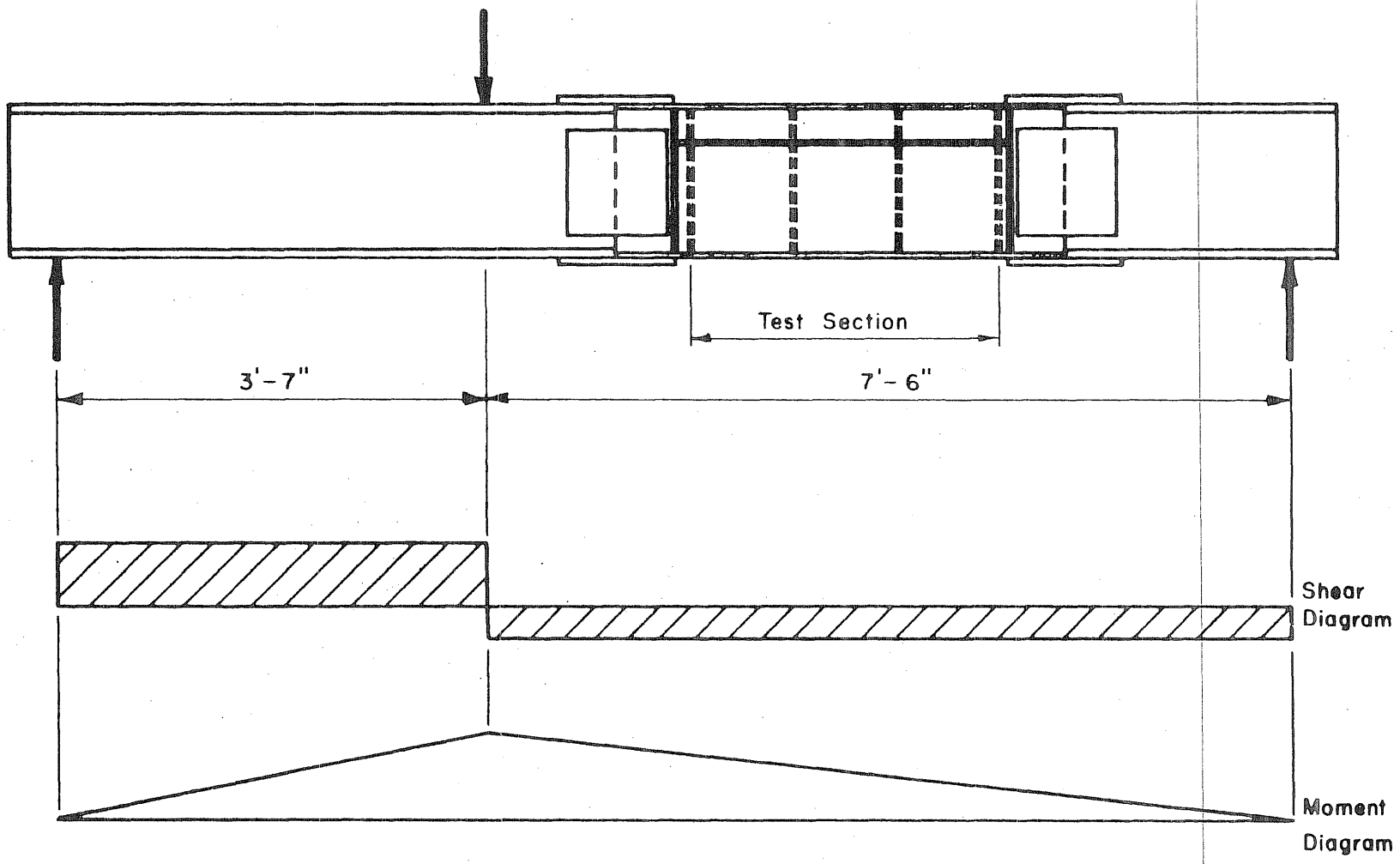

FIG. 11 LONGITUDINALLY STIFFENED GIRDERS WITH VARIOUS TRANSVERSE STIFFENER RIGIDITIES.

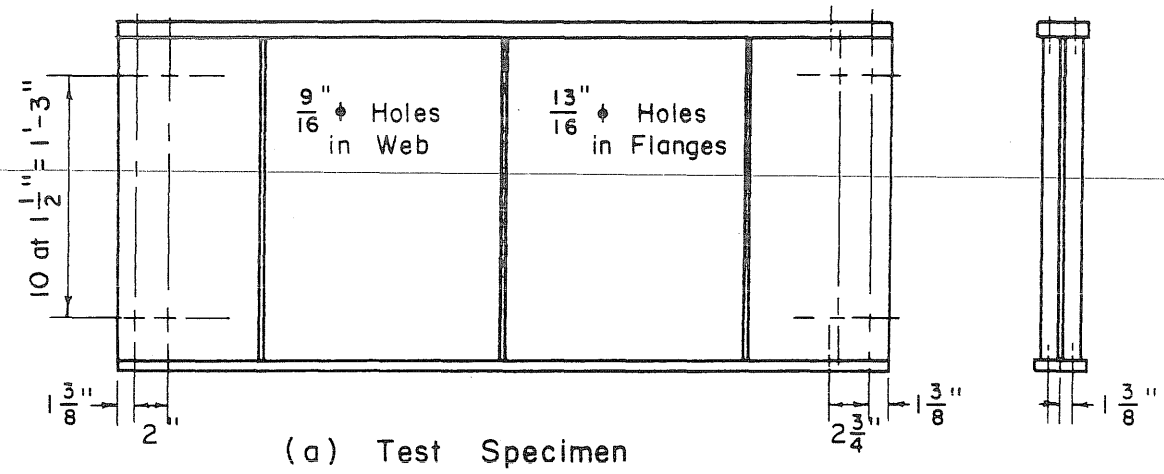

(a) Test Specimen

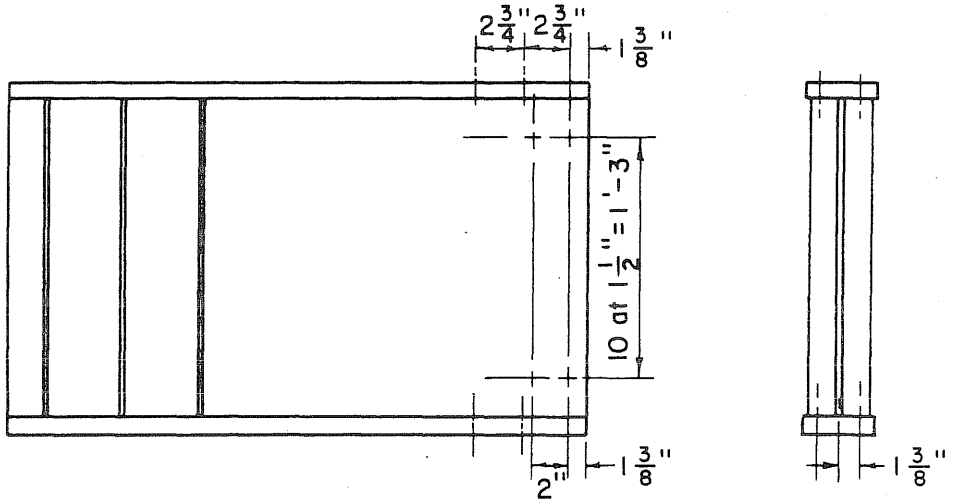

(b) Typical Short End Section

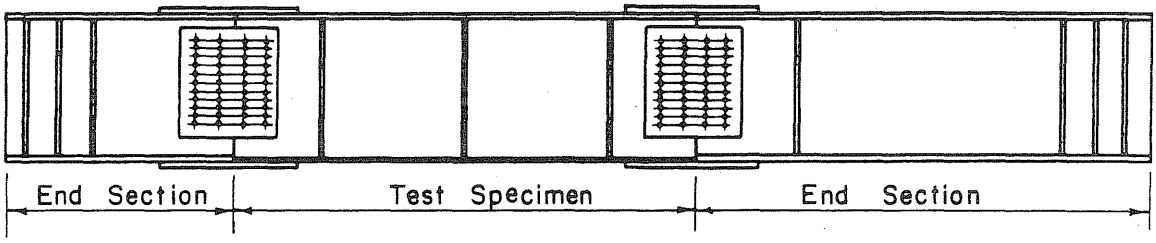

(c) Typical Assembly of Girders

FIG. 12 TYPICAL DIMENSIONS OF CONNECTION DETAILS.

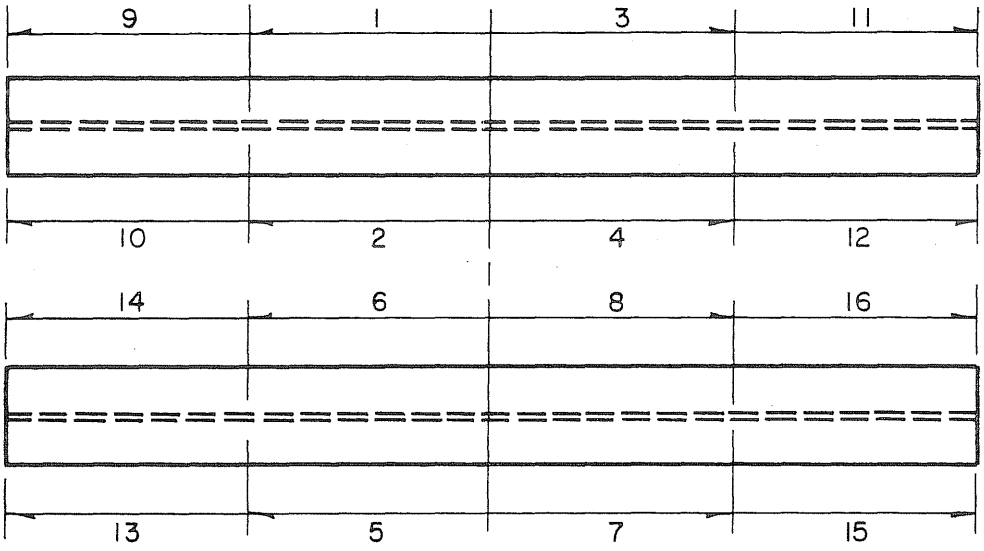

12 inch passes

(a) Web To Flange Welding Sequence

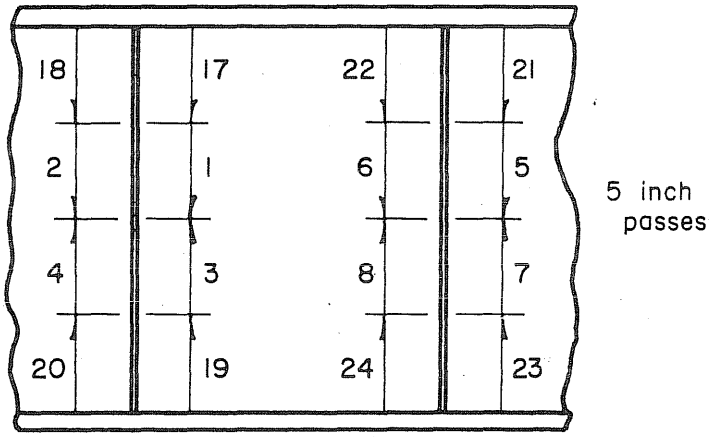

5 inch passes

(b) Stiffener To Web Welding Sequence

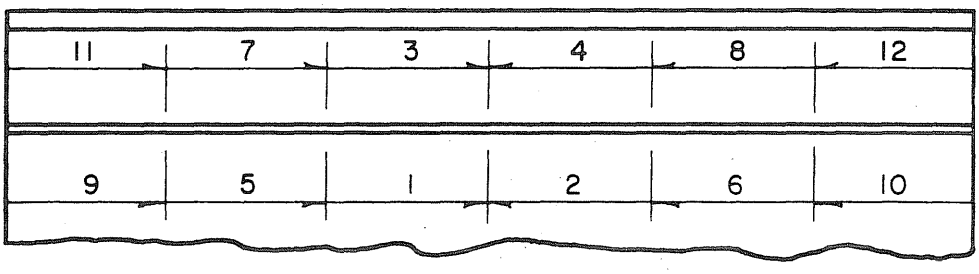

6 inch passes

(c) Longitudinal Stiffener Welding Sequence

FIG. 13 WELDING SEQUENCE FOR TEST SPECIMENS.

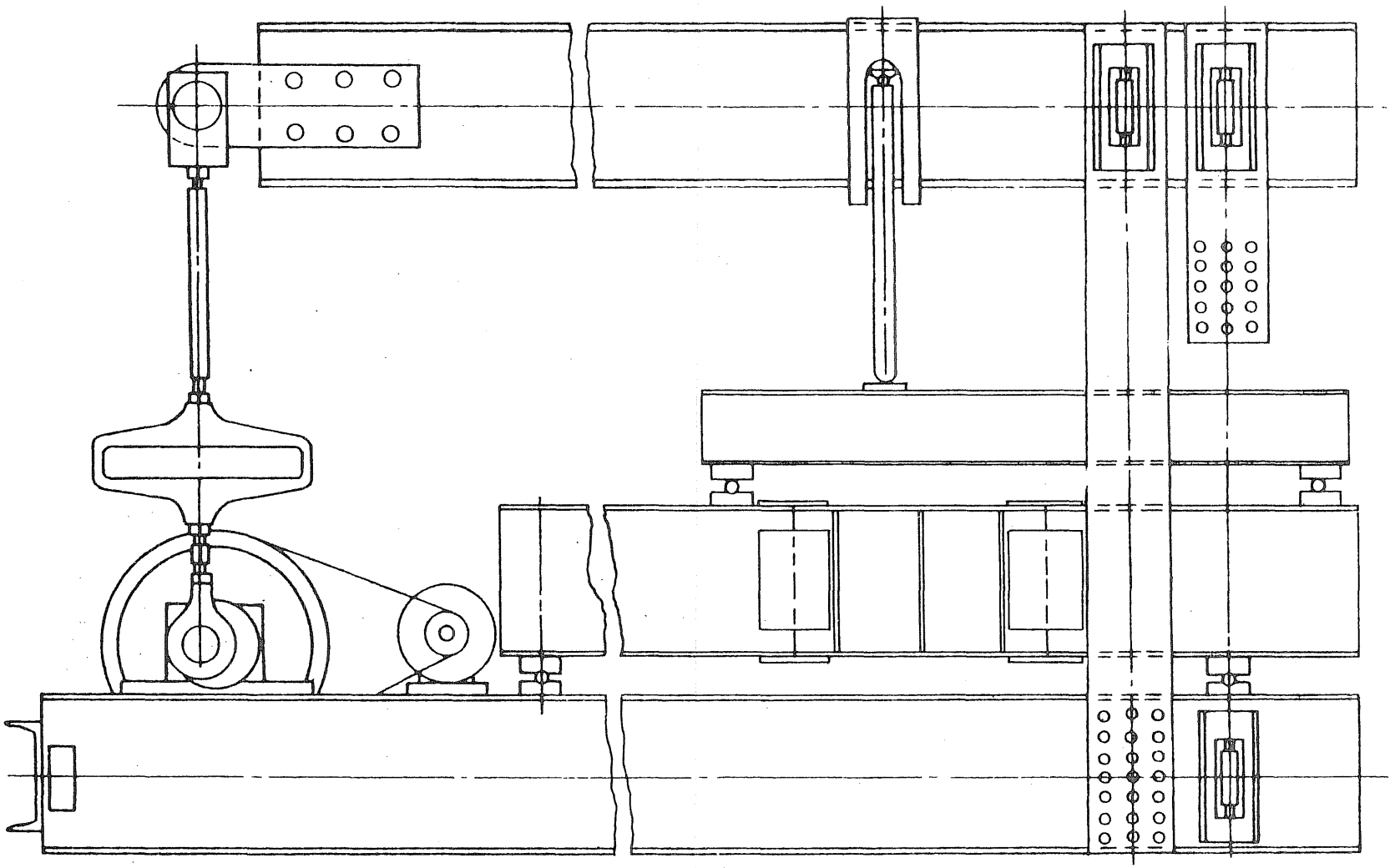

FIG. 14 LOADING ARRANGEMENT IN LEVER FATIGUE MACHINE

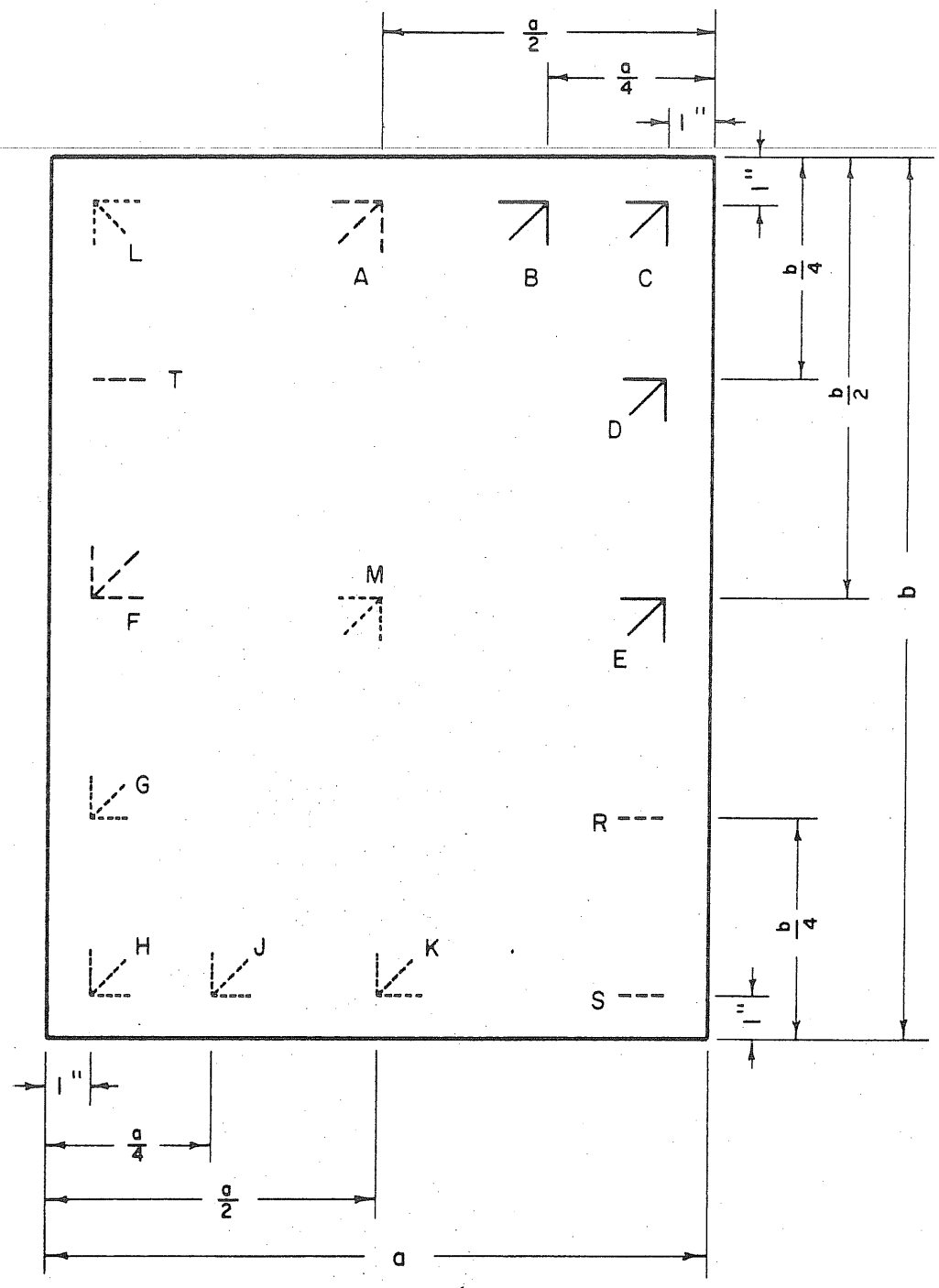

FIG. 15 TYPICAL STRAIN GAGE LOCATIONS.

Note: Web deflections are given in inches.

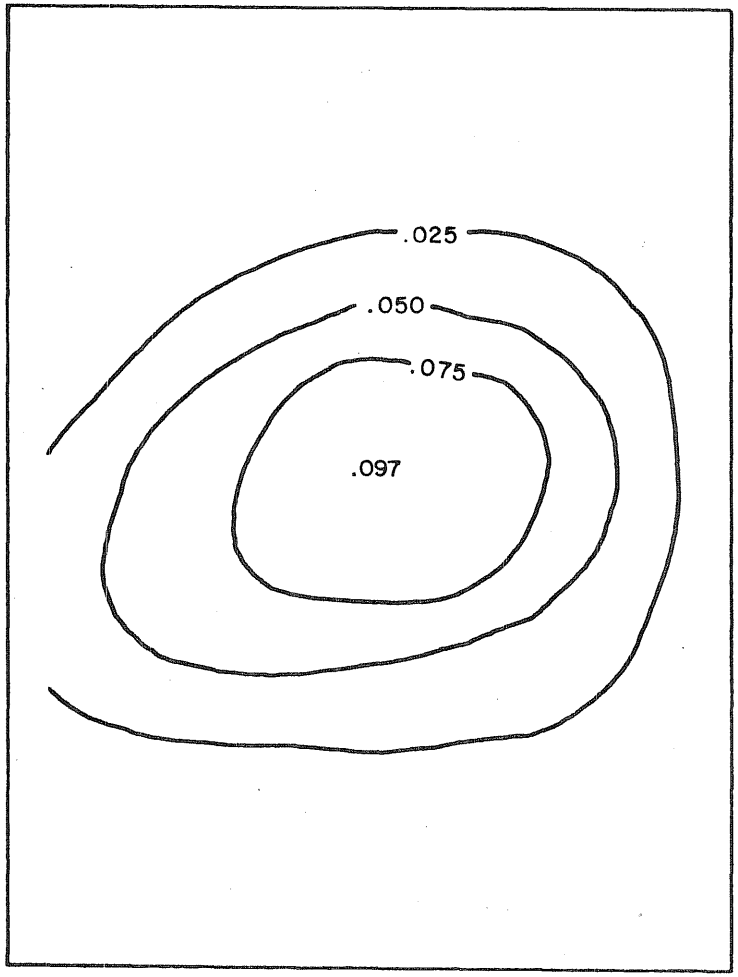

FT-1A

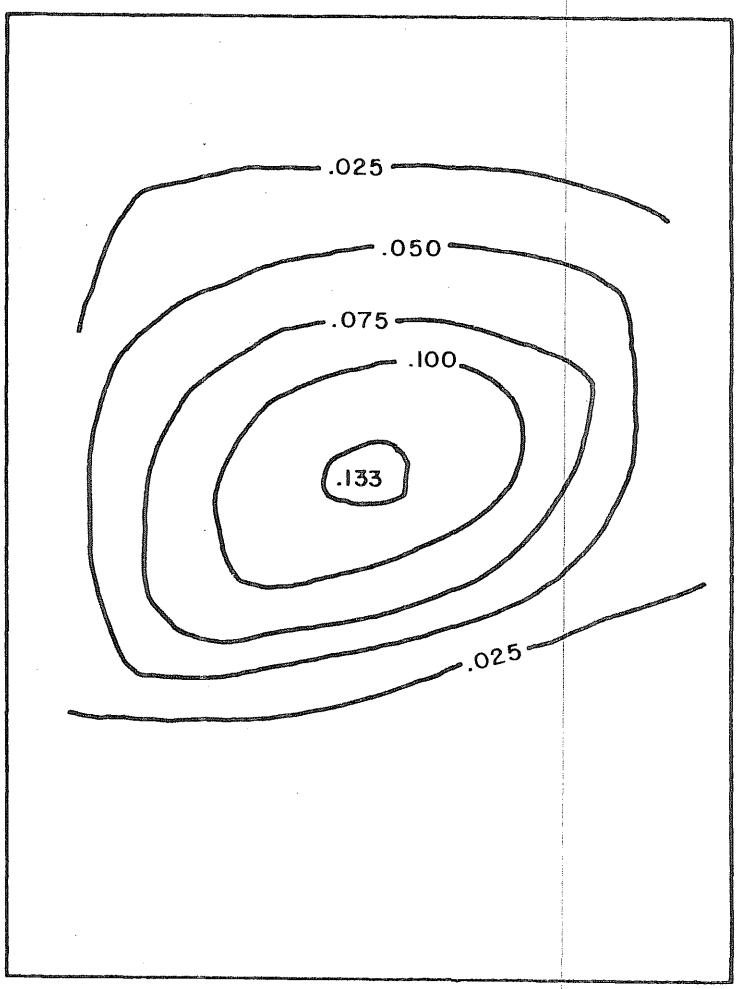

FT-10A

FIG. 16 INITIAL WEB DEFLECTIONS OF FT-1A AND FT-10A.

Note: Web deflections are given in inches.

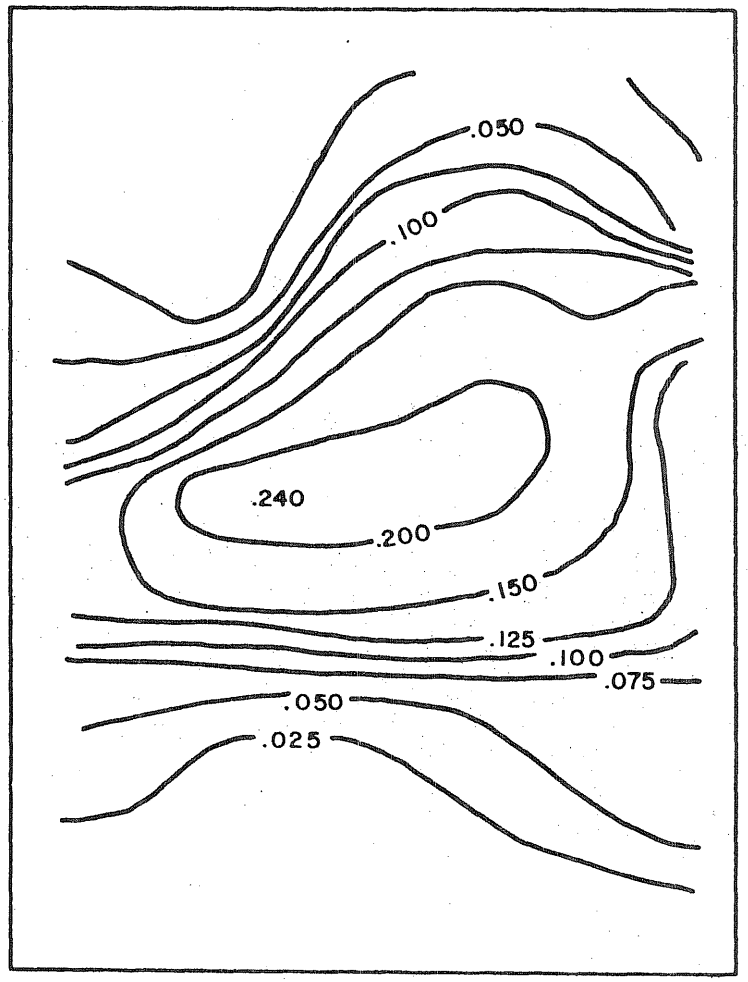

FT-1

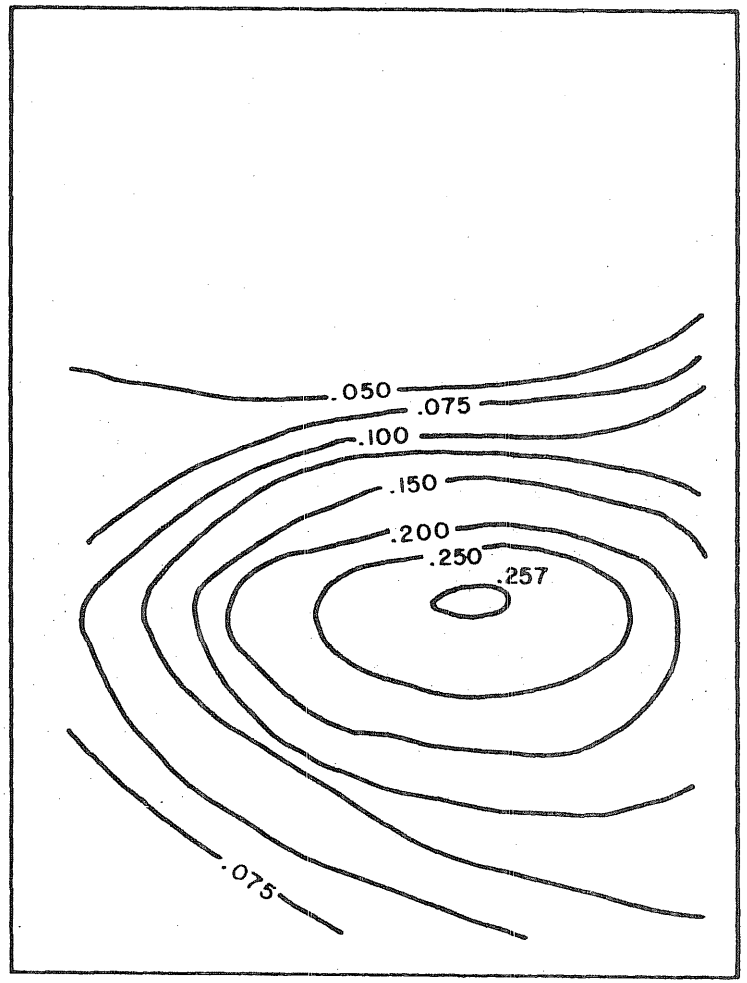

FT-10

FIG. 17 INITIAL WEB DEFLECTIONS OF FT-1 AND FT-10

Note: Web deflections are given in inches.

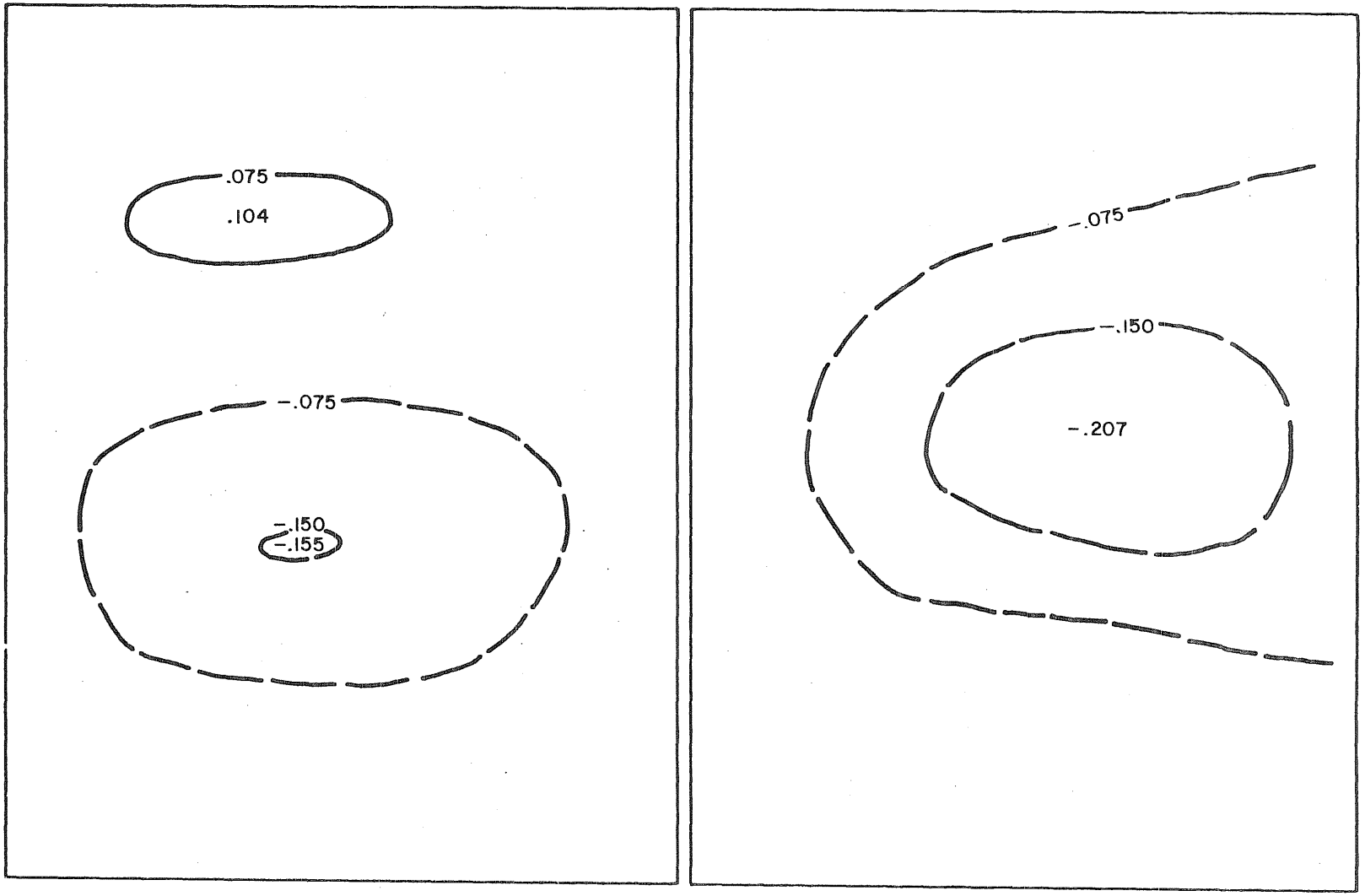

FIG. 18 INITIAL WEB DEFLECTIONS OF FTSB-6A.

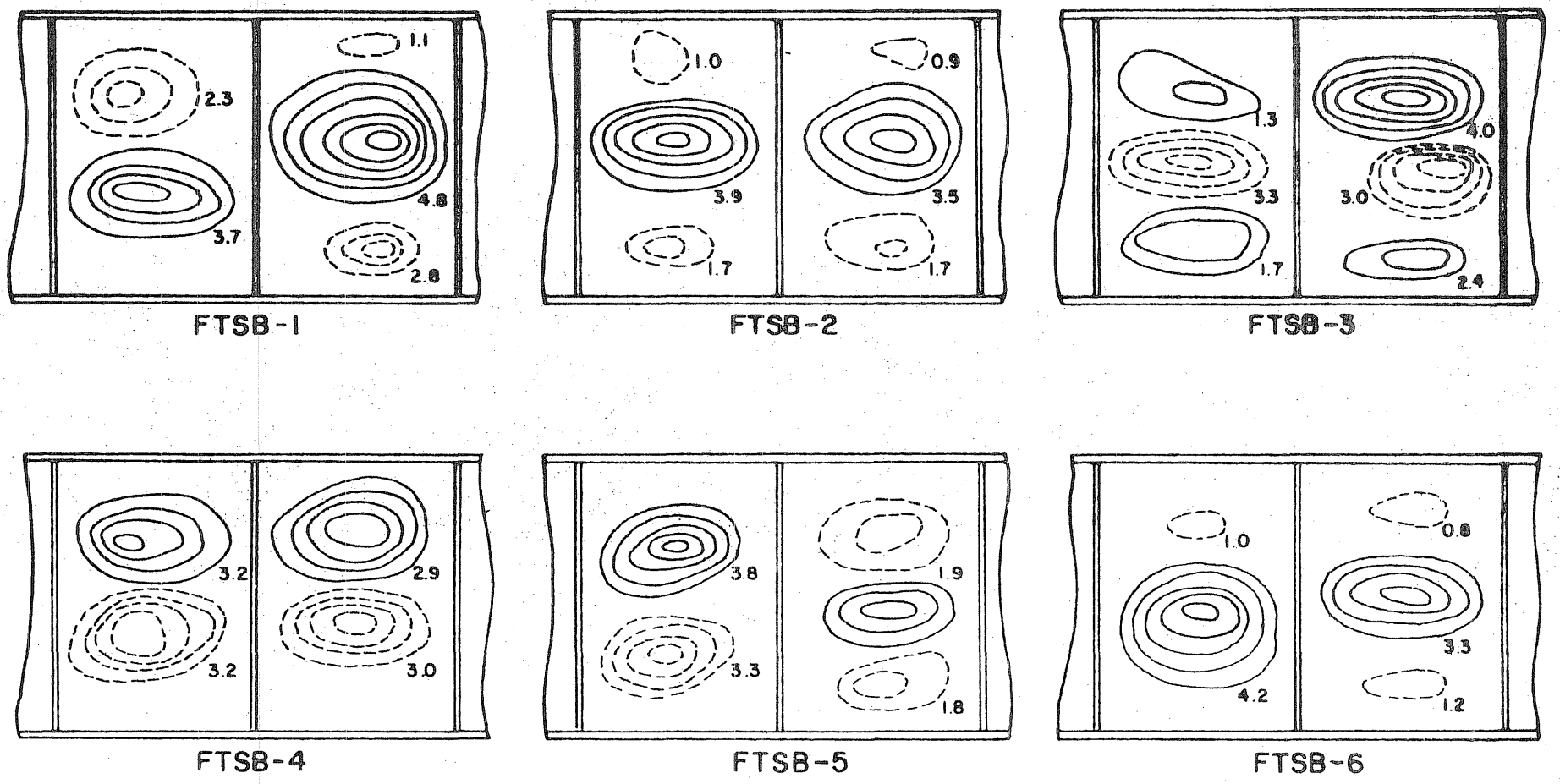

Note : Numbers give values of $w_{max.}/t$ for individual buckles.

FIG. 19 INITIAL WEB DEFLECTION PATTERNS FOR GIRDERS WITH VARIOUS FLANGE SIZES SUBJECTED TO SHEAR AND MOMENT .

Note: Web deflections are given in inches.

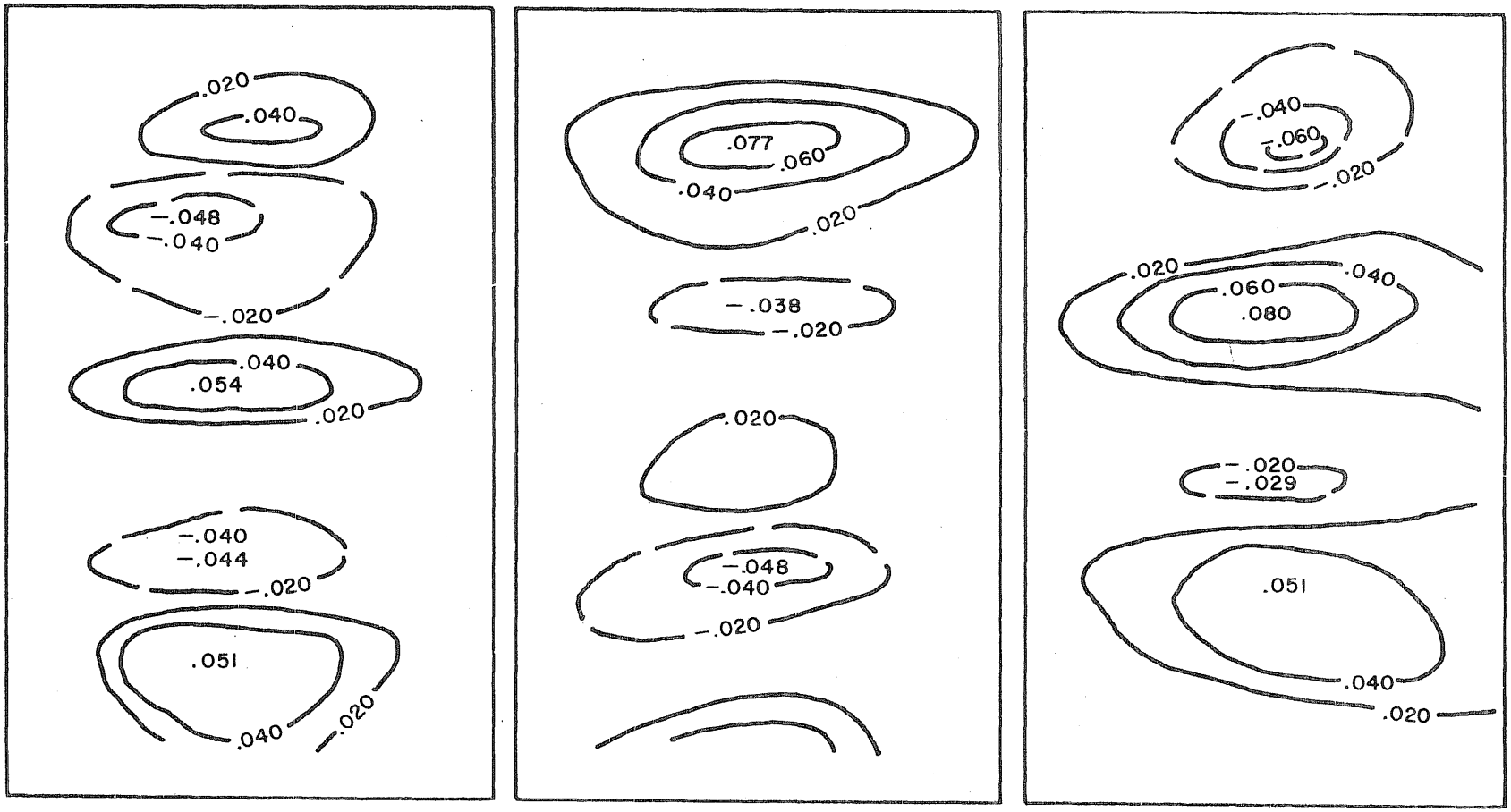

FIG. 20 INITIAL WEB DEFLECTIONS OF VST 8-4A

Note: Web deflections are given in inches.

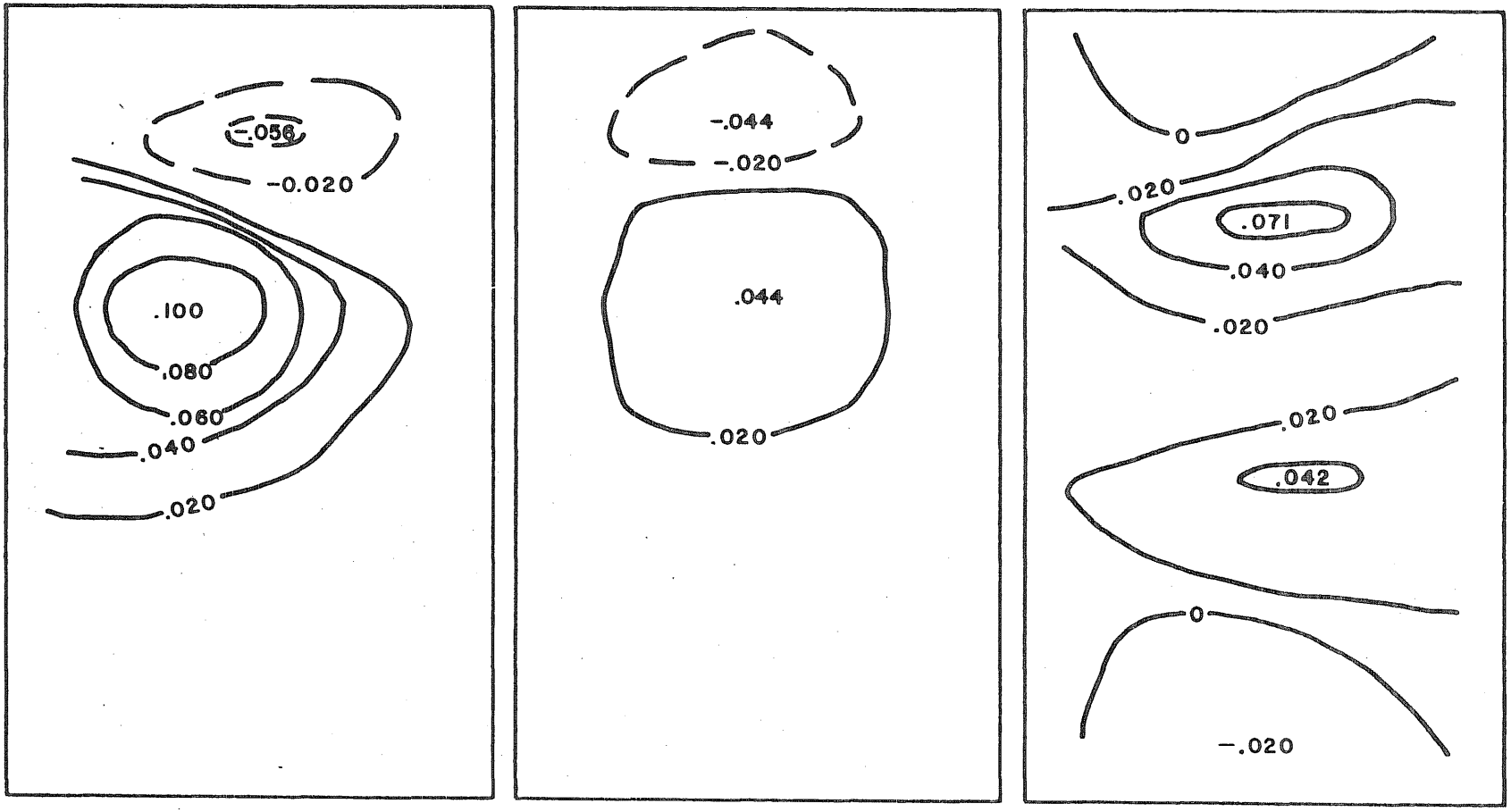

FIG. 21 INITIAL WEB DEFLECTIONS OF VSTB-16A

Note: Web deflections are given in inches.

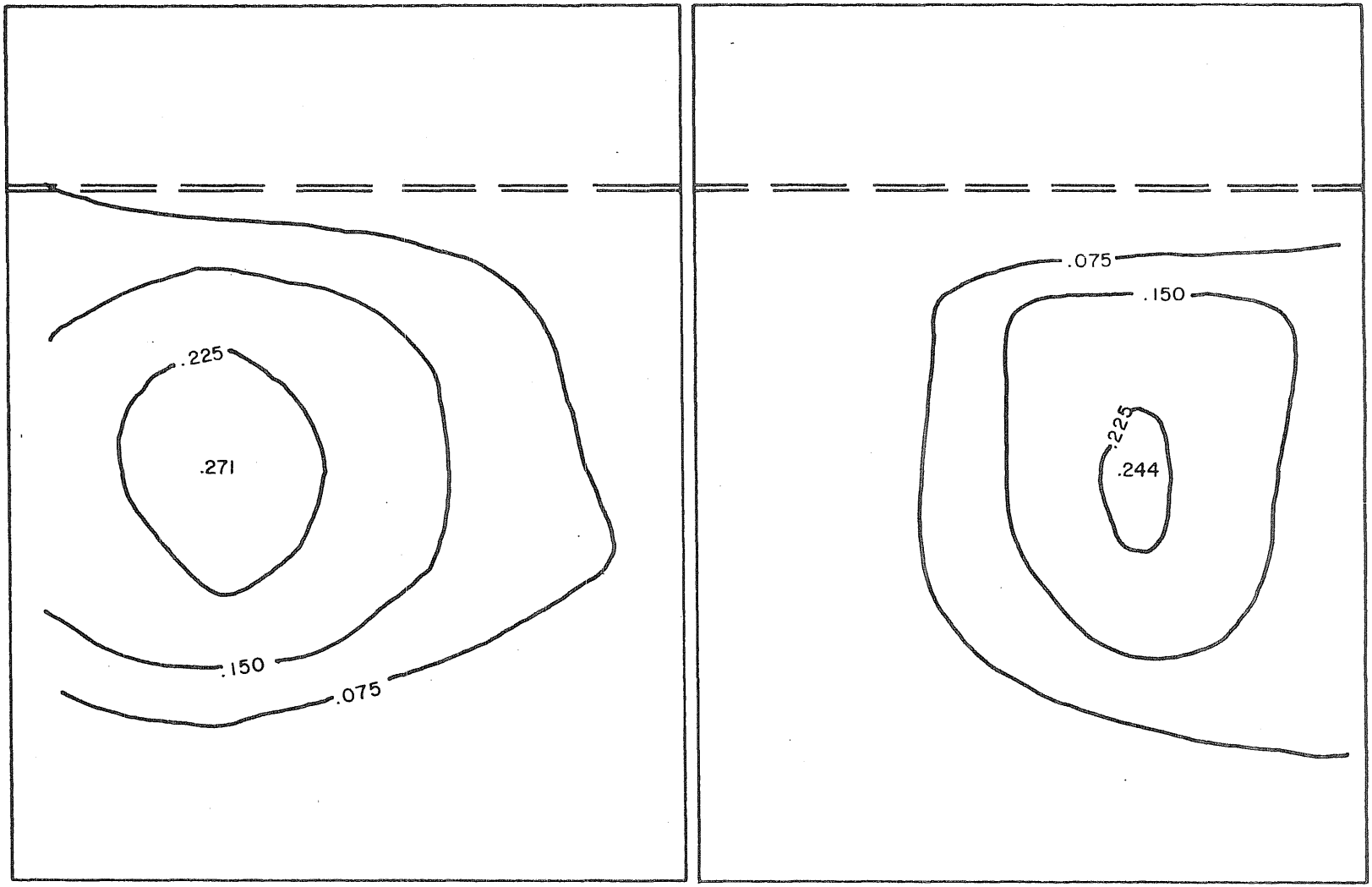

FIG. 22 INITIAL WEB DEFLECTIONS OF HSB-1.

Note: Web deflections are given in inches.

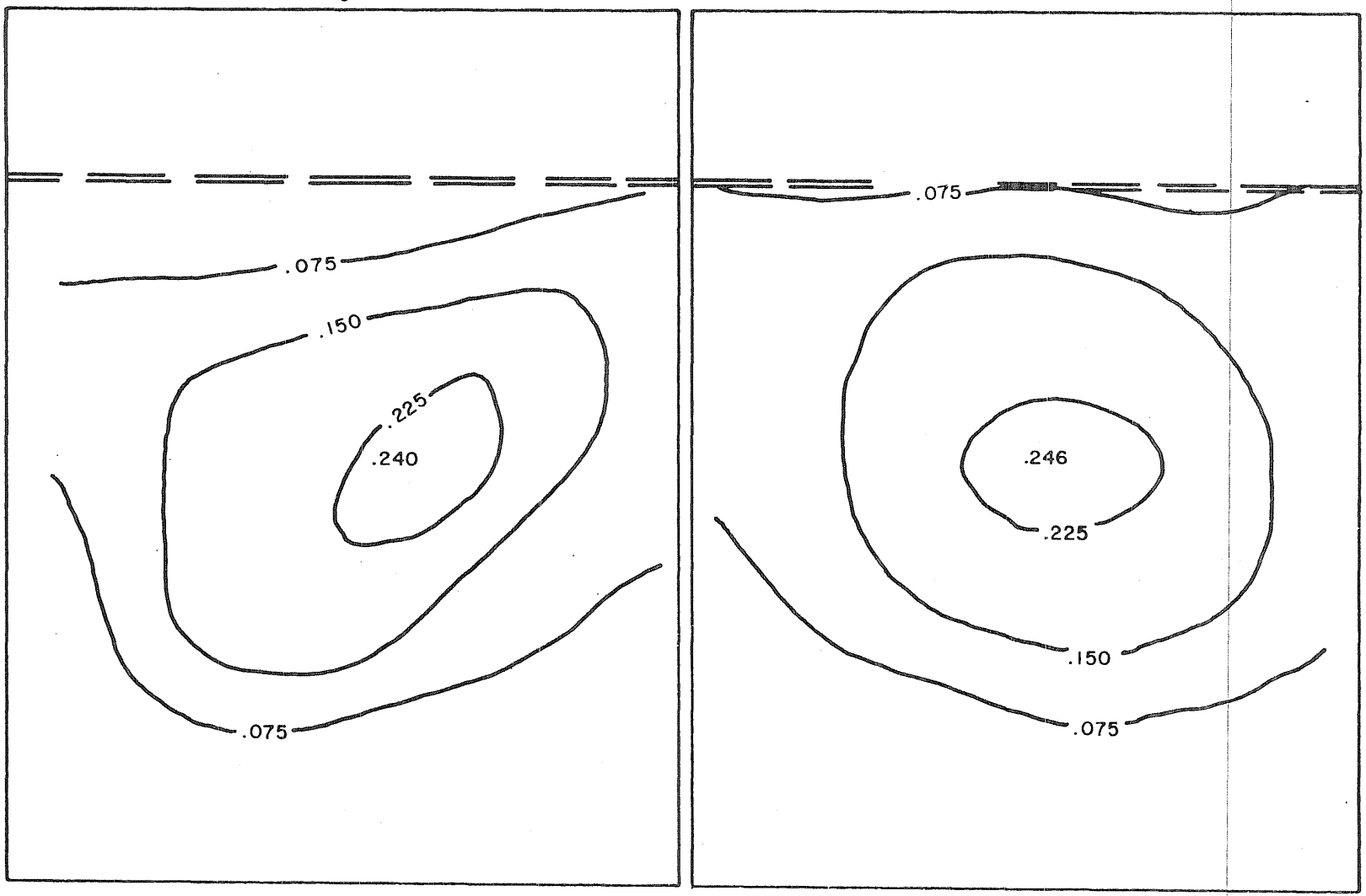

FIG. 23 INITIAL WEB DEFLECTIONS OF HSB-2.

Note: Web deflections are given in inches.

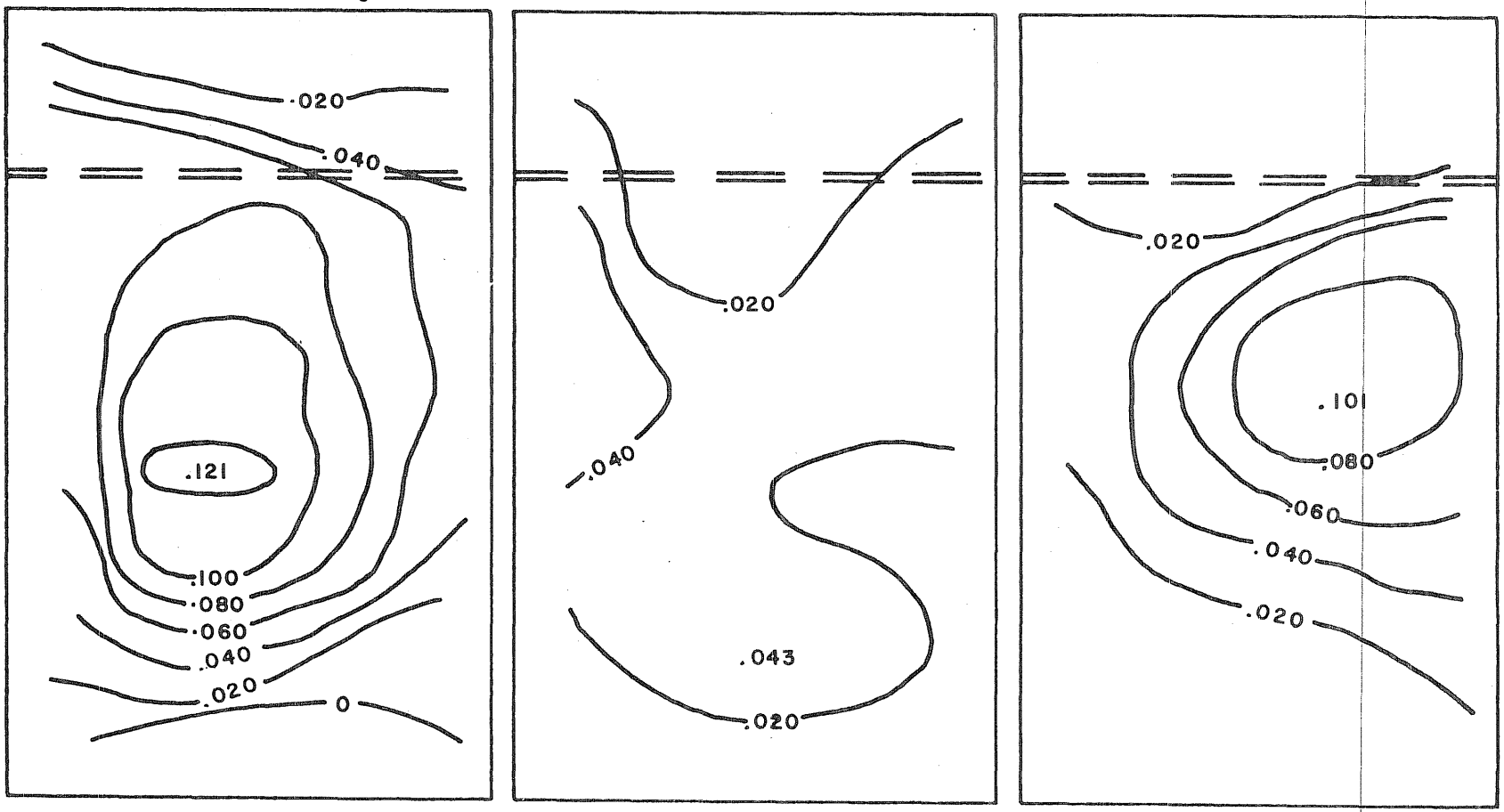

FIG. 24 INITIAL WEB DEFLECTIONS OF HVSB-1

Note: Web deflections are given in inches.

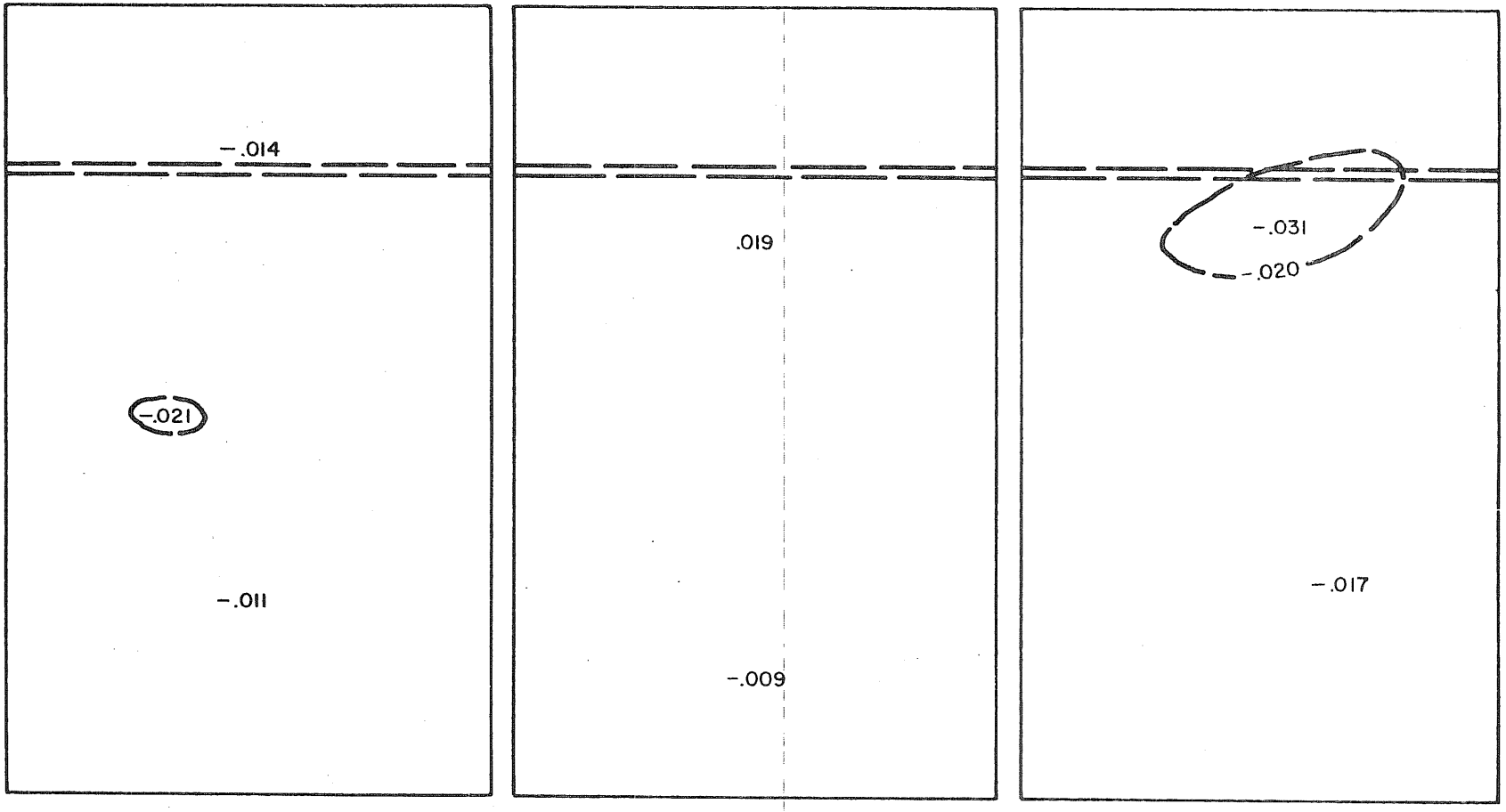

FIG. 25 INITIAL WEB DEFLECTIONS OF HVSB-2.

Note: Web deflections are given in inches.

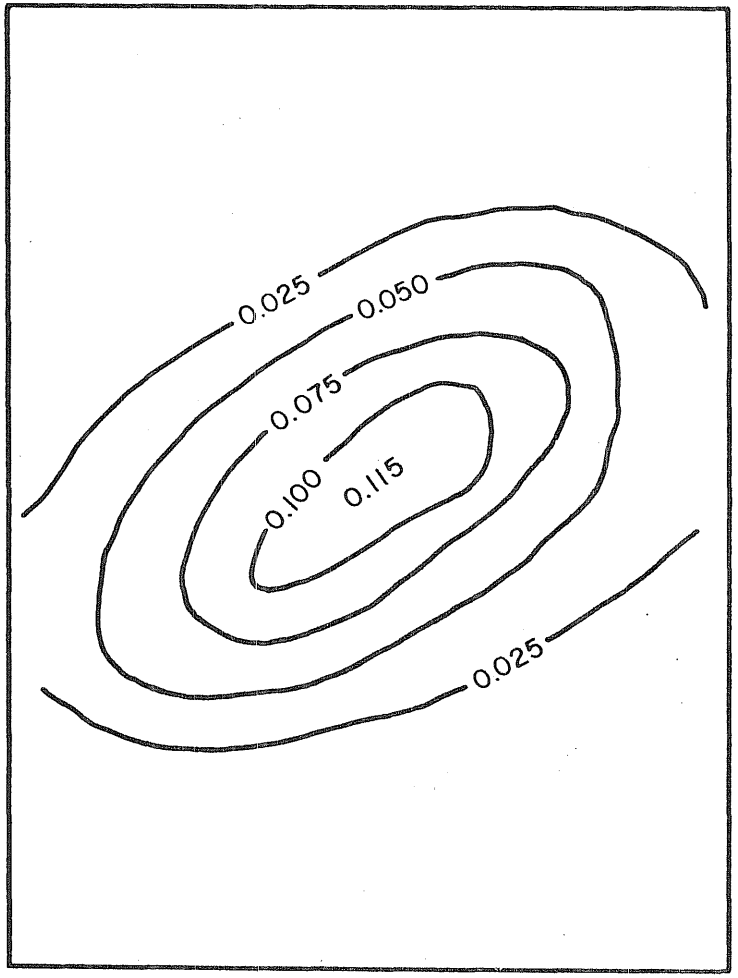

$\frac{W}{W_{mf}} = \frac{1}{4}$

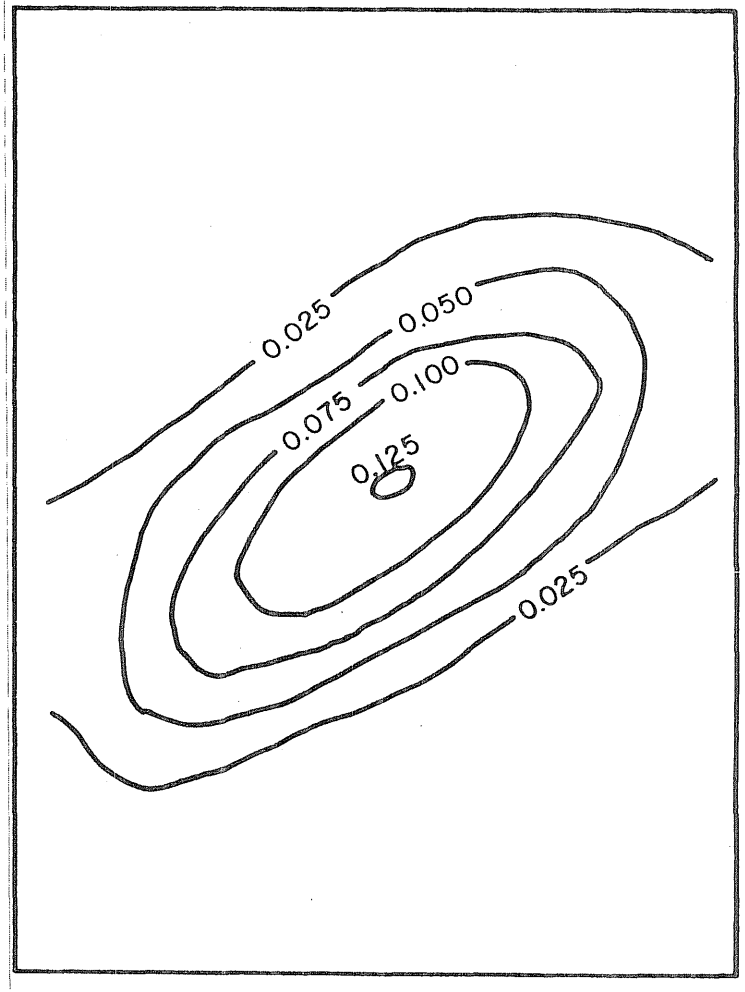

$\frac{W}{W_{mf}} = \frac{1}{2}$

FT—1A
118,000 Cycles

FIG. 26 WEB DEFLECTIONS DUE TO LOAD.

Note: Web deflections are given in inches.

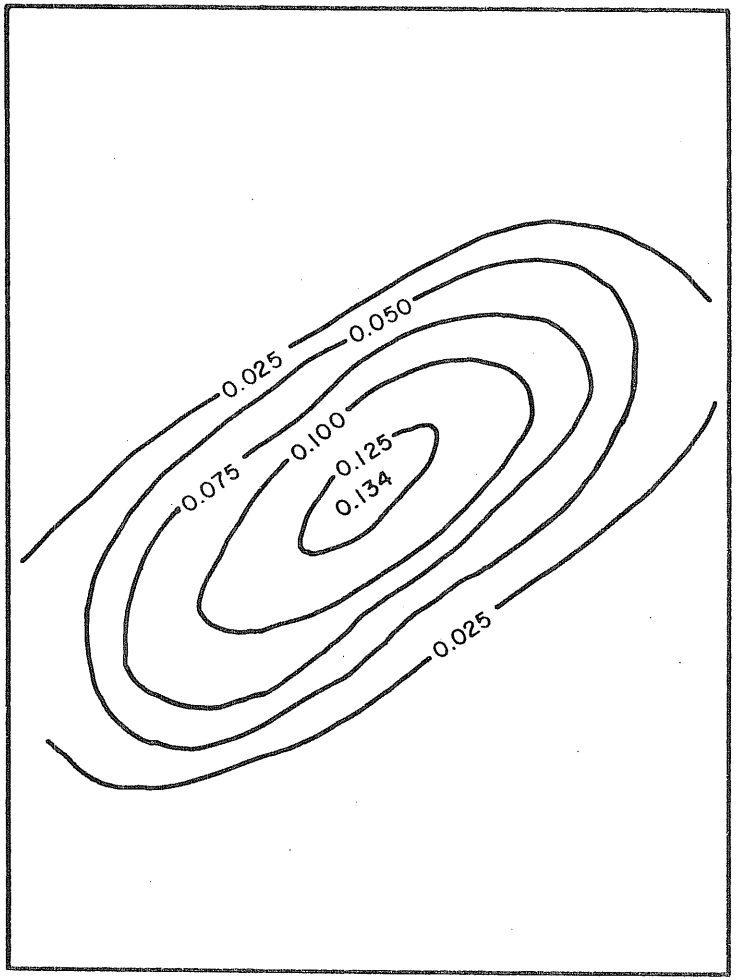

$\frac{W}{W_{mf}} = \frac{3}{4}$

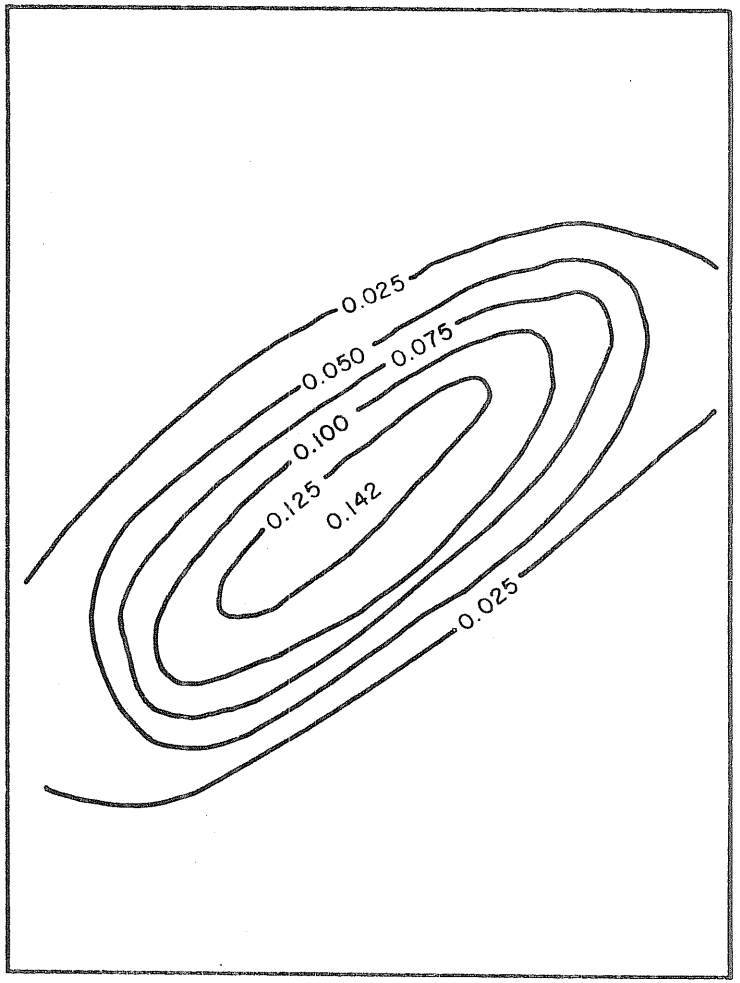

$\frac{W}{W_{mf}} = 1$

FT—1A
118,000 Cycles

FIG. 27 WEB DEFLECTIONS DUE TO LOAD.

Note: Web deflections are given in inches.

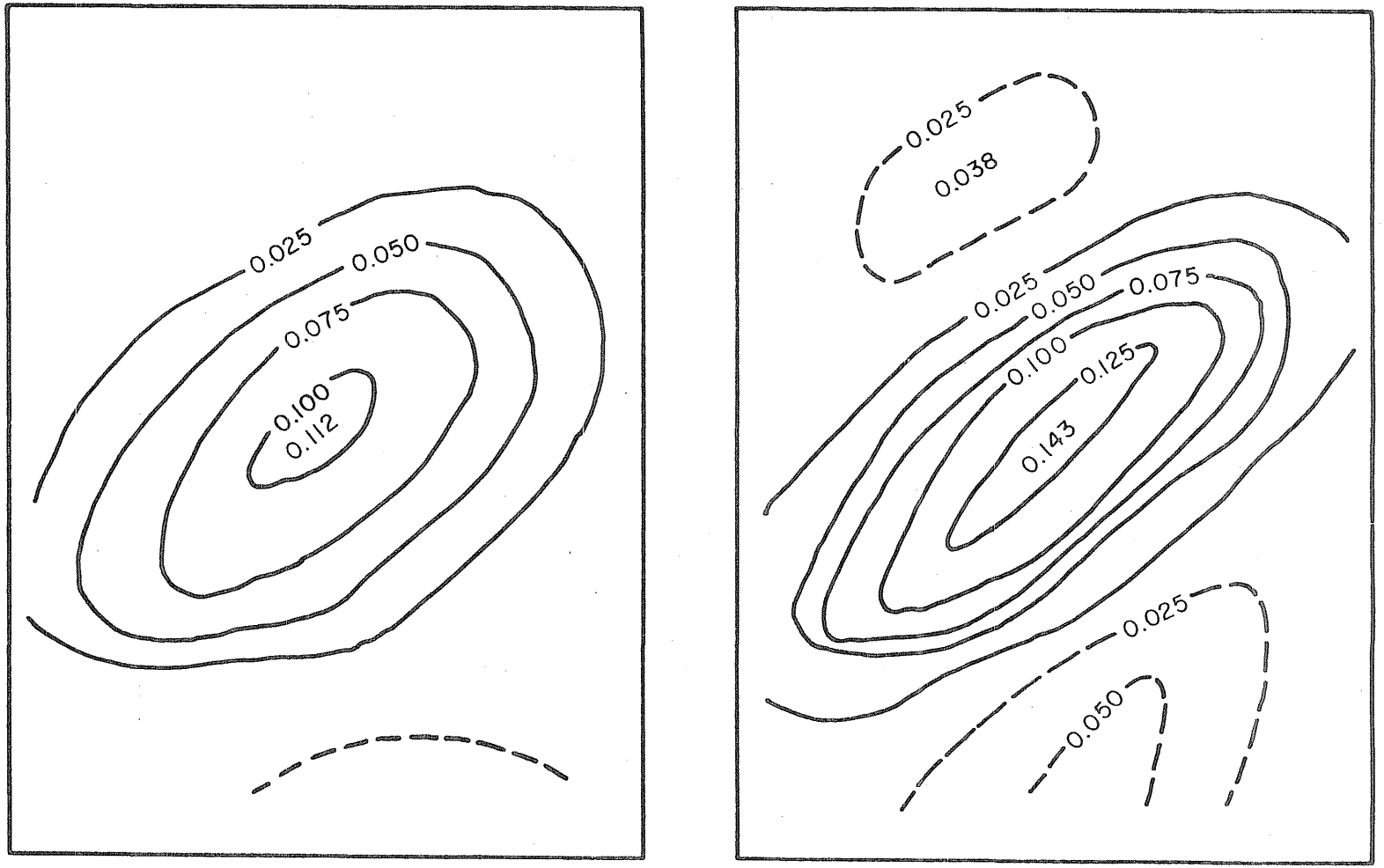

$\frac{W}{W_{mf}} = \frac{1}{4}$

$\frac{W}{W_{mf}} = 1$

FT–1A
1,000,000 Cycles

FIG. 28 WEB DEFLECTIONS DUE TO LOAD.

Note: Web deflections are given in inches.

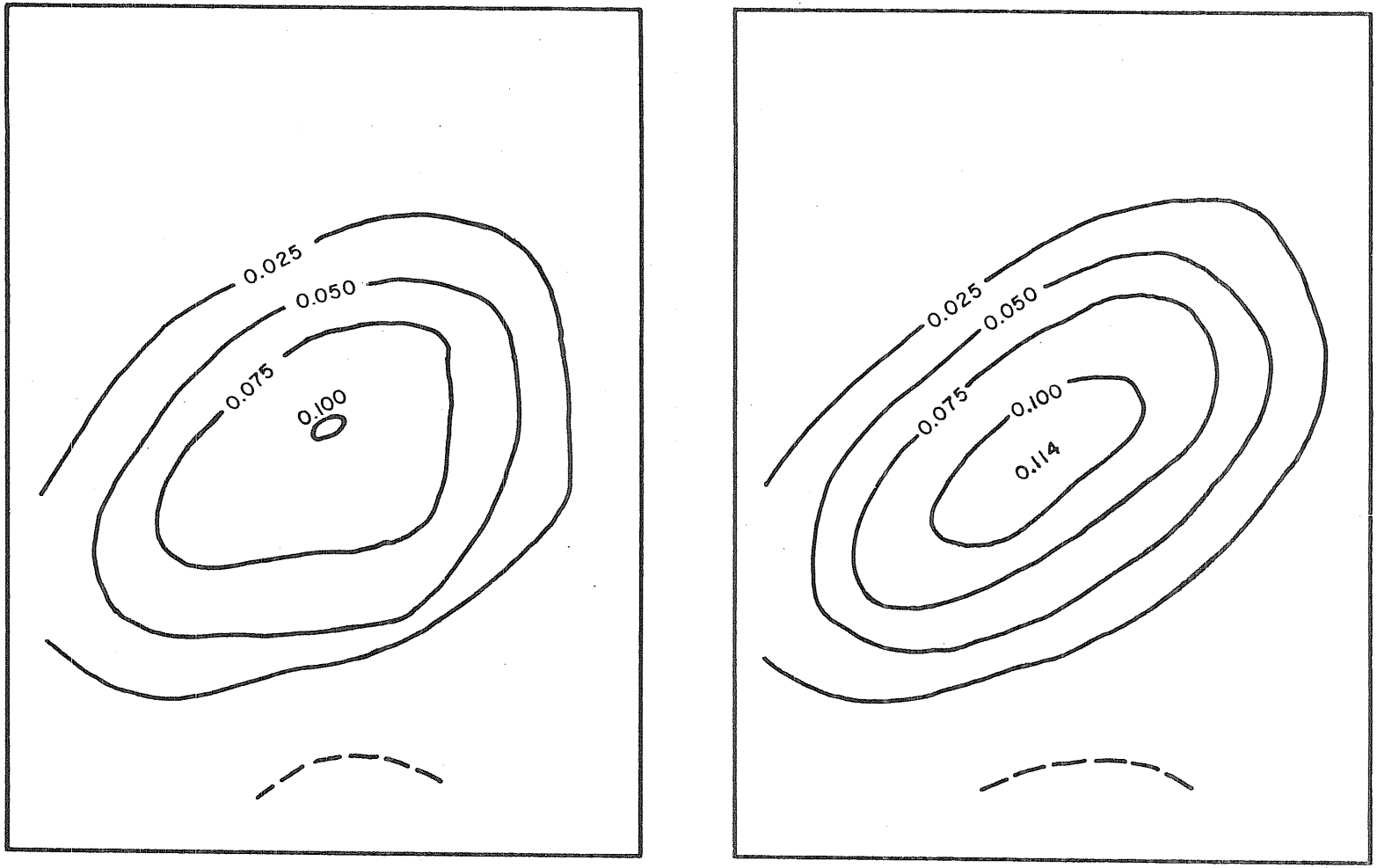

$\frac{W}{W_{mi}} = 0$

$\frac{W}{W_{mf}} = \frac{1}{4}$

FT—1A
2,250,000 Cycles

FIG. 29 WEB DEFLECTIONS DUE TO LOAD.

Note: Web deflections are given in inches.

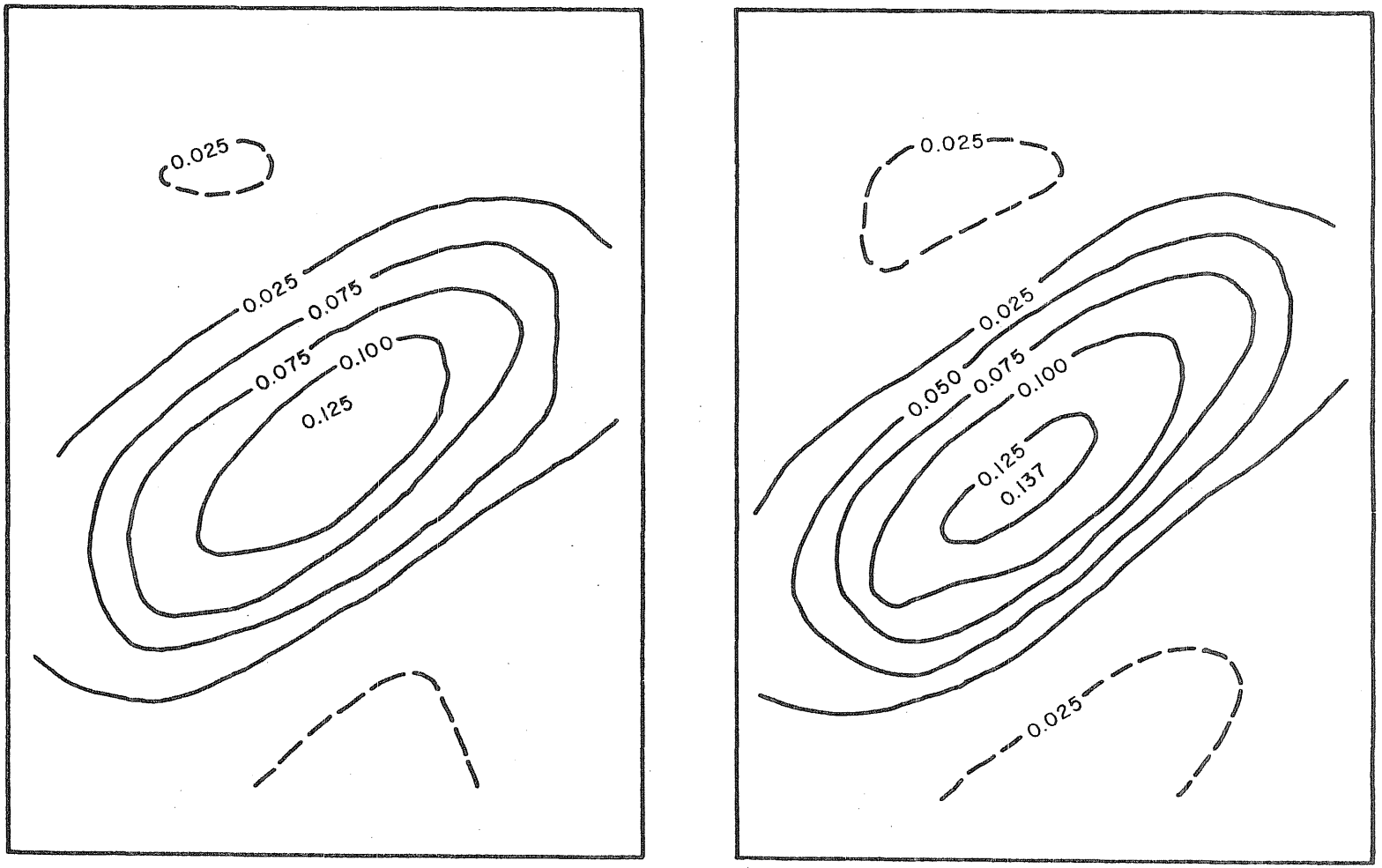

$\frac{W}{W_{mf}} = \frac{1}{2}$

$\frac{W}{W_{mf}} = \frac{3}{4}$

FT−1A
2,250,000 Cycles

FIG. 30 WEB DEFLECTIONS DUE TO LOAD.

Note: Web deflections are given in inches.

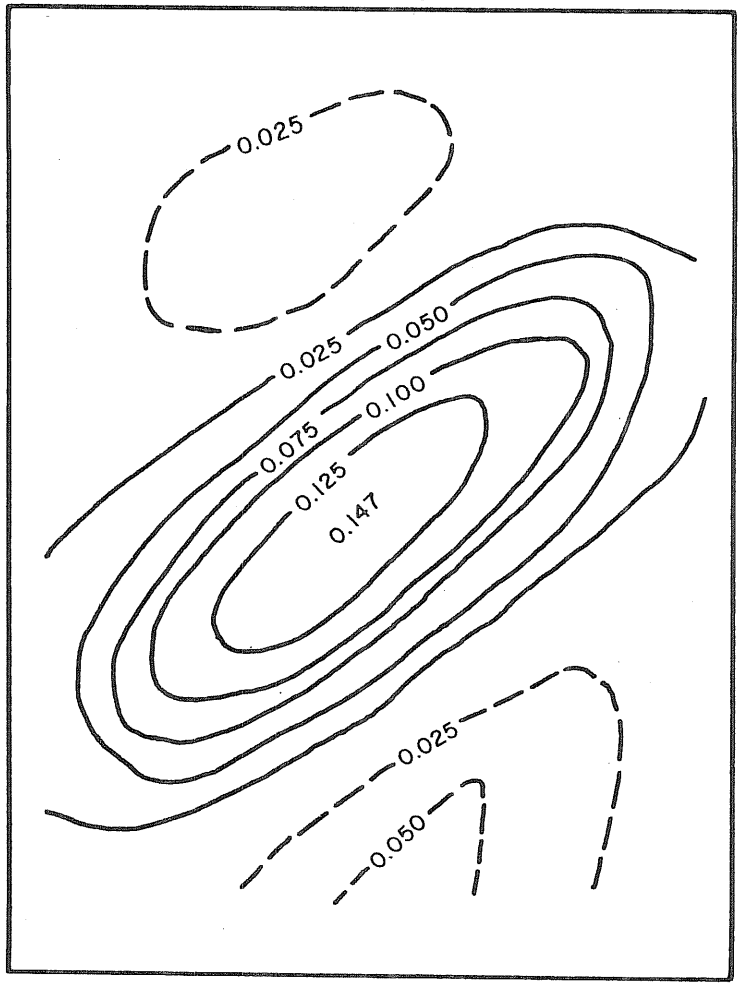

$$\frac{W}{W_{mf}} = 1$$

FT — 1A 2,250,000 Cycles

FIG. 31 WEB DEFLECTIONS DUE TO LOAD.

Note: Web deflections are given in inches.

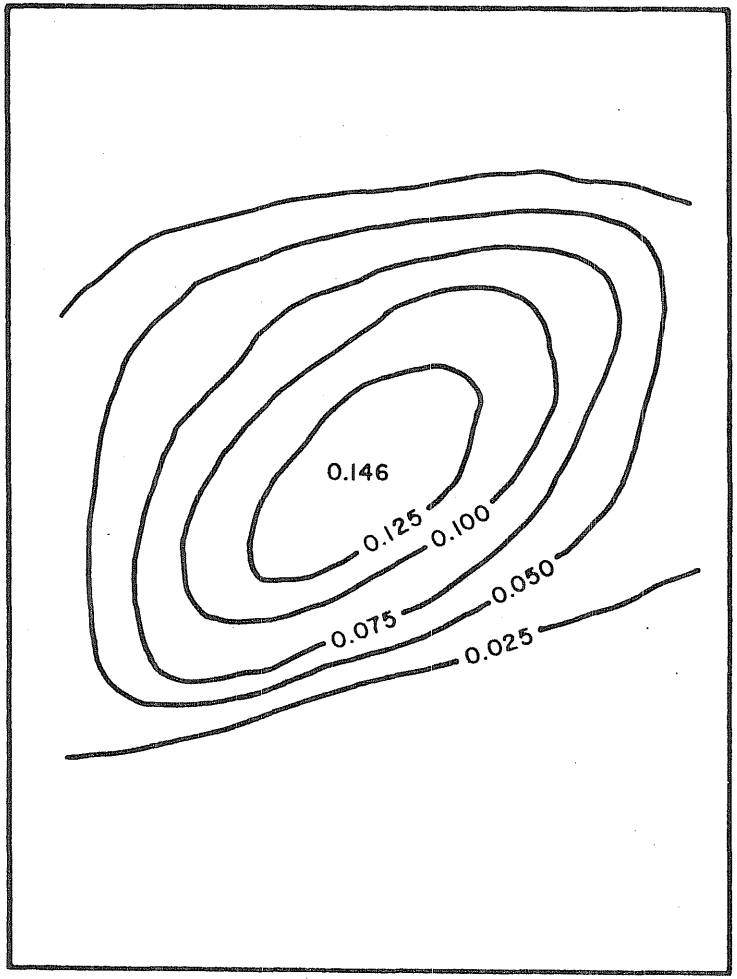

$\frac{W}{W_{mf}} = \frac{1}{4}$

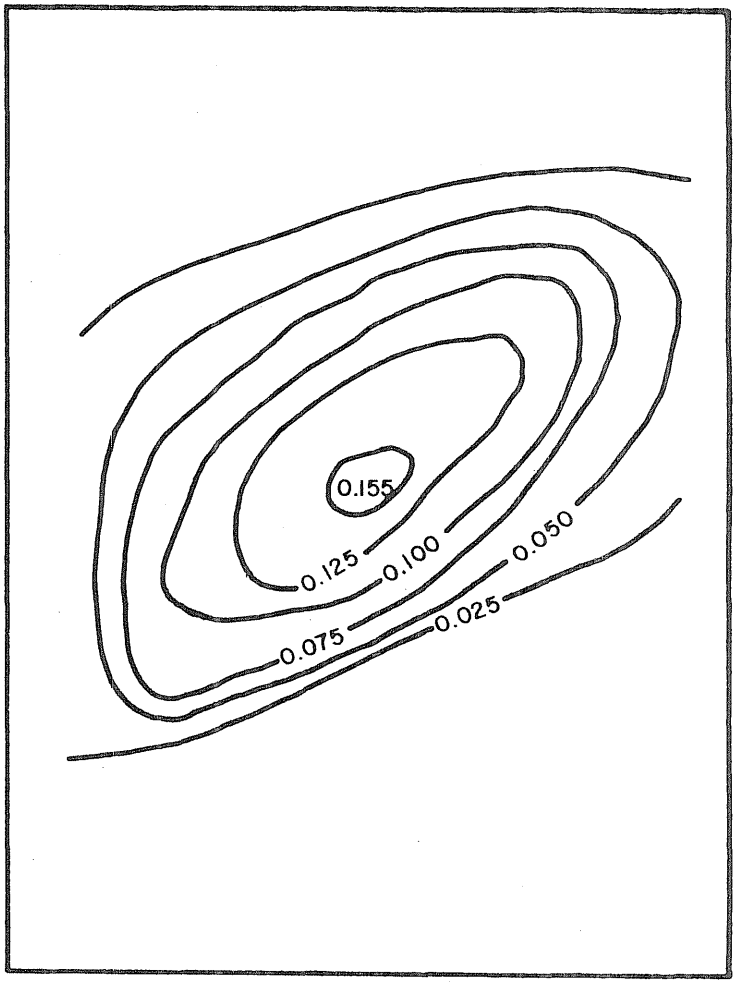

$\frac{W}{W_{mf}} = \frac{1}{2}$

FT—10A
1,000 Cycles

FIG. 32 WEB DEFLECTIONS DUE TO LOAD.

Note: Web deflections are given in inches.

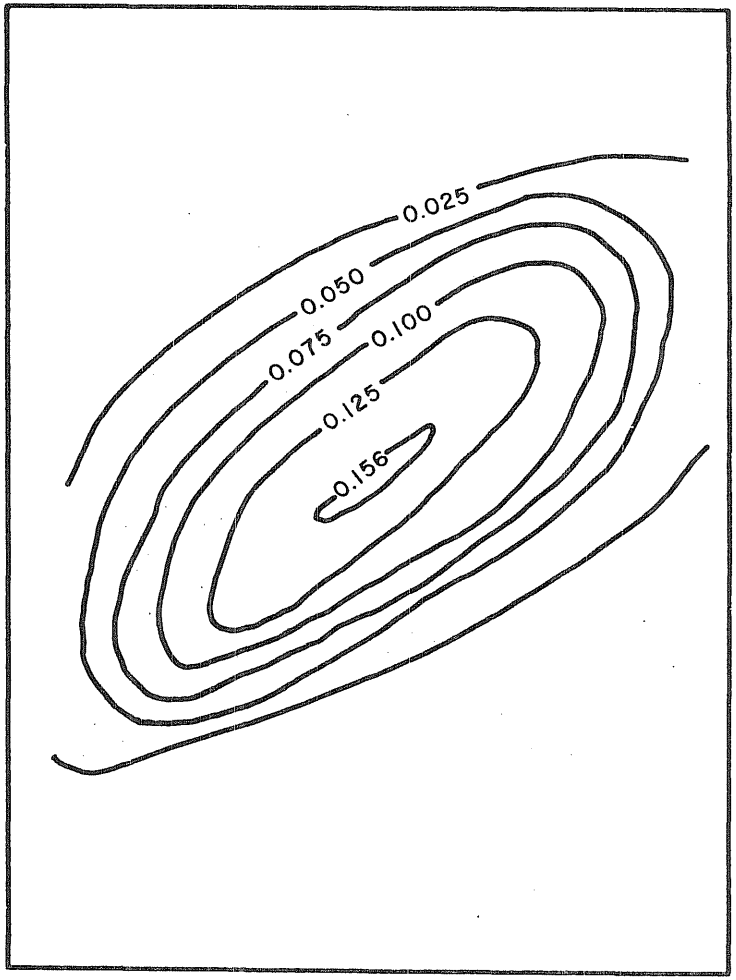

$\frac{W}{W_{mf}} = \frac{3}{4}$

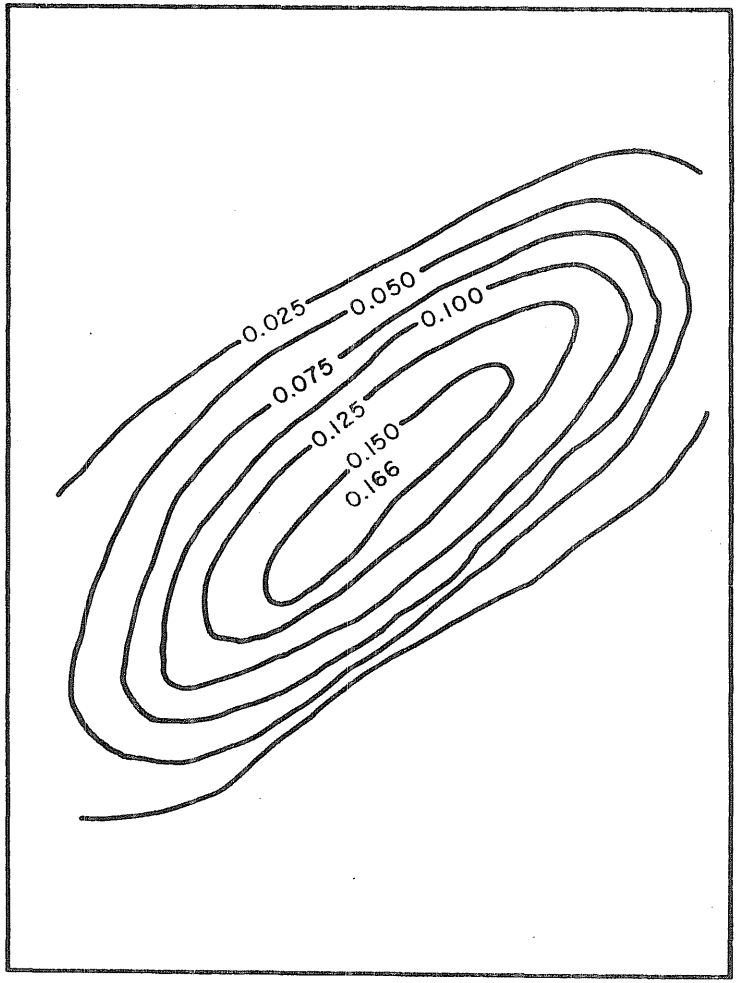

$\frac{W}{W_{mf}} = 1$

FT—10A
1,000 Cycles

FIG. 33 WEB DEFLECTIONS DUE TO LOAD.

Note: Web deflections are given in inches.

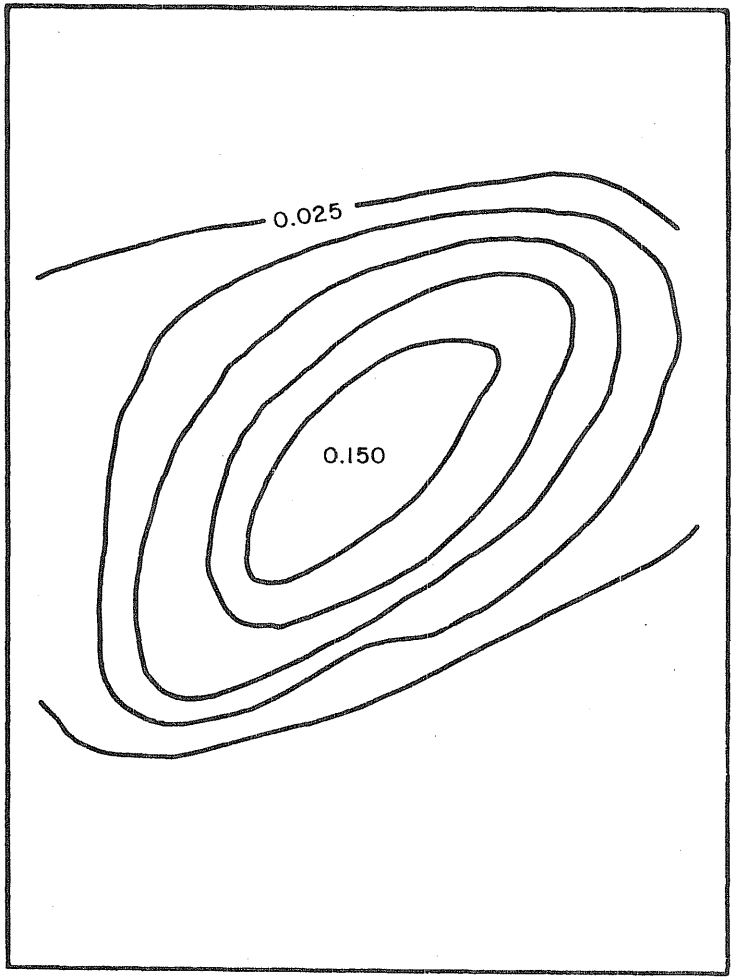

$\frac{W}{W_{mf}} = \frac{1}{4}$

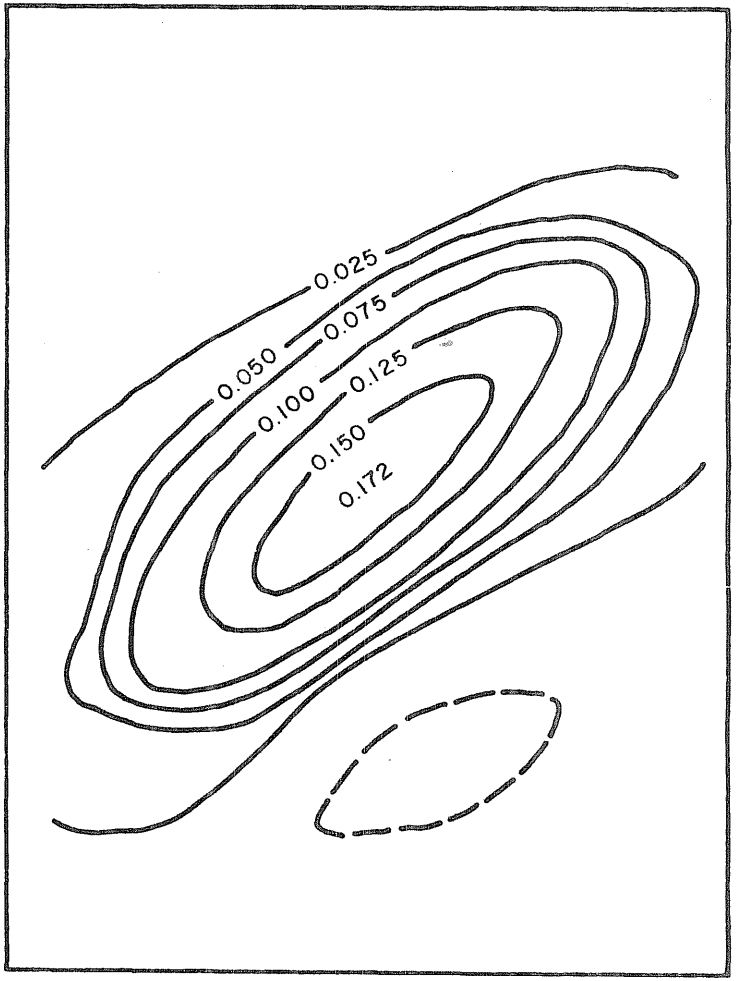

$\frac{W}{W_{mf}} = 1$

FT—10A
2,075,000 Cycles

FIG. 34 WEB DEFLECTIONS DUE TO LOAD.

Note: Web deflections are given in inches

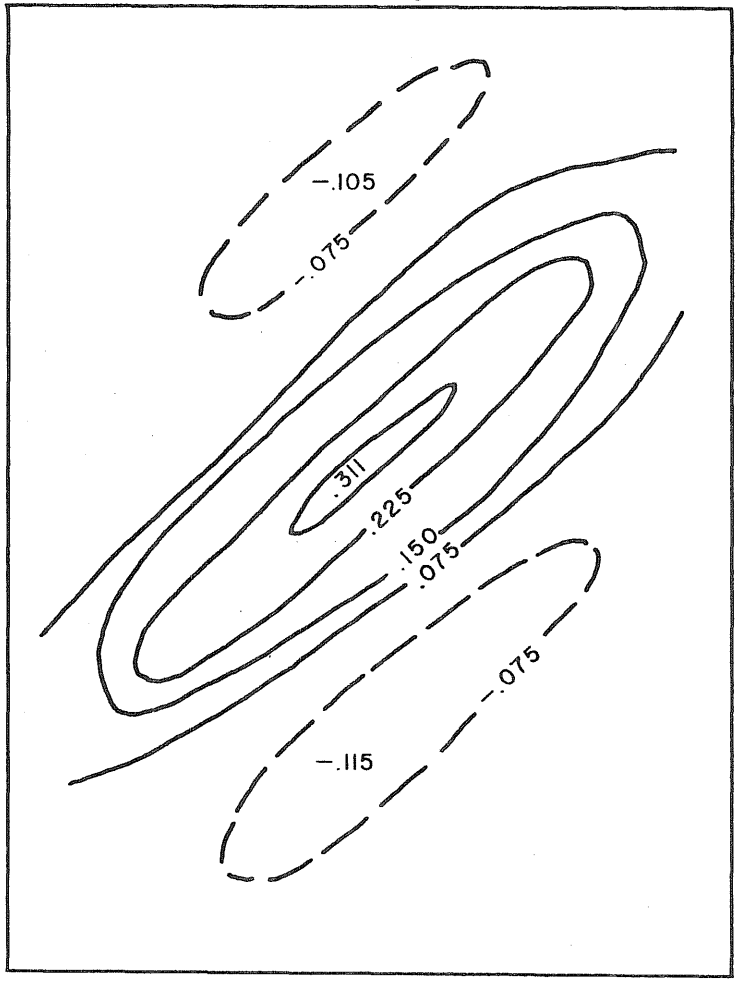

$\frac{W}{W_{mf}} = 1.5$

FIG. 35 WEB DEFLECTIONS OF FT-10A DUE TO LOAD

Note: Web deflections are given in inches.

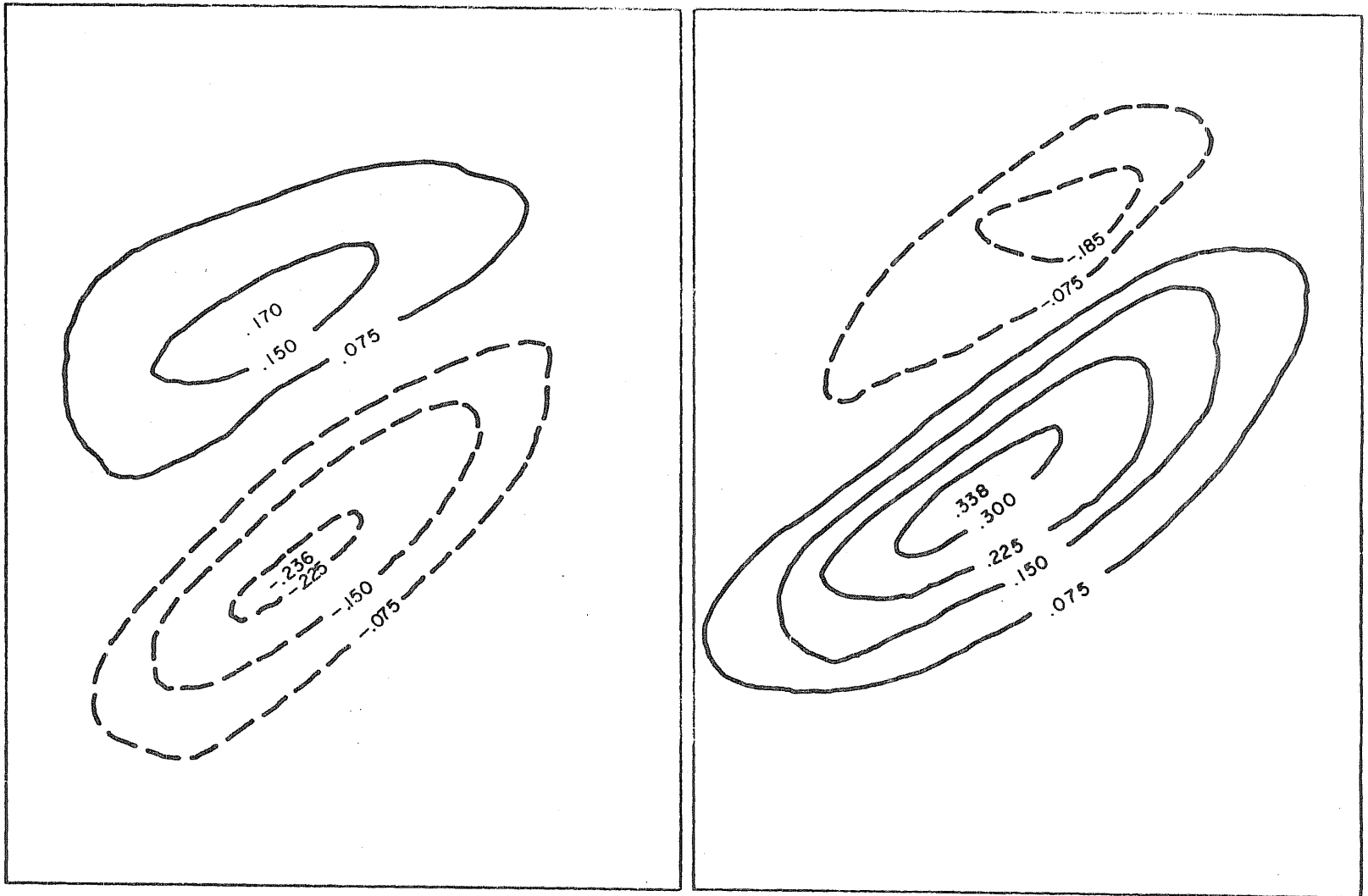

Panel 2

FTSB-2A

$\frac{W}{W_{mf}} = \frac{1}{4}$

Panel 1

600 cycles

FIG. 36 WEB DEFLECTIONS DUE TO LOAD .

Note: Web deflections are given in inches.

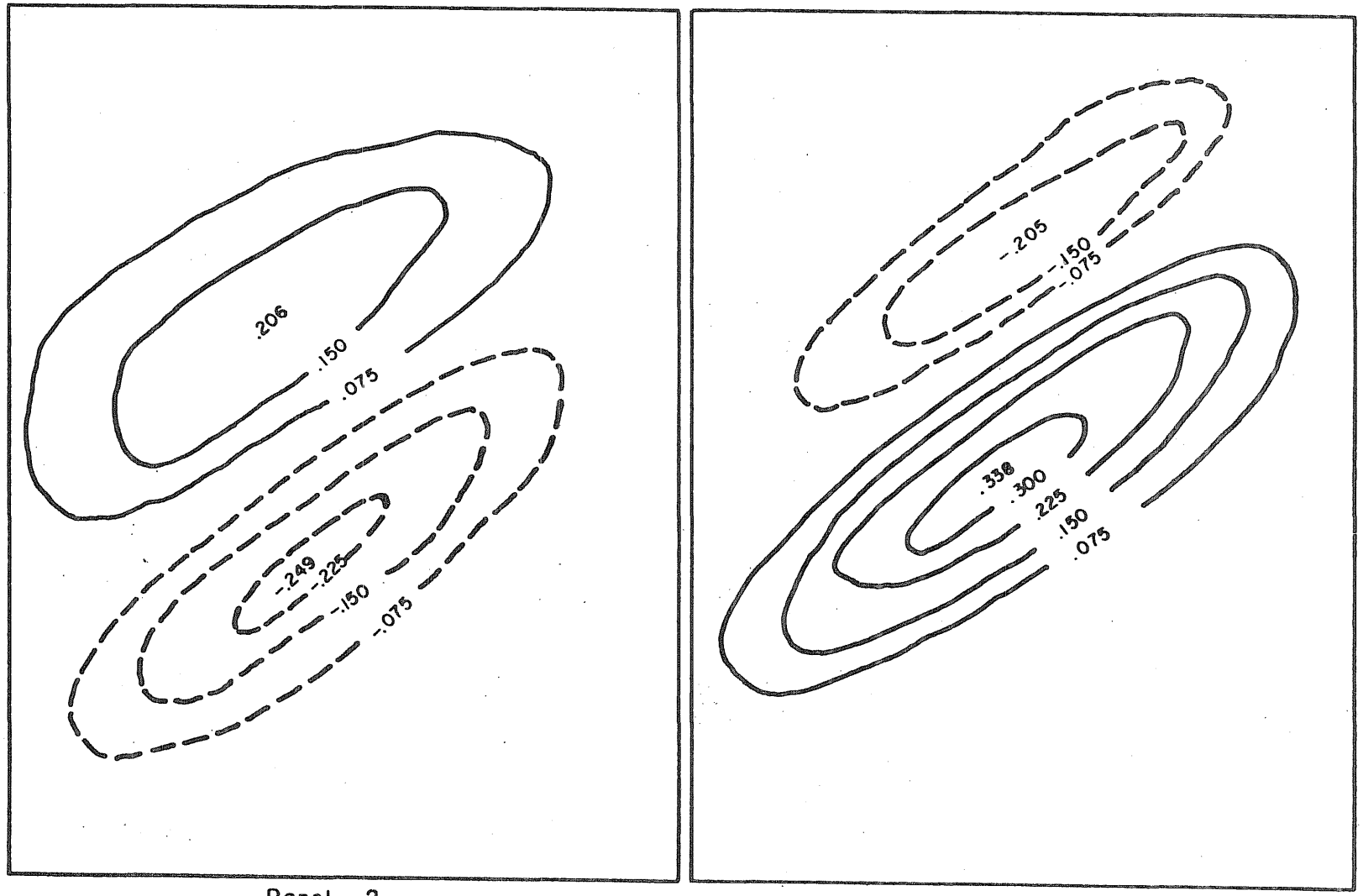

Panel 2

Panel 1

$\frac{W}{W_{mf}} = 1$

FTSB-2A

600 cycles

FIG. 37 WEB DEFLECTIONS DUE TO LOAD .

Note: Web deflections are given in inches.

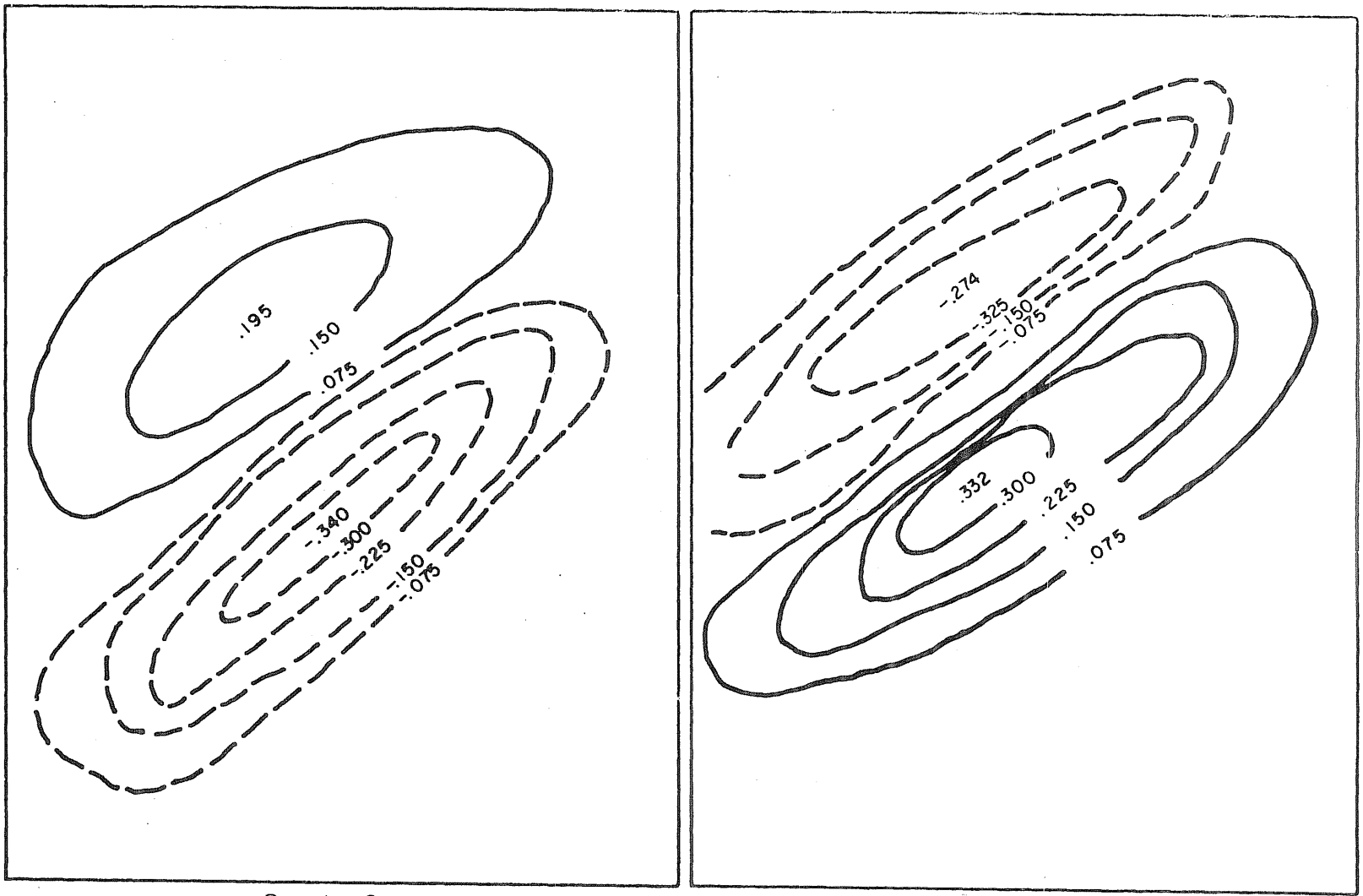

Panel 2

Panel 1

$\frac{W}{W_{mf}} = 1$

FTSB-2A

371,000 cycles

FIG. 38 WEB DEFLECTIONS DUE TO LOAD .

Note: Web deflections are given in inches.

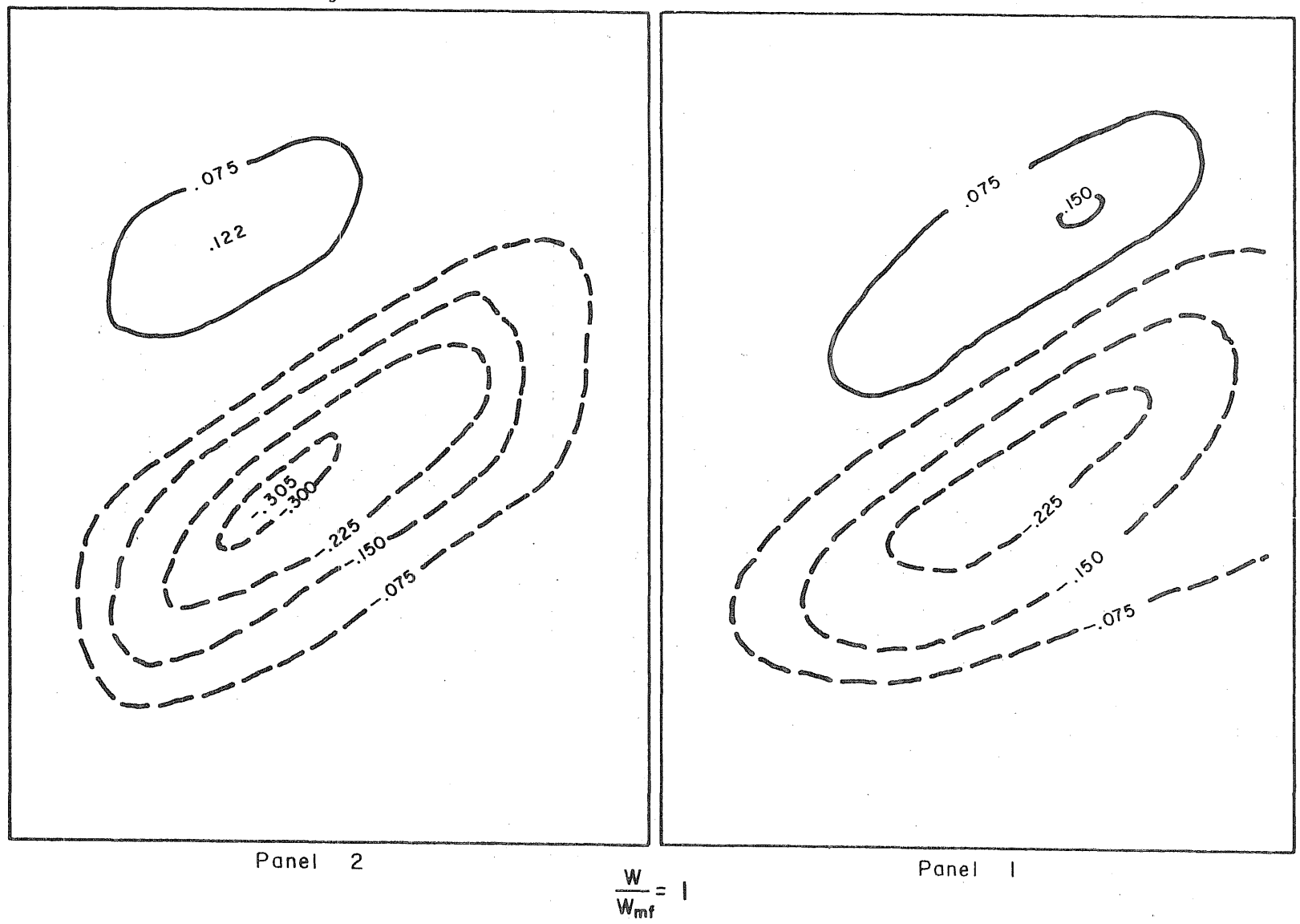

Panel 2

$\frac{W}{W_{mf}} = 1$

Panel 1

FTSB-6A

0 cycles

FIG. 39 WEB DEFLECTIONS DUE TO LOAD .

Note: Web deflections are given in inches.

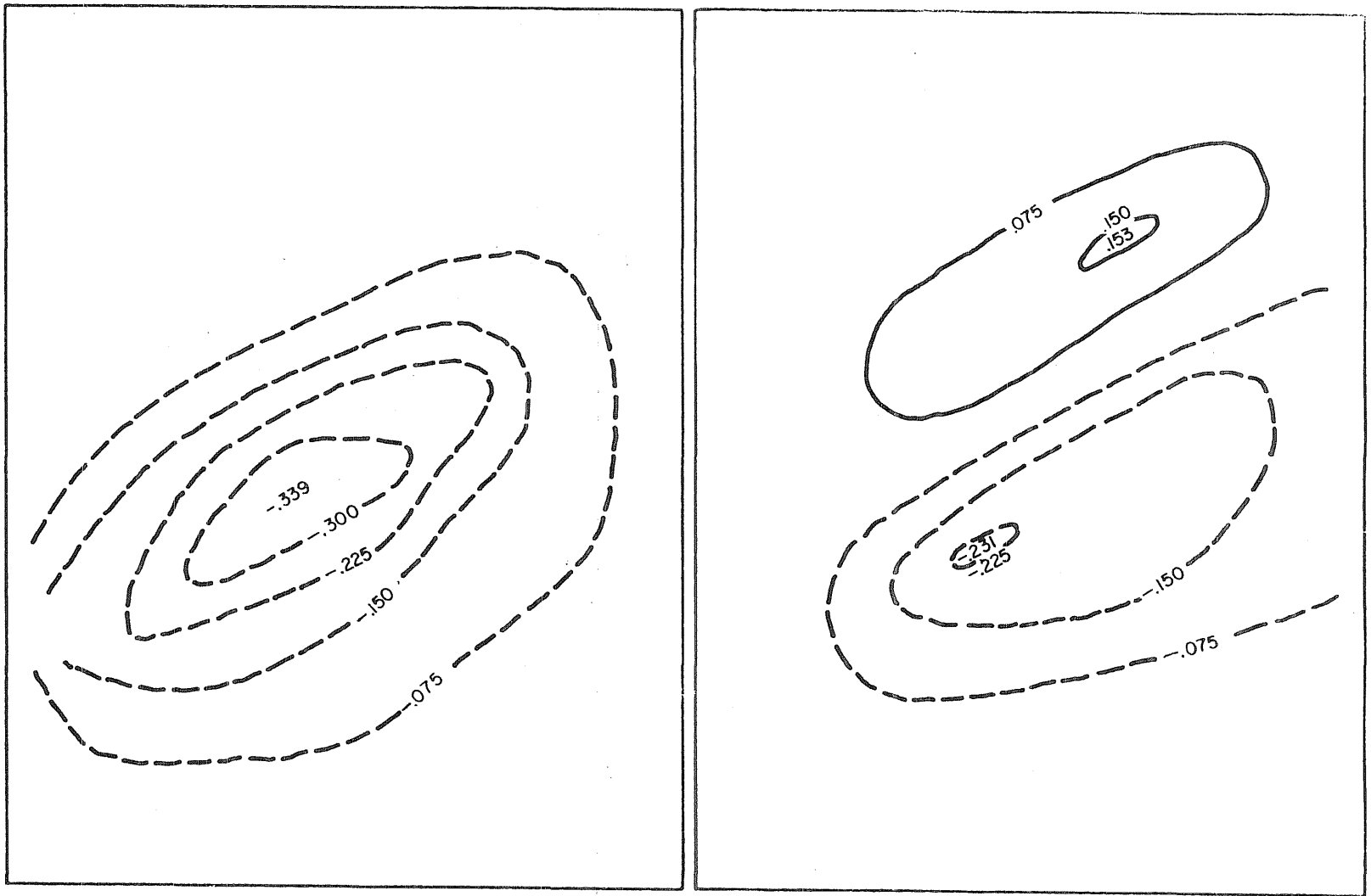

FTSB-6A $\frac{W}{W_{mf}} = 0$ 362,000 cycles

FIG. 40 WEB DEFLECTIONS DUE TO LOAD .

Note: Web deflections are given in inches.

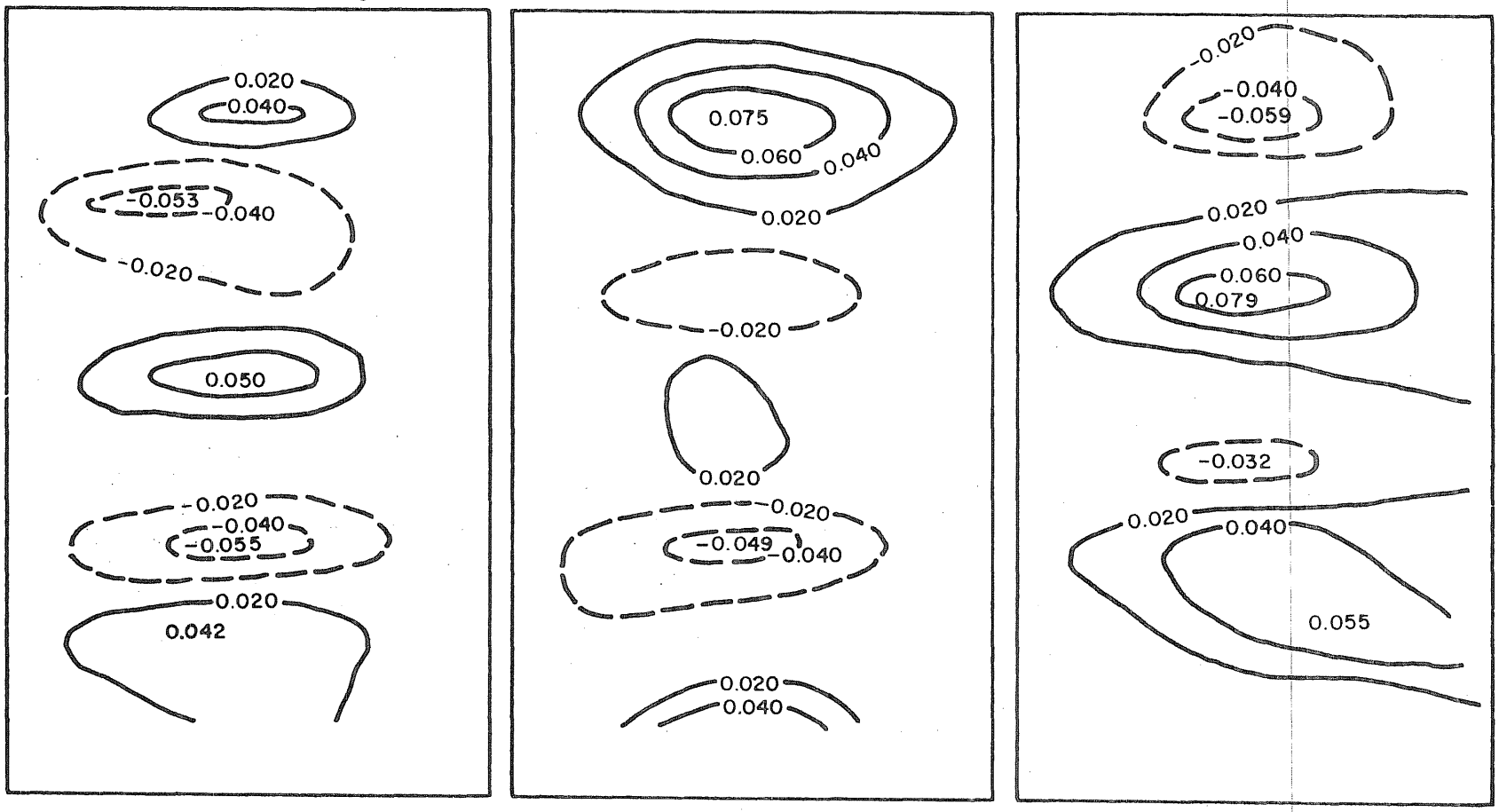

VST 8-4A

$\frac{W}{W_{mf}} = \frac{1}{4}$

0 cycles

FIG. 41 WEB DEFLECTIONS DUE TO LOAD.

Note: Web deflections are given in inches.

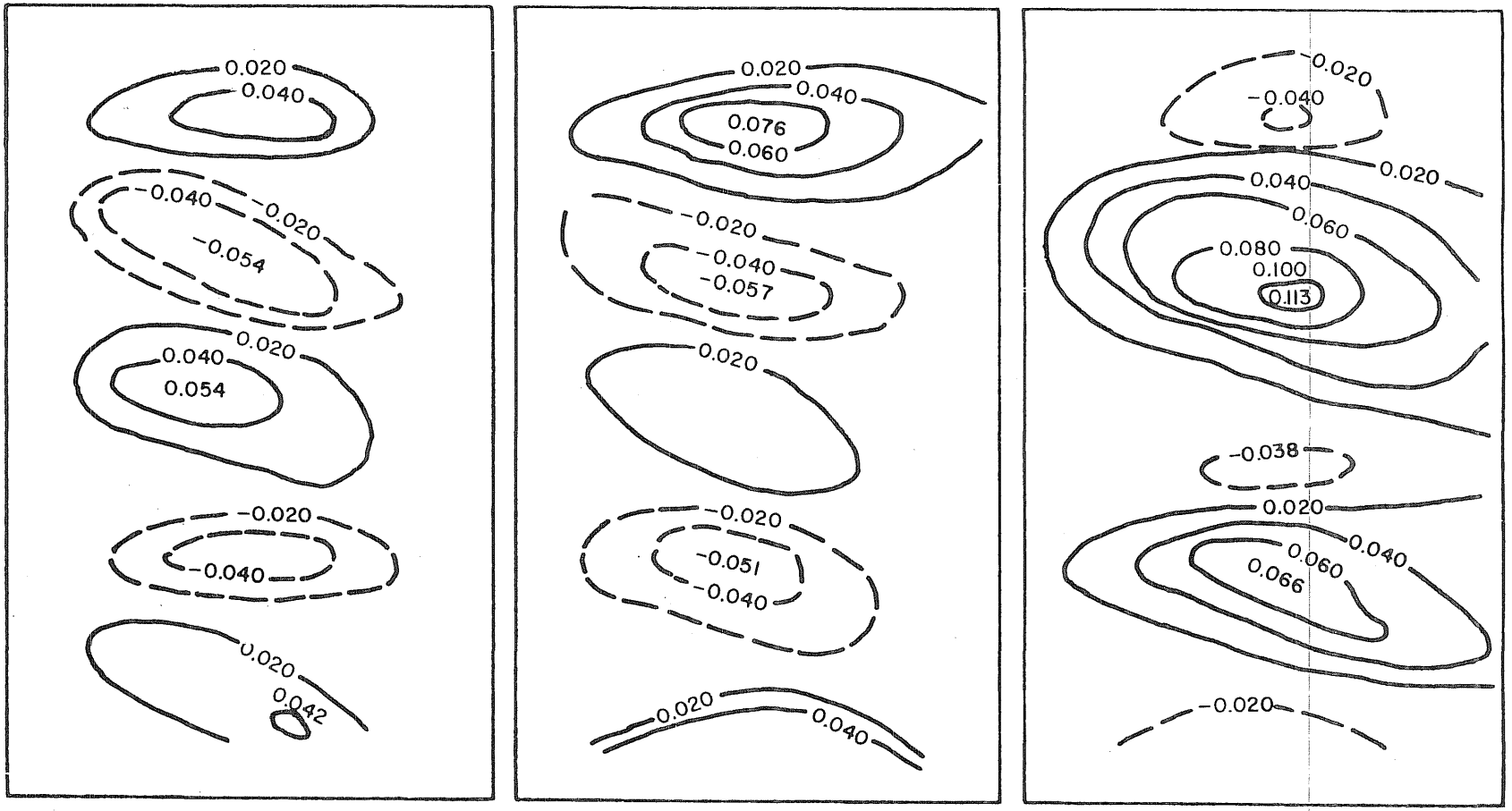

VST 8-4A

$\frac{W}{W_{mf}} = 1$

0 cycles

FIG. 42 WEB DEFLECTION DUE TO LOAD.

Note: Web deflections are given in inches.

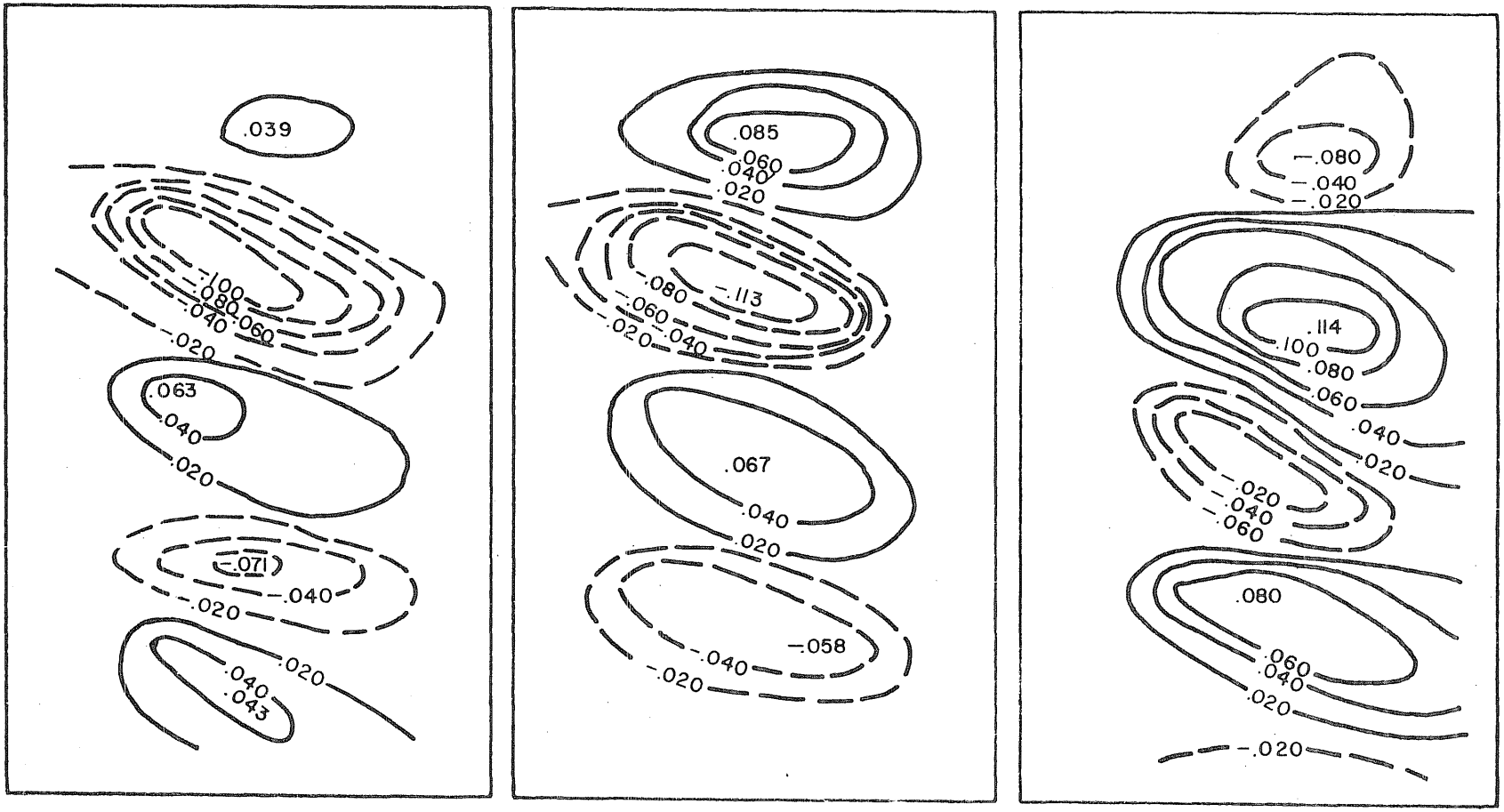

$$\frac{W}{W_{mf}} = 1.5$$

VST 8—4A

STATIC TEST

FIG. 43 WEB DEFLECTIONS DUE TO LOAD.

Note: Web deflections are given in inches.

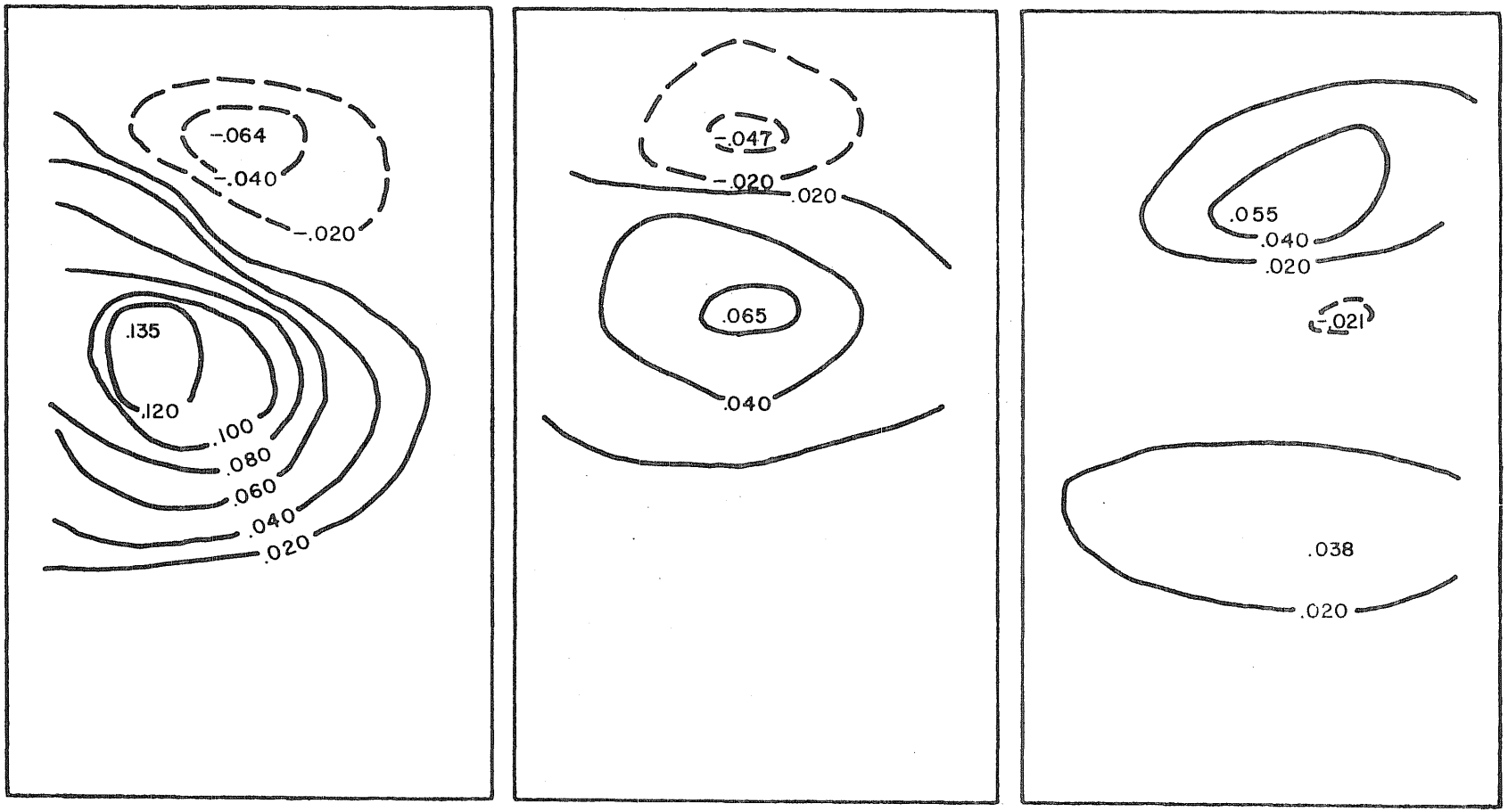

$$\frac{W\text{-}}{W_{mf}} = \frac{1}{4}$$

VST8-16A

STATIC TEST

FIG. 44 WEB DEFLECTIONS DUE TO LOAD.

Note: Web deflections are given in inches.

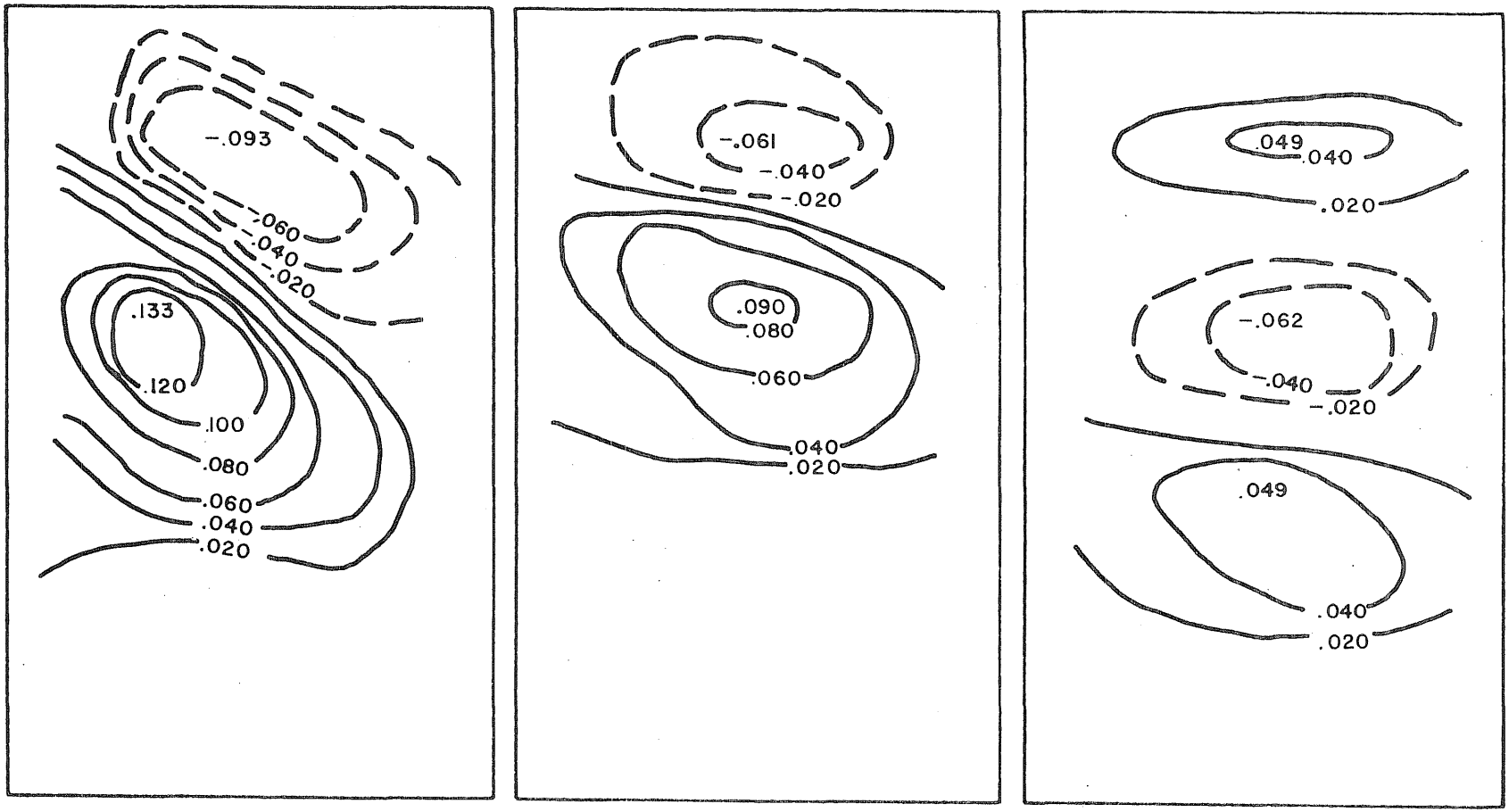

$\frac{W}{W_{mf}} = 1$

VST 8-16A

STATIC TEST

FIG. 45 WEB DEFLECTIONS DUE TO LOAD.

Note: Web deflections are given in inches.

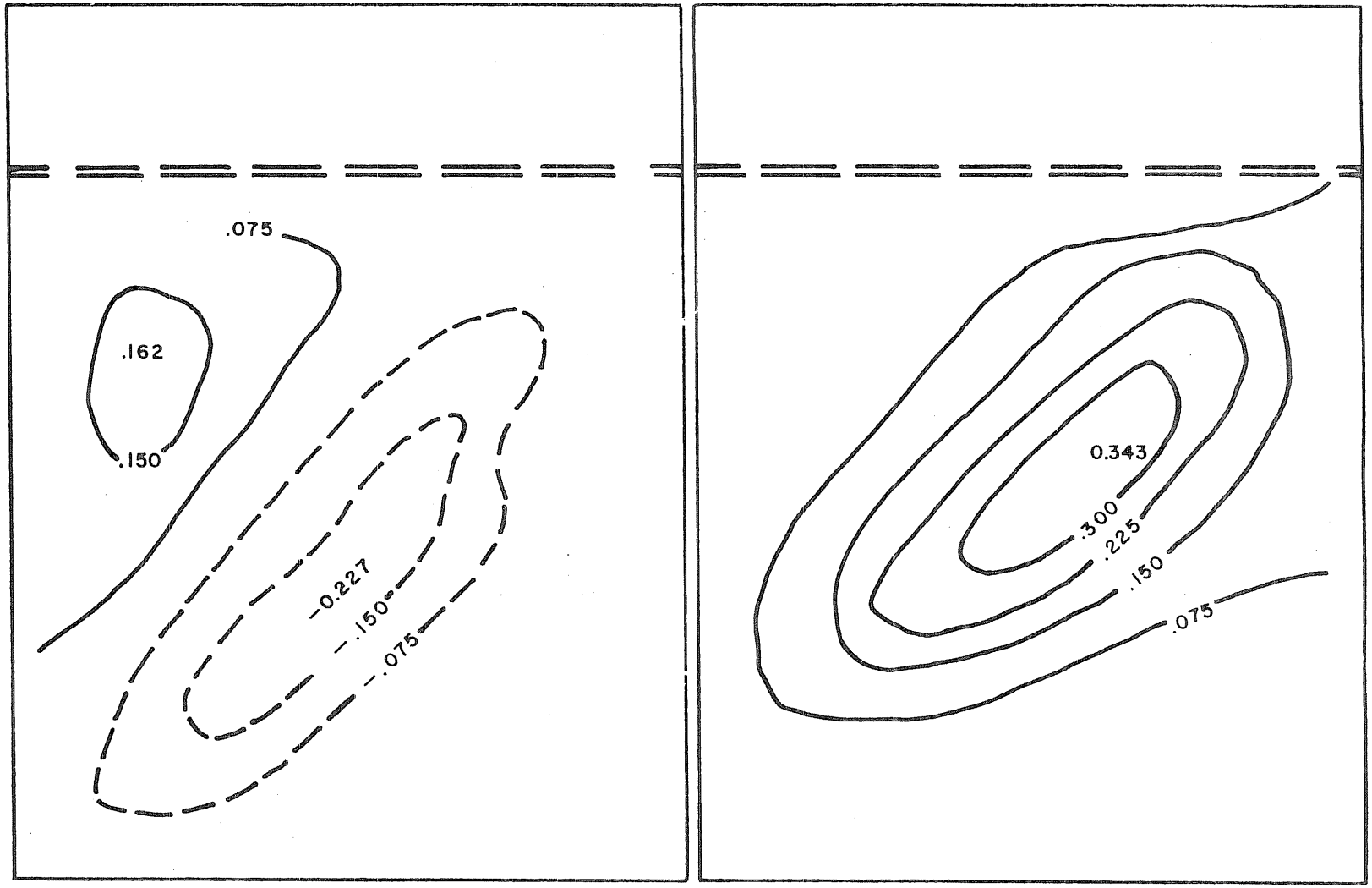

$\frac{W}{W_{mf}} = \frac{1}{4}$

HSB-1

6000 cycles

FIG. 46 WEB DEFLECTIONS DUE TO LOAD .

Note: Web deflections are given in inches.

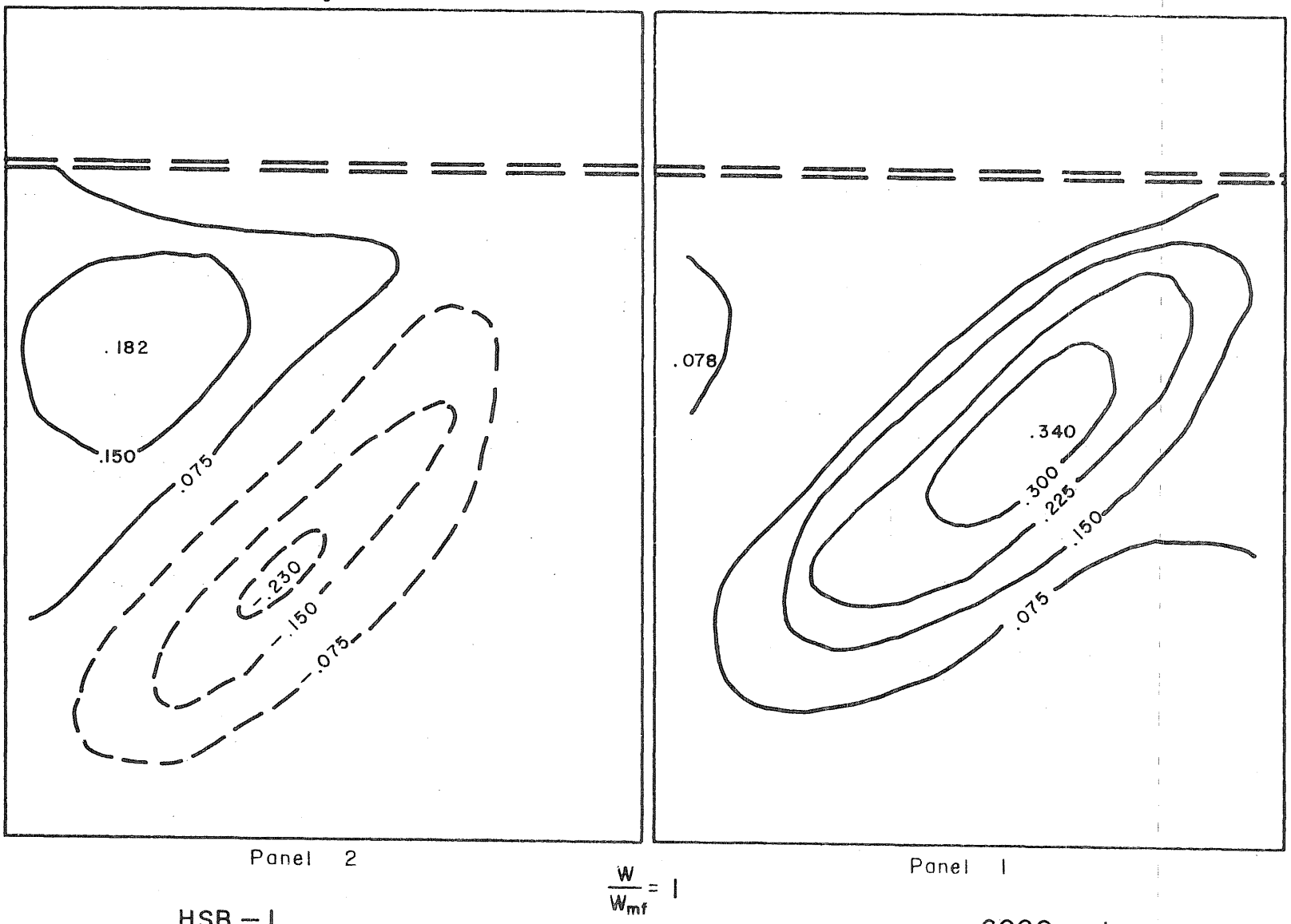

FIG. 47 WEB DEFLECTIONS DUE TO LOAD .

Note: Web deflections are given in inches.

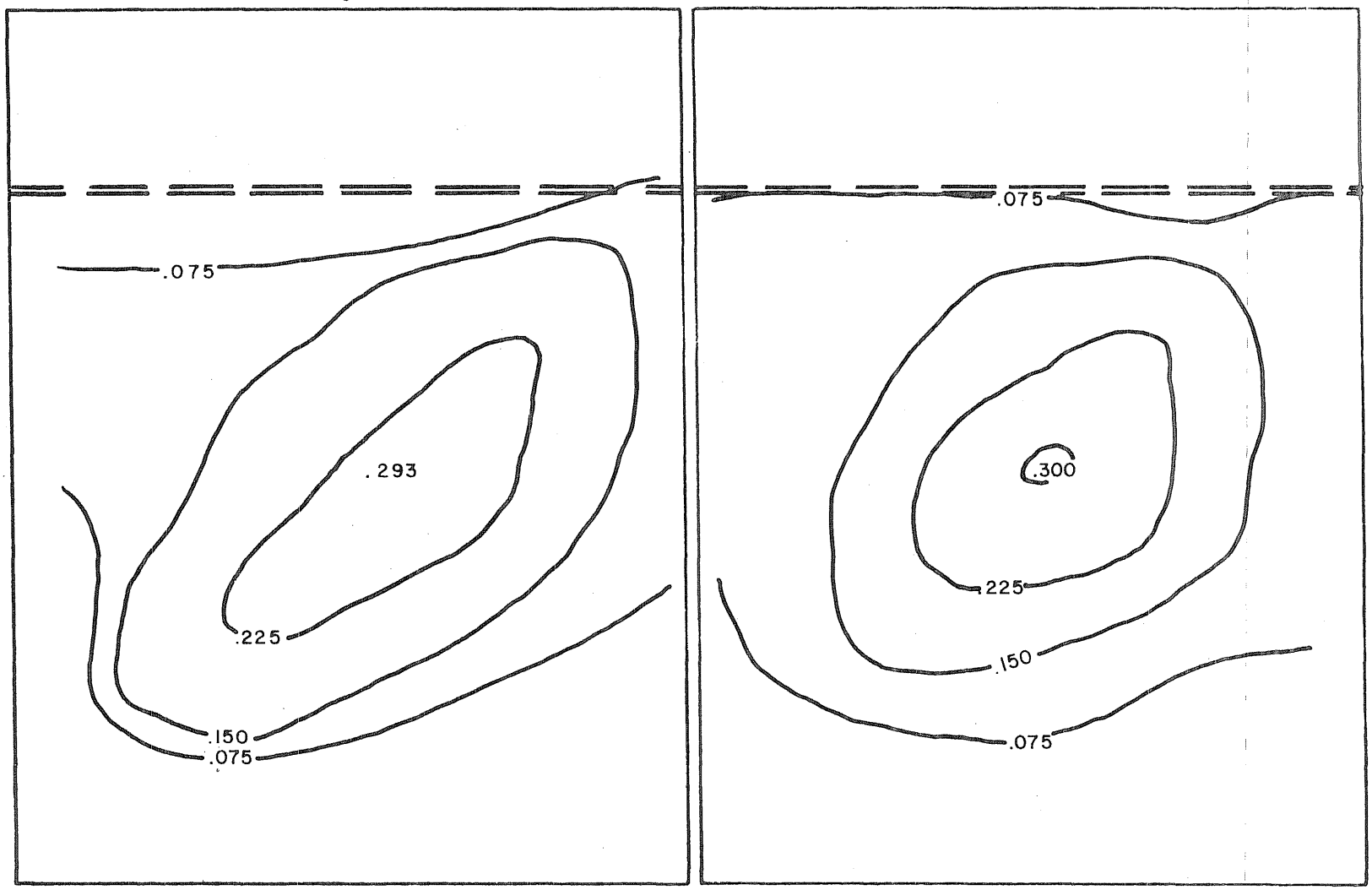

FIG. 48 WEB DEFLECTIONS DUE TO LOAD .

Note: Web deflections are given in inches.

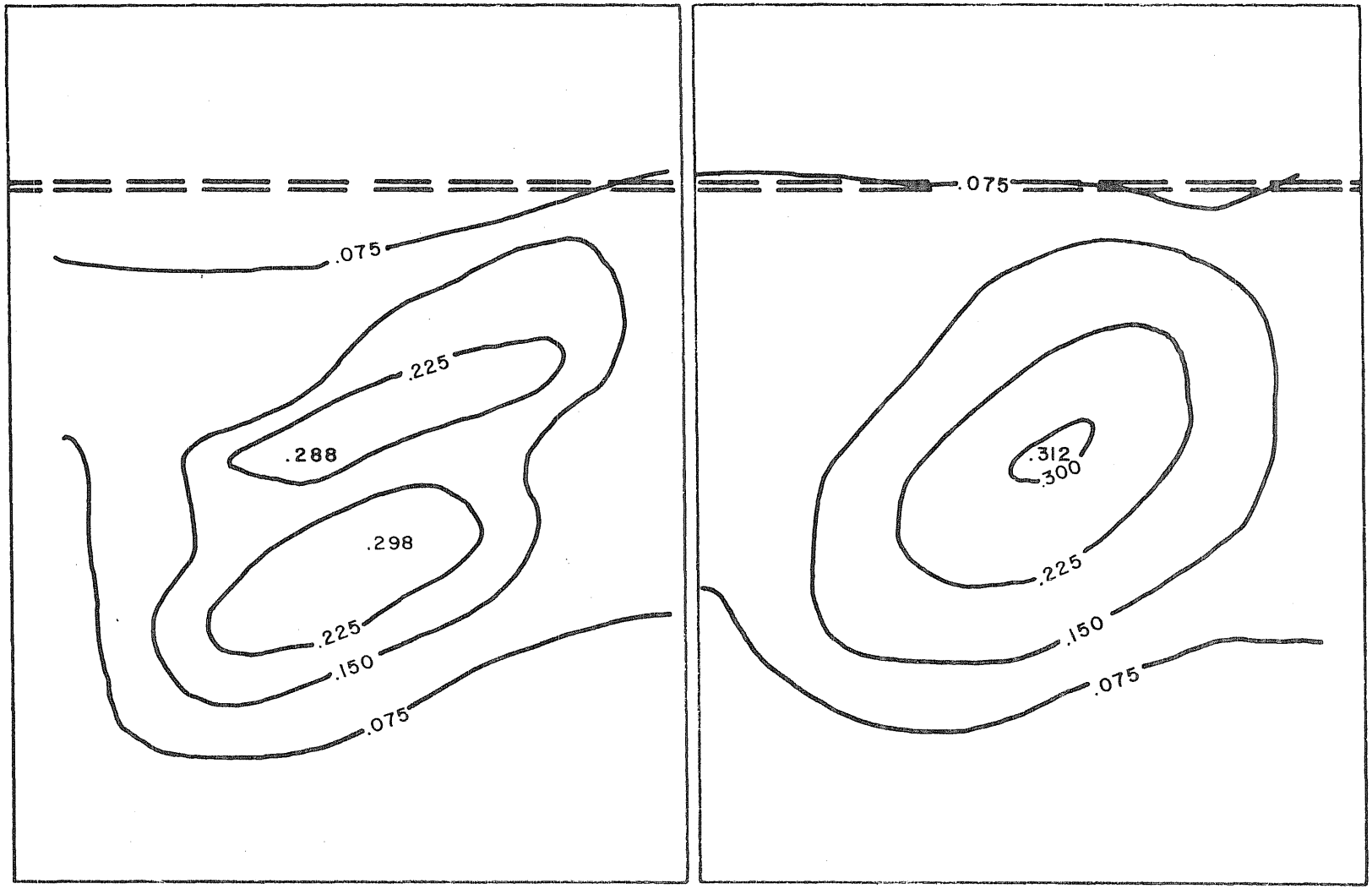

Panel 2

Panel 1

$\frac{W}{W_{mf}} = \frac{1}{2}$

HSB – 2

1000 cycles

FIG. 49 WEB DEFLECTIONS DUE TO LOAD

Note: Web deflections are given in inches.

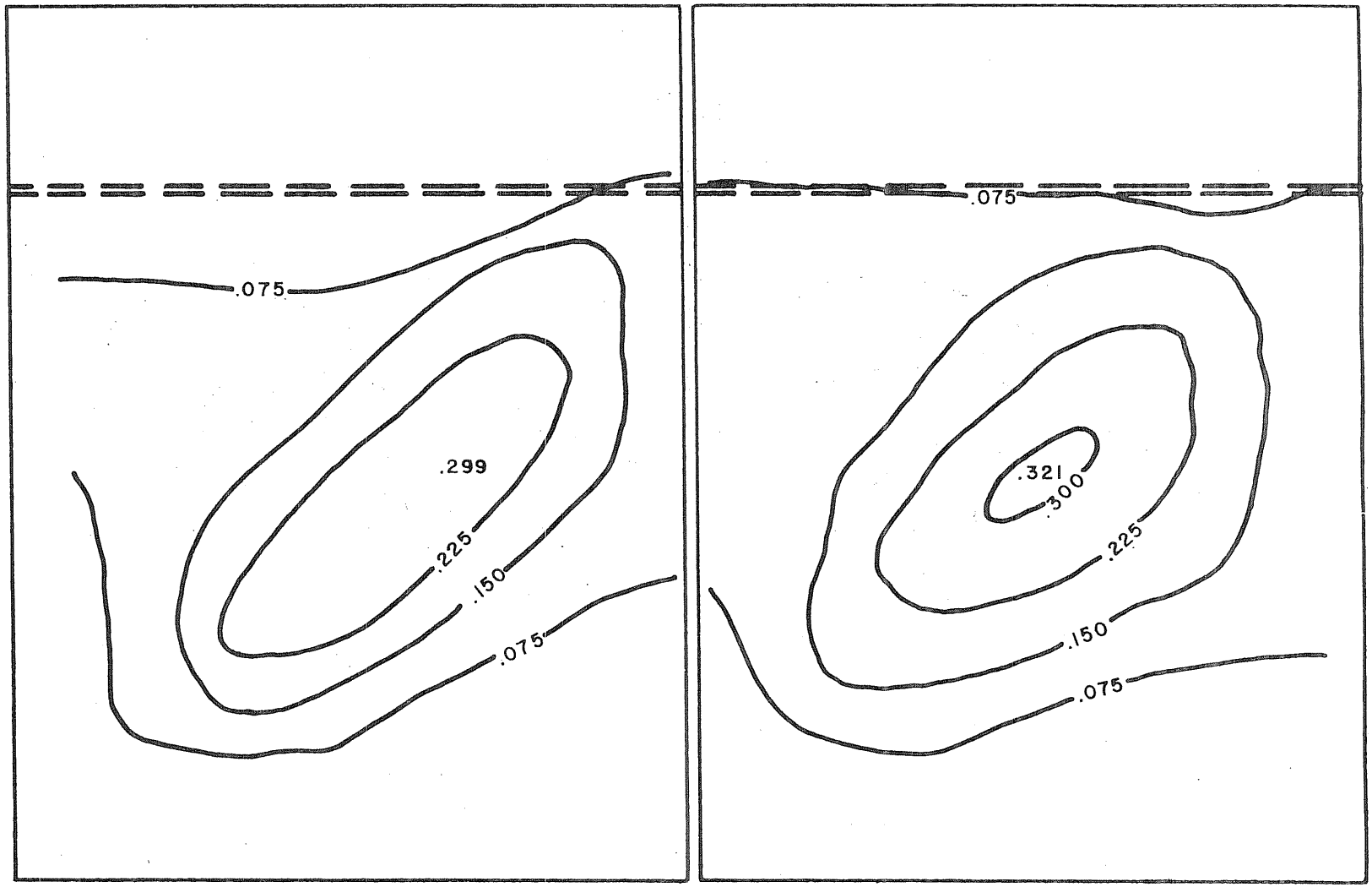

Panel 2

Panel 1

$\frac{W}{W_{mf}} = \frac{3}{4}$

HSB – 2

1000 cycles

FIG. 50 WEB DEFLECTIONS DUE TO LOAD .

Note: Web deflections are given in inches.

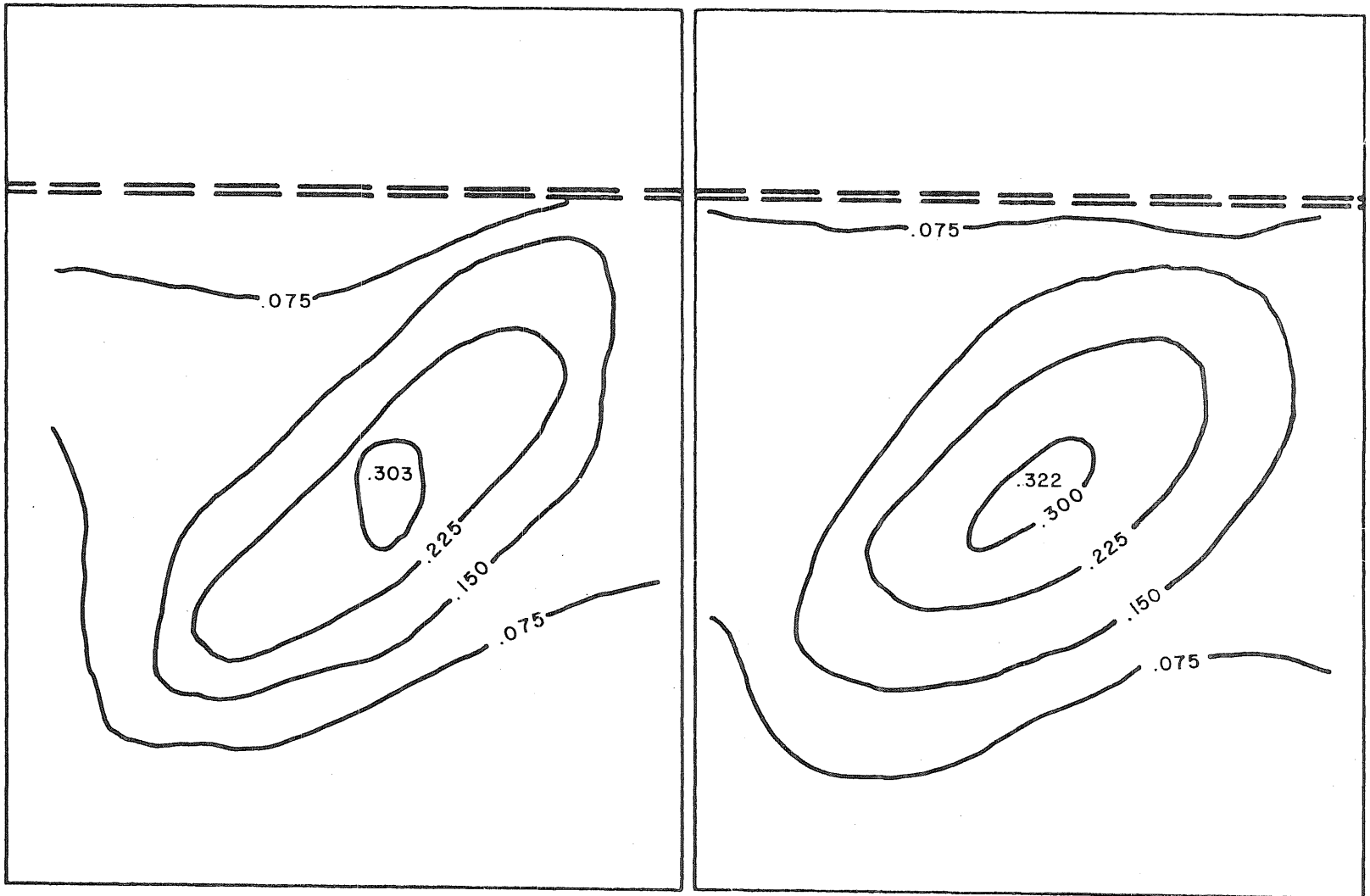

Panel 2

Panel 1

$\frac{W}{W_{mf}} = 1$

HSB – 2

1000 cycles

FIG. 51 WEB DEFLECTIONS DUE TO LOAD.

Note: Web deflections are given in inches.

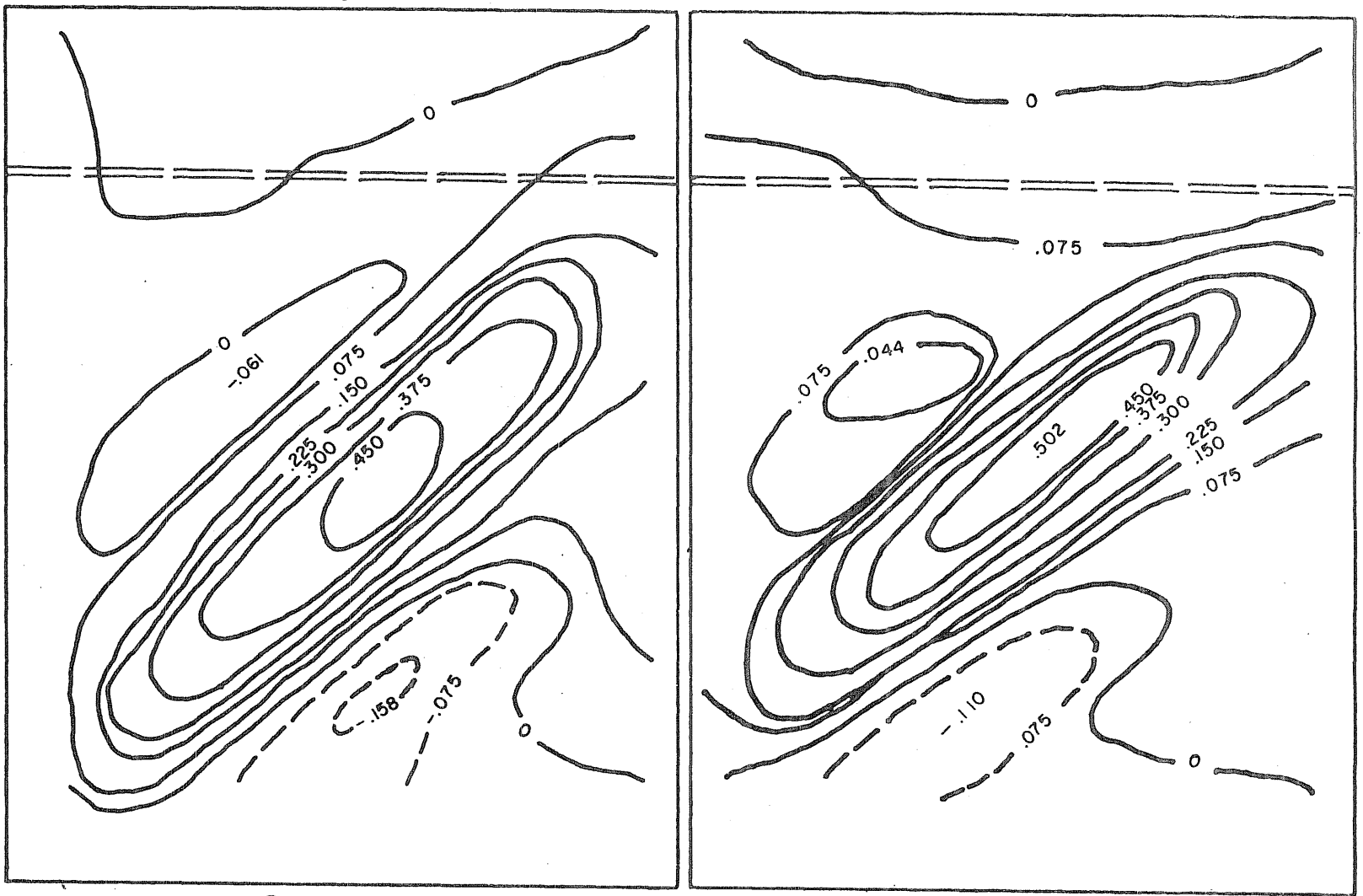

$\frac{W}{W_{mf}} = 1.3$

HSB-2

FIG. 52 WEB DEFLECTIONS OF HSB-2 DURING STATIC TEST.

Note: Web deflections are given in inches.

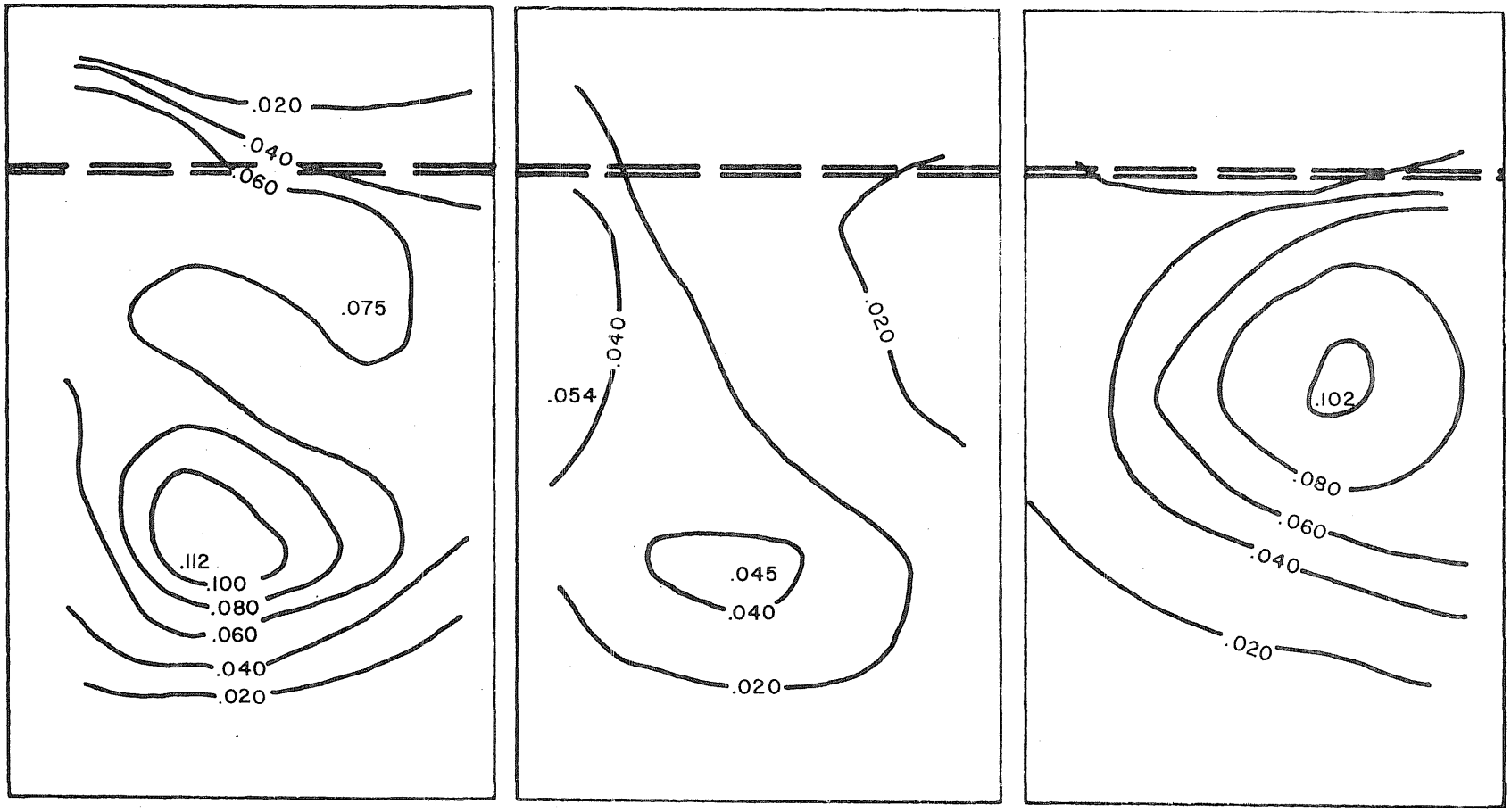

HVSB-I

$\frac{W}{W_{mf}} = \frac{1}{4}$

1000 cycles

FIG. 53 WEB DEFLECTIONS DUE TO LOAD.

Note: Web deflections are given in inches.

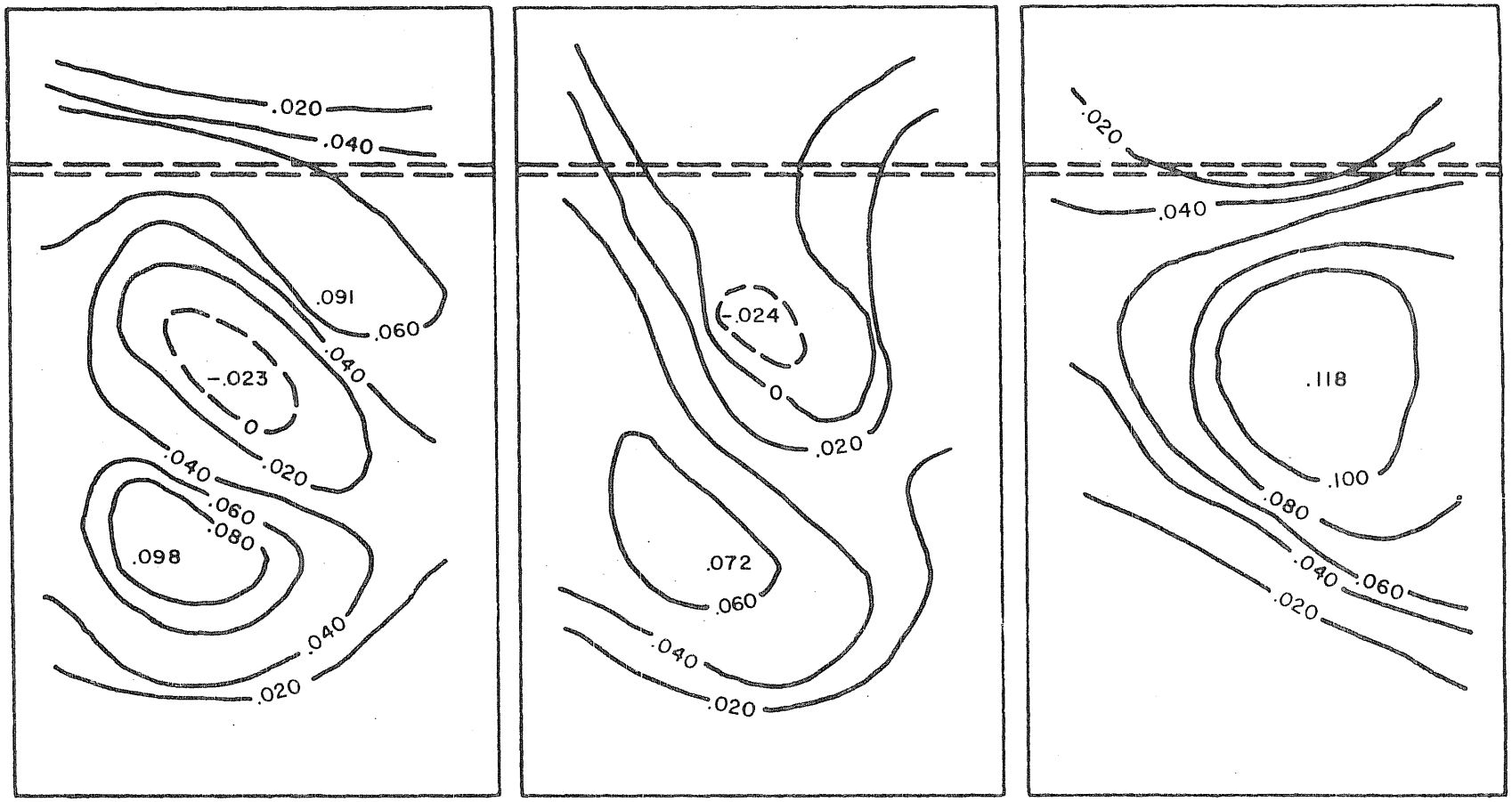

HVSB – 1 $\frac{W}{W_{mf}} = 1$ 1,000 cycles

FIG. 54 WEB DEFLECTIONS DUE TO LOAD.

Note: Web deflections are given in inches.

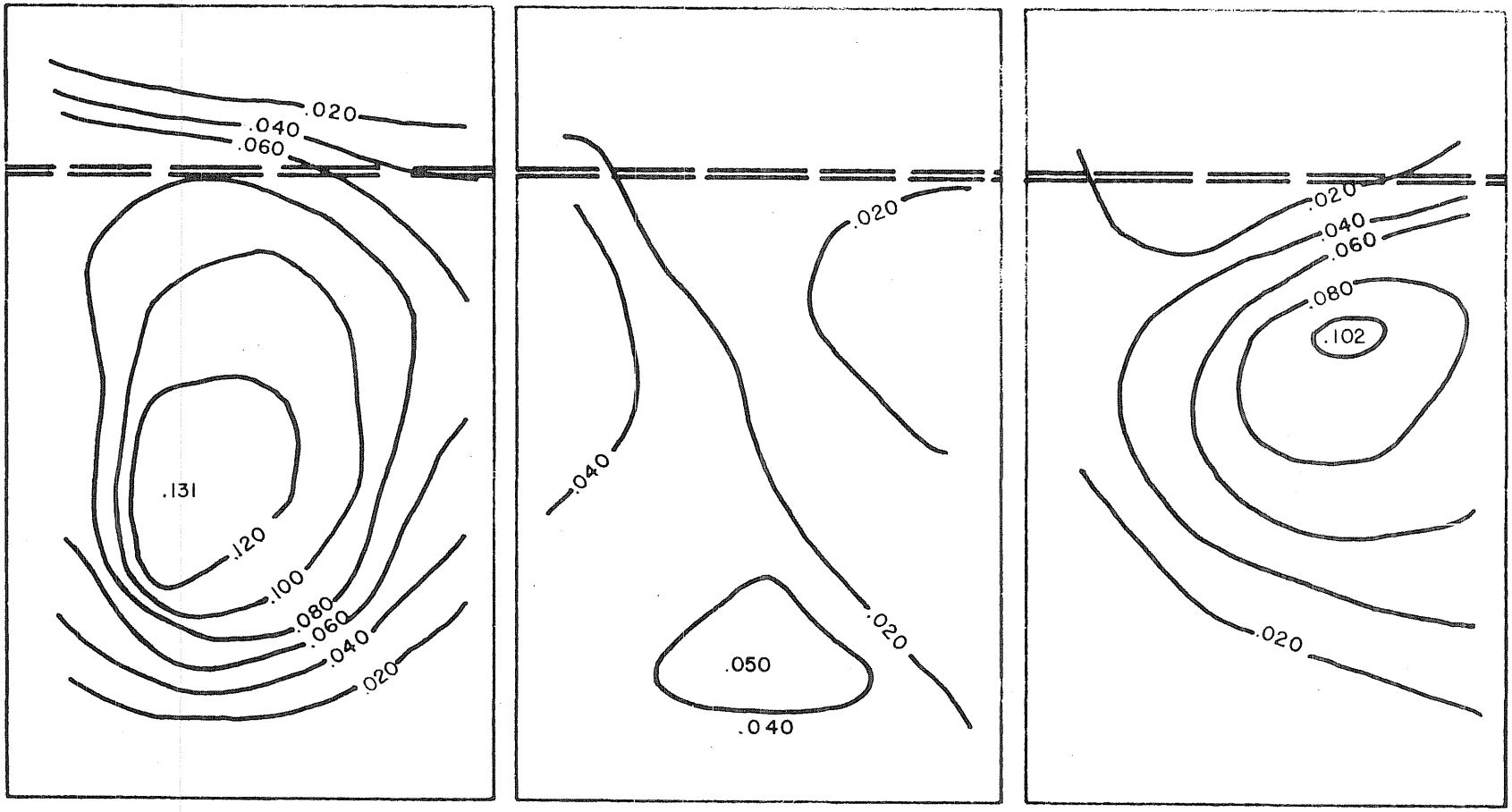

HVSB – 1 $\frac{W}{W_{mf}} = 0$ 478,000 cycles

FIG. 55 WEB DEFLECTIONS OF HVSB-1

Note: Web deflections are given in inches.

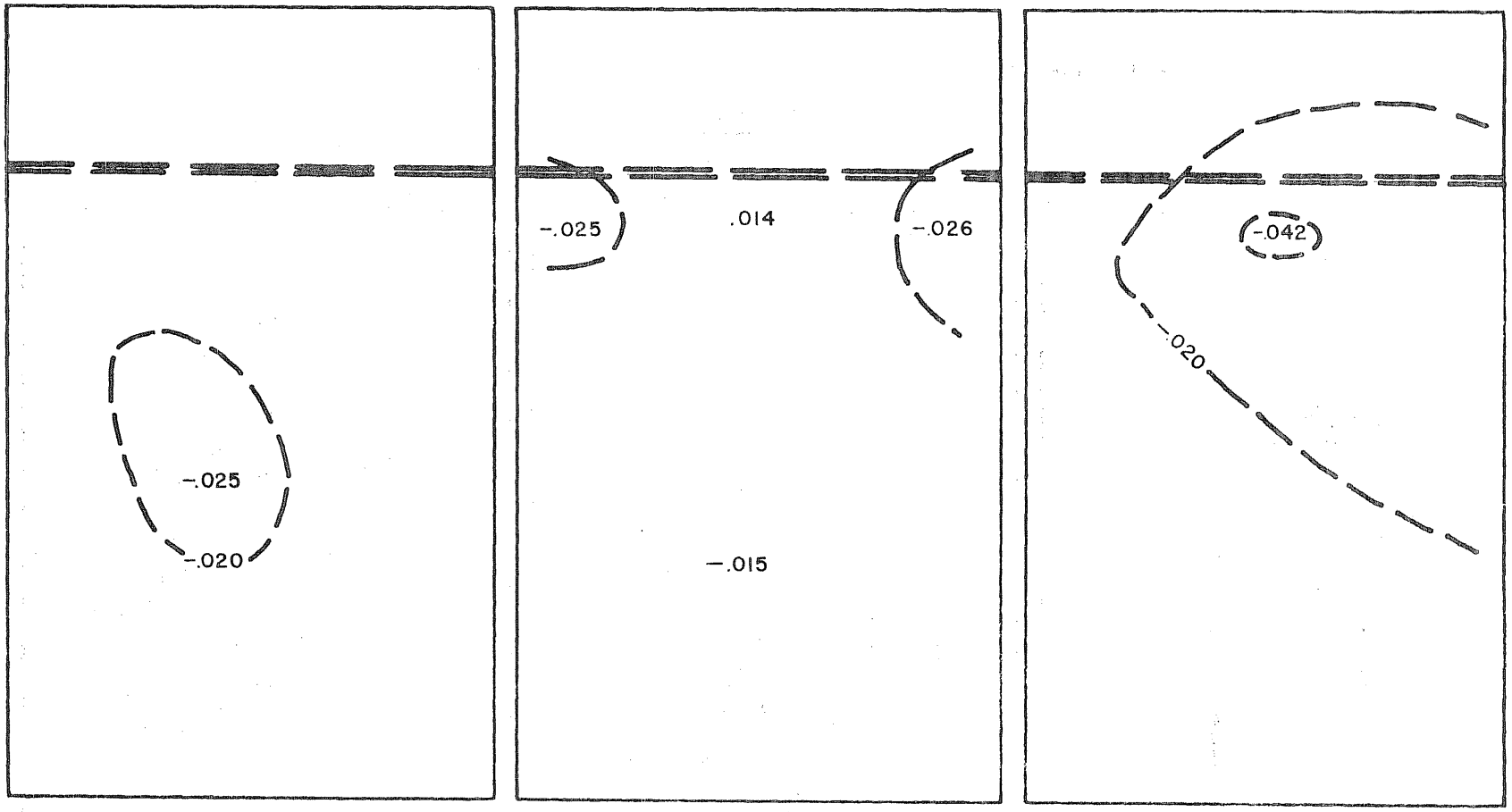

HVSB-2 $\frac{W}{W_{mf}} = \frac{1}{4}$ 3000 cycles

FIG. 56 WEB DEFLECTIONS DUE TO LOAD.

SRS 328

Note: Web deflections are given in inches.

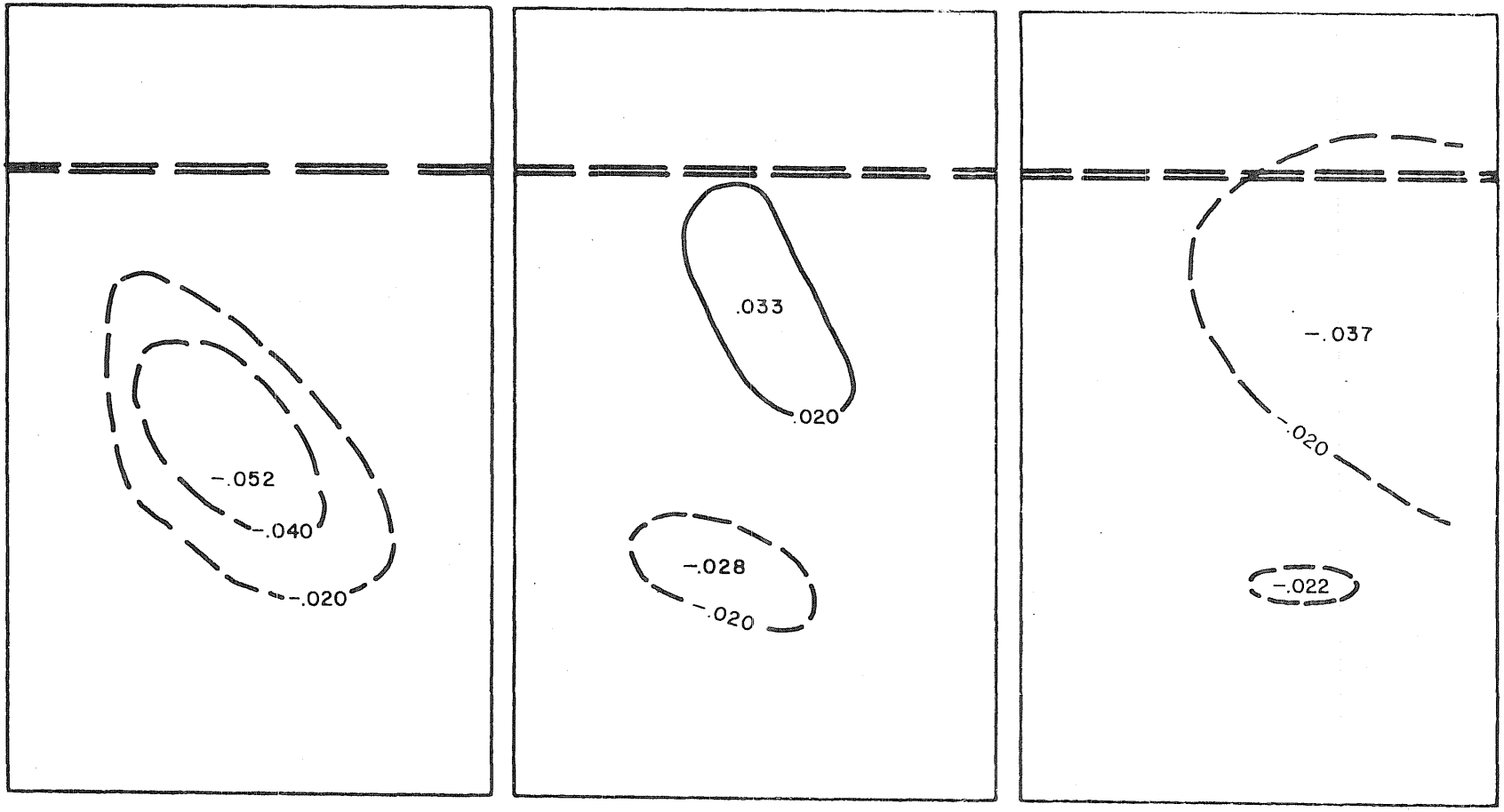

$\frac{W}{W_{mf}} = 1$

HSVB-2

3000 cycles

FIG. 57 WEB DEFLECTIONS DUE TO LOAD.

Note: Web deflections are given in inches.

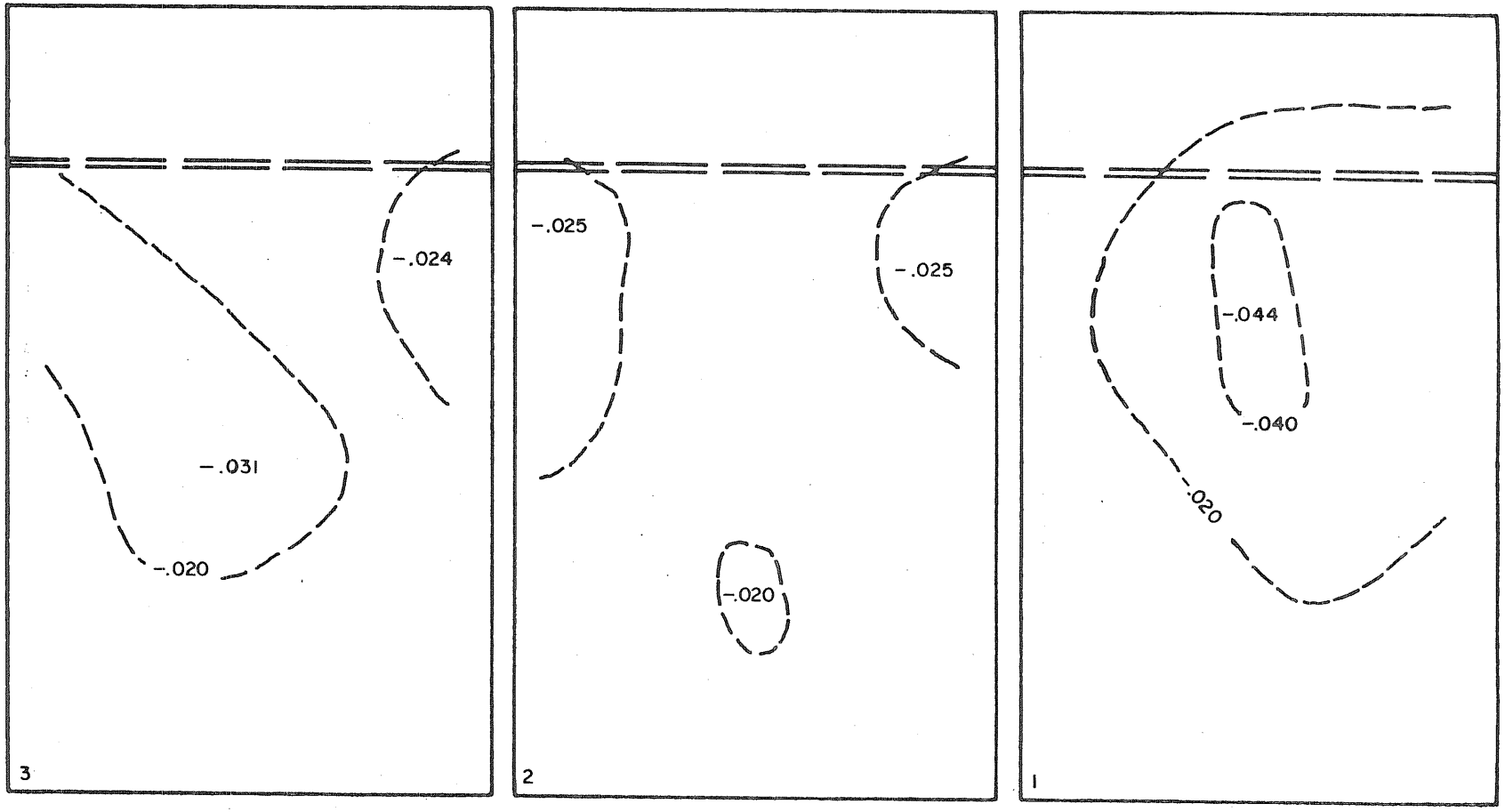

HVSB-2 $\frac{W}{W_{mf}} = \frac{1}{4}$ 3,000,000 cycles

FIG. 58 WEB DEFLECTIONS DUE TO LOAD.

Note: Web deflections are given in inches.

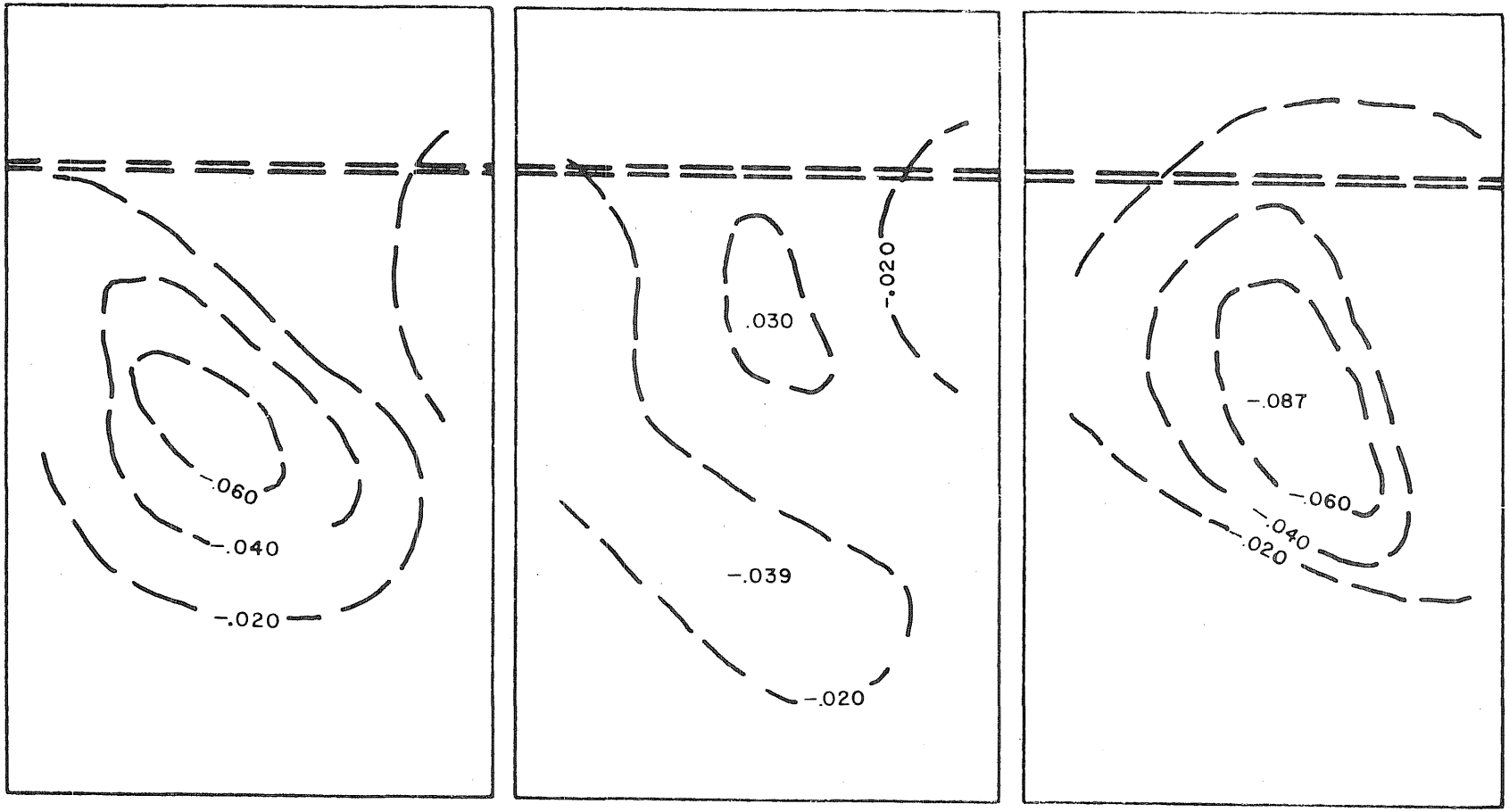

HVSB-2 $\frac{W}{W_{mf}} = 1$ 3,000,000 cycles

FIG. 59 WEB DEFLECTIONS DUE TO LOAD.

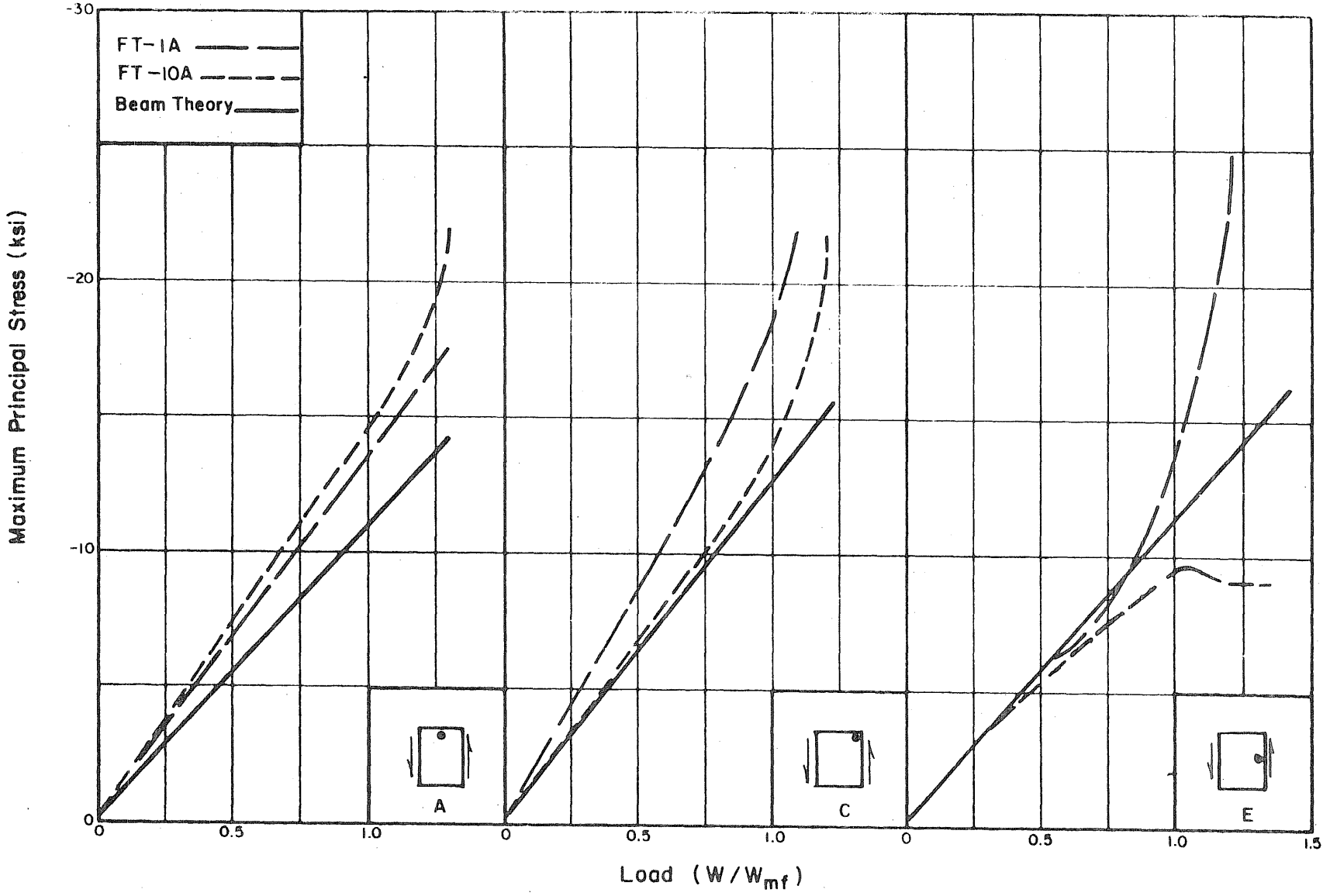

FIG. 60 MAXIMUM PRINCIPAL STRESS vs LOAD AT VARIOUS WEB LOCATIONS.

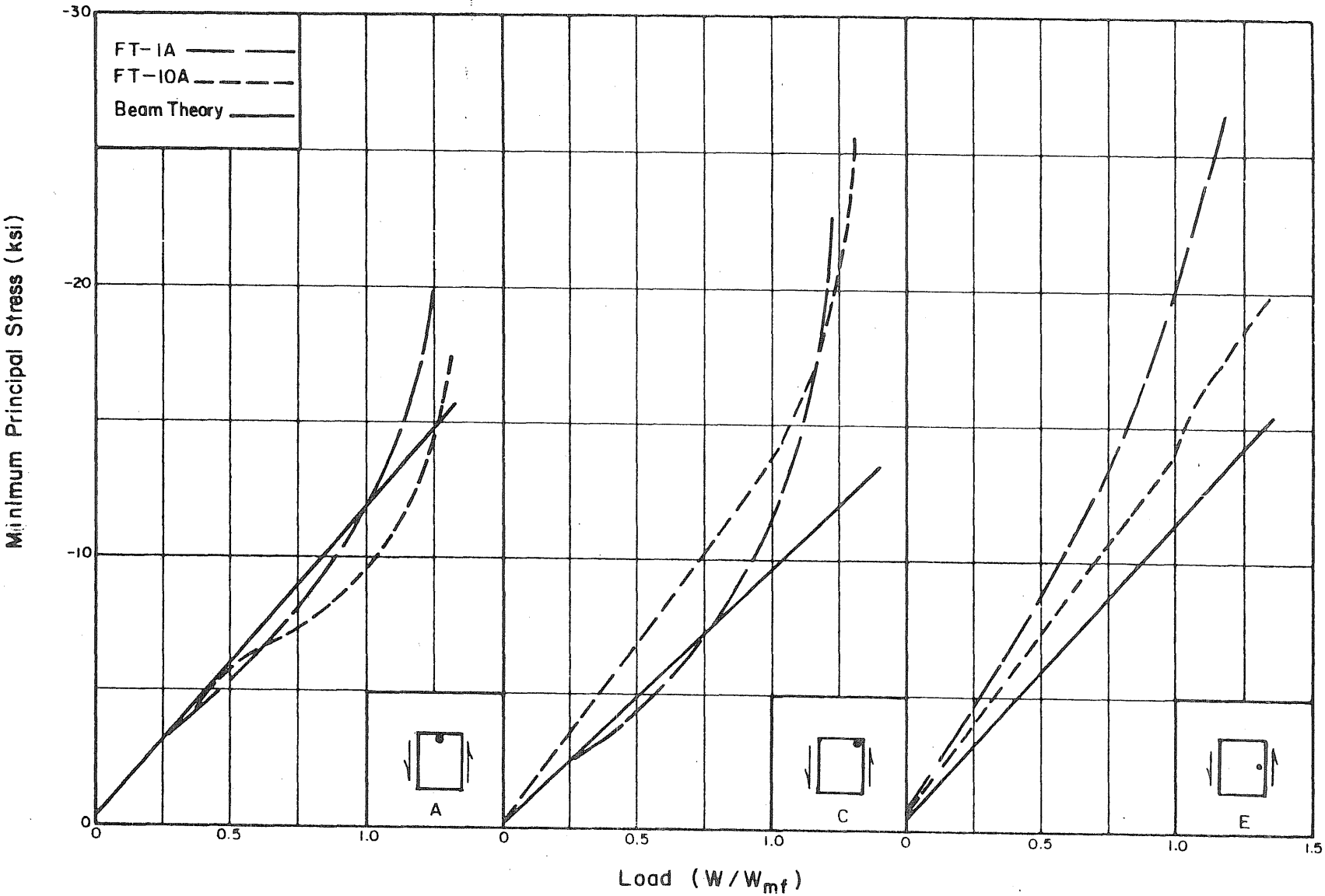

FIG. 61 MINIMUM PRINCIPAL STRESS vs LOAD AT VARIOUS WEB LOCATIONS.

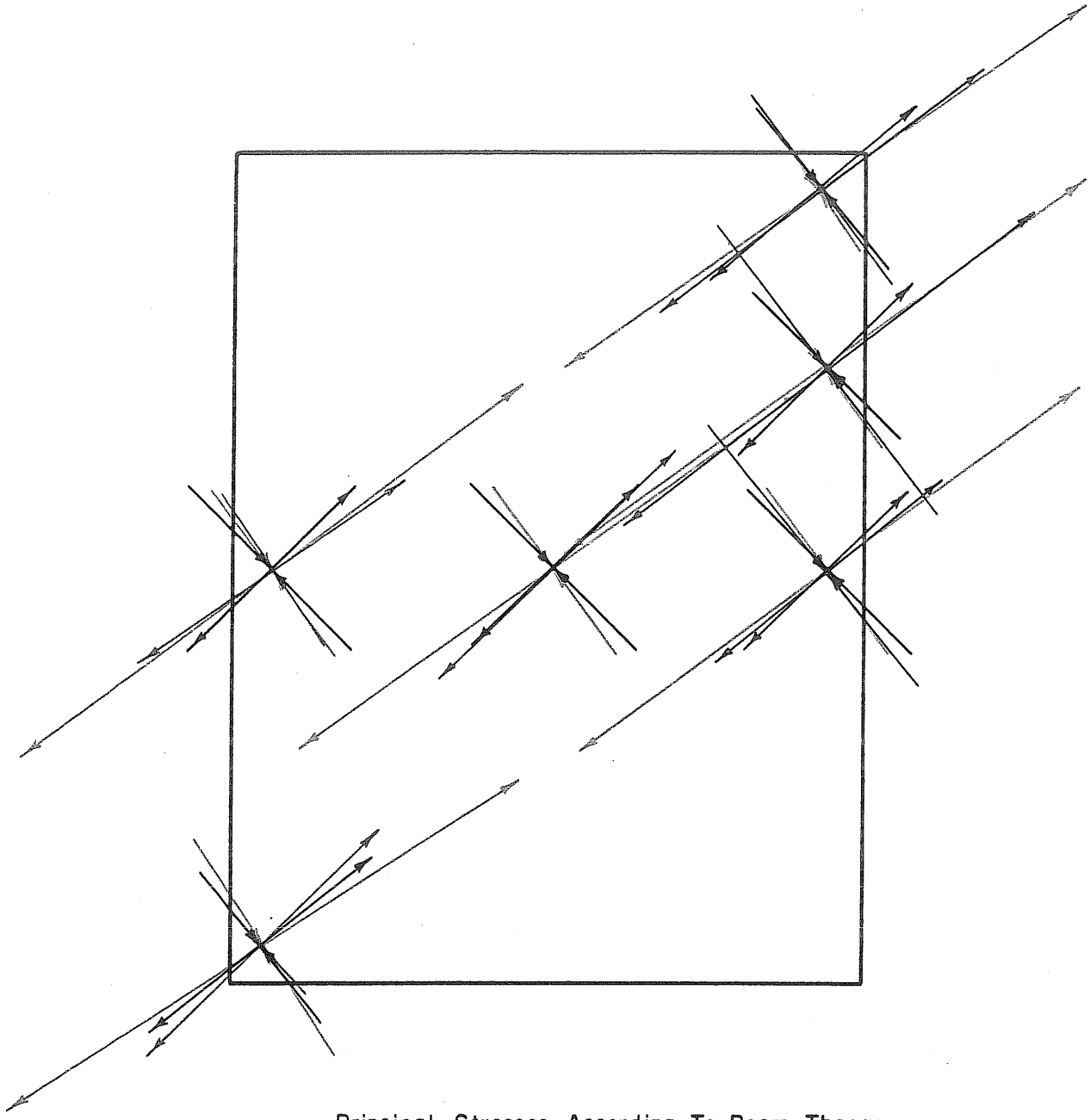

FIG. 62 PRINCIPAL STRESSES AT VARIOUS PANEL LOCATIONS OF SHEAR GIRDER FT-1A.

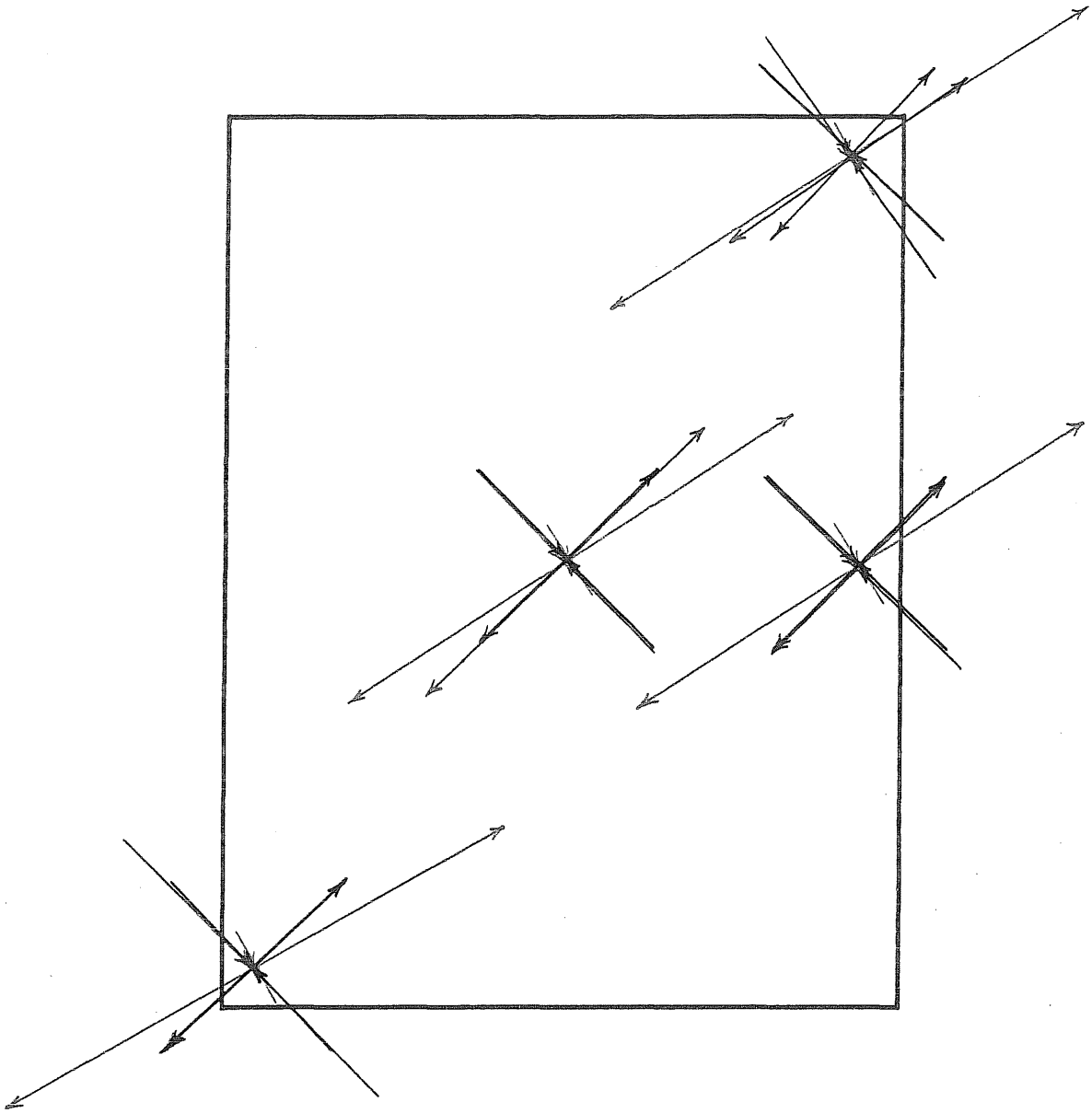

FIG. 63 PRINCIPAL STRESSES AT VARIOUS PANEL LOCATIONS OF SHEAR GIRDER FT-10A.

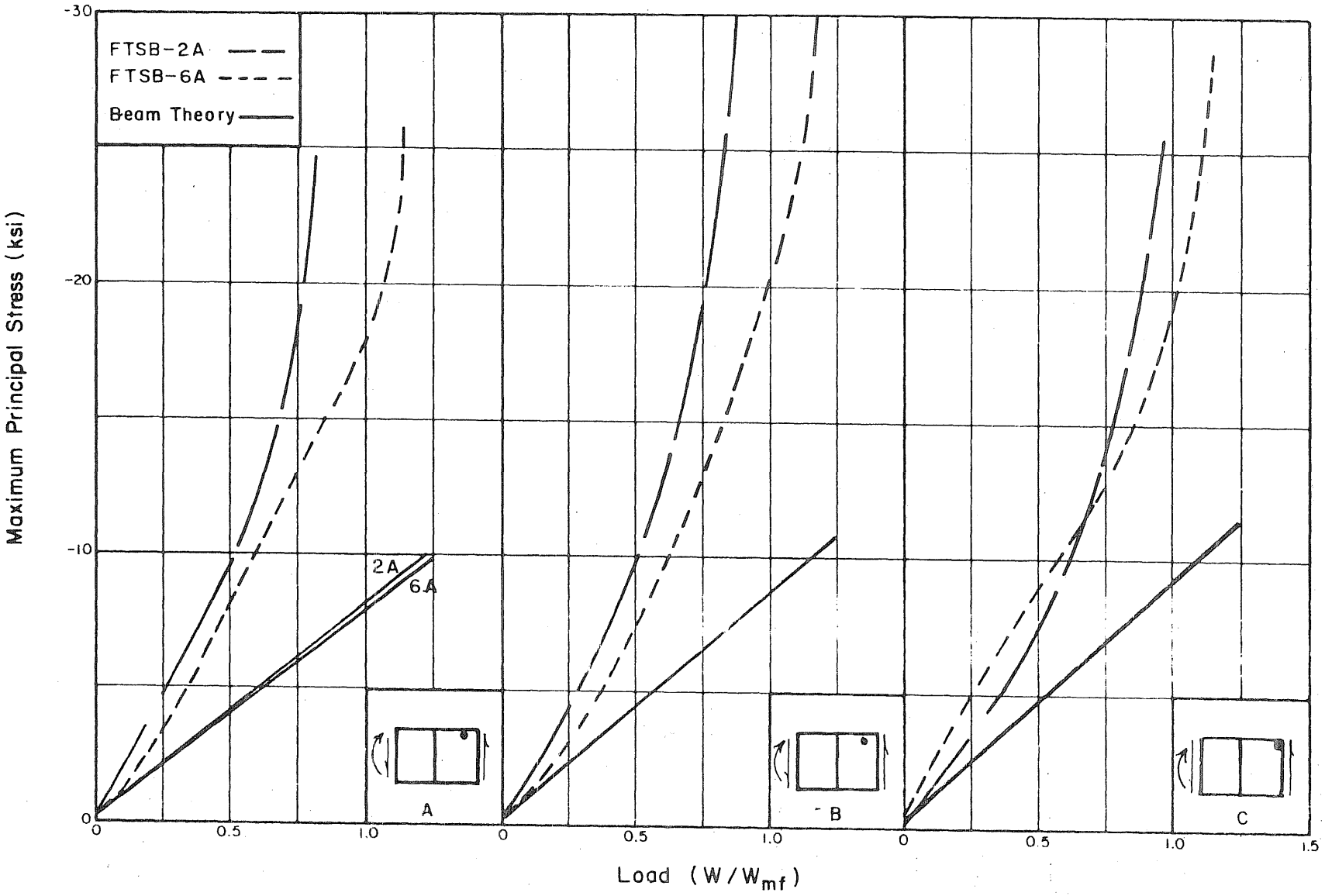

FIG. 64 MAXIMUM PRINCIPAL STRESS vs LOAD AT VARIOUS WEB LOCATIONS.

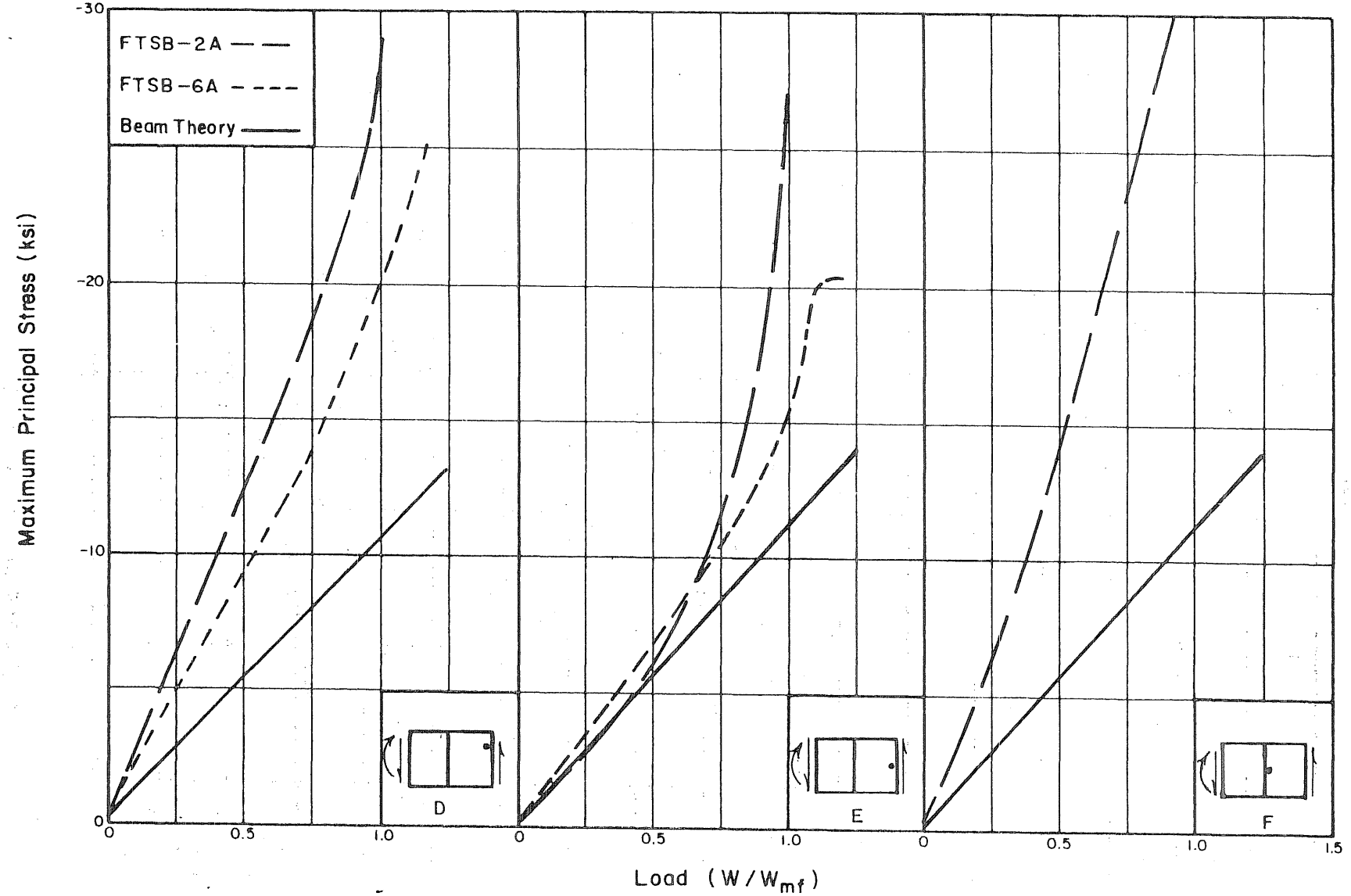

FIG. 65 MAXIMUM PRINCIPAL STRESS vs LOAD AT VARIOUS WEB LOCATIONS.

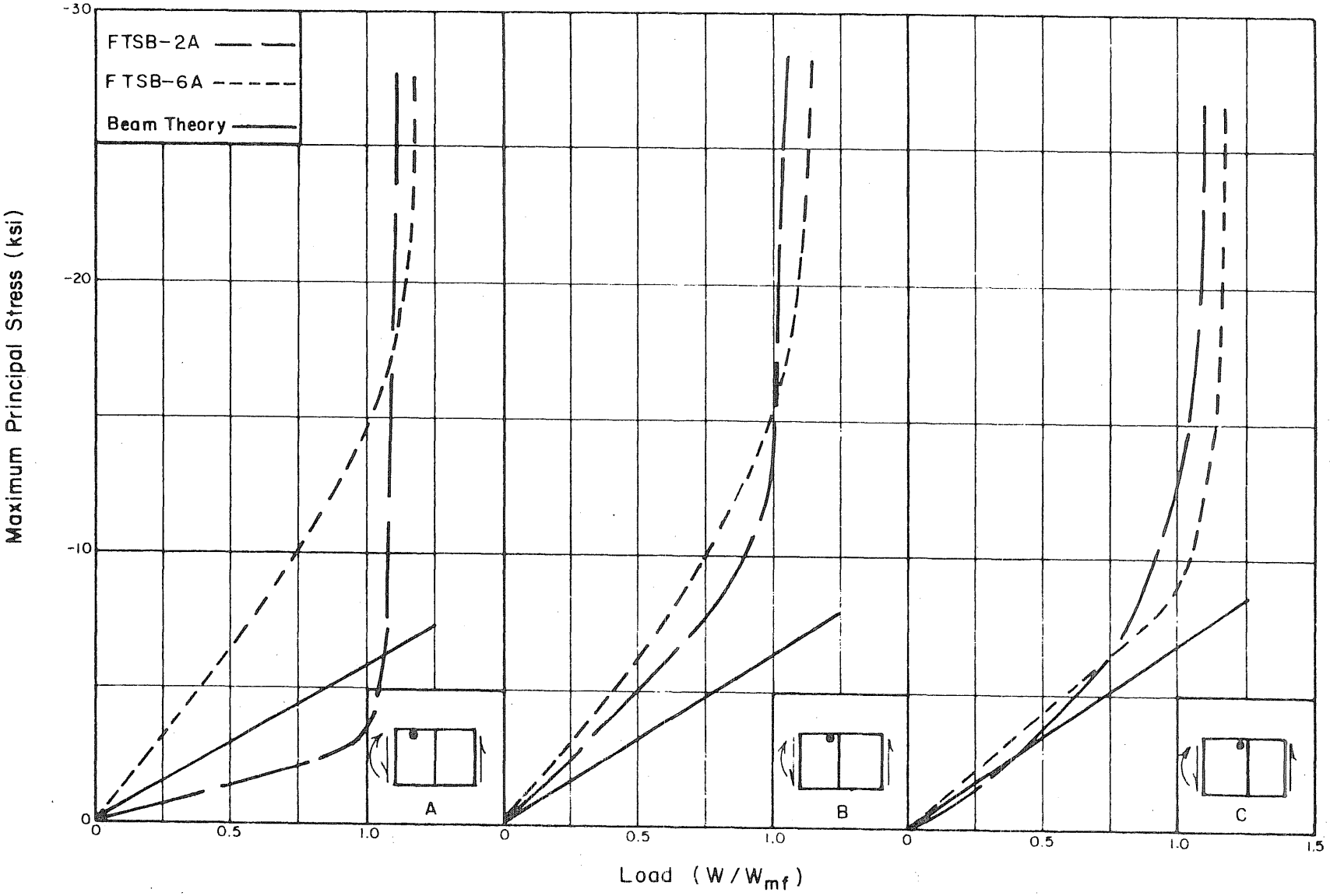

FIG. 66 MAXIMUM PRINCIPAL STRESS vs LOAD AT VARIOUS WEB LOCATIONS.

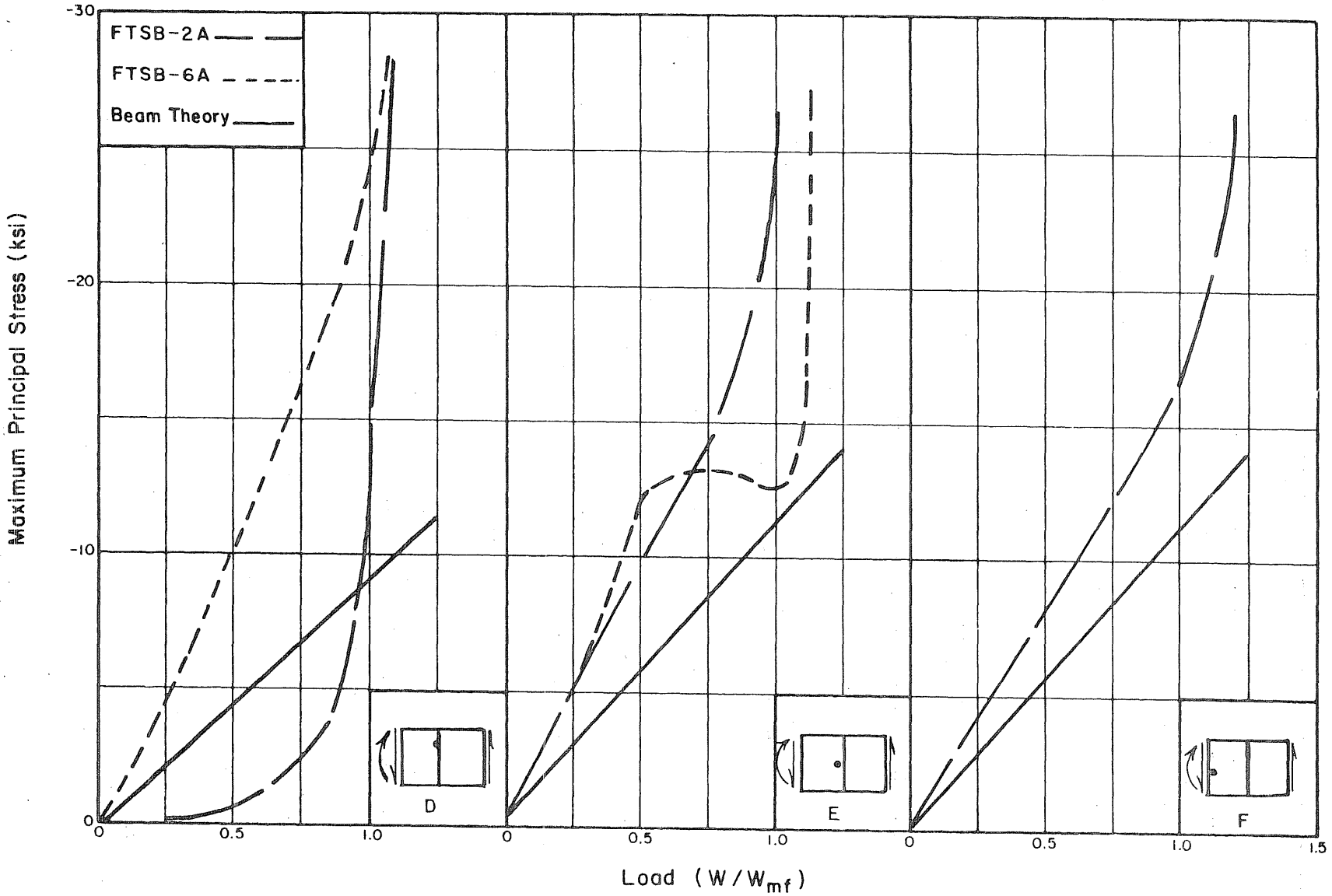

FIG. 67 MAXIMUM PRINCIPAL STRESS vs LOAD AT VARIOUS WEB LOCATIONS.

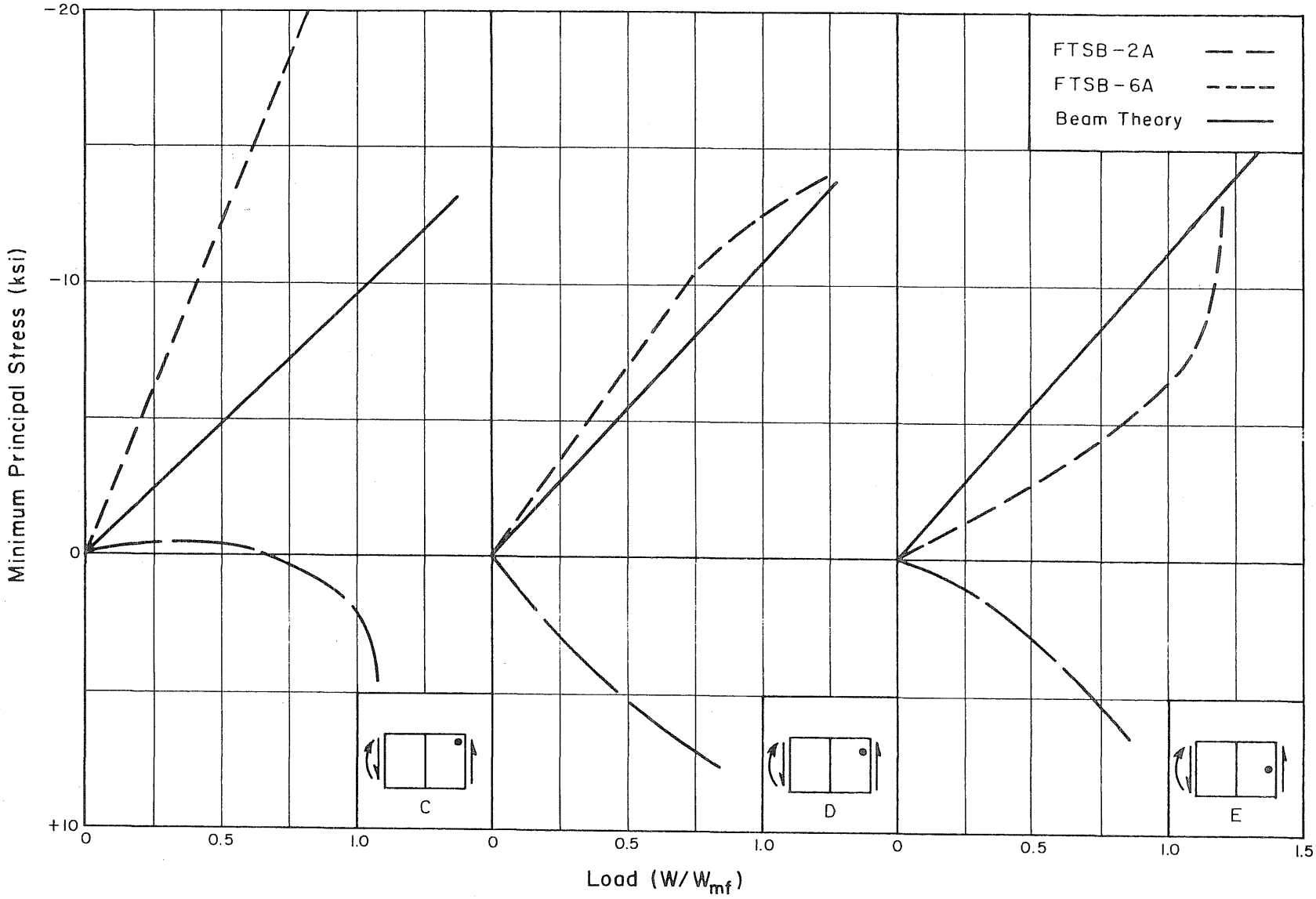

FIG. 68 MINIMUM PRINCIPAL STRESS vs LOAD FOR FTSB GIRDERS.

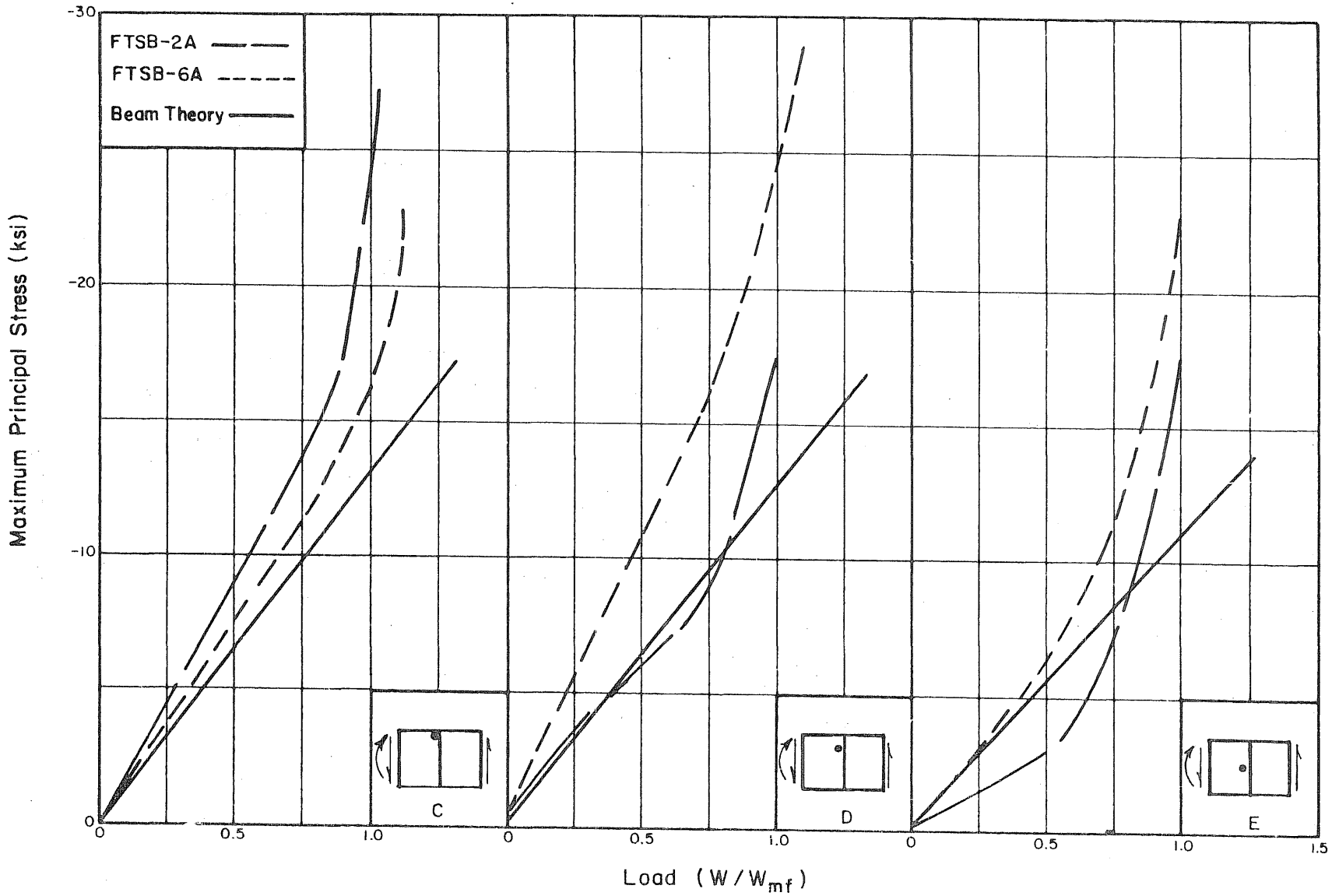

FIG. 69 MAXIMUM PRINCIPAL STRESS vs LOAD AT VARIOUS WEB LOCATIONS.

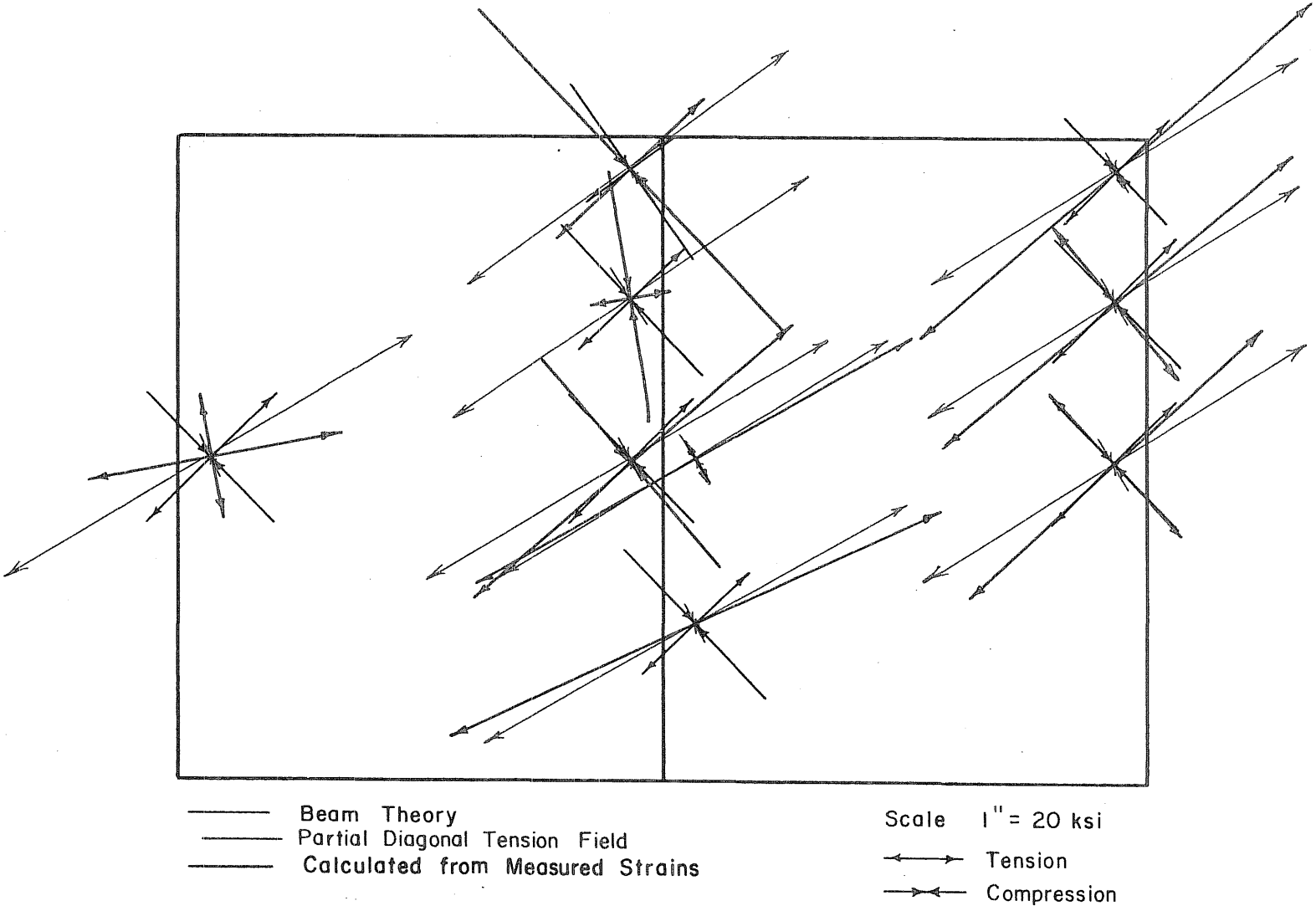

FIG. 70 COMPARISON OF PREDICTED AND MEASURED MEMBRANE STRESSES FOR FTSB-2A.

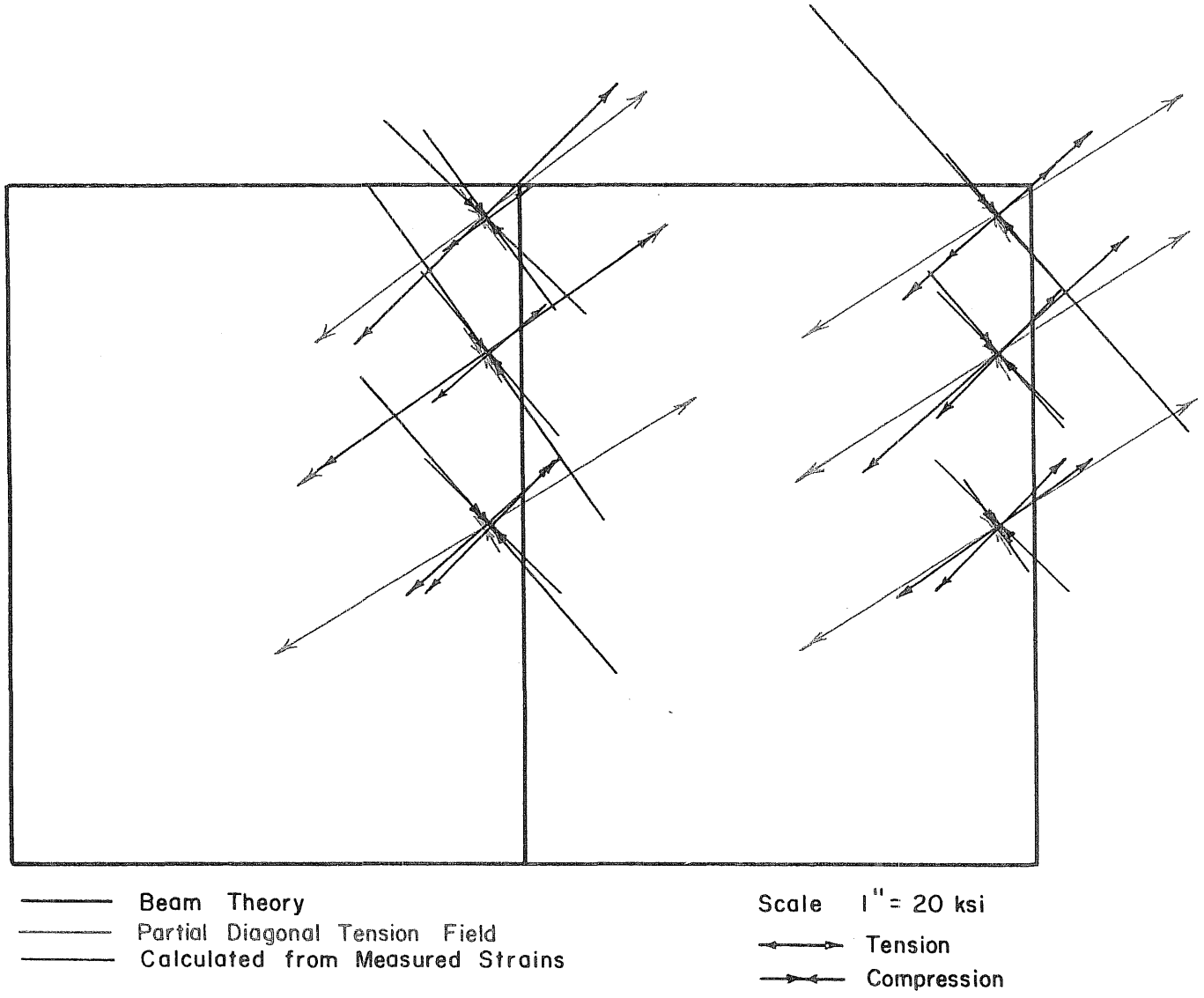

FIG. 71 COMPARISON OF PREDICTED AND MEASURED MEMBRANE STRESSES FOR FTSB-6A.

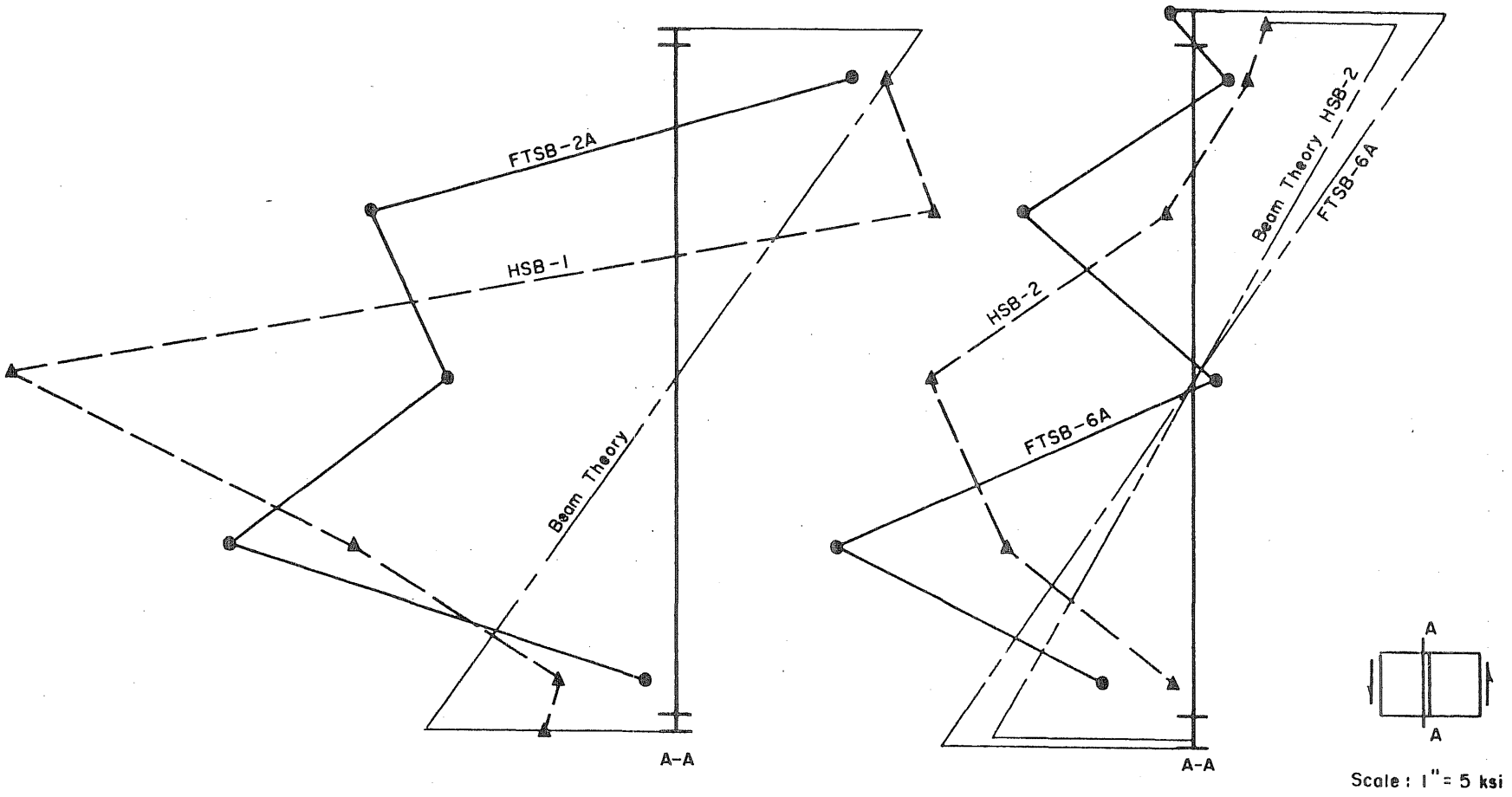

FIG. 72 DISTRIBUTION OF STRESSES ON A VERTICAL CROSS SECTION FOR GIRDERS WITH VARIOUS FLANGE RIGIDITIES.

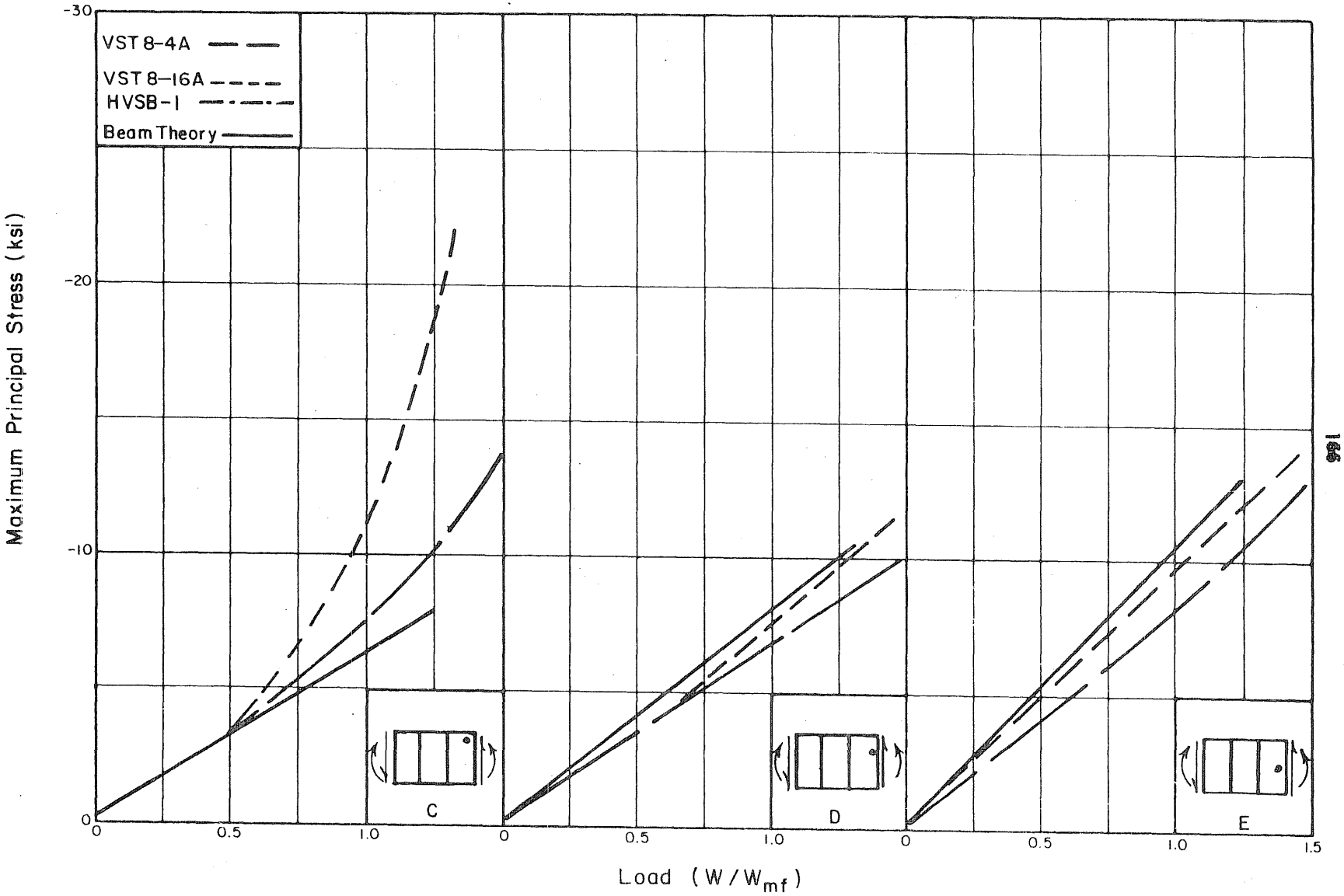

FIG. 73 MAXIMUM PRINCIPAL STRESS vs LOAD AT VARIOUS WEB LOCATIONS.

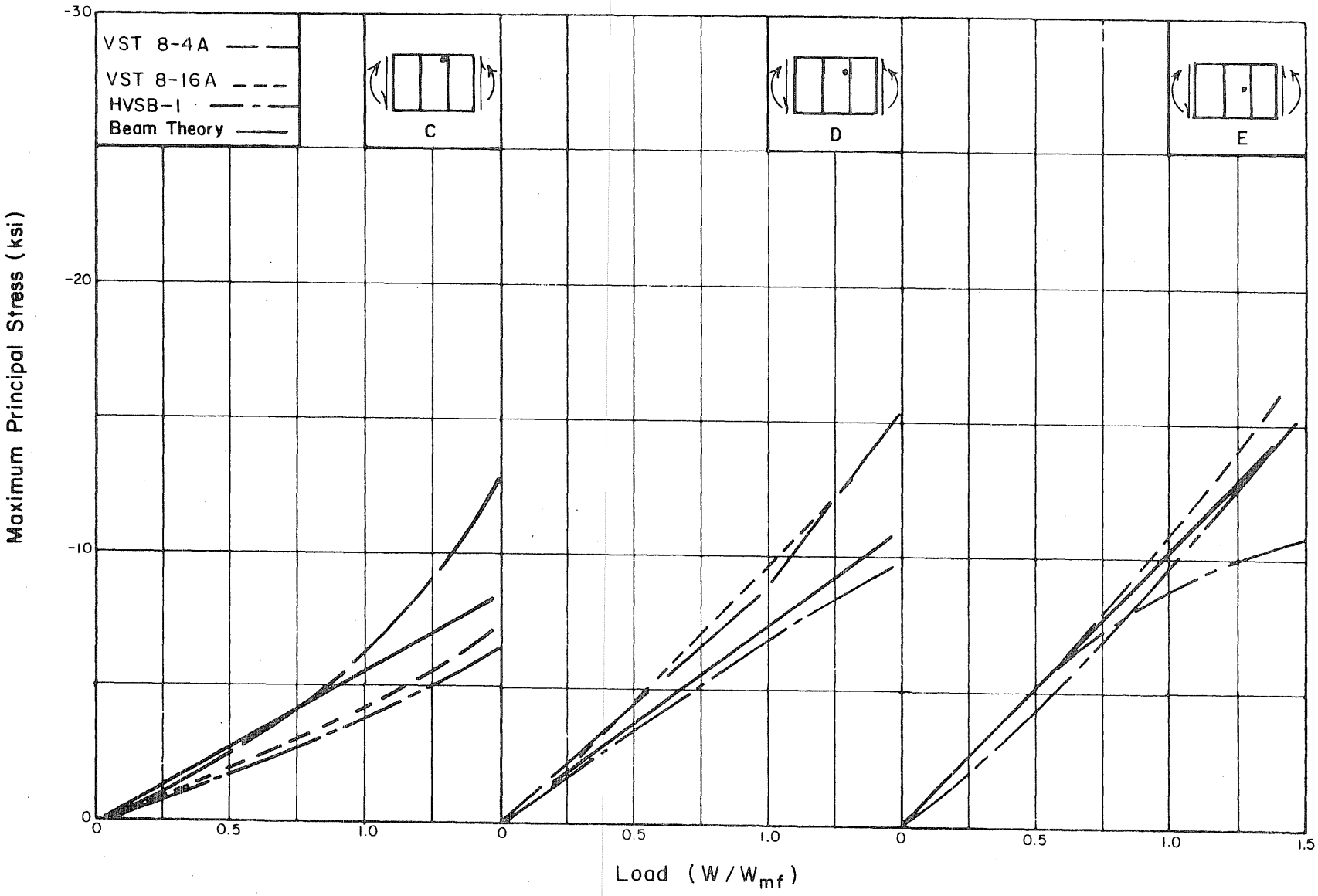

FIG. 74 MAXIMUM PRINCIPAL STRESS vs LOAD AT VARIOUS WEB LOCATIONS.

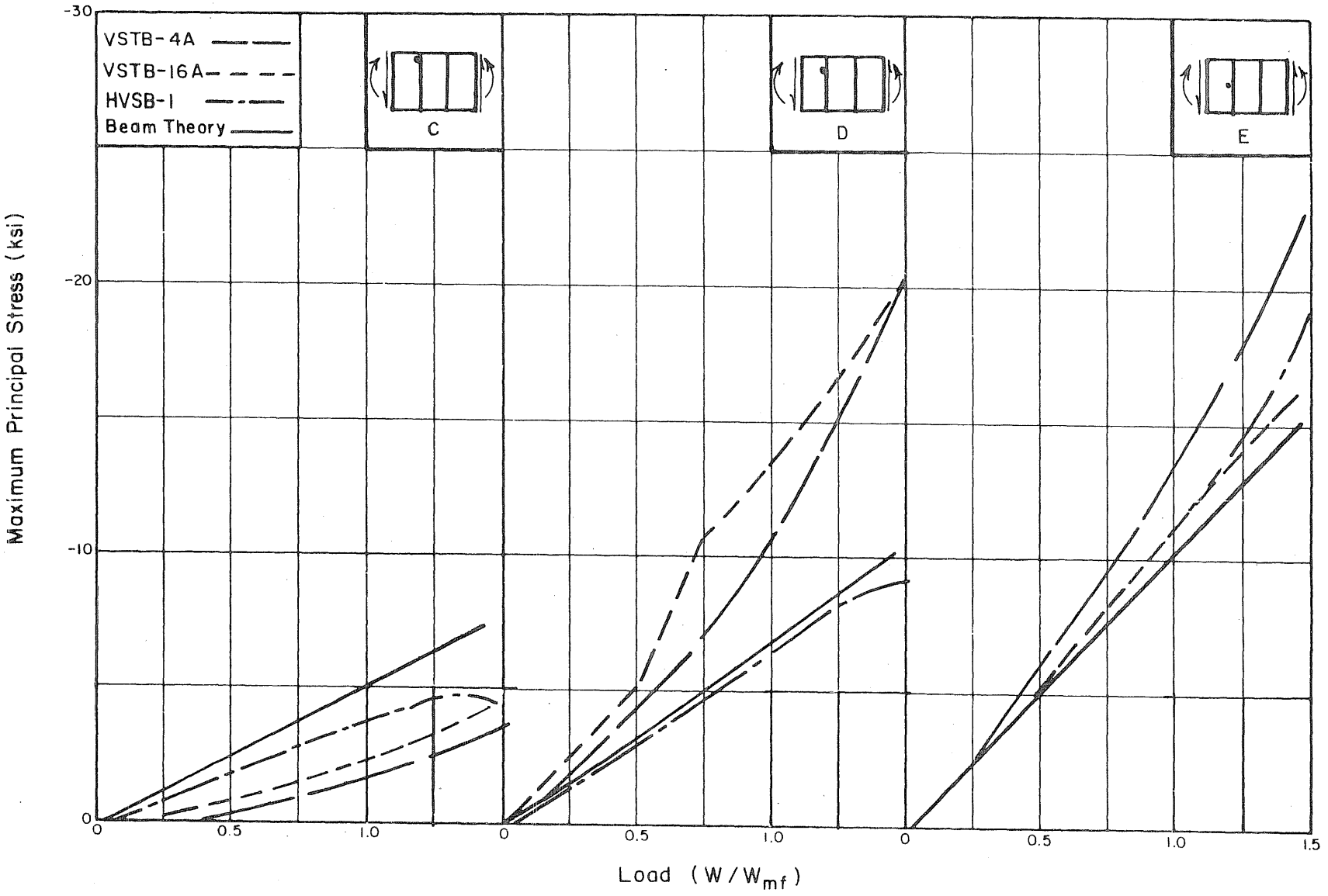

FIG. 75 MAXIMUM PRINCIPAL STRESS vs LOAD AT VARIOUS WEB LOCATIONS.

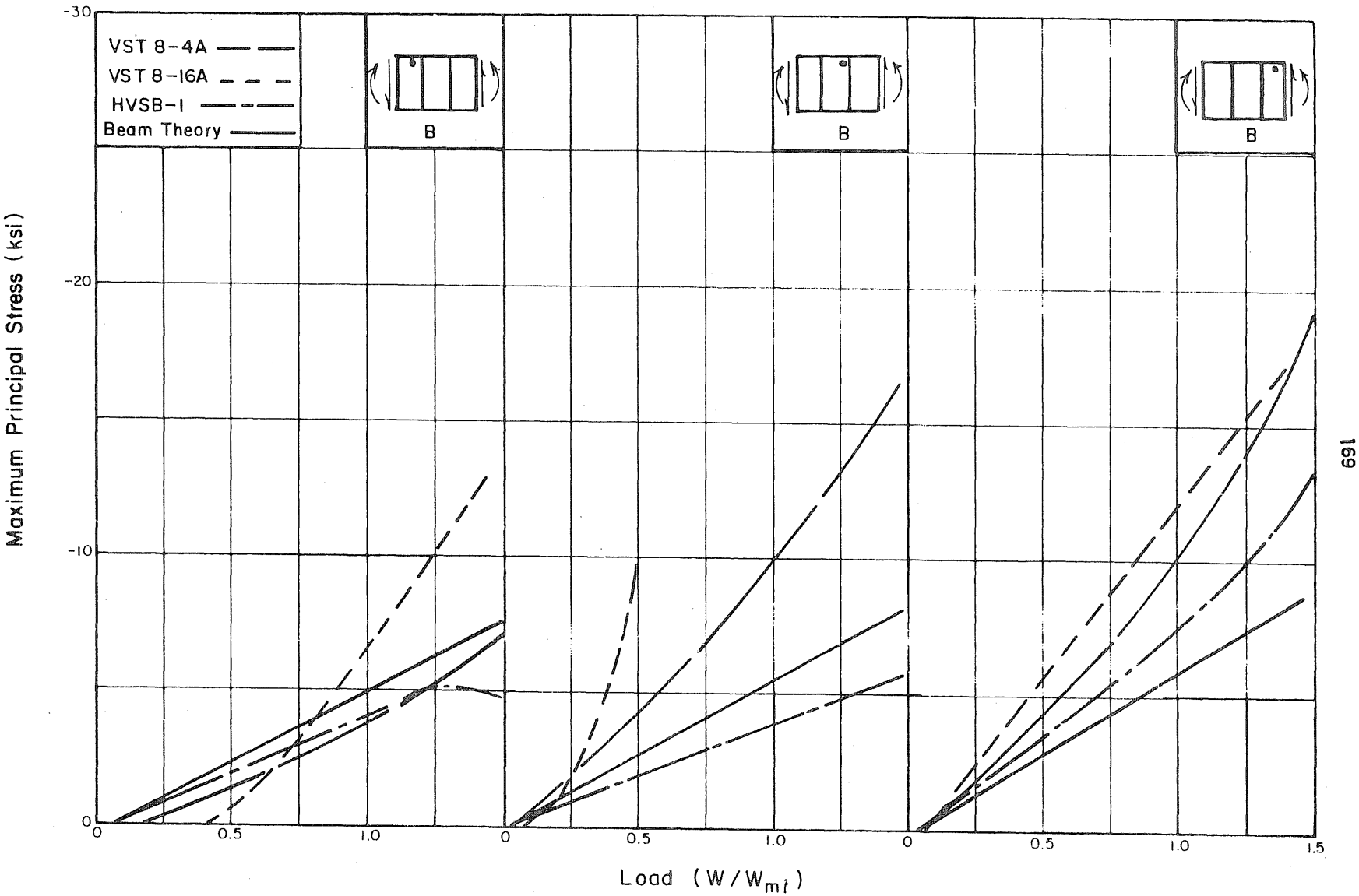

FIG. 76 MAXIMUM PRINCIPAL STRESS vs LOAD AT VARIOUS WEB LOCATIONS.

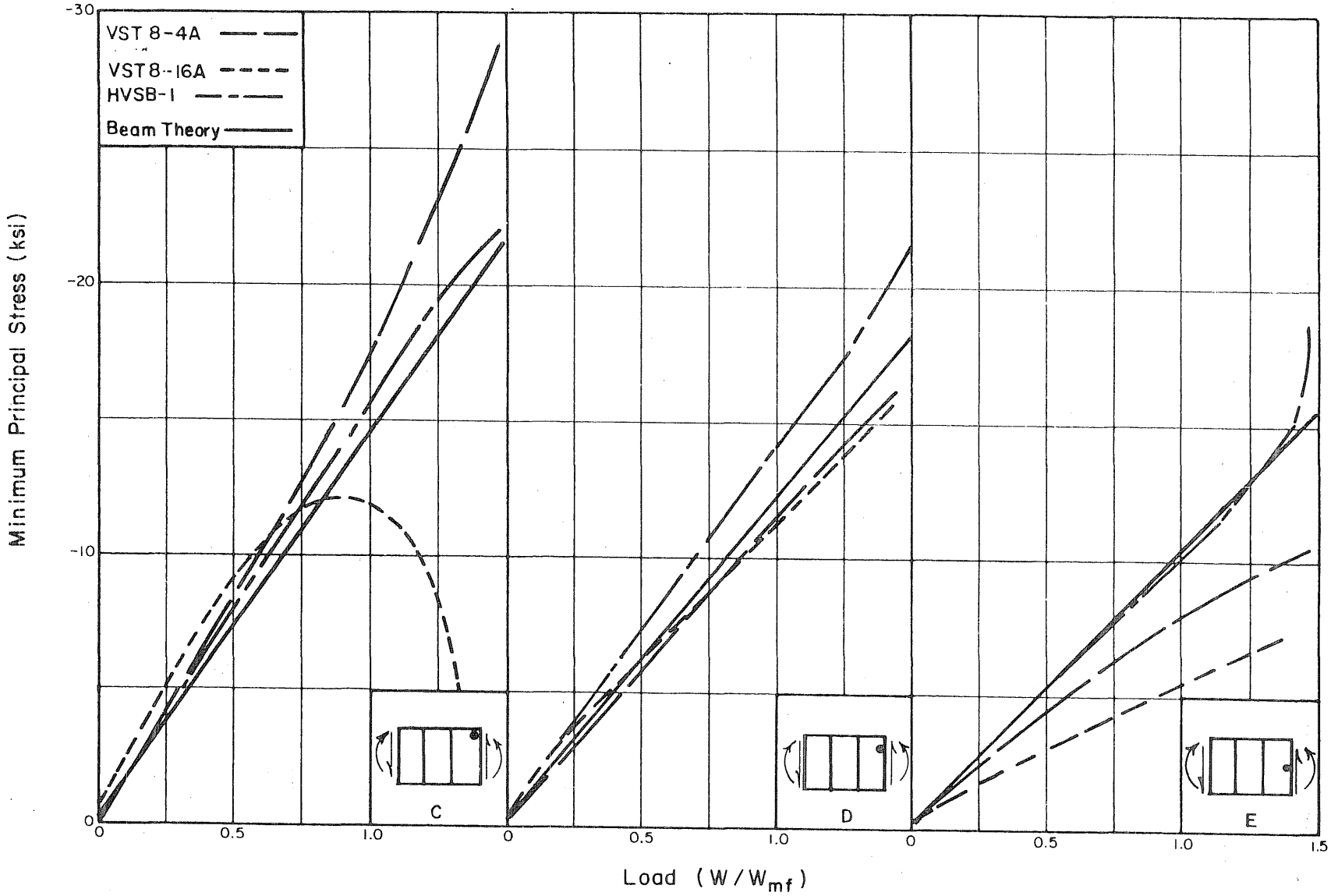

FIG. 77 MINIMUM PRINCIPAL STRESS vs LOAD AT VARIOUS WEB LOCATIONS.

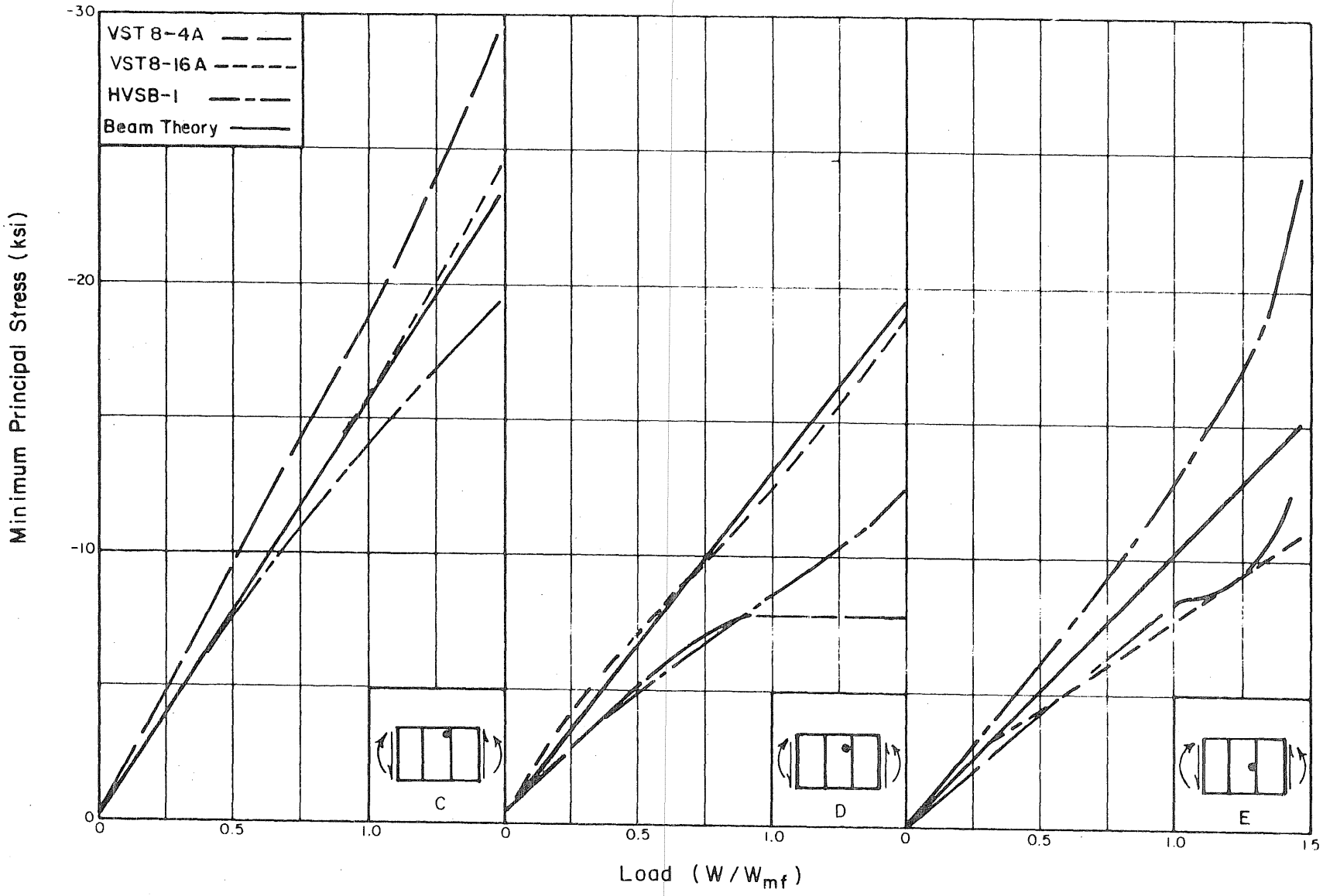

FIG. 78 MINIMUM PRINCIPAL STRESS vs LOAD AT VARIOUS WEB LOCATIONS.

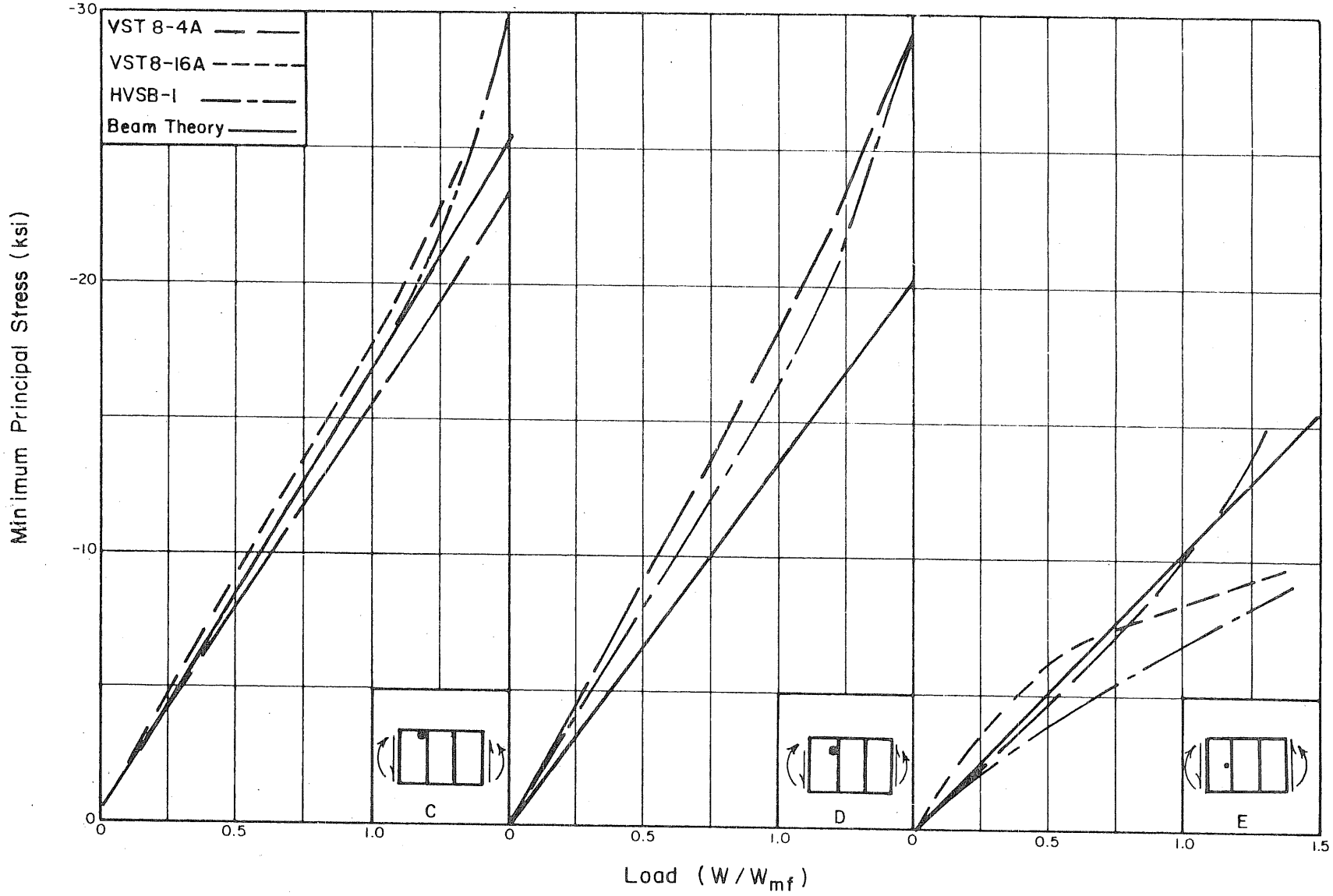

FIG. 79 MINIMUM PRINCIPAL STRESS vs LOAD AT VARIOUS WEB LOCATIONS.

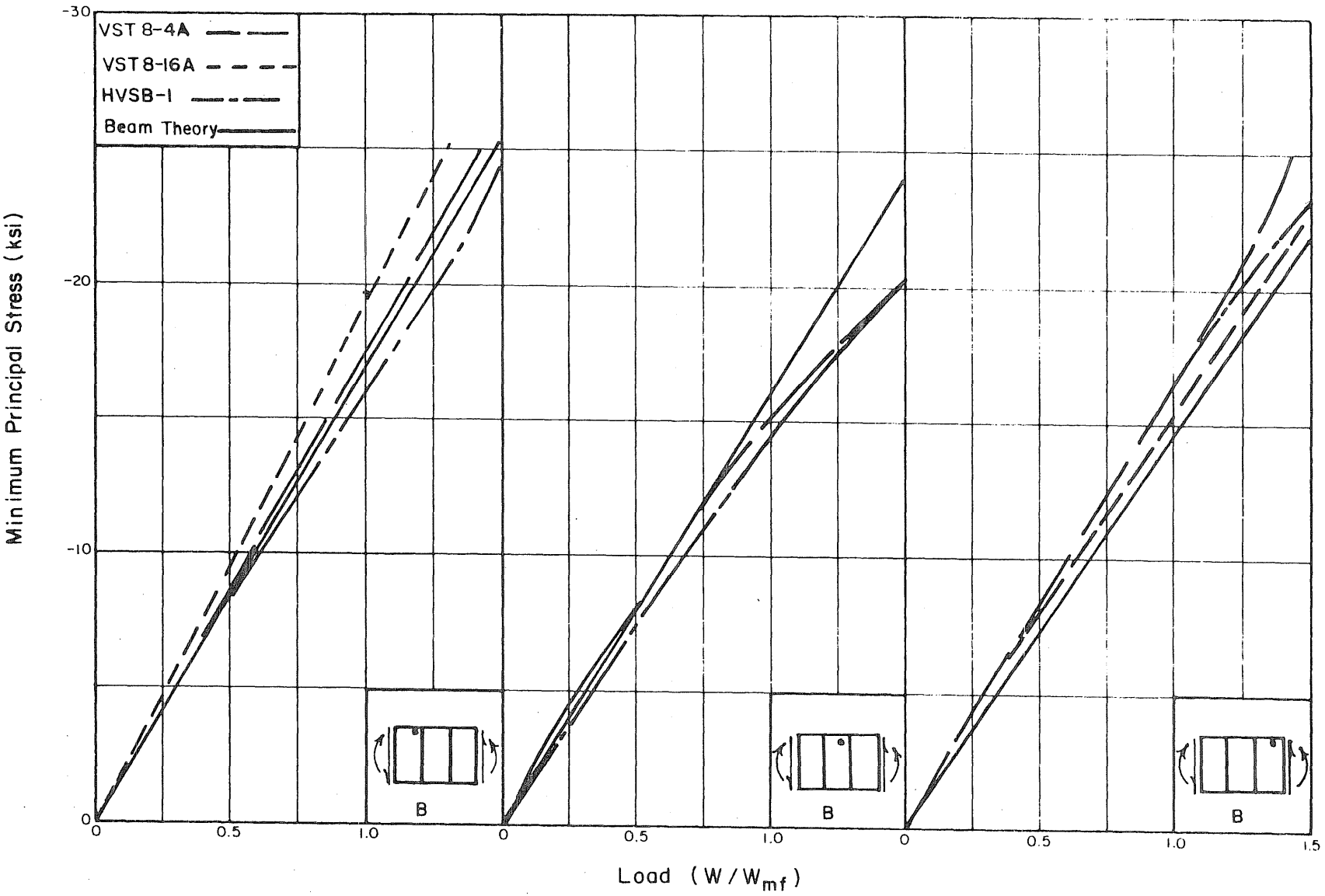

FIG. 80 MINIMUM PRINCIPAL STRESS vs LOAD AT VARIOUS WEB LOCATIONS.

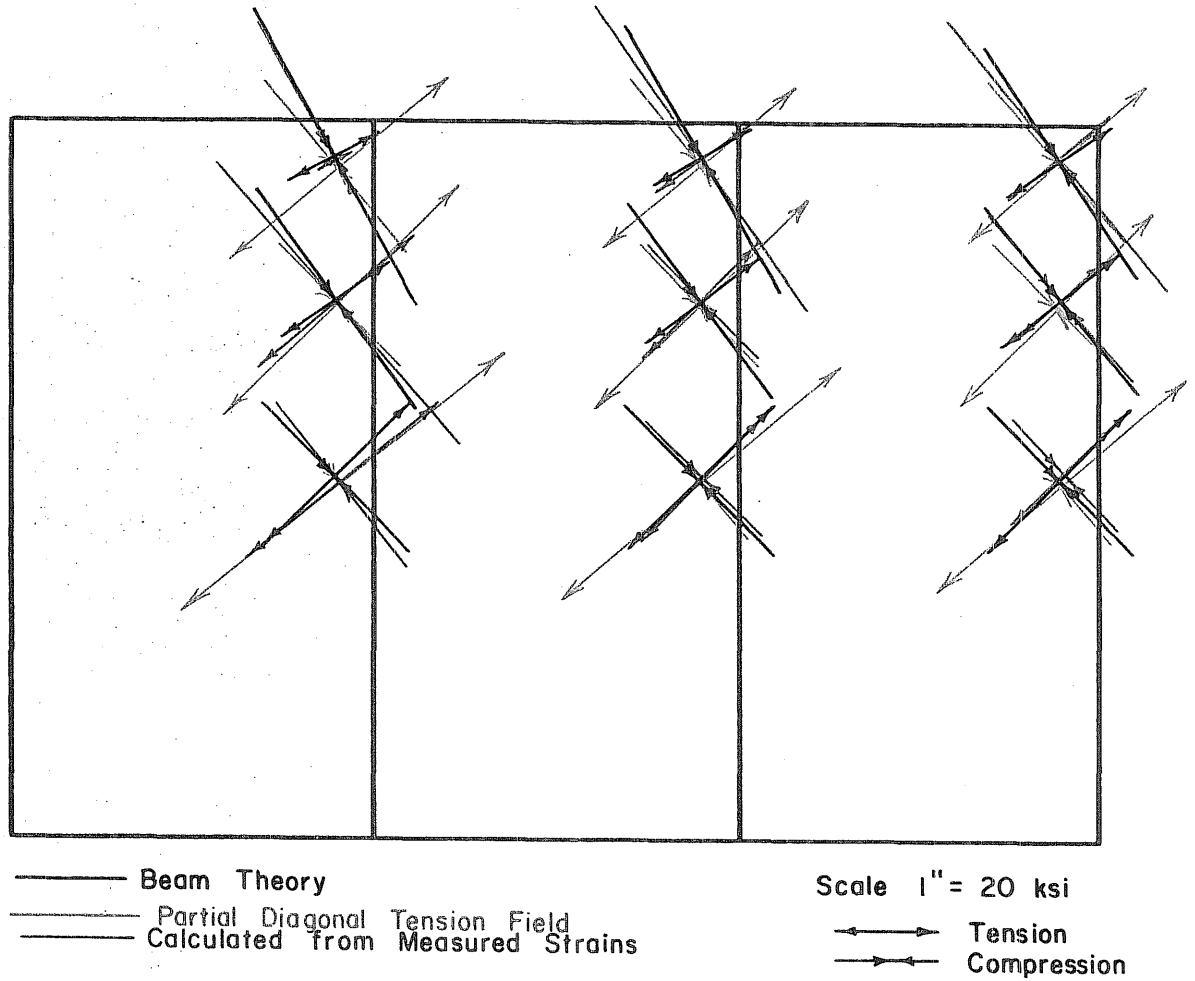

FIG. 81 COMPARISON OF PREDICTED AND MEASURED MEMBRANE STRESSES FOR VST 8-4A.

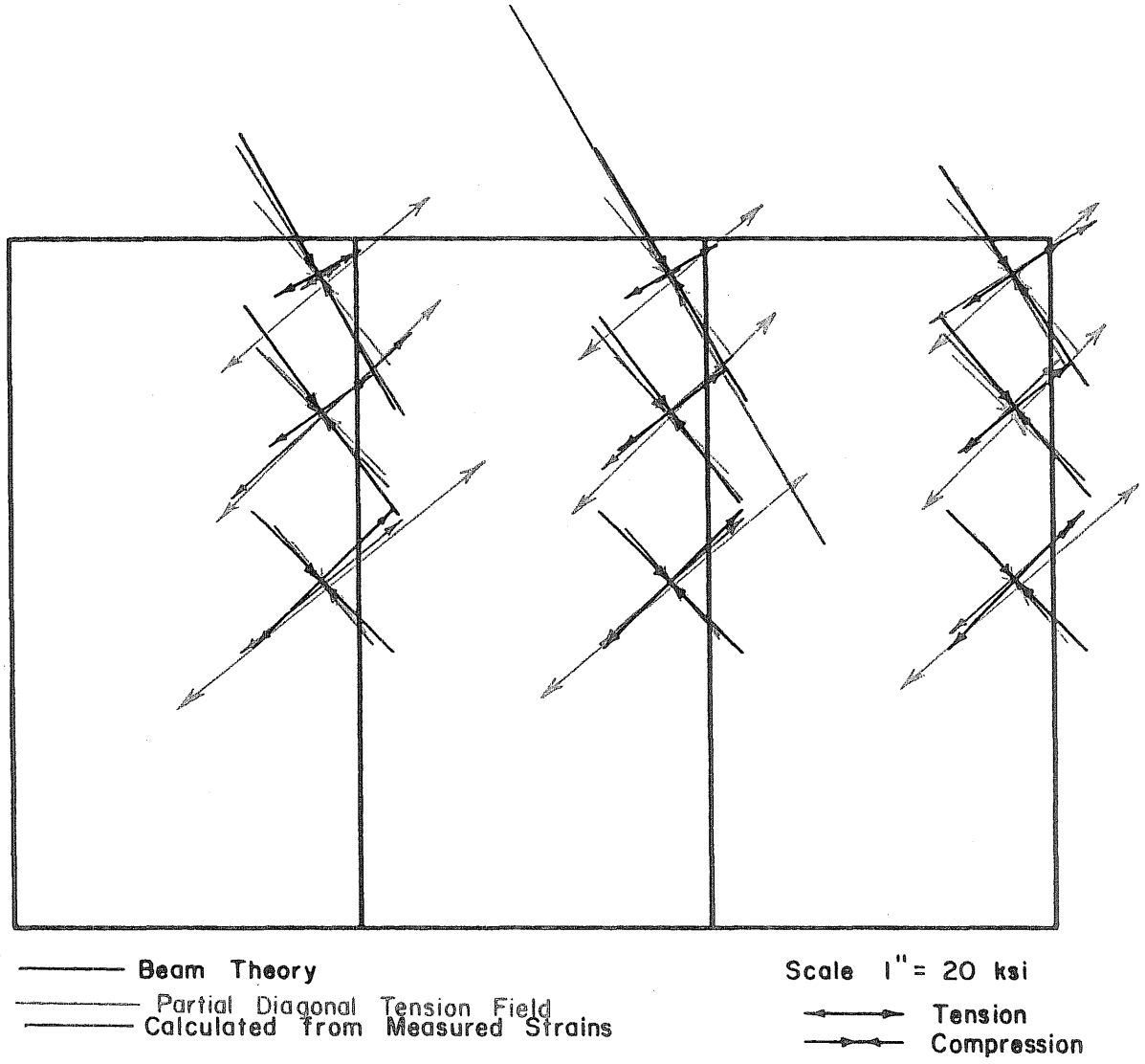

FIG. 82 COMPARISON OF PREDICTED AND MEASURED MEMBRANE STRESSES FOR VST 8-16A.

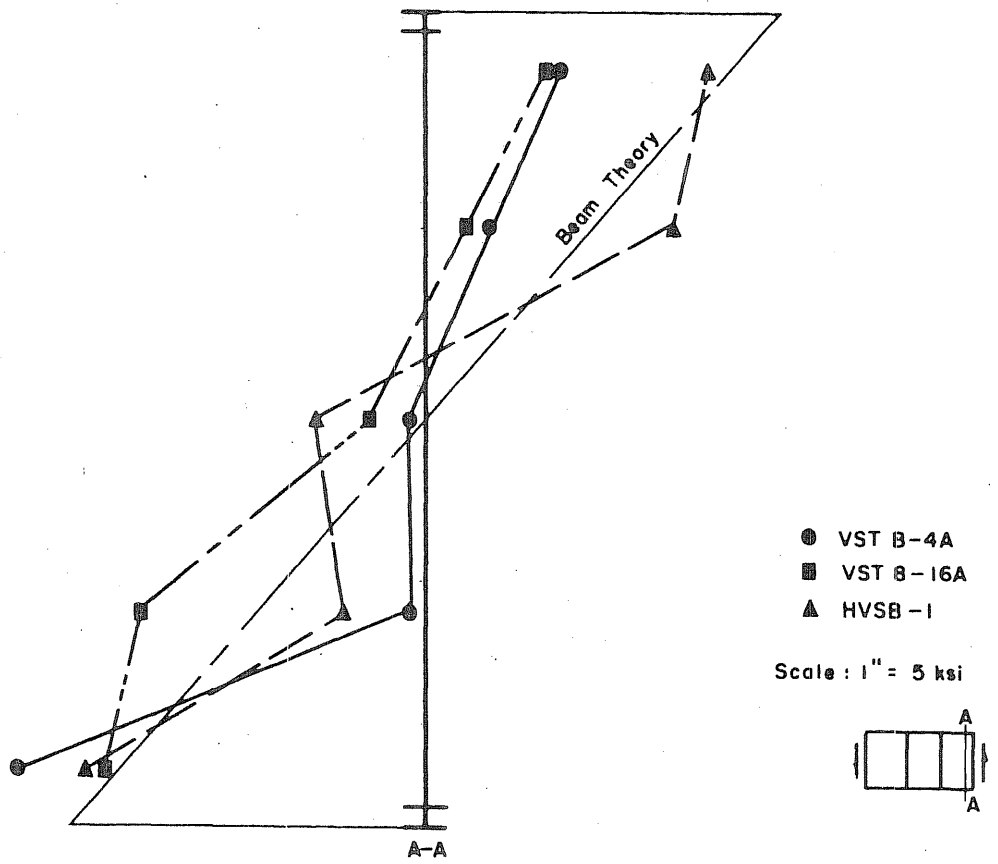

FIG. 83 DISTRIBUTION OF STRESSES ON A VERTICAL CROSS SECTION FOR GIRDERS WITH VARYING TRANSVERSE RIGIDITIES.

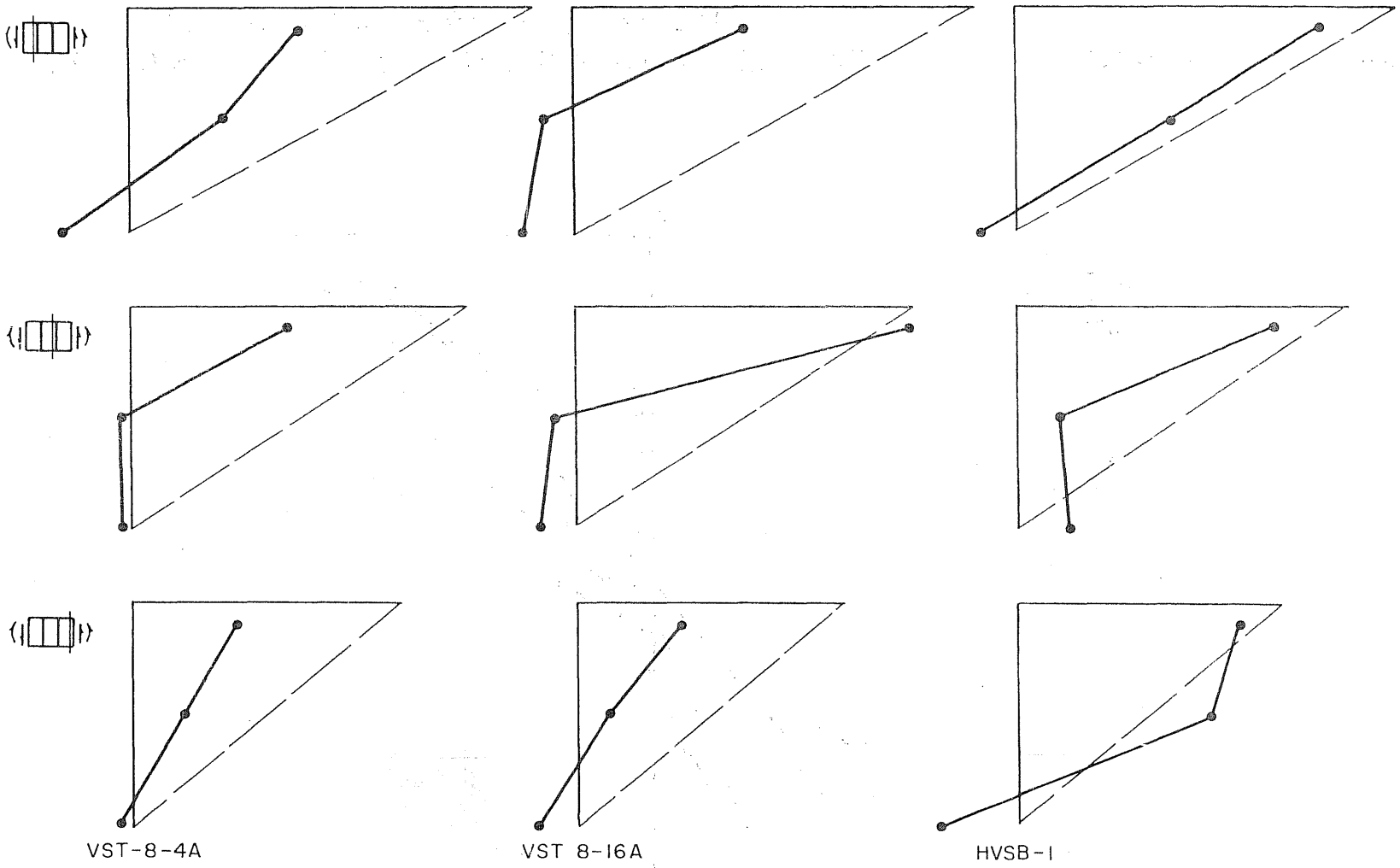

FIG. 84 COMPRESSION ZONE STRESS DISTRIBUTION OF GIRDERS WITH VARIOUS TRANSVERSE STIFFENER RIGIDITIES.

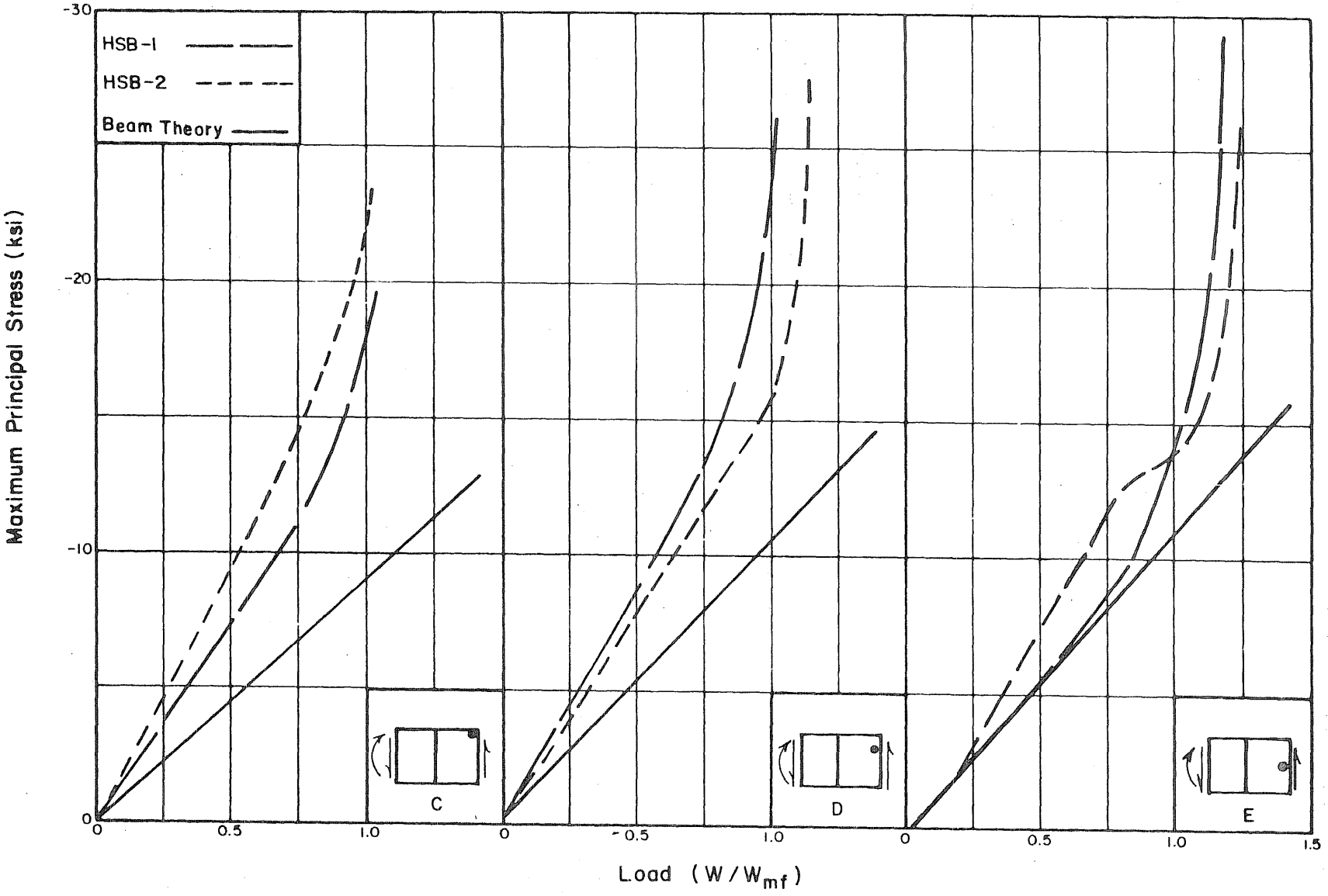

FIG. 85 MAXIMUM PRINCIPAL STRESS vs LOAD AT VARIOUS WEB LOCATIONS.

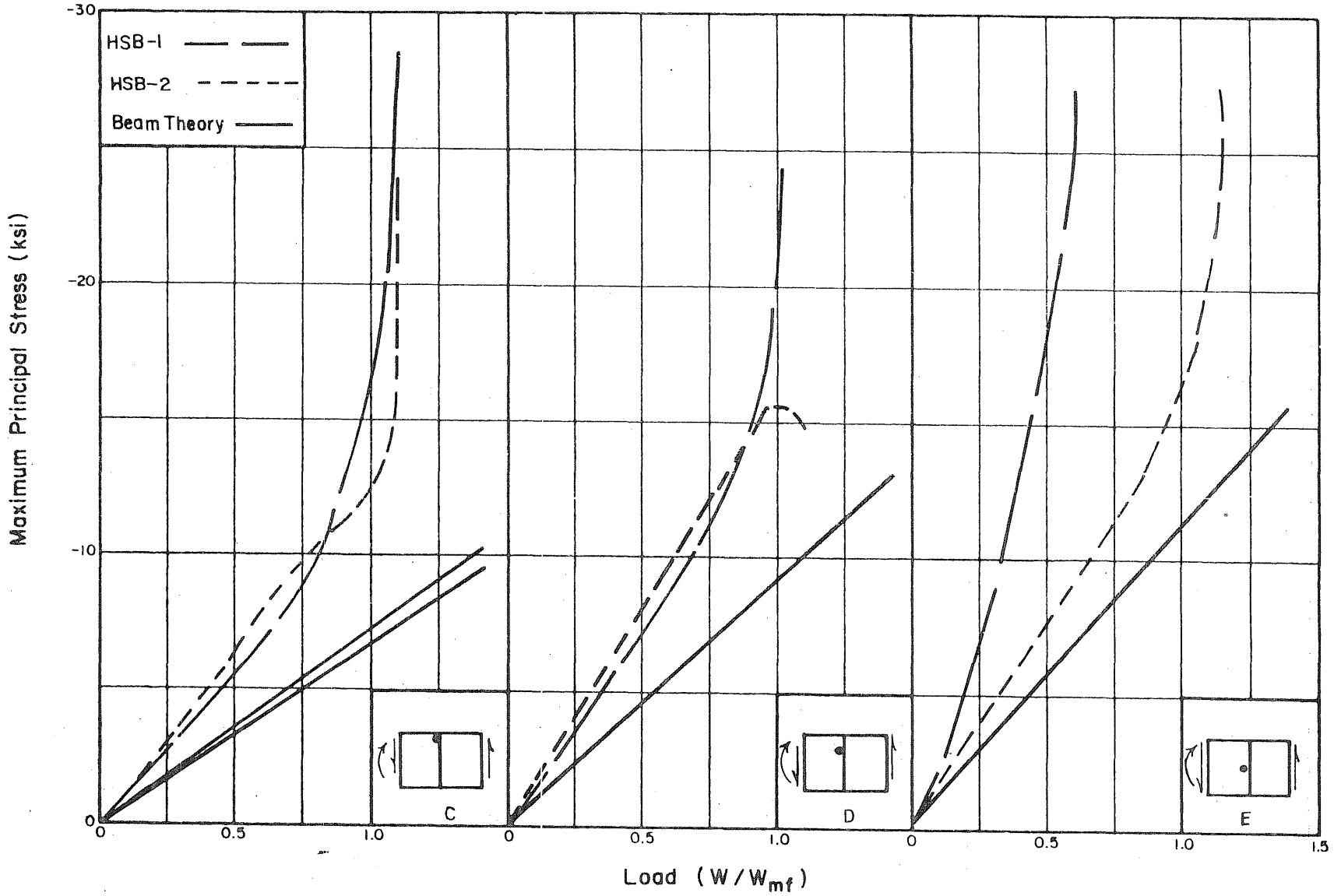

FIG. 86 MAXIMUM PRINCIPAL STRESS vs LOAD AT VARIOUS WEB LOCATIONS.

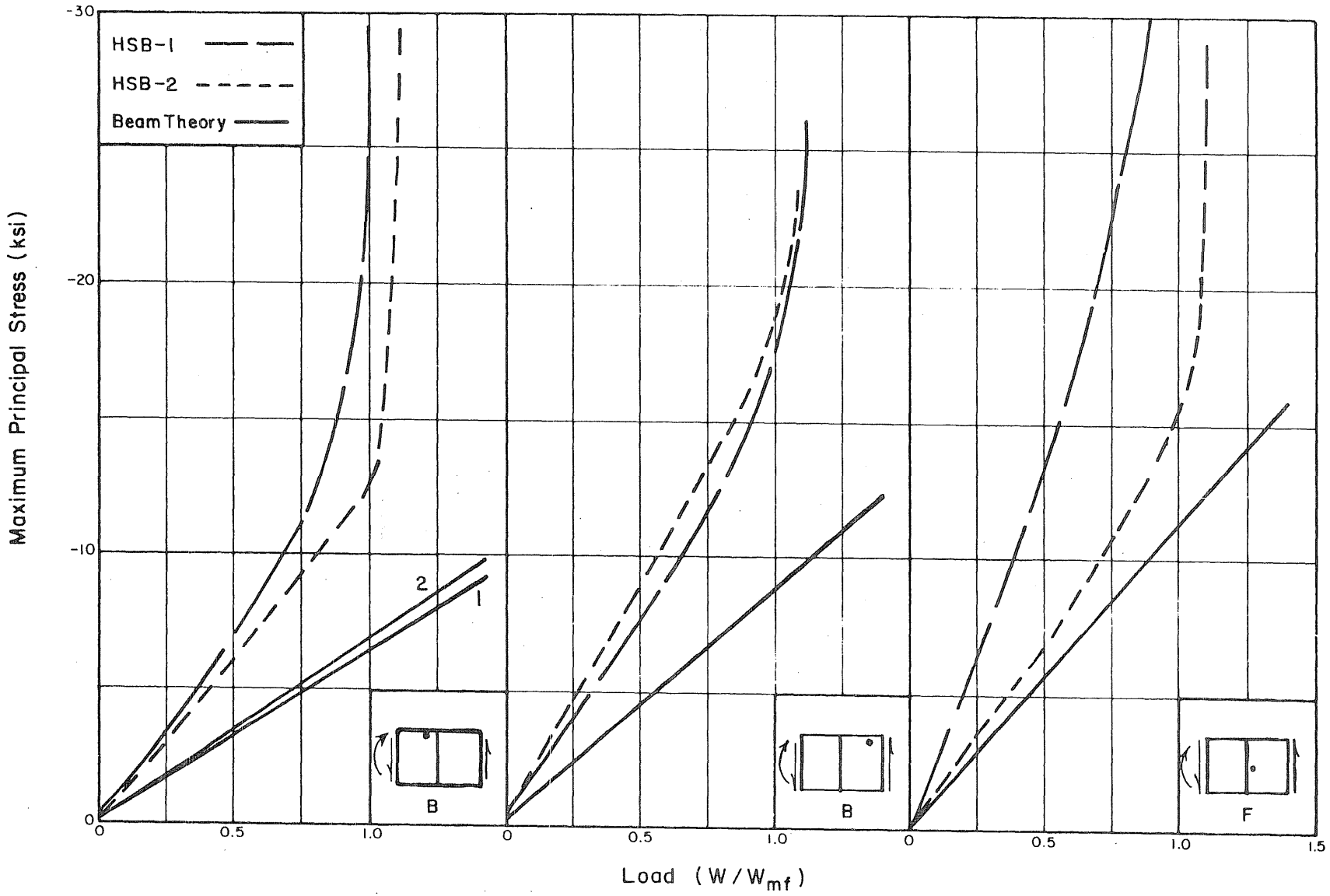

FIG. 87 MAXIMUM PRINCIPAL STRESS vs LOAD AT VARIOUS WEB LOCATIONS.

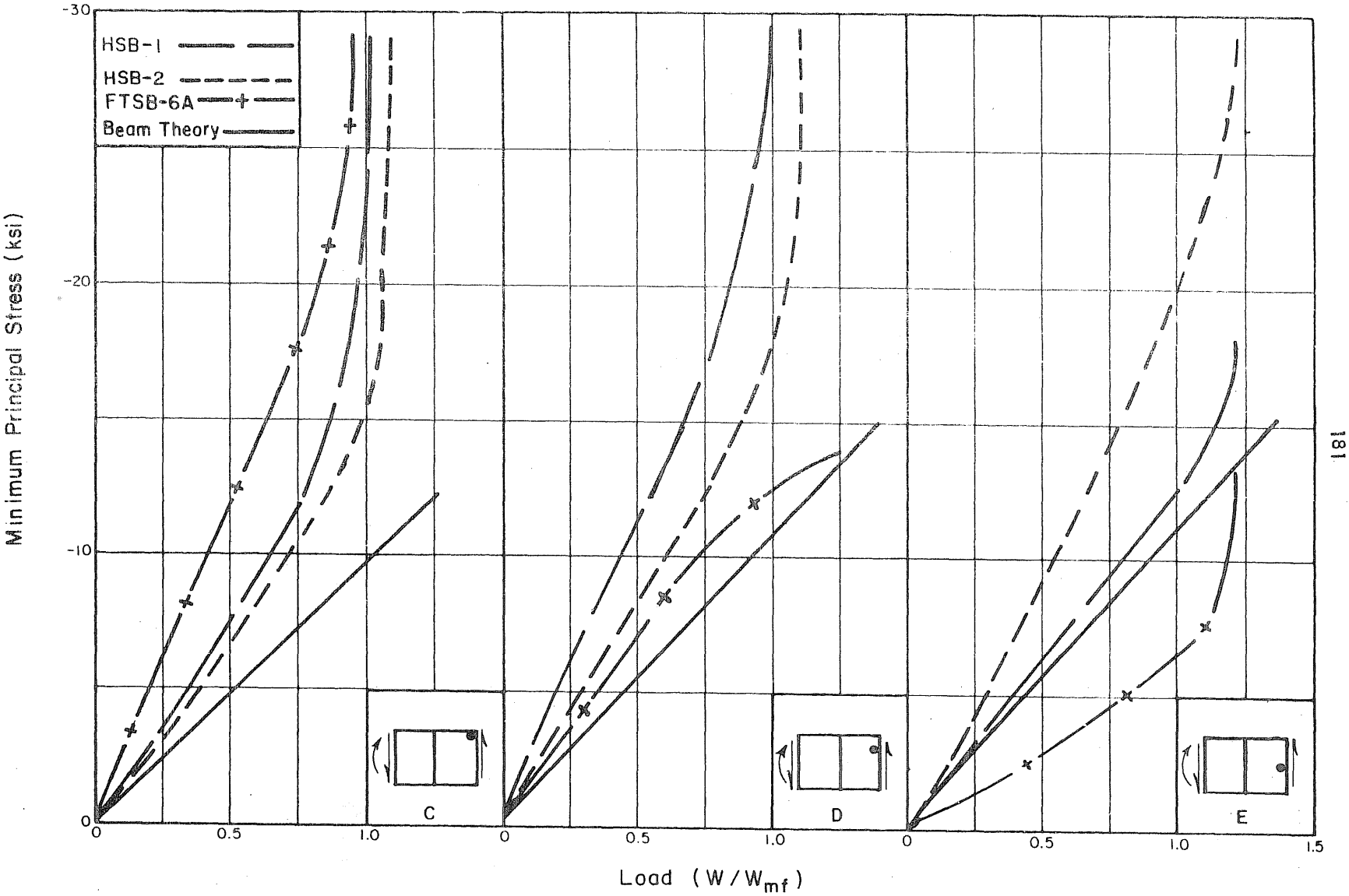

FIG. 88 MINIMUM PRINCIPAL STRESS vs LOAD AT VARIOUS WEB LOCATIONS.

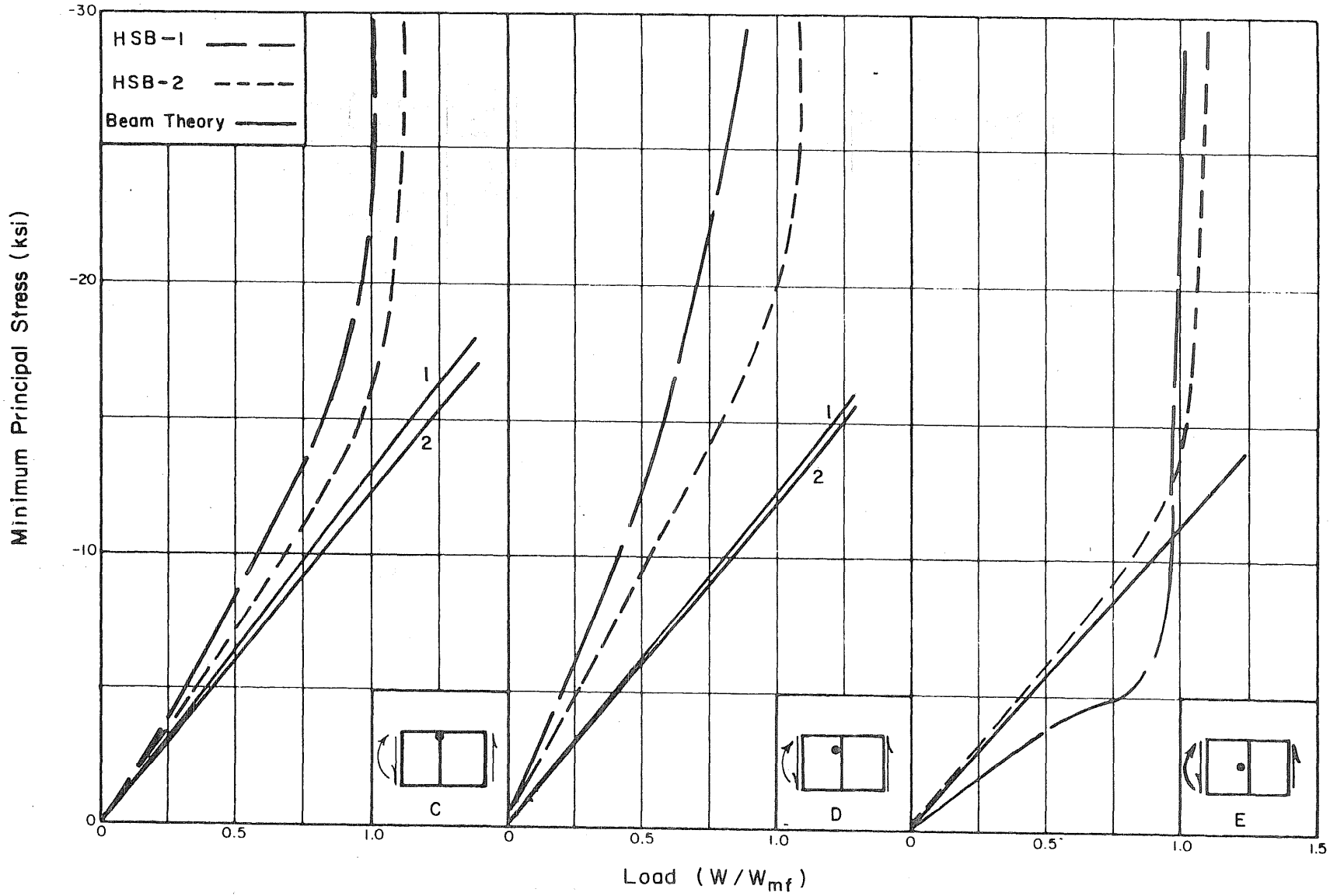

FIG. 89 MINIMUM PRINCIPAL STRESS vs LOAD AT VARIOUS WEB LOCATIONS.

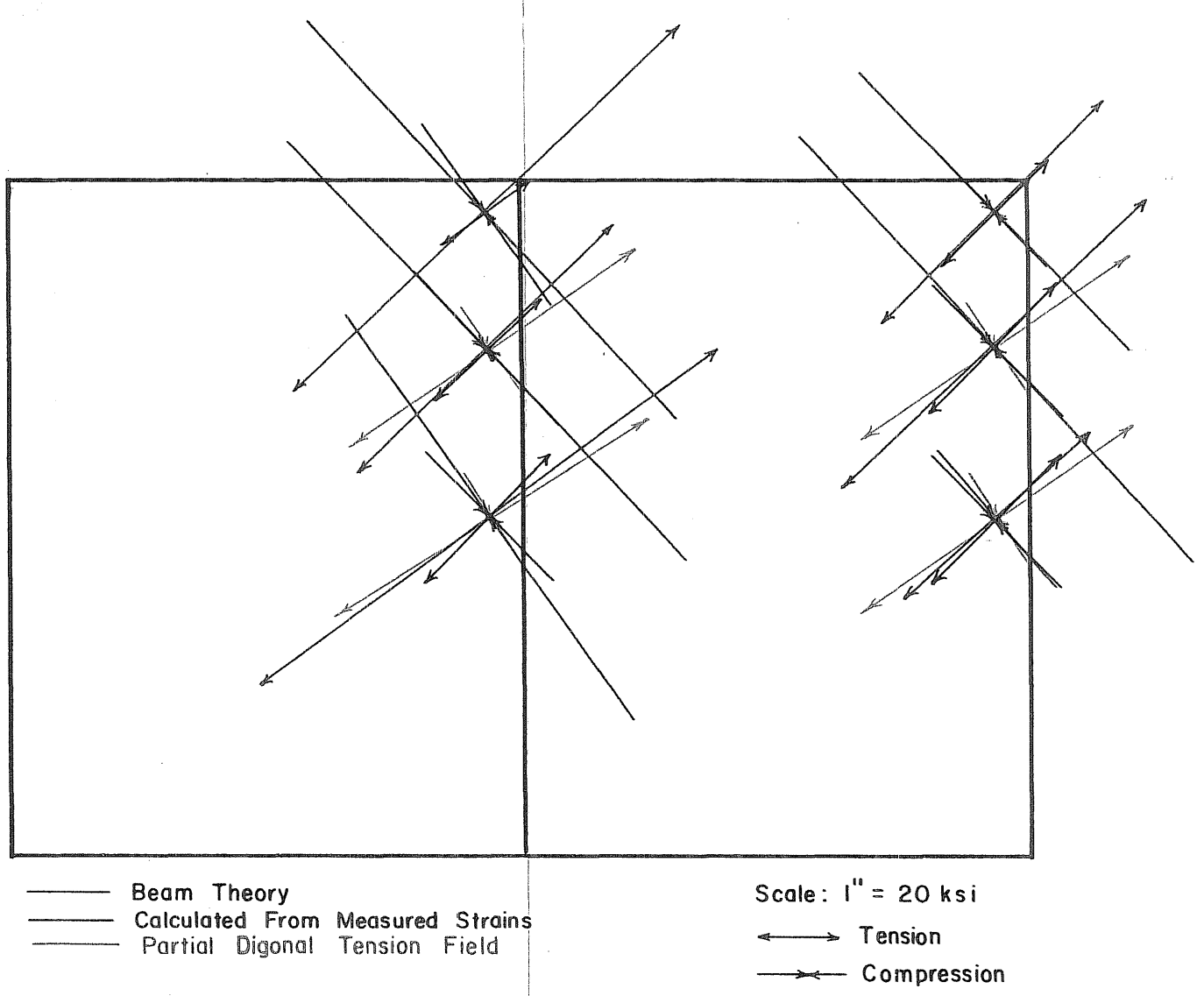

FIG. 90 COMPARISON OF PREDICTED AND MEASURED MEMBRANE STRESSES FOR HSB-1.

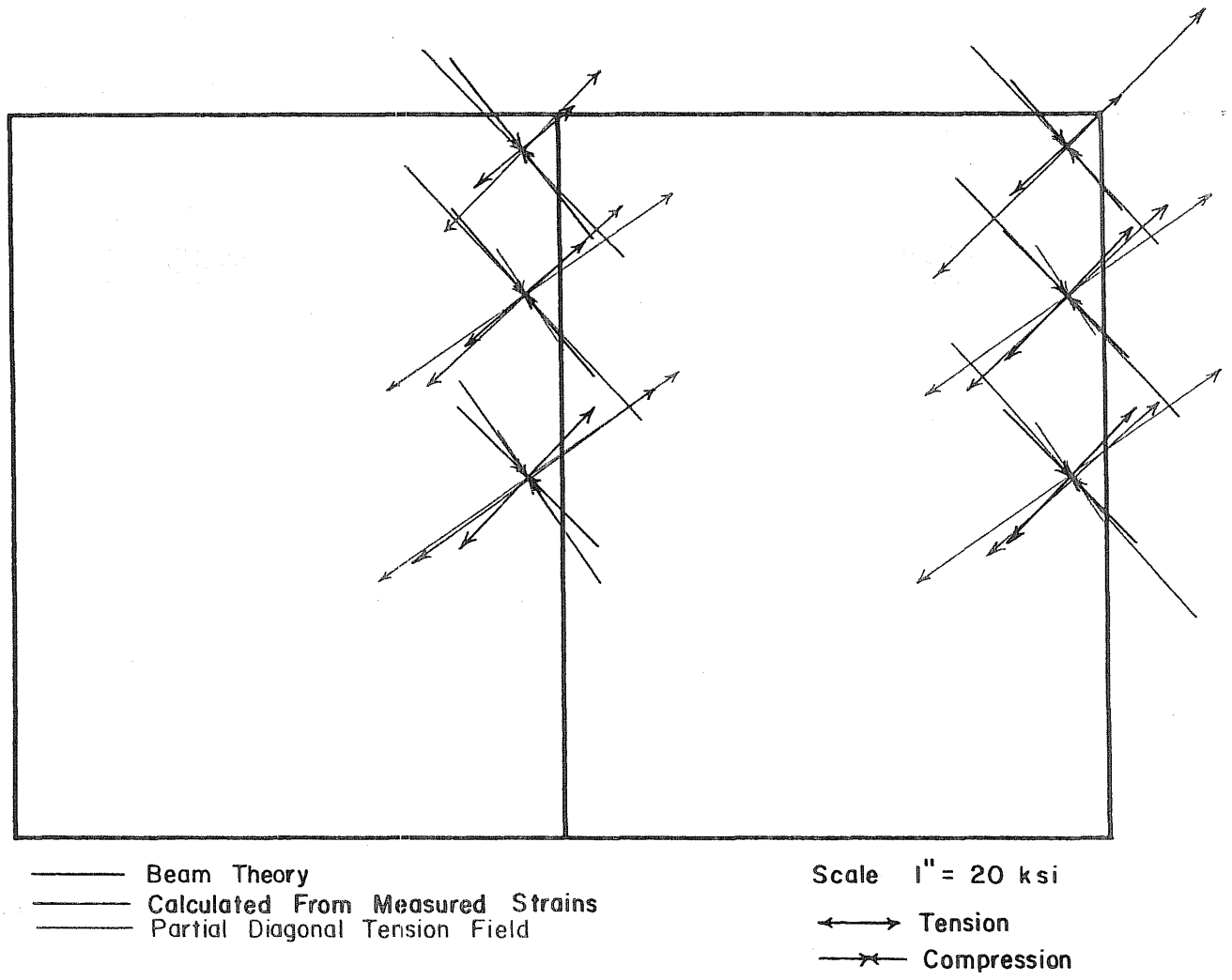

FIG. 91 COMPARISON OF PREDICTED AND MEASURED MEMBRANE STRESSES FOR HSB-2.

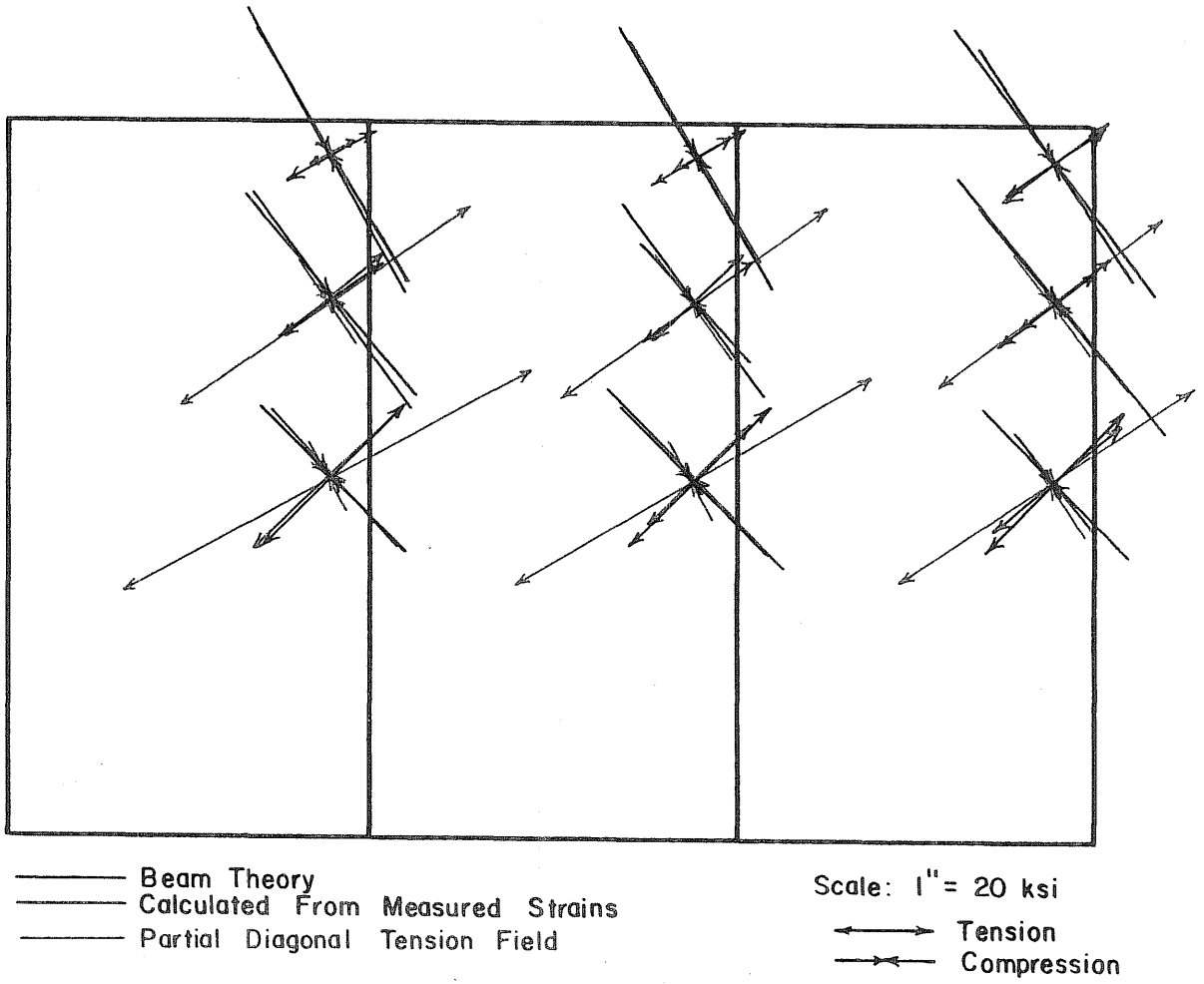

FIG. 92 COMPARISON OF PREDICTED AND MEASURED MEMBRANE STRESSES FOR HVSB-1.

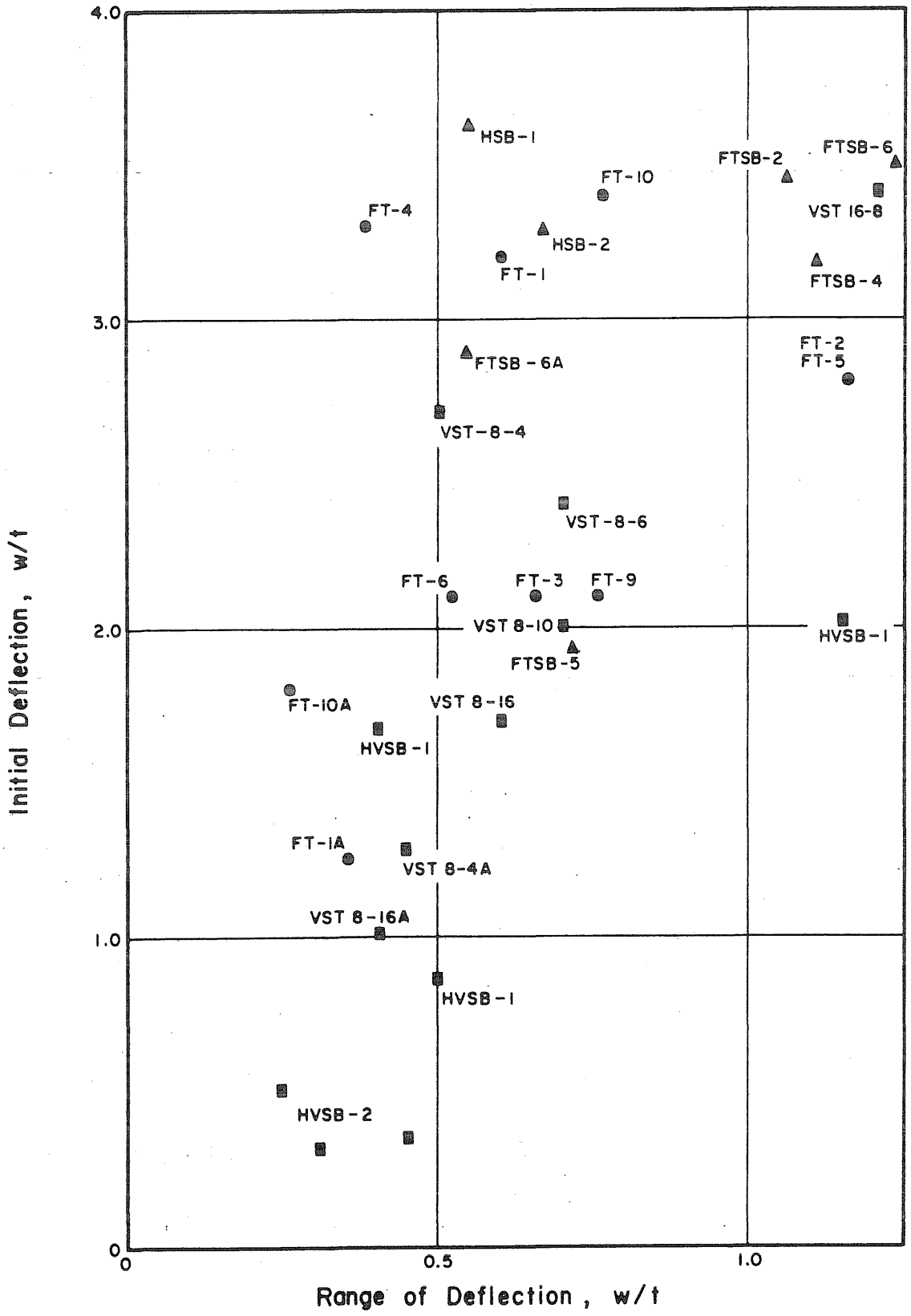

FIG. 93 INITIAL DEFLECTIONS vs RANGE OF DEFLECTIONS FOR A CYCLE OF LOADING.

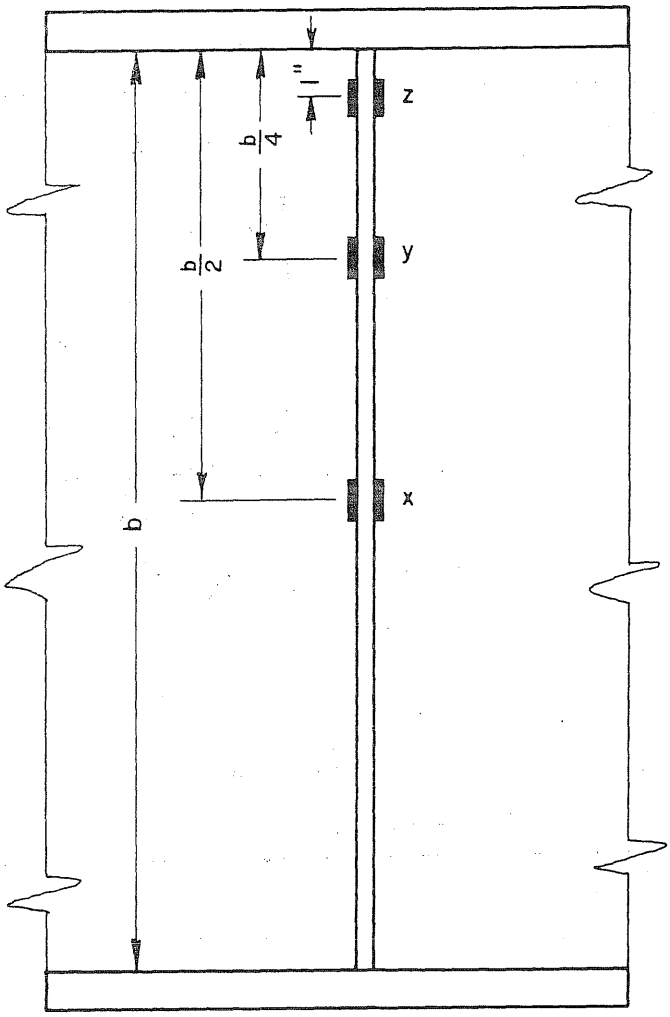

FIG. 94 TYPICAL STRAIN GAGE LOCATIONS ON TRANSVERSE STIFFENERS.

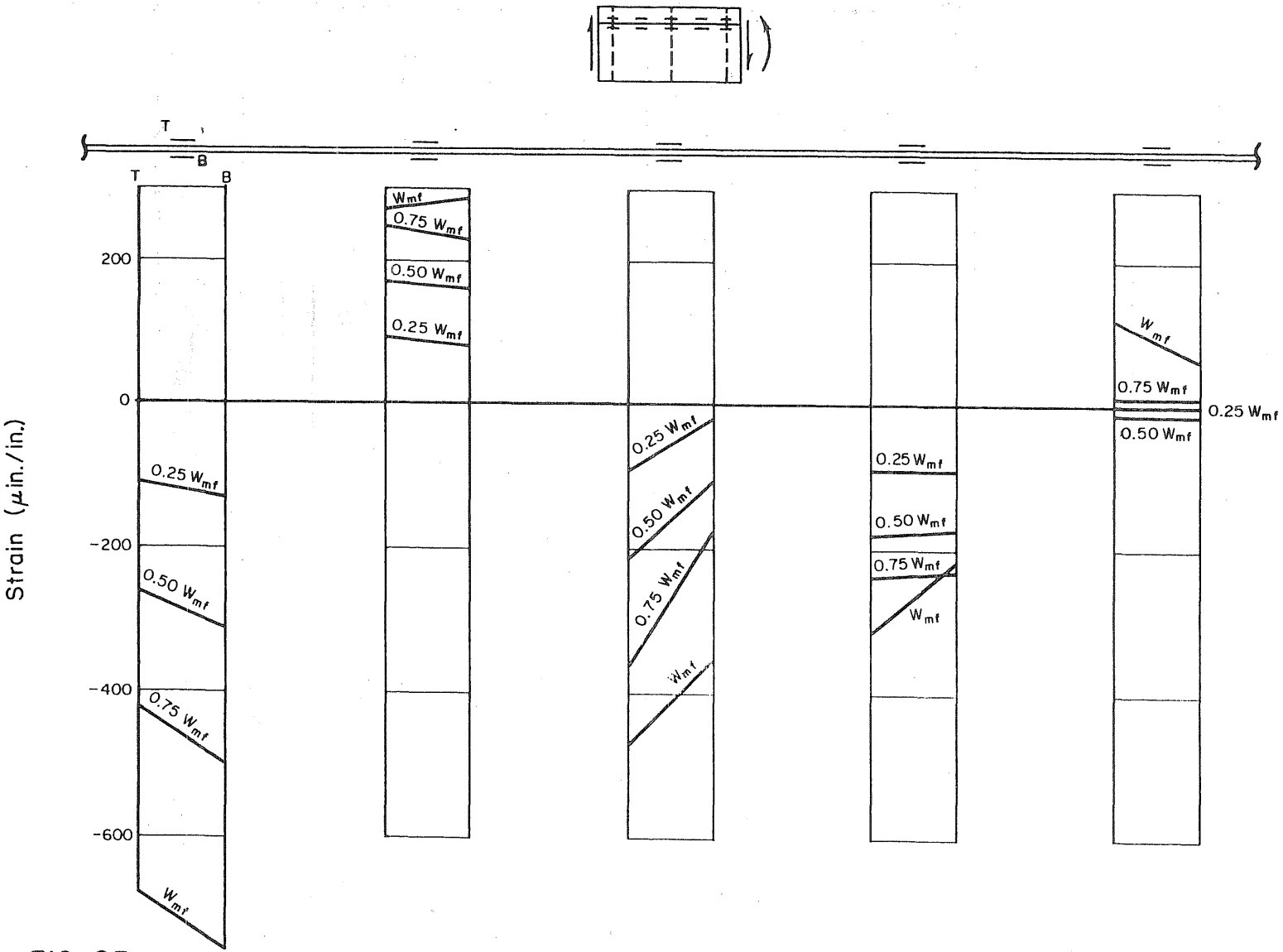

FIG. 95 LONGITUDINAL STIFFENER STRAIN FOR GIRDER HSB-1.

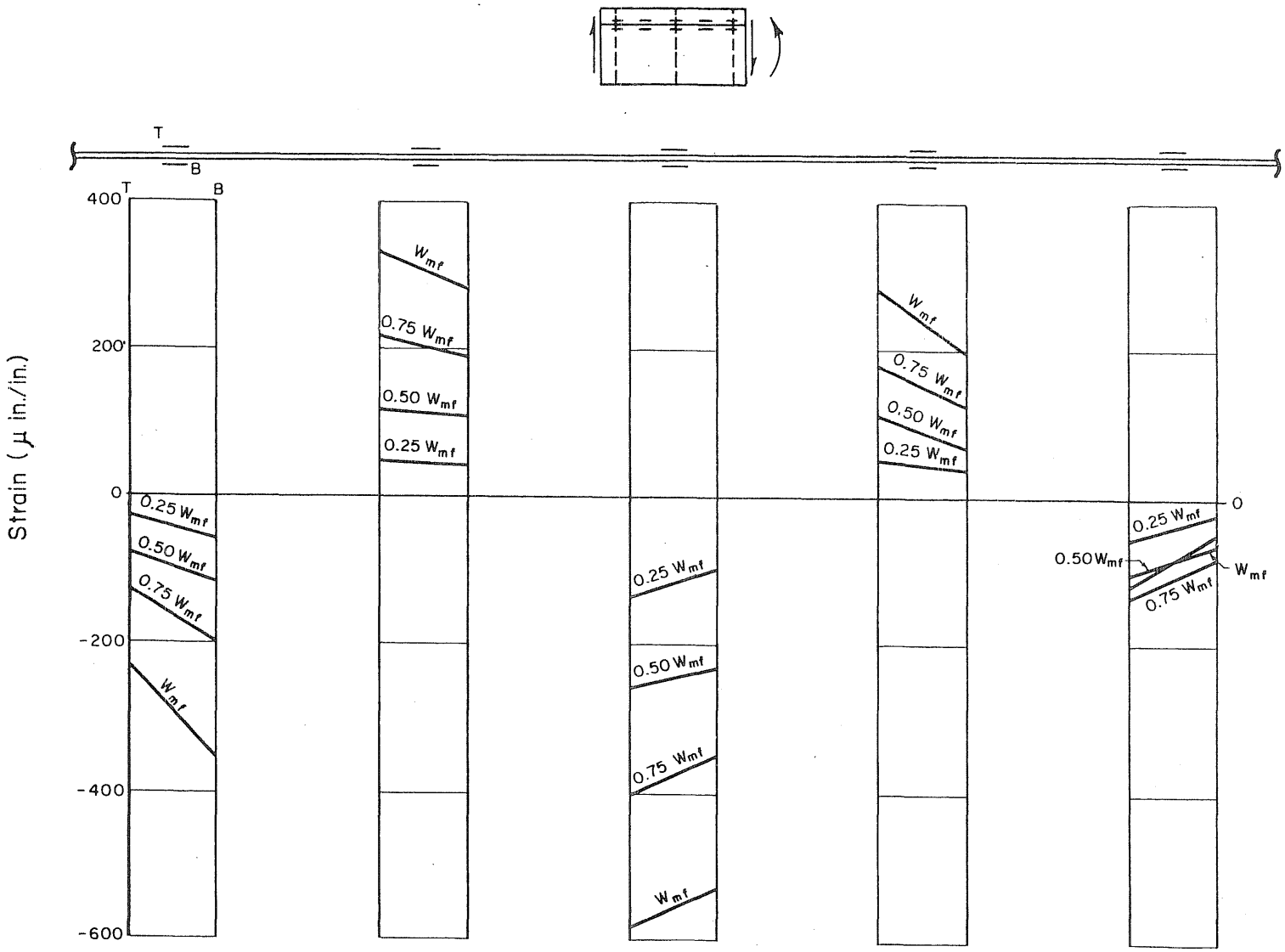

FIG. 96 LONGITUDINAL STIFFENER STRAIN FOR GIRDER HSB-2.

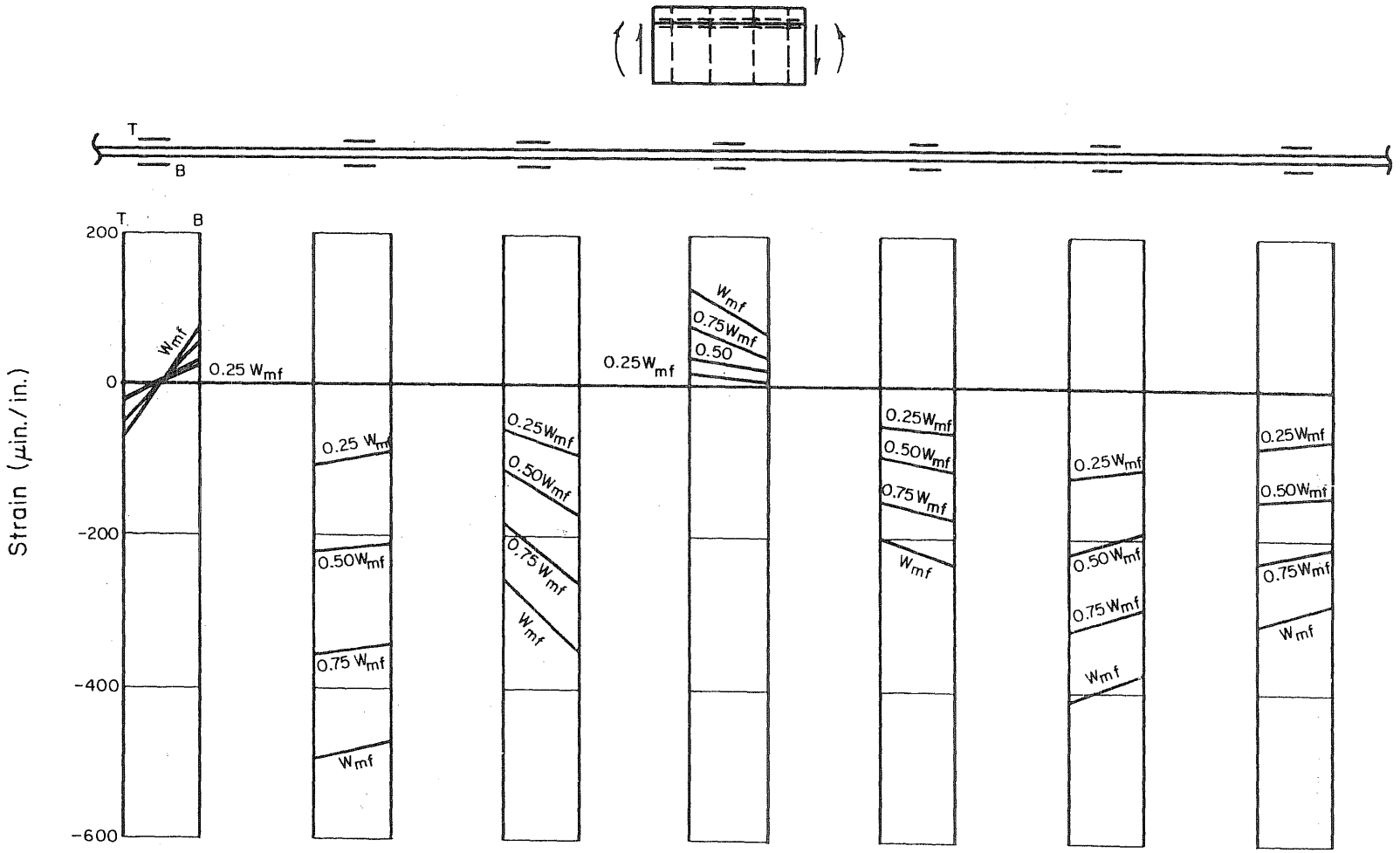

FIG. 97 . LONGITUDINAL STIFFENER STRAIN FOR GIRDER HVSB-1 .

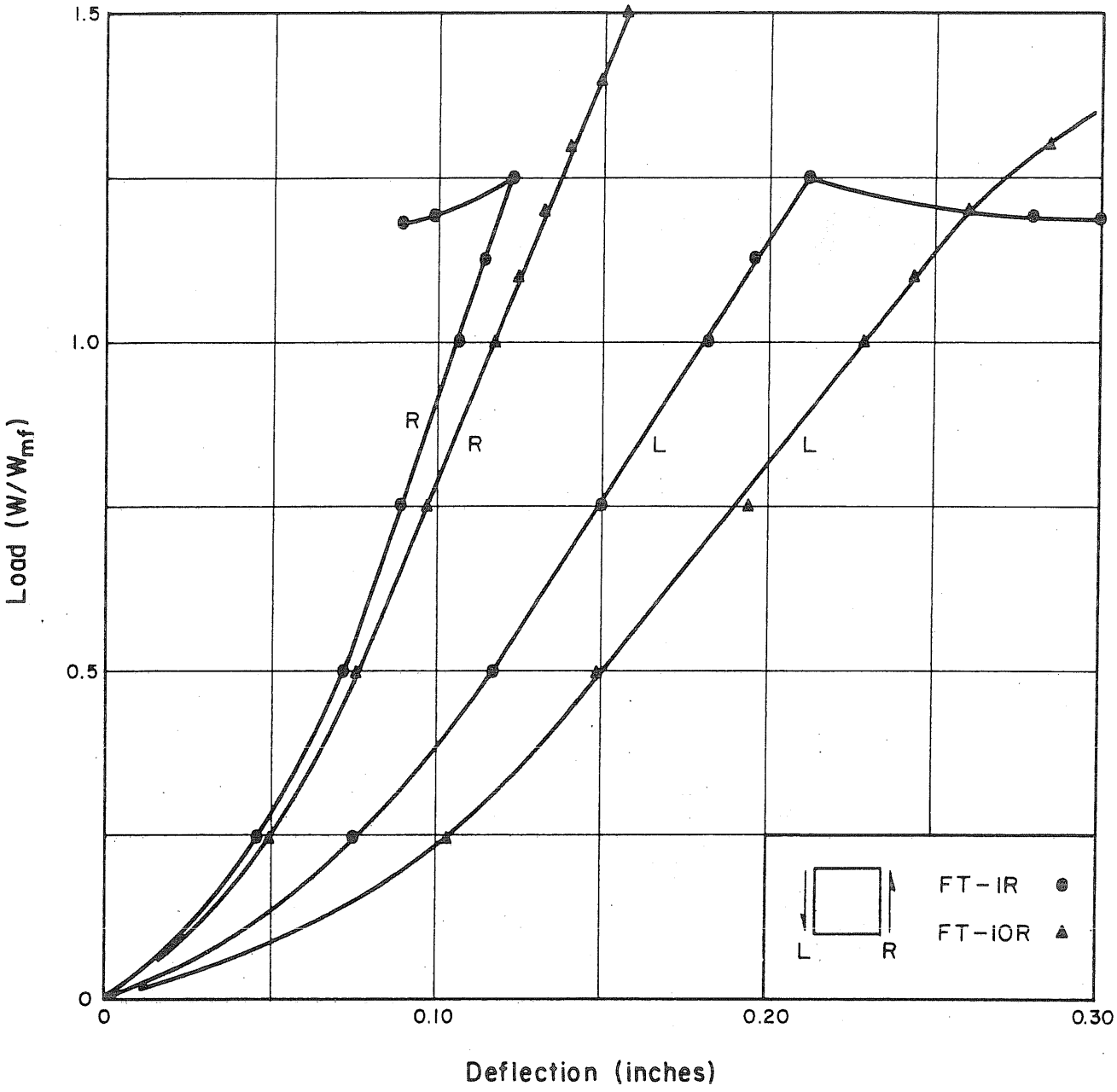

FIG. 98 LOAD DEFLECTION CURVES FOR GIRDERS FT-IA AND FT-IOA.

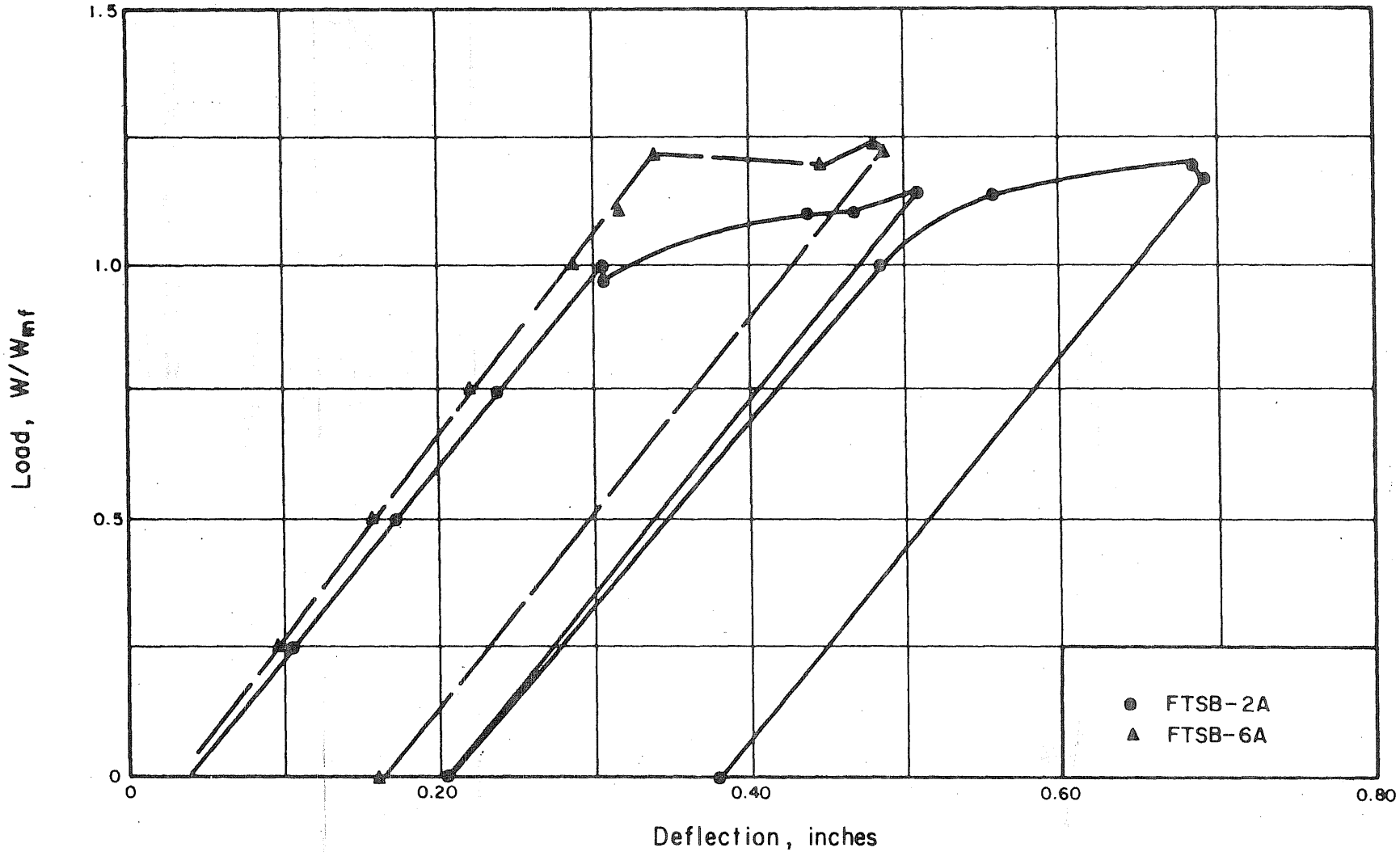

FIG. 99 LOAD DEFLECTION CURVES FOR FTSB GIRDERS.

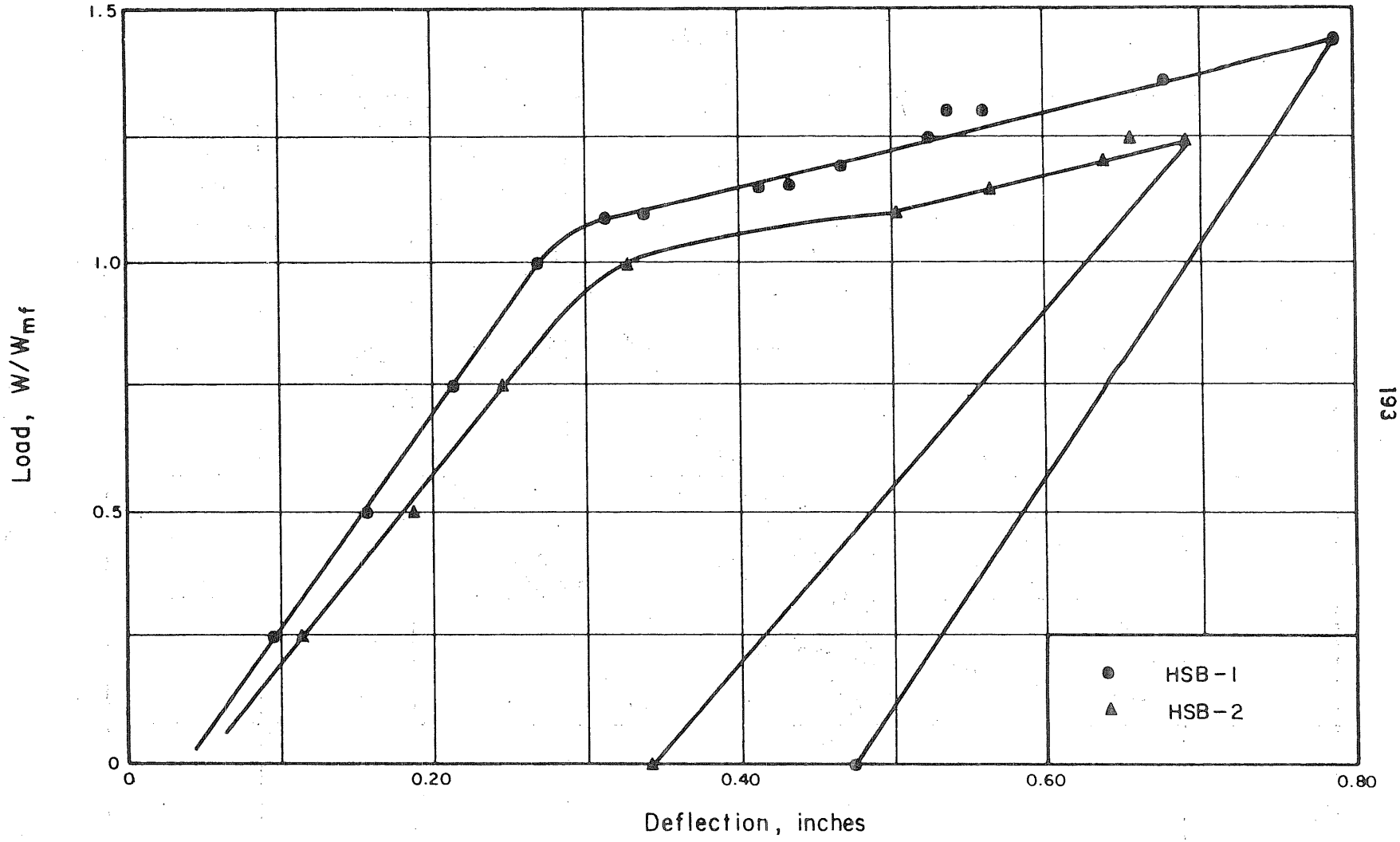

FIG. 100 LOAD DEFLECTION CURVES FOR HSB GIRDERS.

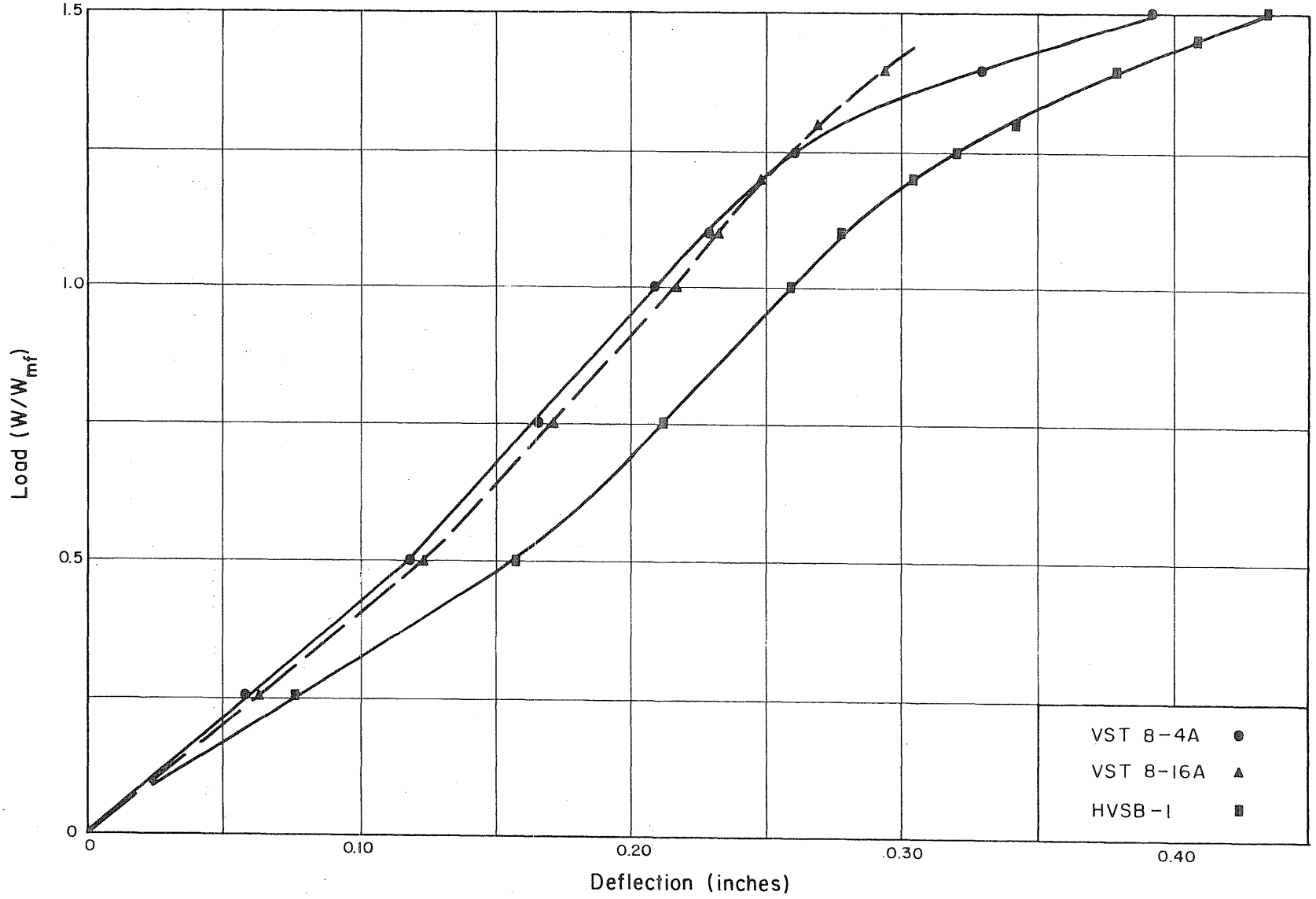

FIG. 101 VERTICAL DEFLECTION vs LOAD FOR VST AND HVSB GIRDERS.

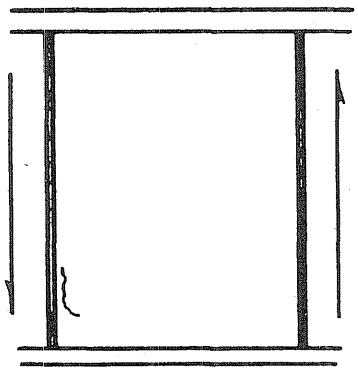

FT-1A

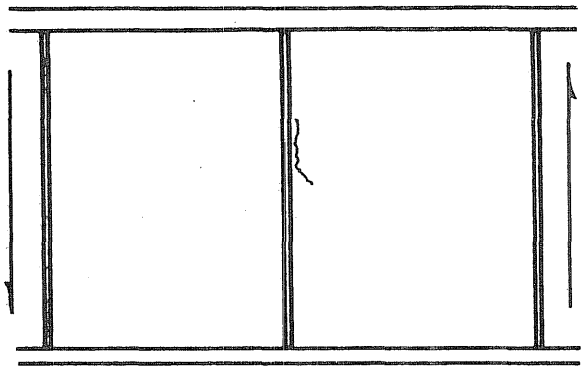

FTSB-2A

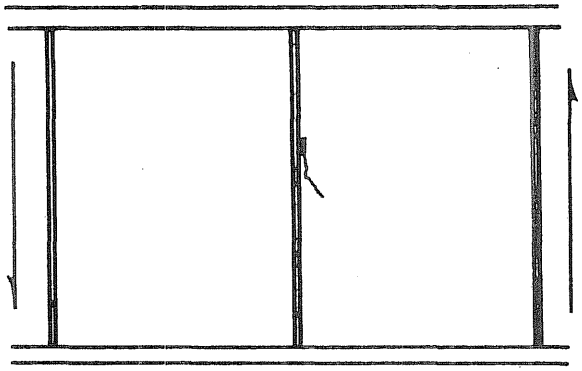

FTSB-6A

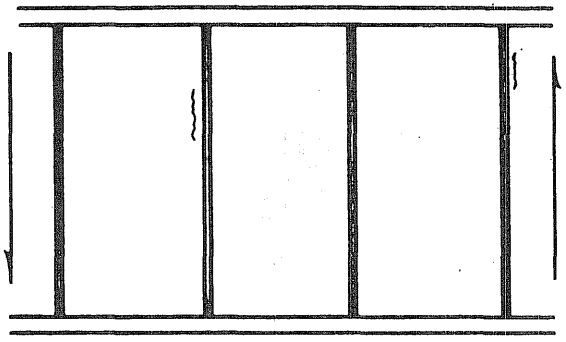

VST 8-4A

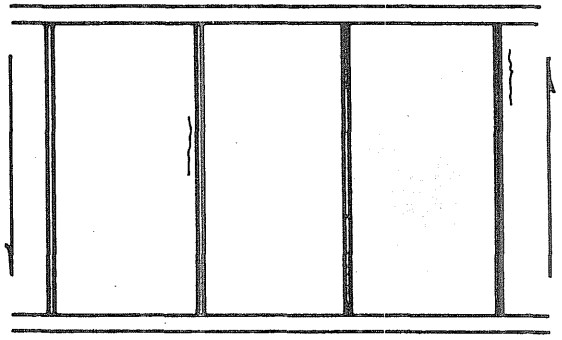

VST 8-16A

FIG. 102 LOCATIONS OF FAILURES.

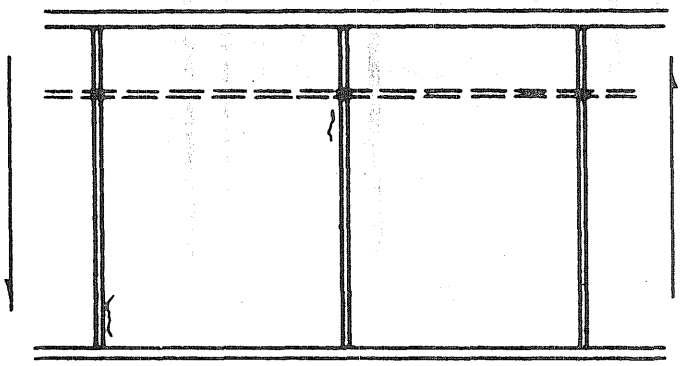

HSB-1

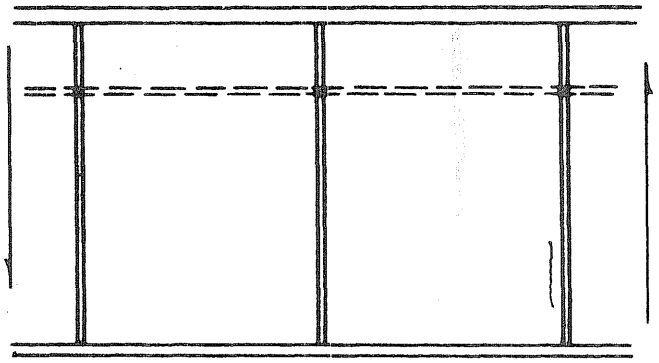

HSB-2

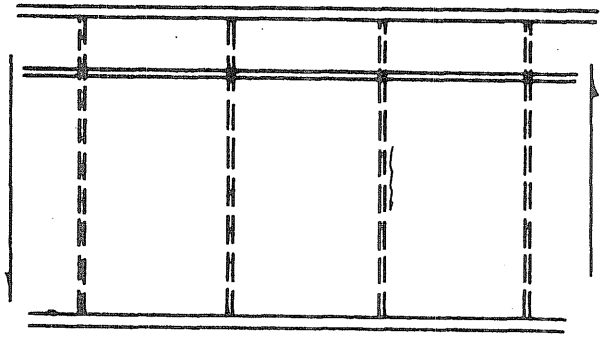

HVSB-1

FIG. 103 LOCATIONS OF FAILURES.

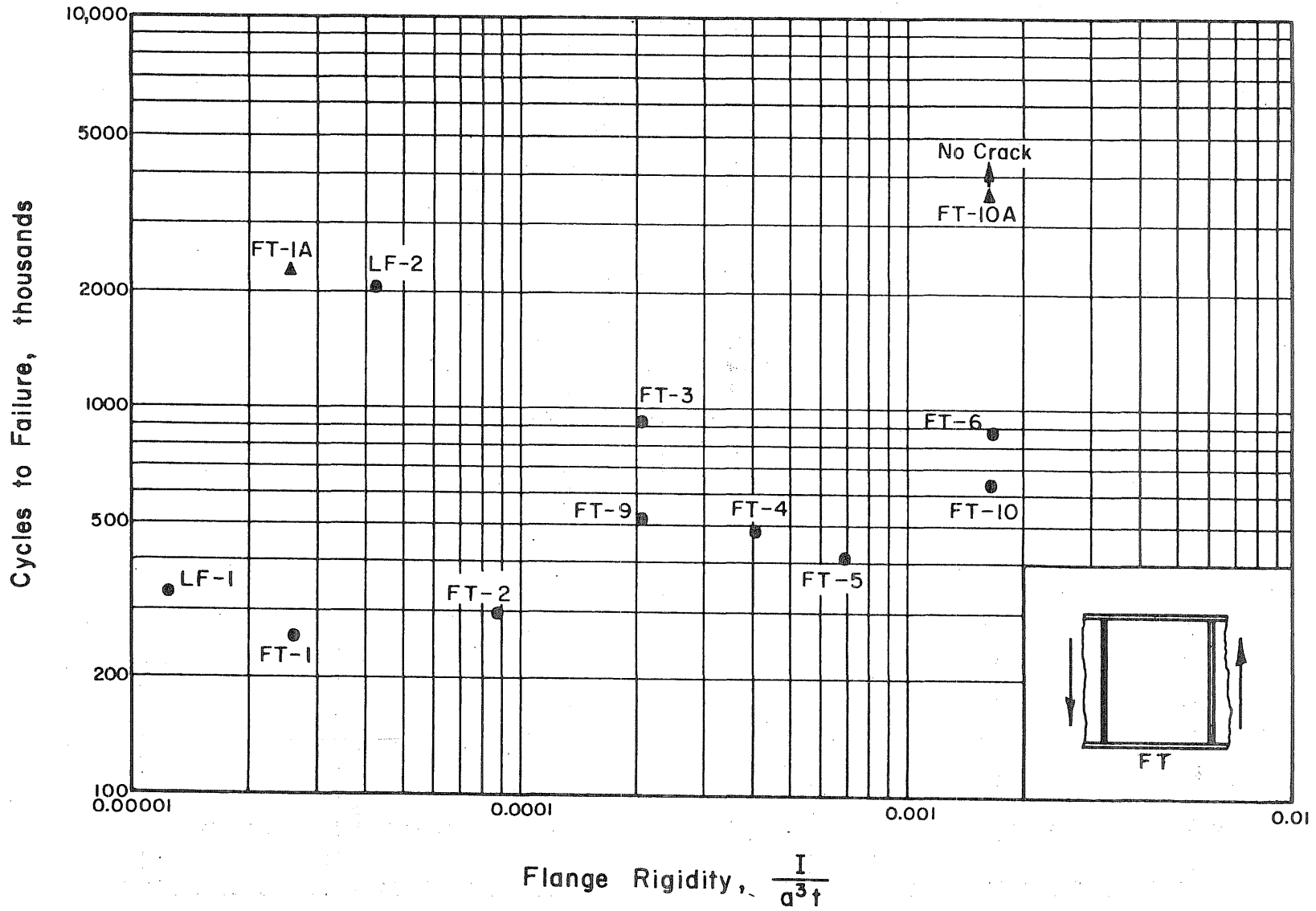

FIG. 104 FATIGUE LIFE OF SHEAR GIRDERS VERSUS FLANGE RIGIDITY PARAMETER.

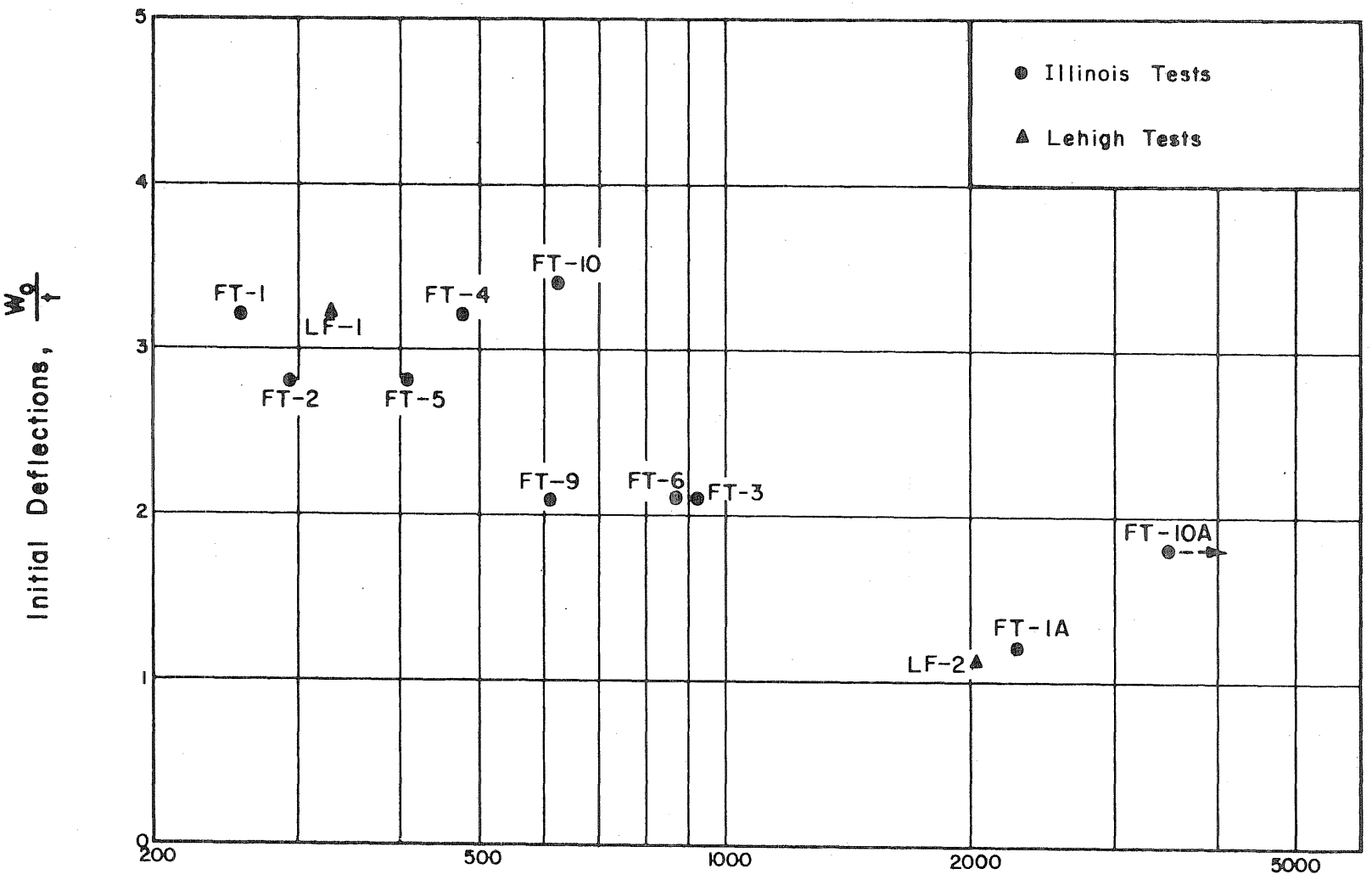

FIG. 105 INITIAL DEFLECTIONS VERSUS FATIGUE LIFE OF SHEAR GIRDERS.

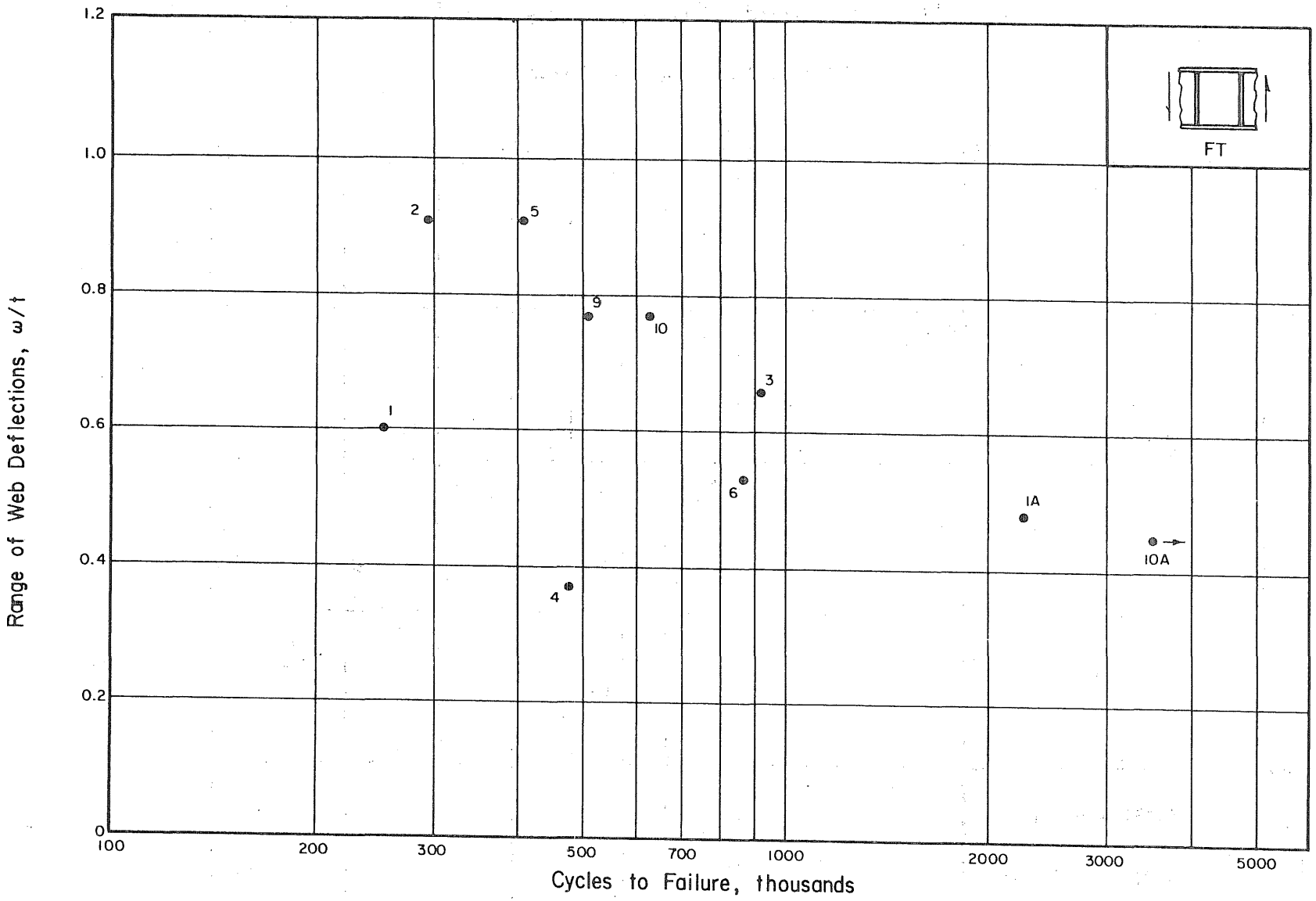

FIG. 106 RANGE OF WEB DEFLECTIONS vs FATIGUE LIFE OF SHEAR GIRDERS.

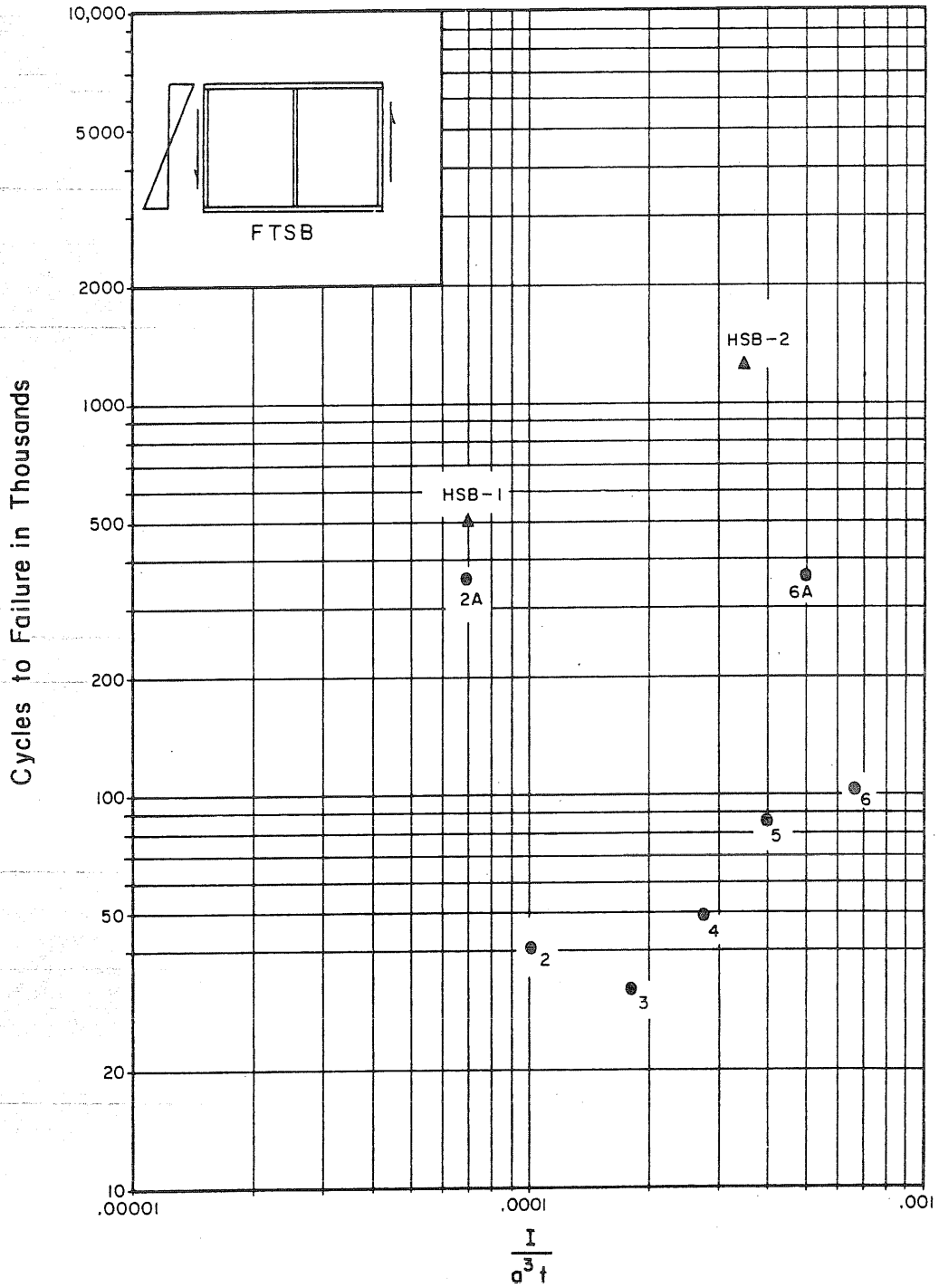

FIG. 107 FATIGUE LIFE vs FLANGE RIGIDITY PARAMETER FOR GIRDERS WITH VARIOUS FLANGE RIGIDITIES SUBJECTED TO SHEAR AND BENDING.

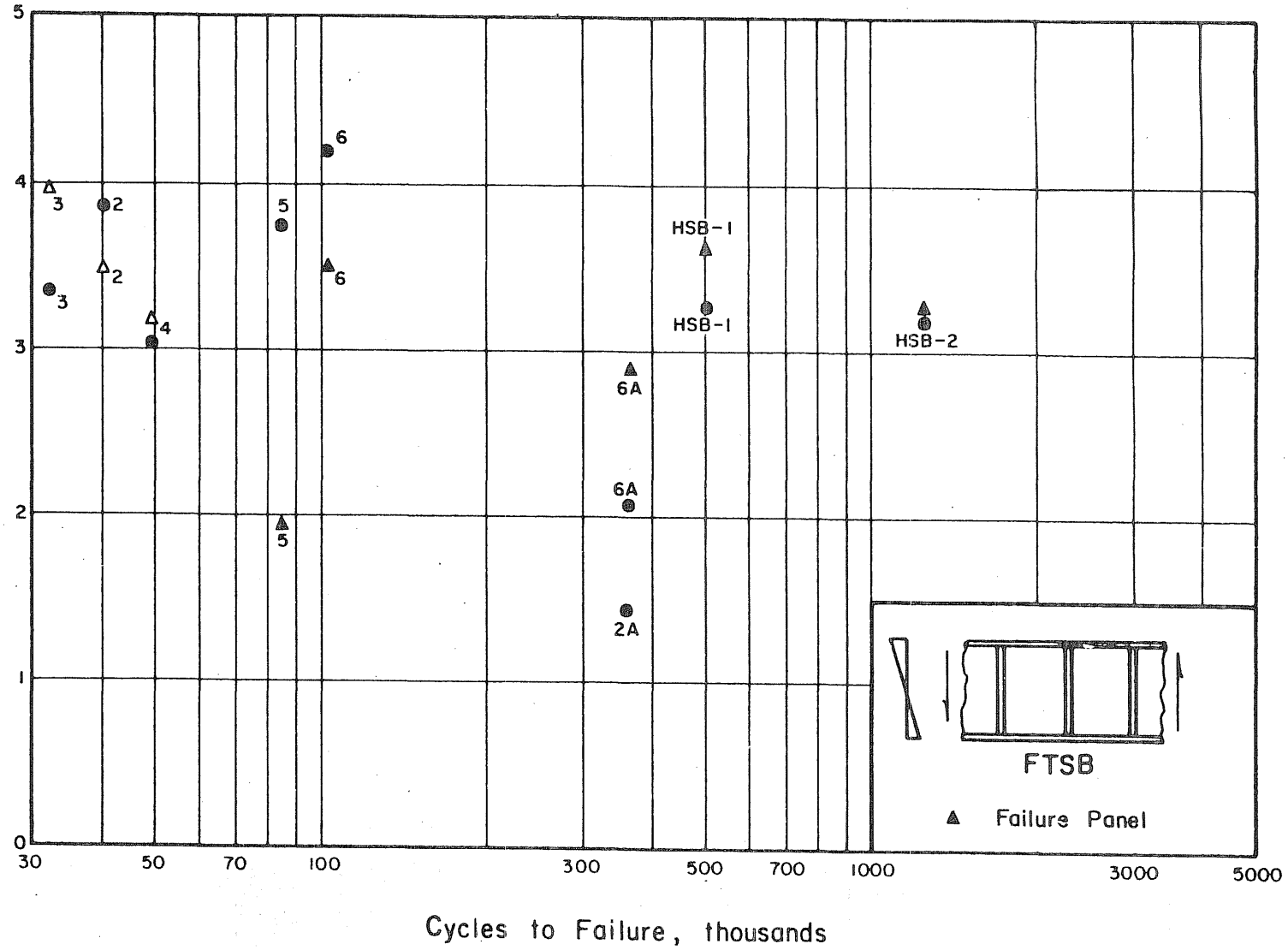

FIG. 108 INITIAL DEFLECTIONS vs FATIGUE LIFE OF GIRDERS WITH VARIOUS FLANGE RIGIDITIES SUBJECTED TO SHEAR AND BENDING.

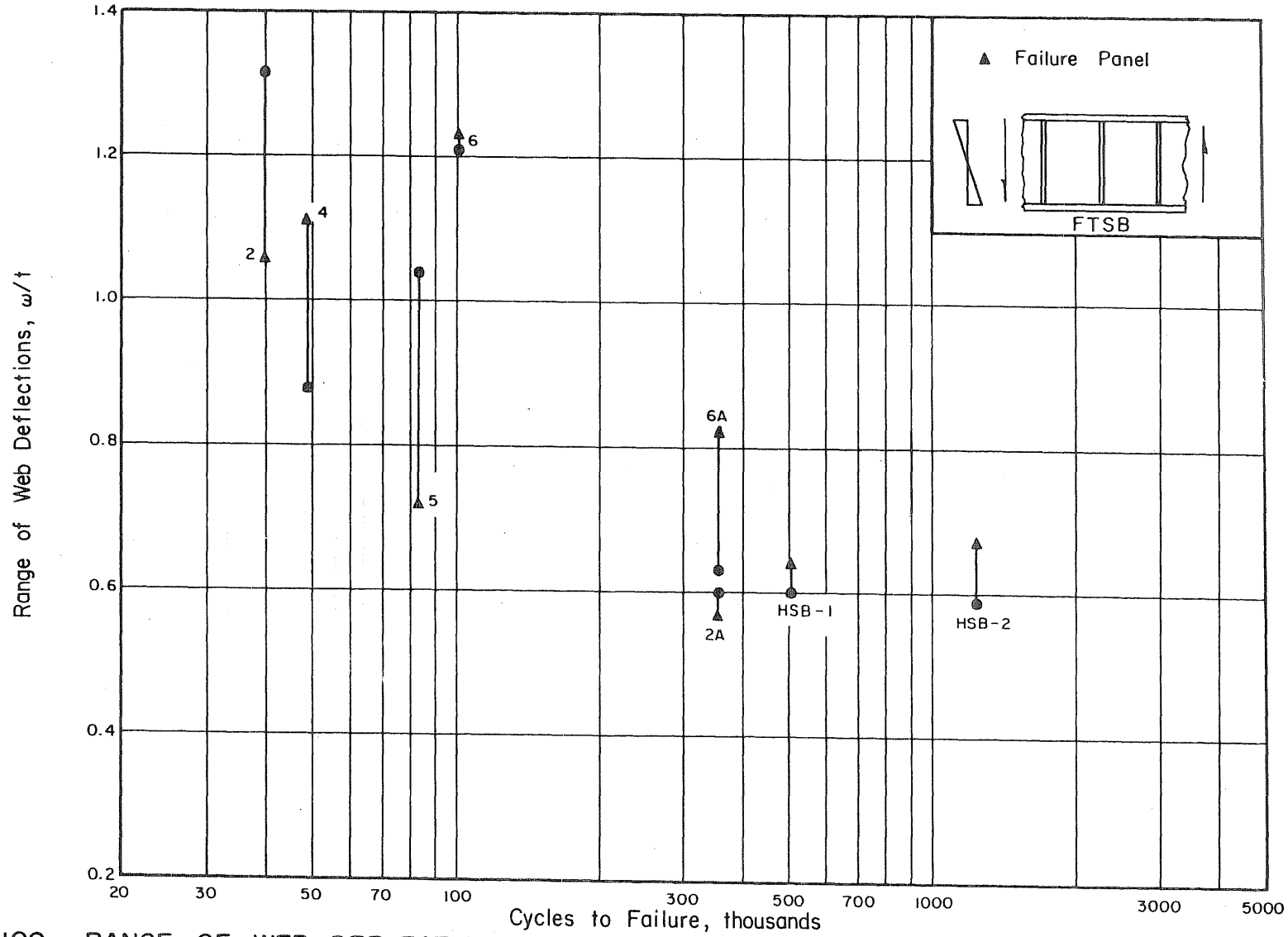

FIG. 109 RANGE OF WEB DEFLECTIONS vs FATIGUE LIFE OF GIRDERS WITH VARIOUS FLANGE RIGIDITIES SUBJECTED TO SHEAR AND BENDING.

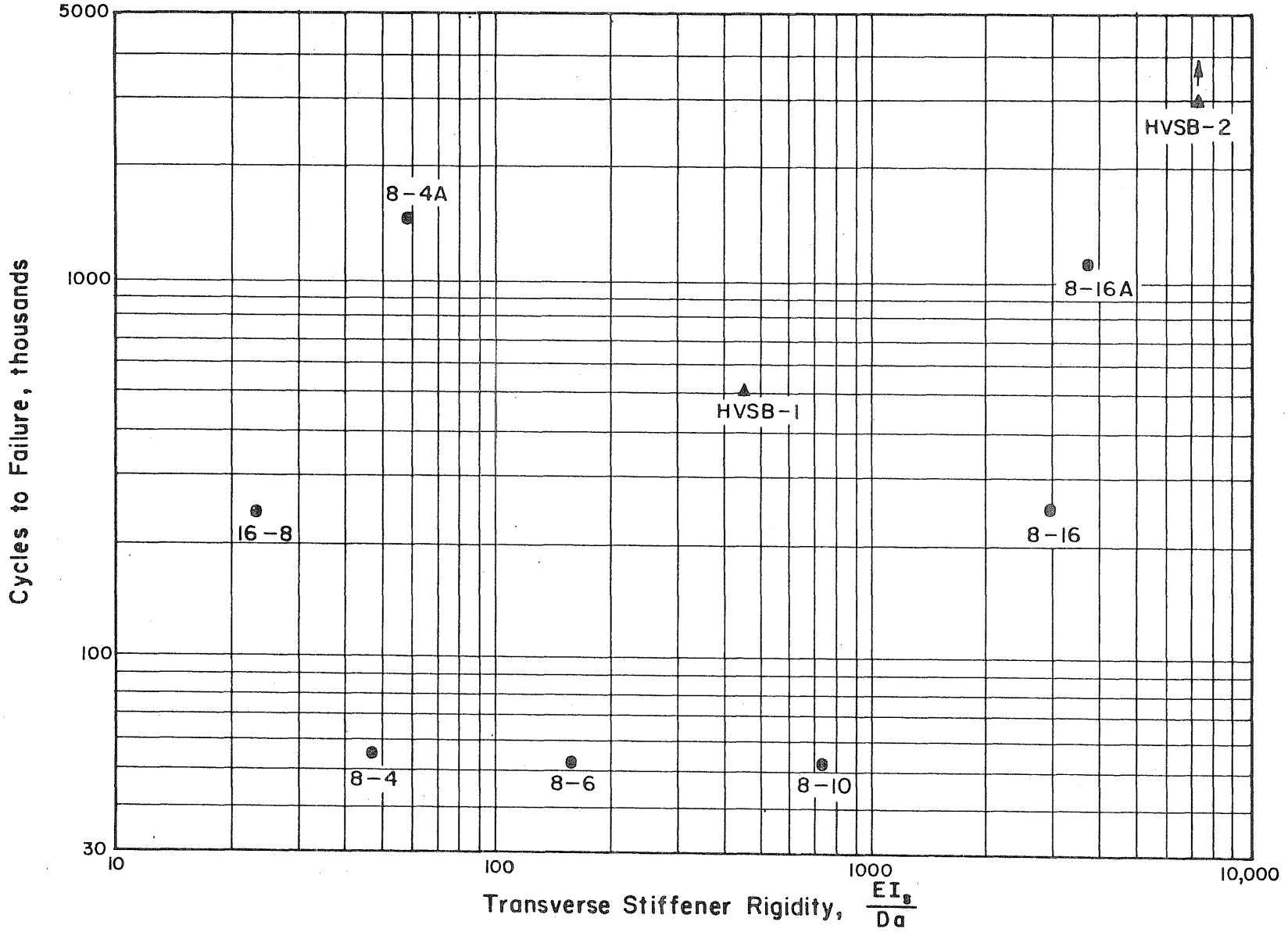

FIG. 110 FATIGUE LIFE vs STIFFENER RIGIDITY PARAMETER FOR GIRDERS WITH VARIOUS TRANSVERSE STIFFENER SIZES.

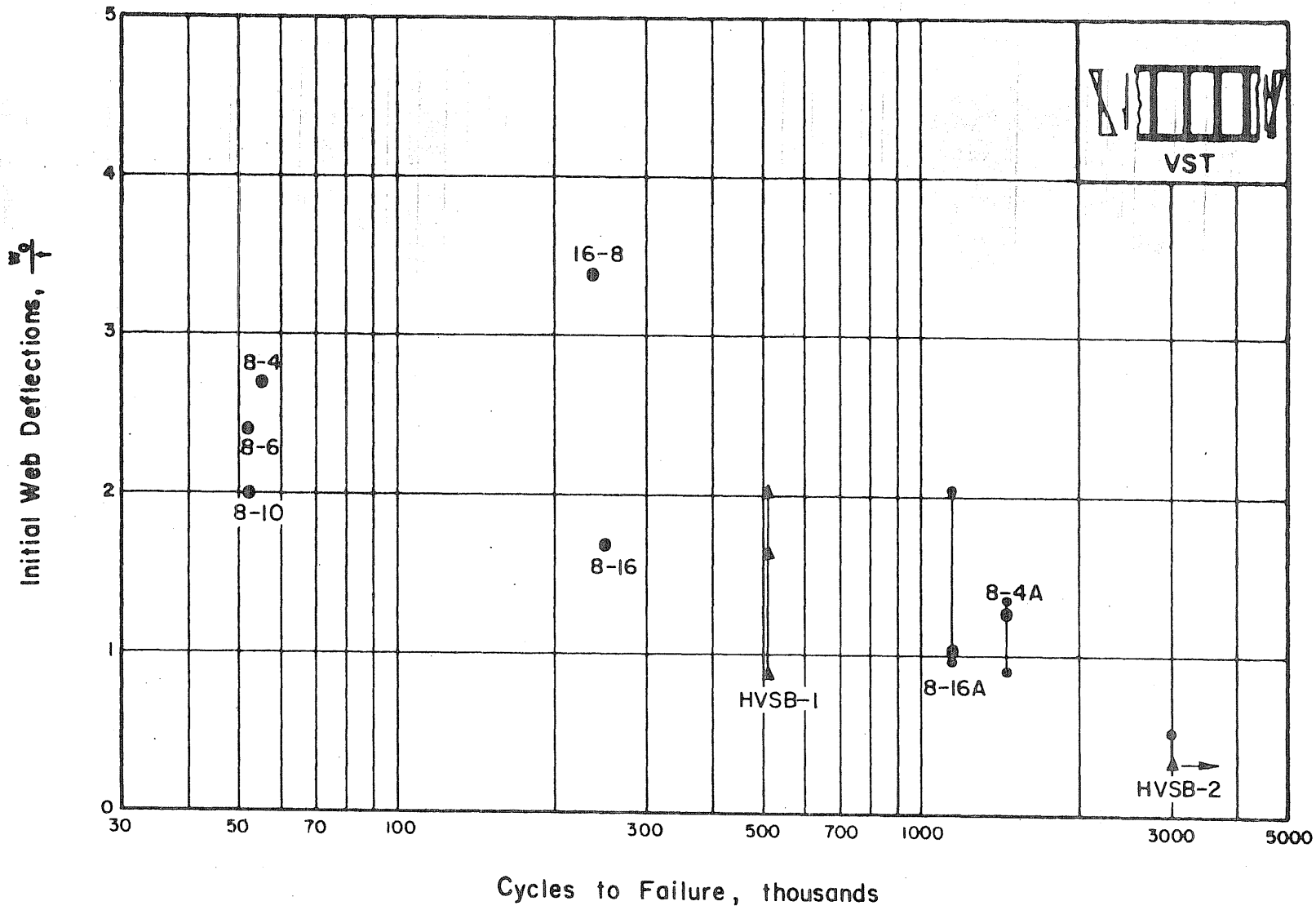

FIG. III INITIAL WEB DEFLECTIONS vs FATIGUE LIFE OF GIRDERS WITH VARIOUS TRANSVERSE STIFFENER RIGIDITIES .

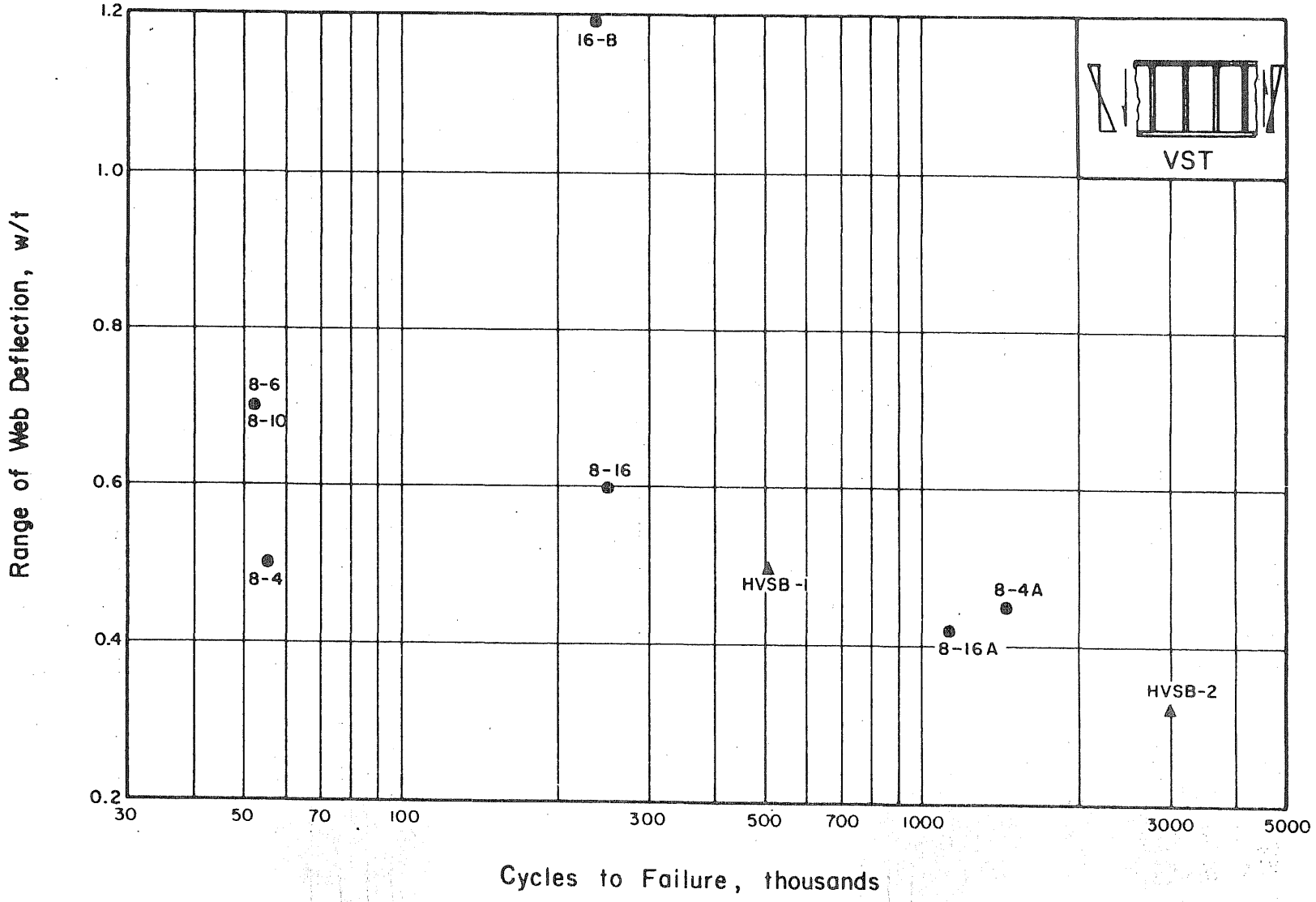

FIG. 112 RANGE OF WEB DEFLECTIONS vs FATIGUE LIFE FOR GIRDERS WITH VARIOUS TRANSVERSE STIFFENER RIGIDITIES.